Charles University in Prague
Faculty of Mathematics and Physics

DOCTORAL THESIS

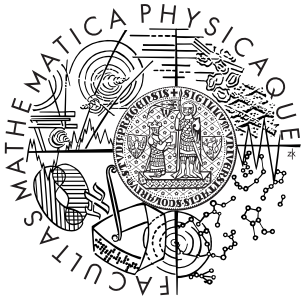

Jaroslav Trnka

Lagrangians for effective field theories and their properties

Institute of Particle and Nuclear Physics

Supervisor of the doctoral thesis: Jiří Novotný
Study programme: Physics
Specialization: f-9 Subnuclear Physics

Prague 2013

I would like to thank Jiří Novotný and Karol Kampf for their help during my years in Prague and for the collaboration on the first and third projects presented in this thesis, and to Juan Jose Sanz-Cillero for working with me on the second project. I am also grateful to Nima Arkani-Hamed and David McGady for their useful comments. I also thank my friends and family for their continuous support.

I declare that I carried out this doctoral thesis independently, and only with the cited sources, literature and other professional sources.

I understand that my work relates to the rights and obligations under the Act No. 121/2000 Coll., the Copyright Act, as amended, in particular the fact that the Charles University in Prague has the right to conclude a license agreement on the use of this work as a school work pursuant to Section 60 paragraph 1 of the Copyright Act.

In Prague, October 25, 2013

Název práce: Studium efektivních Lagrangianů a jejich aplikace

Autor: Jaroslav Trnka

Katedra: Ústav částicové a jaderné fyziky

Vedoucí disertační práce: RNDr. Jiří Novotný, CSc., ÚČJF

Abstrakt: V této práci studujeme různé aspekty efektivních teorií pole pro kvantovou chromodynamiku (QCD). V prvních dvou kapitolách se zaměříme na efektivní teorii pro resonance, která interpoluje mezi nízkoenergetickou efektivní teorií (Chirální poruchová teorie) a vysokoenergetickou QCD. V rámci této teorie studujeme jednosmyčkovou renormalizaci, jak z pohledu výpočetního pomocí SS-PP korelátoru, tak i čistě koncepčního studiem dynamicky generovaných stupňů volnosti. Ve čtvrté kapitole studujeme amplitudy rozptylu v rámci nelineárního sigma modelu, který představuje vedoucí člen nízkoenergetické efektivní teorie pro QCD. V návaznosti na nedávné objevy v rámci Yang-Mills teorie se nám podaří v rámci tohoto modelu zkonstruovat rekurzivní relace pro stromové amplitudy. Kromě čistě teoretické důležitosti tohoto faktu představuje tato metoda efektivní výpočetní nástroj nezávislý na formulaci amplitud pomocí Feynmanovských diagramů.

Klíčová slova: efektivní teorie pole, kvantová chromodynamika, nelineární sigma model

Title: Lagrangians for effective field theories and their properties

Author: Jaroslav Trnka

Department: Institute of Particle and Nuclear Physics

Supervisor: RNDr. Jiří Novotný, CSc., Institute of Particle and Nuclear Physics

Abstract: In this thesis we study various aspects of effective field theories for Quantum Chromodynamics (QCD). In first two chapters we focus on effective field theory for resonances which interpolates between the low energy field theory and the high energy QCD description. In this theory we study one-loop renormalization: we calculate one-loop corrections to SS-PP correlator and also study more conceptual problem – dynamical generations of new poles in propagators. In chapter four we study scattering amplitudes in the non-linear sigma model which is the leading low energy approximation to QCD. We make a contact with recent discoveries in the context of Yang-Mills theory by constructing recursion relations for all tree-level amplitudes. These relations are important not only conceptually but they also provide an effective tool to determine all tree-level amplitude in a way which is independent on the standard Feynman diagrams expansion.

Keywords: Effective field theories, Quantum chromodynamics, Non-linear sigma model

Contents

1 Overview of the thesis **4**
1.1 Introduction . . . 4
1.1.1 Effective field theory for resonances . . . 4
1.1.2 Amplitudes in the non-linear sigma model . . . 5
1.2 SS-PP correlator in the resonance region . . . 6
1.2.1 One-loop renormalization . . . 6
1.2.2 Phenomenology . . . 8
1.3 Renormalization in the effective theory for spin-1 resonances . . . 8
1.3.1 Vector field formalism . . . 9
1.3.2 Organization of counterterms . . . 11
1.3.3 The self-energy at one loop . . . 12
1.4 Amplitudes in the Non-linear sigma model . . . 13
1.4.1 Color stripped amplitudes . . . 13
1.4.2 Semi-on-shell amplitudes and Berends-Giele relations . . . 15
1.4.3 BCFW-like recursion relations . . . 16

2 High energy constraints in the octet $SS-PP$ correlator **19**
2.1 Introduction . . . 19
2.2 Resonance chiral theory lagrangian . . . 22
2.2.1 Leading order lagrangian . . . 23
2.2.2 Subleading Lagrangian . . . 24
2.2.3 Equations of motion and redundant operators . . . 25
2.3 Chiral octet $SS-PP$ correlator . . . 26
2.4 One-loop computation in resonance chiral theory . . . 27
2.4.1 Goldstone boson renormalizations . . . 28
2.4.2 Scalar resonance renormalization . . . 31
2.4.3 Pseudo-scalar resonance renormalization . . . 33
2.4.4 1PI contributions . . . 34
2.4.5 Correlator at NLO . . . 35
2.5 High energy constraints . . . 36
2.5.1 Alternative renormalization schemes . . . 38
2.6 Low-energy expansion . . . 40
2.6.1 $\widetilde{MS}$–subtraction scheme . . . 40
2.6.2 Pole masses and WSR–scheme for c_m and d_m . . . 42
2.7 Correlator with the extended RχT lagrangian . . . 42
2.7.1 Meson self-energies . . . 43
2.7.2 P–ϕ mixing . . . 45
2.7.3 New $s \to S$ and $p \to P$ vertex functions . . . 45
2.8 Phenomenology . . . 46
2.8.1 Phenomenology with Ecker *et al.*'s lagrangian $\mathcal{L}_G + \mathcal{L}_R$ . . . 47
2.8.2 Improving one $R\pi$ channel: extending the lagrangian . . . 48
2.8.3 Improving the $V\pi$, $S\pi$, $A\pi$ and $P\pi$ channels . . . 49
2.8.4 Impact of the RR' channels . . . 51
2.9 Conclusions . . . 51
2.10 Appendix . . . 53

2.10.1 Running of the renormalized parameters with $\mathcal{L}_G + \mathcal{L}_R$ . . 53
2.10.2 On-shell scheme for c_m and d_m 53
2.10.3 Feynman integrals 54
2.10.4 Useful expansions 54

3 Renormalization in the effective theory for spin-1 resonances 55
3.1 Introduction 55
3.2 Propagators and poles 58
3.2.1 Proca formalism 59
3.2.2 Antisymmetric tensor formalism 63
3.2.3 First order formalism 69
3.3 Organization of the counterterms 72
3.4 The self-energies at one loop 78
3.4.1 The Proca field case 78
3.4.2 The antisymmetric tensor case 81
3.4.3 The first order formalism 85
3.4.4 Note on the counterterms 90
3.5 From self-energies to propagators 91
3.5.1 The number of poles using Argument principle 92
3.5.2 The Källén-Lehman representation and nature of the poles 94
3.5.3 Examples of the poles 98
3.6 Summary and discussion 102
3.7 Appendix 105
3.7.1 Additional degrees of freedom in the path integral - the Proca field 105
3.7.2 The additional degrees of freedom in the path integral-the antisymmetric tensor case 108
3.7.3 Path integral formulation of the first order formalism . . . 110
3.7.4 The parameters α_i and β_i in terms of LECs 113
3.7.5 Proof of the positivity of the spectral functions 116

4 Amplitudes in the Non-linear sigma model 118
4.1 Introduction 118
4.2 Nonlinear sigma model 119
4.2.1 Leading order Lagrangian 119
4.2.2 General properties of the tree-level scattering amplitudes . 121
4.2.3 Tree-level amplitudes for $G = SU(N)$ 122
4.2.4 Explicit examples of $SU(N)$ on-shell amplitudes 125
4.3 Recursive methods for scattering amplitudes 126
4.3.1 BCFW recursion relations 126
4.3.2 Reconstruction formula with subtractions 128
4.4 BCFW-like relations for semi-on-shell amplitudes 129
4.4.1 Semi-on-shell amplitudes and Berends-Giele relations . . . 130
4.4.2 Cayley parametrization 132
4.4.3 Scaling properties of semi-on-shell amplitudes 134
4.4.4 BCFW reconstruction 137
4.4.5 Explicit example of application of BCFW relations: 6pt amplitude 141
4.5 More properties of stripped semi-on-shell amplitudes 142

4.5.1 Adler zeroes 144
4.5.2 Double-soft limit 147
4.6 Summary and conclusion 152
4.7 Appendix 153
4.7.1 General parametrization 153
4.7.2 More examples of amplitudes 157
4.7.3 Relative efficiency of Feynman diagrams and Berends-Giele relations 158
4.7.4 Other example of scaling properties of the semi-on-shell amplitudes 162
4.7.5 Double soft limit of Goldstone boson amplitudes 163

Conclusion **170**

Bibliography **171**

1. Overview of the thesis

1.1 Introduction

Standard Model is a very successful theory in describing elementary particles and their interaction. Over the last decades it has passed incredible number of experimental checks and there is no evidence that the theory is wrong. Moreover, the discovery of the Higgs boson in July 2012 completed the experimental search for all particles contained in this model. However, it is clear that this is not an ultimate theory of the universe but rather just a low energy approximation of the final theory. It is known for long time that the Standard model suffers from several problems where the most important role play: the hierarchy problem which is the large split between electroweak scale and unification/Planck scale and the incorporation of gravity. These are fundamental problems that will be definitely the biggest challenges of theoretical physics in 21th century.

The important part of the Standard model is the sector of strong interactions which is described by Quantum Chromodynamics. The fundamental degrees of freedom are gluons and quarks which are asymptotically free at high energies. At low energies the theory is strongly coupled and gluons and quarks are confined into hadrons. This means that at low energies there are other degrees of freedom - pions and other pseudoscalar mesons that arise from spontaneous chiral symmetry breaking. These particles are not present in the original QCD Lagrangian and their description requires the effective field theory approach provided by the chiral Lagrangian, ie. $SU(3)$ non-linear sigma model. The extension beyond the leading order is captured by the Chiral Perturbation Theory which provides a consistent momentum expansion. This theory has been very successful in describing the dynamics of the low energy sector of QCD.

This thesis focuses on two big open questions in this direction:

1. Extension of the effective field theory for QCD approach beyond the lowest energies.

2. Theoretical studies of the effective field Lagrangians using computations of scattering amplitudes.

1.1.1 Effective field theory for resonances

Chiral Perturbation Theory is an effective field theory for pseudoscalar mesons which is the lowest multiplet in the spectrum of hadrons. The effect of all higher resonances is effectively included in the coupling constants. Therefore, this effective theory breaks down when dynamics of resonances become important. This happens at the scale $\Lambda = M_\rho$ where M_ρ is the mass of the rho meson which is the lightest resonance. For energies $E \geq 1\,\mathrm{GeV}$ we need a new theory that also includes resonances as dynamical degrees of freedom, Resonance Chiral Theory. In the simplest approximation we consider only lowest multiplets of vector, axial vector, scalar and pseudoscalar resonances but in principle we could consider the infinite tower of them.

Resonance Chiral Theory is an effective field theory that describes interactions of pseudoscalar mesons and higher resonances. Because we are in intermediate energetic region there is no good expansion parameter. At lower energies we expand in small momenta while at high energies we can use $1/N_C$ expansion. In the resonance sector we have to combine both expansion parameters in order to get phenomenologically relevant results. The approach is to write a general Lagrangian compatible with the symmetries (chiral building blocks coupled to resonance fields). Then we calculate correlation functions in this theory and compare it with correlation functions computed at low energies (in Chiral Perturbation Theory) and at high energies with Operator Product Expansion (OPE). We require that our result matches both of them which gives consistency constraints on the coupling constants of our effective Lagrangian.

This thesis addresses this problem in two chapters. In chapter 2 we follow the approach outlined above by calculating $SS - PP$ correlator at one-loop. We match the result at low and high energies and provide set of conditions on coupling constants together with the saturation of low-energy constants in the chiral Lagrangians. In chapter 3 we study more conceptual point of validity of the resonance approach for loops. We find that in certain cases non-physical degrees of freedom can appear in the loop calculations and discuss the implications.

1.1.2 Amplitudes in the non-linear sigma model

In the low energy sector of QCD the dynamics of pseudoscalar mesons (pions, kaons) can be described by the $SU(3)$ non-linear sigma model. This theory plays an extremely important role in particle physics. It describes the dynamics of the octet of pseudo-Goldstone bosons that arise in the spontaneous symmetry breaking $SU(3) \times SU(3) \to SU(3)$. The Lagrangian is given by

$$\mathcal{L} = \frac{F^2}{4} \partial_\mu e^{\frac{i}{F}\phi} \partial^\mu e^{-\frac{i}{F}\phi} \qquad \text{where } \phi = \phi^a T^a \tag{1.1}$$

There is infinite tower of terms in this Lagrangian but all of them have two derivatives only. To study the properties of this Lagrangian it is suggestive to calculate the most basic physical observables which are scattering amplitudes. There are many interesting results in the literature but they are mostly from 1970's and 1980's: and none of them make any connection with the discoveries made in the context of Yang-Mills theory.

In last decade many new and powerful methods have been used to calculate scattering amplitudes in Yang-Mills theory. The most prominent role play the BCFW recursion relations that use the analytic properties of the S-matrix and reconstructs arbitrary scattering amplitude recursively from three point amplitudes. More recently, new amazing mathematical structures have been uncovered for supersymmetric Yang-Mills theories making close connections with active research in number of mathematical disciplines, from algebraic geometry to number theory.

However, most of the activity has been limited to Yang-Mills theory (and gravity) and there is a very little application to any other theories, especially not to effective field theories where these methods were believed to fail due. The non-linear sigma model here serves as a very good test case because it is a simple but still effective field theory.

In chapter 4 we construct BCFW-like recursion relations for all tree-level amplitudes of pseudo-Goldstone bosons in the non-linear sigma model. This shows that the modern methods developed in the context of Yang-Mills theory can be used more generally. We also discuss some further implications like the presence of Adler zero for color stripped amplitudes.

Before discussing these projects in details in chapter 2-4 we review main results in following three sections.

1.2 SS-PP correlator in the resonance region

Within the large–N_C approach the mesons will be classified within $U(3)$ multiplets. The chiral Goldstone bosons are introduced by means of the basic building block,

$$u(\phi) = \exp\left(i\frac{\phi}{\sqrt{2}F}\right) \tag{1.2}$$

where $\phi = \frac{1}{\sqrt{2}}\lambda^a\phi^a$ and

$$\phi(x) \;=\; \begin{pmatrix} \frac{1}{\sqrt{2}}\pi^0 + \frac{1}{\sqrt{6}}\eta_8 + \frac{1}{\sqrt{3}}\eta_1 & \pi^+ & K^+ \\ \pi^- & -\frac{1}{\sqrt{2}}\pi^0 + \frac{1}{\sqrt{6}}\eta_8 + \frac{1}{\sqrt{3}}\eta_1 & K^0 \\ K^- & \overline{K}^0 & -\frac{2}{\sqrt{6}}\eta_8 + \frac{1}{\sqrt{3}}\eta_1 \end{pmatrix} . \tag{1.3}$$

The Goldstone bosons couple to massive $U(3)$ multiplets of the type $V(1^{--})$, $A(1^{++})$, $S(0^{++})$ and $P(0^{-+})$. The vector multiplet, for instance, is given by

$$V_{\mu\nu} \;=\; \begin{pmatrix} \frac{1}{\sqrt{2}}\rho^0 + \frac{1}{\sqrt{6}}\omega_8 + \frac{1}{\sqrt{3}}\omega_1 & \rho^+ & K^{*+} \\ \rho^- & -\frac{1}{\sqrt{2}}\rho^0 + \frac{1}{\sqrt{6}}\omega_8 + \frac{1}{\sqrt{3}}\omega_1 & K^{*0} \\ K^{*-} & \overline{K}^{*0} & -\frac{2}{\sqrt{6}}\omega_8 + \frac{1}{\sqrt{3}}\omega_1 \end{pmatrix}_{\mu\nu} , \tag{1.4}$$

where we use the antisymmetric tensor formalism for spin–1 fields to describe the vector and axial-vector resonances [8, 9, 13].

The resonance fields R are chosen to transform covariantly under the chiral group as in Eq. (2.5) [8]. The interaction terms which are linear in the resonance fields can be obtained from the seminal work [8]:

$$\begin{aligned} \mathcal{L}_R \;&=\; c_d\langle Su^\mu u_\mu\rangle + c_m\langle S\chi_+\rangle + id_m\langle P\chi_-\rangle \\ &\quad + \frac{F_V}{2\sqrt{2}}\langle V_{\mu\nu}f_+^{\mu\nu}\rangle + \frac{iG_V}{2\sqrt{2}}\langle V_{\mu\nu}[u^\mu,u^\nu]\rangle + \frac{F_A}{2\sqrt{2}}\langle A_{\mu\nu}f_-^{\mu\nu}\rangle . \end{aligned} \tag{1.5}$$

1.2.1 One-loop renormalization

For our analysis of the $SS-PP$ correlator, the relevant bilinear terms will be [15]

$$\mathcal{L}_{RR'} \;=\; i\lambda_1^{PV}\langle\,[\nabla^\mu P, V_{\mu\nu}]\,u^\nu\,\rangle \;+\; \lambda_1^{SA}\langle\,\{\nabla^\mu S, A_{\mu\nu}\}\,u^\nu\,\rangle \;+\; \lambda_1^{SP}\langle\,\{\nabla^\mu S, P\}\,u_\mu\,\rangle\,. \tag{1.6}$$

Only single flavor–trace operators are considered for the construction of the large–N_C lagrangian. At tree-level, the octet $SS-PP$ correlator only gets contributions from this kind of terms, even at subleading orders in $1/N_C$. Operators

with two or more traces might appear in the vertices of one loop diagrams but, since these multi-trace terms are $1/N_C$–suppressed, these contributions would go to next-to-next-to-leading order and they will be neglected in the present work.

If one now uses the perturbative calculation, the $SS-PP$ octet correlator takes up to NLO in $1/N_C$ the form,

$$\begin{aligned}
\frac{1}{B_0^2}\,\Pi(p^2) &= \frac{1}{M_S^2-p^2}\left(16c_m^2 - 32c_m\lambda_{18}^S p^2 + \frac{16c_m^2 X_S p^4}{M_S^2-p^2}\right) \\
&\quad - \frac{16c_m^2}{(M_S^2-p^2)^2}\Sigma_S^r(p^2)^{1\ell} - \frac{8c_m}{M_S^2-p^2}\,\frac{1}{B_0}\Phi_{sS}^r(p^2)^{1\ell} \\
&\quad - \frac{1}{M_P^2-p^2}\left(16d_m^2 - 32d_m\lambda_{13}^P p^2 + \frac{16d_m^2 X_P p^4}{M_P^2-p^2}\right) \\
&\quad + \frac{16d_m^2}{(M_P^2-p^2)^2}\Sigma_P^r(p^2)^{1\ell} + \frac{8d_m}{M_P^2-p^2}\,\frac{1}{B_0}\Phi_{pP}^r(p^2)^{1\ell} \\
&\quad + \frac{2F^2}{p^2}\left(1 - \frac{8\widetilde{L}_{11}p^2}{F^2} - \frac{4\widetilde{L}_{12}p^2}{F^2}\right) + \frac{2F^2}{p^4}\Sigma_\phi^r(p^2)^{1\ell} + \frac{2F}{p^2}\,\frac{\sqrt{2}}{B_0}\Phi_{p\phi}^r(p^2)^{1\ell} \\
&\quad + 32\widetilde{L}_8 + 16\widetilde{L}_{11} + 8\widetilde{L}_{12} \;+\; \Pi_{ss-pp}^r(p^2)^{1\ell}\,. \qquad (1.7)
\end{aligned}$$

The couplings shown here are the renormalized ones even if the superscript "r" is not explicitly present. The first two lines are the contribution from the scalar exchanges. The third and fourth ones come from the pseudoscalar resonance exchanges, whereas the fifth one is produced by the Goldstone exchanges. The last line is given by the 1PI diagrams in the $SS-PP$ correlator.

The NLO expression for the correlator contains plenty of resonance parameters that are not fully well known. A typical procedure to improve the determination of these couplings is the use of the short-distance conditions [9].

The operator product expansion tells us that the $SS-PP$ correlator vanishes like $1/p^4$ for the large Euclidean momentum. Indeed, due to the smallness of its dimension–four condensate ($\frac{1}{B_0^2}\langle\,\mathcal{O}_4^{SS-PP}\,\rangle \simeq 12\pi\alpha_S F^4 \sim 3\cdot 10^{-4}$ GeV^4 [49]), it is a good approximation to consider that it vanishes like $1/p^6$ when $p^2\to-\infty$ [49].

The correlator does not follow this short-distance behaviour for arbitrary values of its couplings. This imposes severe constraints on the coefficients of the high-energy expansion of our NLO correlator,

$$\frac{1}{B_0^2}\,\Pi(p^2) \;=\; \sum_{n=0,1,2\ldots}\frac{1}{(p^2)^k}\left(\alpha_{2n}^{(p)} \,+\, \alpha_{2n}^{(\ell)}\ln\frac{-p^2}{\mu^2}\right). \qquad (1.8)$$

The proper OPE short-distance behaviour is therefore recovered by demanding [47]

$$\alpha_k^{(\ell)} = \alpha_k^{(p)} = 0\,, \qquad \text{for} \quad k=0,2,4\,. \qquad (1.9)$$

At large N_C, there are no logarithmic terms ($\alpha_k^{(\ell)}=0$) and for the remaining coefficients one has $\alpha_0^{(p)}=0$ (no $\widetilde{L}_8$ or higher local couplings at large N_C) and the two Weinberg sum-rules (WSR),

$$\begin{aligned}
\alpha_2^{(p)} &= 2F^2 + 16d_m^2 - 16c_m^2 \;=\; 0\,, \\
\alpha_4^{(p)} &= 16d_m^2 M_P^2 - 16c_m^2 M_S^2 \;=\; 0\,. \qquad (1.10)
\end{aligned}$$

At NLO, in the case when the interactions only contain operators $\mathcal{L}_R$ with at most one resonance field [8], the high-energy expansion log–term coefficients result

$$\begin{aligned}
\frac{8\pi^2F^2}{3}\alpha_0^{(\ell)} &= 8c_m^2 - 8d_m^2 - 4c_dc_m + 2c_d^2 + G_V^2 - \frac{8c_d^2c_m^2}{F^2} - \frac{F^2}{2}\,,\\
\frac{8\pi^2F^2}{3}\alpha_2^{(\ell)} &= 8d_m^2M_P^2 - 8c_m^2M_S^2 - \frac{16M_S^2c_d^2c_m^2}{F^2} + 20c_dc_mM_S^2 - 6c_d^2M_S^2 - 3G_V^2M_V^2\,,\\
\frac{8\pi^2F^2}{3}\alpha_4^{(\ell)} &= -\frac{24c_d^2c_m^2M_S^4}{F^2} - 4c_dc_mM_S^4 + 6c_d^2M_S^4 + 3G_V^2M_V^4\,,
\end{aligned} \tag{1.11}$$

and the high-energy coefficients $\alpha_{0,2,4}^{(p)}$ are given by

$$\begin{aligned}
\alpha_0^{(p)} &= -\alpha_0^{(l)} \;+\; 32\,\widetilde{L}_8\,,\\
\alpha_2^{(p)} &= 2F^2 + 16d_m^2 - 16c_m^2 \;+\; A(\mu)\,,\\
\alpha_4^{(p)} &= 16d_m^2M_P^2 - 16c_m^2M_S^2 \;+\; B(\mu)\,,
\end{aligned} \tag{1.12}$$

with the NLO corrections that depend on the renormalization scale μ through functions $A(\mu)$ and $B(\mu)$.

1.2.2 Phenomenology

First, we will extract the value of the LECs at large N_C within the single resonance approximation. We will use the formerly referred $M_S = 980 \pm 20$ MeV and $M_P = 1300 \pm 50$ MeV, $F = 90 \pm 2$ MeV and the standard reference χPT renormalization scale $\mu_0 = 770$ MeV. The short-distance constraints determine c_m and d_m in terms of the scalar and pseudo-scalar masses, producing

$$L_8 \,=\, (0.83 \pm 0.05)\,\cdot 10^{-3}\,, \qquad\qquad C_{38} \,=\, (8.4 \pm 1.0)\cdot\, 10^{-6}\,. \tag{1.13}$$

Naively, if the uncertainty on the saturation scale is estimated by observing the variation with μ in the range 0.5–1 GeV, one would expect the former values to be deviated from the actual ones at the order of $\Delta L_8 \sim 0.3\cdot 10^{-3}$, $\Delta C_{38} \sim 5\cdot 10^{-6}$.

In order to go beyond the naive estimate of the subleading $1/N_C$ uncertainty, we consider now the one-loop contributions computed in previous sections. The analysis needs the detailed discussion of parameters and different schemes. Finally, it leads to our final LEC estimates,

$$L_8(\mu_0) \,=\, (1.0 \pm 0.4)\,\cdot\, 10^{-3}\,, \qquad\qquad C_{38}(\mu_0) \,=\, (8 \pm 5)\,\cdot\, 10^{-6}\,. \tag{1.14}$$

These numbers are compared to previous determinations in Fig. 2.14. Although there is still a clear dispersion between the various measurements, at the present error level we remain essentially compatible. Further efforts should be focused on the extraction of the scalar and pseudo-scalar pole masses in order to sizably reduce the uncertainties in the resonance calculations.

1.3 Renormalization in the effective theory for spin-1 resonances

In this chapter we discuss the issue of the additional degrees of freedom in all three formalisms for the description of spin-one resonances (vector, antisymmetric

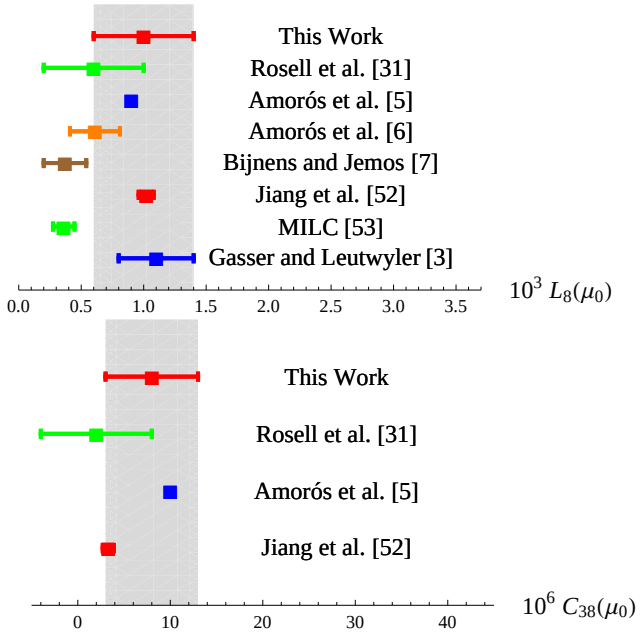

Figure 1.1: Comparison of the LEC predictions in this work with previous results in the bibliography.

tensor and combined). We use the path integral formulation where the protective symmetry analogous to the Rarita-Schwinger case is manifest. We formulate a formal self-consistent organization of the counterterms and one-particle irreducible graphs, which sorts the operators in the Lagrangian according to the number of derivatives as well as number of the resonance fields and which is useful for the proof of renormalizability of the Resonance chiral theory as an effective theory. This is used to explicitly calculate self-energies and give a list of counterterms and briefly discuss the renormalization prescription. Finally, we construct their propagators and discuss the pole structure. In this review, we focus just on the case of vector field description, discussion for other two formalisms is analogous.

1.3.1 Vector field formalism

The full propagator for the spin-1 field is

$$\Delta_{\mu\nu}(p) = -\frac{1}{p^2 - M^2 - \Sigma^T(p^2)} P^T_{\mu\nu} + \frac{1}{M^2 + \Sigma^L(p^2)} P^L_{\mu\nu}. \tag{1.15}$$

where

$$P^L_{\mu\nu} = \frac{p_\mu p_\nu}{p^2} \tag{1.16}$$

$$P^T_{\mu\nu} = g_{\mu\nu} - \frac{p_\mu p_\nu}{p^2} \tag{1.17}$$

are the usual longitudinal and transverse projectors and $\Sigma^{T,L}$ are the corresponding transverse and longitudinal self-energies, which vanish in the free field limit.

The possible (generally complex) poles of such a propagator are of two types; either at $p^2 = s_V$, where s_V is given by the solutions of

$$s_V - M^2 - \Sigma^T(s_V) = 0, \tag{1.18}$$

or at $p^2 = s_S$ where s_S is the solution of

$$M^2 + \Sigma^L(s_S) = 0. \tag{1.19}$$

Let us first discuss the poles of the first type. Assuming that (3.8) is satisfied for $s_V = M_V^2 > 0$, then for $p^2 \to M_V^2$

$$\begin{aligned} \Delta_{\mu\nu}(p) &= \frac{Z_V}{p^2 - M_V^2}\left(-g_{\mu\nu} + \frac{p_\mu p_\nu}{M^2}\right) + O(1) \\ &= \frac{Z_V}{p^2 - M_V^2}\sum_\lambda \varepsilon_\mu^{(\lambda)}(p)\varepsilon_\nu^{(\lambda)*}(p) + O(1) \end{aligned} \tag{1.20}$$

where

$$Z_V = \frac{1}{1 - \Sigma'^T(M_V^2)} \tag{1.21}$$

and where $\varepsilon_\mu^{(\lambda)}(p)$ are the usual spin-one polarization vectors. Under the condition $Z_V > 0$ the poles of this type correspond to spin-one one particle states $|p, \lambda, V\rangle$ which couple to the Proca field as

$$\langle 0|V_\mu(0)|p, \lambda, V\rangle = {Z_V}^{1/2}\varepsilon_\mu^{(\lambda)}(p). \tag{1.22}$$

At least one of these states is expected to be perturbative in the sense that its mass and coupling to V_μ can be written as

$$M_V^2 = M^2 + \delta M_V^2 \tag{1.23}$$

$$Z_V = 1 + \delta Z_V, \tag{1.24}$$

where δM_V^2 and δZ_V are small corrections vanishing in the free field limit. This solution corresponds to the original degree of freedom described by the free part of the Lagrangian $\mathcal{L}_0$. The additional one particle states corresponding to the other possible (non-perturbative) solutions of (3.8) decouple in the free field limit.

The second type of poles is given by (intrinsically nonperturbative) solutions of (3.9). Suppose that this condition is satisfied by $s_S = M_S^2 > 0$. For $p^2 \to M_S^2$

$$\Delta_{\mu\nu}(p) = \frac{Z_S}{p^2 - M_S^2}\frac{p_\mu p_\nu}{M_S^2} + O(1) \tag{1.25}$$

where

$$Z_S = \frac{1}{\Sigma'^L(M_S^2)}. \tag{1.26}$$

Assuming $Z_S > 0$ this pole corresponds to the spin-zero one particle state $|p, S\rangle$ which couples to V_μ as

$$\langle 0|V_\mu(0)|p, S\rangle = \mathrm{i}p_\mu\frac{{Z_S}^{1/2}}{M_S}. \tag{1.27}$$

For the free field this scalar mode is frozen and does not propagate according to the special form of the vector field Lagrangian. Therefore, in the limit of vanishing interaction the extra scalar state decouples. Without any additional assumptions on the symmetries of the interaction Lagrangian we can therefore expect the appearance of additional dynamically generated degrees of freedom.

1.3.2 Organization of counterterms

In the process of the loop calculation we are lead to the problem of performing a classification of the countertems, which have to be introduced in order to renormalize infinities. For this purpose, it is convenient to have a scheme, which allows us to assign to each operator in the Lagrangian and to each Feynman graph an appropriate expansion index. Indices of the counterterms, which are necessary in order to cancel the divergences of the given Feynman graph, should be then correlated with the indices of the vertices of the graph as well as with the number of the loops. When we restrict ourselves to the (one-particle irreducible) graphs with a given index, the number of the allowed operators contributing to the graph as well as that of necessary counterterms should be finite. There are several possibilities how to do it, some of them being quite efficient but purely formal and unphysical, some of them having good physical meaning, but not very useful in practise.

The problem is obvious: we are trying to build the effective theory in the intermediate energy region which is hard because we do not have useful expansion parameters. Therefore, in the standard cases one uses either small momentum or large N_C expansion which always leads to problems. Our approach combines the advantages of both approaches and it classifies all graphs based on the combined expansion. Let us start with the familiar formula for the degree of superficial divergence d_Γ of a given *one particle irreducible* graph Γ, which provides us with the upper bound on the number of derivatives $d_{\mathcal{O}_{ct}}$ in a counterterm $\mathcal{O}_{ct}$ needed for the renormalization of Γ. Because in the vector field formalism the spin 1 resonance propagator behaves as $O(1)$ for $p \to \infty$, we get

$$d_{\mathcal{O}_{ct}} \leq d_\Gamma = 4L - 2I_{GB} + \sum_{\mathcal{O}} d_{\mathcal{O}} \tag{1.28}$$

where $d_{\mathcal{O}}$ means the number of derivatives of the vertex V derived from the operator $\mathcal{O}$. We can derive the analog of the Weinberg formula, now in the form of an upper bound

$$i_{\mathcal{O}_{ct}} \leq i_\Gamma = 2L + \sum_{\mathcal{O}} i_{\mathcal{O}}. \tag{1.29}$$

The counting rules can be summarized as follows

$$R_{\mu\nu},\, V_\mu = O(p),\, M = O(1) \tag{1.30}$$

and for the external sources as usual

$$v^\mu, a^\mu = O(p),\ \chi, \chi^+ = O(p^2). \tag{1.31}$$

Note also that, the index $i_{\mathcal{O}}$ can be rewritten as

$$i_{\mathcal{O}} = D_{\mathcal{O}} - 2\left(1 - \frac{n_R^{\mathcal{O}}}{2}\right) \tag{1.32}$$

and in the last bracket we recognize the exponent controlling the leading large N_C behavior of the coupling constant in front of the operator $\mathcal{O}$. Remember, however, that the loop induced counterterms have an additional $1/N_C$ suppression for each

loop (cf. (3.121)). Therefore it is natural to modify the index $i_{\mathcal{O}}$ and i_Γ as follows (the coefficient 1/2 is a matter of convenience, see bellow)

$$\widehat{i}_{\mathcal{O}} = \frac{1}{2}D_{\mathcal{O}} - \left(1 - \frac{n_R^{\mathcal{O}}}{2} - s_{\mathcal{O}}\right) \qquad \widehat{i}_\Gamma = 2L + \sum_{\mathcal{O}} \widehat{i}_{\mathcal{O}}$$

With such a modified indices $\widehat{i}_{\mathcal{O}}$, $\widehat{i}_\Gamma$ the formula (3.126) has the form

$$\widehat{i}_{\mathcal{O}_{ct}} \leq \widehat{i}_\Gamma = 2L + \sum_{\mathcal{O}} \widehat{i}_{\mathcal{O}} \tag{1.33}$$

The content of this redefinition of $i_{\mathcal{O}}$ is evident: the operators are now classified according to the combined derivative and large N_C expansion according to the counting rules (for pure χPT introduced in [82], [83])

$$p = O(\delta^{1/2}),\ v, a = O(\delta^{1/2}),\ \chi, \chi^+ = O(\delta),\ \frac{1}{N_C} = O(\delta) \tag{1.34}$$

In what follows we shall use for the classification of the counterterms and for the organization of our calculation the index $i_{\mathcal{O}}$ given by (3.125) and (3.126). Note however, that these formulae similarly to the previous cases, do not have much of physical content and serve only as a *formal* tool for the proof of the renormalizability and for the ordering of the counterterms. Namely, the index i_Γ which is by construction related to the superficial degree of the divergence (and which applies to one-particle irreducible graphs only) does not reflect the infrared behavior of the (one-particle irreducible) graph Γ, rather it refers to its ultraviolet properties.

1.3.3 The self-energy at one loop

Our starting point is the following Lagrangian for 1^{--} resonances [85] (see also [86])

$$\begin{aligned}\mathcal{L}_V &= -\frac{1}{4}\langle \widehat{V}_{\mu\nu}\widehat{V}^{\mu\nu}\rangle + \frac{1}{2}M^2\langle V_\mu V^\mu\rangle \\ &\quad -\frac{\mathrm{i}}{2\sqrt{2}}g_V\langle \widehat{V}^{\mu\nu}[u_\mu, u_\nu]\rangle + \frac{1}{2}\sigma_V\varepsilon_{\alpha\beta\mu\nu}\langle\{V^\alpha, \widehat{V}^{\mu\nu}\}u^\beta\rangle + \dots\end{aligned} \tag{1.35}$$

where we have written down explicitly only the terms contributing to the self-energy. In order to cancel the infinite part of the loops we have therefore to introduce a set of counterterms with two resonance fields and indices[1] $i_{\mathcal{O}} \leq 6$, namely

$$\begin{aligned}\mathcal{L}_V^{ct} &= \frac{1}{2}M^2 Z_M\langle V_\mu V^\mu\rangle + \frac{Z_V}{4}\langle \hat{V}_{\mu\nu}\hat{V}^{\mu\nu}\rangle - \frac{Y_V}{2}\langle (D_\mu V^\mu)^2\rangle \\ &\quad + \frac{X_{V1}}{4}\langle\{D_\alpha, D_\beta\}V_\mu\{D^\alpha, D^\beta\}V^\mu\rangle + \frac{X_{V2}}{4}\langle\{D_\alpha, D_\beta\}V_\mu\{D^\alpha, D^\mu\}V^\beta\rangle \\ &\quad + \frac{X_{V3}}{4}\langle\{D_\alpha, D_\beta\}V^\beta\{D^\alpha, D^\mu\}V_\mu\rangle + \frac{X_{V4}}{2}\langle D^2V_\mu\{D^\mu, D^\beta\}V_\beta\rangle + X_{V5}\langle D^2V_\mu D^2V^\mu\rangle \\ &\quad + \mathcal{L}_V^{ct(6)}.\end{aligned} \tag{1.36}$$

[1] Note that, for these counterterms the index $i_{\mathcal{O}}$ coincides with the usual chiral order $D_{\mathcal{O}}$.

Here the last term accumulates the operators with six derivatives ($i_{\mathcal{O}} = 6$), which we do not write down explicitly. The bare couplings are split into a finite part renormalized at a scale μ and a divergent part. The result for self-energies can be written in the form (in the following formulae $x = s/M^2$)

$$\begin{aligned}\Sigma_T^r(s) &= M^2\left(\frac{M}{4\pi F}\right)^2\left[\sum_{i=0}^{3}\alpha_i x^i - \frac{1}{2}g_V^2\left(\frac{M}{F}\right)^2 x^3\widehat{B}(x) - \frac{40}{9}\sigma_V^2(x-1)^2 x\widehat{J}(x)\right]\\ \Sigma_L^r(s) &= M^2\left(\frac{M}{4\pi F}\right)^2\sum_{i=0}^{3}\beta_i x^i\end{aligned}$$

In the above formulae α_i and β_i can be expressed in terms of the renormalization scale independent combinations of the counterterm couplings and χlogs.

It is easy to show that these results lead to the generation of new poles in the propagators that for some reasonable values of coupling constants are inside the region of applicability of this theory. The detailed discussion together with numerical analysis is provided in chapter 3 of the thesis. As a result, the concept of renormalization for the effective theory for resonances must be studied in more details taking into account this phenomenon.

1.4 Amplitudes in the Non-linear sigma model

The focus of this chapter is on scattering amplitudes of Goldstone bosons within the $SU(N)$ nonlinear sigma model described by the leading order Lagrangian. In principle, the standard Feynman diagram approach allows us to calculate arbitrary amplitude. Because the model is effective, and the Lagrangian contains an infinite tower of terms the calculation becomes very complicated for amplitudes of many external Goldstone bosons even at tree-level. It would be therefore desirable to find alternative non-diagrammatic methods which could save the computational effort and provide us with a tool to get the amplitudes more efficiently.

We find the new recursion relations for all on-shell tree-level amplitudes of Goldstone bosons within $SU(N)$ nonlinear sigma model. This shows that on-shell methods can be applied also for effective field theories and it gives new computational tool in this model. Using these recursion relations we are also able to prove more properties of tree-level amplitudes that are invisible in the Feynman diagram approach.

1.4.1 Color stripped amplitudes

The most general chiral invariant leading order effective Lagrangian in general number d of space-time dimensions describing the dynamics of the Goldstone bosons corresponding to the spontaneous symmetry breaking $G_L \times G_R \to G_V$ as

$$\mathcal{L}^{(2)} = \frac{F^2}{4}\langle\partial_\mu U\partial^\mu U^{-1}\rangle = -\frac{F^2}{4}\langle(U^{-1}\partial_\mu U)(U^{-1}\partial^\mu U)\rangle, \tag{1.37}$$

where F is a constant[2] with the canonical dimension $d/2-1$. Here and in what follows we use the notation $\langle\cdot\rangle = \mathrm{Tr}(\cdot)$ and the trace is taken in the defining

[2]The decay constant of the Goldstone bosons.

representation of G. The overall normalization factor is dictated by the form of the parametrization of the matrix U in terms of the Goldstone boson fields ϕ^a which we write for the purposes of this subsection[3] as

$$U = \exp\left(\sqrt{2}\frac{\mathrm{i}}{F}\phi\right) \tag{1.38}$$

where $\phi = \phi^a t^a$ and t^a, $a = 1, \ldots, \dim G$ are generators of G satisfying

$$\langle t^a t^b \rangle = \delta^{ab} \tag{1.39}$$

$$[t^a, t^b] = \mathrm{i}\sqrt{2} f^{abc} t^c. \tag{1.40}$$

Here f^{abc} are totally antisymmetric structure constants of the group G. According to (4.2), the fields ϕ^a transform linearly under the little group G_V as the vector in the adjoint representation of G while the general chiral transformations of ϕ^a are nonlinear.

The Lagrangian $\mathcal{L}^{(2)}$ can be rewritten in terms of the Goldstone boson fields as follows. We have

$$U^{-1}\partial_\mu U = -\frac{\exp\left(-\sqrt{2}\frac{\mathrm{i}}{F}\mathrm{Ad}(\phi)\right) - 1}{\mathrm{Ad}(\phi)}\partial_\mu\phi = -\frac{1}{\sqrt{2}} t \cdot \frac{\exp\left(-\frac{2\mathrm{i}}{F}D_\phi\right) - 1}{D_\phi} \cdot \partial\phi \tag{1.41}$$

where

$$\mathrm{Ad}(\phi)\partial_\mu\phi = [\phi, \partial_\mu\phi] = \sqrt{2} t^a D^{ab}_\phi \partial_\mu \phi^b \equiv \sqrt{2} t \cdot D_\phi \cdot \partial\phi, \tag{1.42}$$

the matrix D^{ab}_ϕ is given as

$$D^{ab}_\phi = -\mathrm{i} f^{cab}\phi^c \tag{1.43}$$

and the dot means contraction of the indices in the adjoint representation. Inserting this in (4.3) we get finally

$$\mathcal{L}^{(2)} = \frac{F^2}{4}\partial\phi^T \cdot \frac{1 - \cos\left(\frac{2}{F}D_\phi\right)}{D^2_\phi} \cdot \partial\phi = -\partial\phi^T \cdot \left(\sum_{n=1}^{\infty} \frac{(-1)^n}{(2n)!}\left(\frac{2}{F}\right)^{2n-2} D^{2n-2}_\phi\right) \cdot \partial\phi. \tag{1.44}$$

Note that, the only group factors which enter the interaction vertices are the structure constants f^{abc}. In any tree Feynman diagram each f^{abc} is contracted either with another structure constant within the same vertex or via propagator factor δ^{ab} with some structure constant entering next vertex. Therefore, using the standard argumentation for a general tree graph [105], i.e. expressing any f^{abc} as a trace $f^{abc} = -\langle \mathrm{i}[t^a, t^b]t^c\rangle/\sqrt{2}$ and then successively using the relations like $f^{cde}t^c = -\mathrm{i}[t^d, t^e]/\sqrt{2}$ in order to replace the contracted structure constants with the commutators of the generators inside the single trace, we can prove that any tree level on-shell amplitude has a simple group structure, namely

$$\mathcal{M}^{a_1 a_2 \ldots a_n}(p_1, p_2, \ldots, p_n) = \sum_{\sigma \in S_n/Z_n} \langle t^{a_{\sigma(1)}} t^{a_{\sigma(2)}} \ldots t^{a_{\sigma(n)}}\rangle \mathcal{M}_\sigma(p_1, \ldots, p_n). \tag{1.45}$$

Here all the momenta treated as incoming and the sum is taken over the permutation of the n indices $1, 2, \ldots, n$ modulo cyclic permutations.

[3] In what follows we will use also more general parametrization of U.

1.4.2 Semi-on-shell amplitudes and Berends-Giele relations

The semi-on-shell amplitudes $J_n^{a_1 a_2 \dots a_n}(p_1, p_2, \dots, p_n)$ (or *currents* in the terminology of the original paper [131], where they were introduced for QCD and more generally for the $SU(N)$ Yang-Mills theory) can be defined in our case as the matrix elements of the Goldstone boson field $\phi^a(0)$ between vacuum and the n Goldstone boson states $|\pi^{a_1}(p_1) \dots \pi^{a_n}(p_n)\rangle$

$$J_n^{a,a_1 a_2 \dots a_n}(p_1, p_2, \dots, p_n) = \langle 0|\phi^a(0)|\pi^{a_1}(p_1) \dots \pi^{a_n}(p_n)\rangle. \tag{1.46}$$

Here the momentum p_{n+1} attached to $\phi^a(0)$

$$p_{n+1} = -\sum_{j=1}^{n} p_j. \tag{1.47}$$

is off-shell. Note that $J_n^{a,a_1 a_2 \dots a_n}(p_1, p_2, \dots, p_n)$ has a pole for $p_{n+1}^2 = 0$.

In complete analogy with the on-shell amplitudes, at the tree level the right hand side of (4.52) can be expressed in terms of the flavor-stripped semi-on-shell amplitudes $J_n(p_1, p_2, \dots, p_n)$ in the form

$$\langle 0|\phi^a(0)|\pi^{a_1}(p_1) \dots \pi^{a_n}(p_n)\rangle|_{\text{tree}} = \sum_{\sigma \in S_n} \text{Tr}(t^a t^{a_{\sigma(1)}} \dots t^{a_{\sigma(n)}}) J_n(p_{\sigma(1)}, p_{\sigma(2)}, \dots, p_{\sigma(n)}). \tag{1.48}$$

Let us note that, at higher orders in the loop expansion the group structure contains also multiple trace terms. We normalize the one particle states according to

$$J_1(p) = 1. \tag{1.49}$$

In this section the above semi-on-shell flavor-stripped amplitudes $J_n(p_1, p_2, \dots, p_n)$ will be the main subject of our interest. The on-shell stripped amplitudes $\mathcal{M}(p_1, p_2, \dots, p_{n+1})$ can be extracted from them by means of the Lehmann-Symanzik-Zimmermann (LSZ) formulas

$$\mathcal{M}(p_1, p_2, \dots, p_{n+1}) = -\lim_{p_{n+1}^2 \to 0} p_{n+1}^2 J_n(p_1, p_2, \dots, p_n). \tag{1.50}$$

The main advantage of the semi-on-shell amplitudes $J_n(p_1, p_2, \dots, p_n)$ (in what follows we also use short-hand notation $J(1, 2, \dots, n)$) is that they allow to abandon the Feynman diagram approach using appropriate recursive relation. The latter has been first formulated by Berends and Giele in the context of QCD [131] and proved to be very efficient for the calculation of the tree-level multi-gluon amplitudes. For the $U(N)$ nonlinear sigma model the generalized recurrent relations of Berends-Giele type can be written in the form (see Fig.4.3)

$$J(1, 2, \dots, n) = \frac{\mathrm{i}}{p_{1,n}^2} \sum_{m=2}^{n} \sum_{\{j_k\}} \mathrm{i} V_{m+1}(p_{1,j_1}, p_{j_1+1,j_2}, \dots p_{j_{m-1}+1,n}, -p_{1,n}) \prod_{k=1}^{m} J(j_{k-1}+1, \dots, j_k) \tag{1.51}$$

where the sum is over all splittings of the ordered set $\{1, 2, \dots, n\}$ into m non-empty ordered subsets $\{j_{k-1} + 1, j_{k-1} + 2, \dots, j_k\}$, (here $j_0 = 0$ and $j_m = n$),

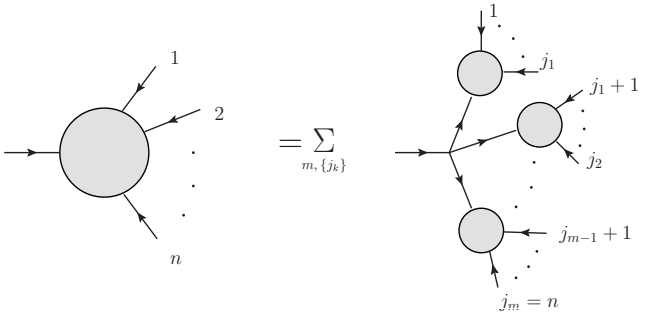

Figure 1.2: Graphical representation of the Berends-Giele recursive relations

V_{m+1} is the flavor-stripped Feynman rule for vertices with $m+1$ external legs and $p_{i,k} = \sum_{j=i}^{k} p_j$ as above.

Using Cayley parametrization we show in the thesis that semi-on-shell currents have interesting behavior under the scaling of external momenta, $t \to 0$

$$J_{2n+1}(tp_1, p_2, tp_3, p_4, \ldots, p_{2r}, tp_{2r+1}, p_{2r+2}, \ldots, p_{2n}, tp_{2n+1}) = O(t^2) \tag{1.52}$$

and

$$\lim_{t\to 0} J_{2n+1}(p_1, tp_2, p_3, tp_4, \ldots, tp_{2r}, p_{2r+1}, tp_{2r+2}, \ldots, tp_{2n}, p_{2n+1}) = \frac{1}{(2F^2)^n}. \tag{1.53}$$

This will allow us to construct recursion relations for the on-shell amplitudes.

1.4.3 BCFW-like recursion relations

The standard BCFW-like deformation [111,112] of the external momenta p_i yields deformed amplitudes which behave as a non-negative power of z for $z \to \infty$. As a result, for the reconstruction of the amplitude from its pole structure we need to use the general reconstruction formula (4.49) for which additional information on the on-shell amplitude (its values at several points) is necessary. However, such an information is not at our disposal. We solve this problems by the following trick: we relax some demands placed on the usual BCFW-like deformation and allow more general ones for which either the reconstruction formula without subtractions can be applied or additional information on the deformed amplitudes is accessible. The momentum conservation cannot be evidently avoided, what remains is the on-shell condition of all the external momenta. It seems therefore to be natural to relax this constraint and instead of the on-shell amplitudes $\mathcal{M}_{2n+2}$ to use the semi-on-shell amplitudes J_{2n+1}, or the cut semi-on-shell amplitudes M_{2n+1} defined as

$$M_{2n+1}(p_1, \ldots, p_{2n+1}) = p_{1,2n+1}^2 J_{2n+1}(p_1, \ldots, p_{2n+1}). \tag{1.54}$$

Motivated by the results of the previous section let us assume the following deformation of the semi-on-shell amplitude M_{2n+1} in the Cayley parametrization

$$M_{2n+1}(z) \equiv M_{2n+1}(p_1, zp_2, p_3, zp_4, \ldots, zp_{2r}, p_{2r+1}, zp_{2r+2}, \ldots, zp_{2n}, p_{2n+1}) \tag{1.55}$$

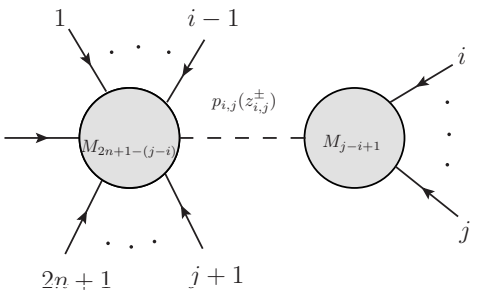

Figure 1.3: Graphical representation of the right hand side of the relation (4.95).

i.e. all even momenta are scaled by the complex parameter z and the odd momenta are not deformed

$$p_{2k}(z) = zp_{2k}, \quad p_{2k+1}(z) = p_{2k+1} \tag{1.56}$$

Note that in contrast to the standard BCFW shift this deformation is possible for general number of space-time dimensions d. The physical amplitude corresponds to $z = 1$. For $n = 1$ we get explicitly

$$M_3(z) = \frac{1}{F^2}(p_1 \cdot p_3) \tag{1.57}$$

For general n let us denote the sums of all odd (even) momenta as

$$p_{\text{-}} = \sum_{k=0}^{n} p_{2k+1}, \quad p_{+} = \sum_{k=1}^{n} p_{2k} \ . \tag{1.58}$$

Then in general case the function $M_{2n+1}(z)$ has the following important properties:

1. With generic fixed p_i it is a meromorphic function of z with simple poles.

2. The asymptotics of $M_{2n+1}(z)$ can be deduced form the known properties of J_{2n+1}, namely for $n > 1$ we get as a consequence of (4.79)

$$M_{2n+1}(z) = (p_+ z + p_-)^2 J_{2n+1}(p_1, zp_2, \ldots, zp_{2n}, p_{2n+1}) = O(z^0). \tag{1.59}$$

3. For $n \geq 1$ we have according to known scaling property (4.68) of J_{2n+1}

$$\lim_{z\to 0} M_{2n+1}(z) = \frac{1}{(2F^2)^n} p_-^2 \tag{1.60}$$

The first two properties allows us to write for $M_{2n+1}(z)$ the reconstruction formula with one subtraction, i.e. the relation (4.49) with $k = 0$. The third property is the key one for the complete reconstruction and determines both the "subtraction point" $a_1 = 0$ and the "subtraction constant" $M_{2n+1}(a_1) = p_-^2/(2F^2)^n$.

As a final result we get then using (4.95), (4.98), (4.91), (4.93) and (4.94)

$$M_{2n+1}(p_1,\ldots,p_{2n+1}) = \frac{1}{(2F^2)^n}p_-^2 + \sum_P M_L^{(P)}(z_P)\frac{R_P}{p_P^2}M_R^{(P)}(z_P). \tag{1.61}$$

Note that there is an extra function R_P in contrast to the standard BCFW formula (4.44), namely

$$R_P = \begin{cases} z_P^{-2} & \text{for} \quad z_P = z_{2j,2j+2} \\ z_P^{-1} & \text{for} \quad z_P = z_{2j-1,2j+1} \\ \frac{1}{z_{i,j}^{\pm}-z_{i,j}^{\mp}}\frac{1-z_{i,j}^{\mp}}{z_{i,j}^{\pm}} & \text{for} \quad z_P = z_{i,j}^{\pm} \end{cases} \tag{1.62}$$

The on-shell amplitude is then

$$\mathcal{M}_{2n}(1,2,\ldots,2n-1;2n) = -\lim_{p_{1,2n-1}^2\to 0} M_{2n-1}(1). \tag{1.63}$$

2. High energy constraints in the octet $SS - PP$ correlator

2.1 Introduction

The effective field theory (EFT) approach is a very powerful tool for the investigation of Quantum Chromodynamics (QCD) at long distances. Chiral Perturbation theory (χPT) [1–3] is the EFT for the description of the chiral (pseudo) Goldstones in the low energy domain $p^2 \ll \Lambda_H^2 \sim 1$ GeV^2, with Λ_H typically the scale of the lowest resonance masses. The calculation of the QCD matrix elements is then organized at long distances in growing powers of the external momenta and light quark masses. Recent progress has allowed to carry χPT up to $\mathcal{O}(p^6)$, i.e., up to the two-loop level [4–7].

In the intermediate resonance region, $\Lambda_H \lesssim E \lesssim 2$ GeV, χPT stops being valid and one must explicitly include the resonance fields in the Lagrangian description. Unfortunately, this is not a straightforward process because there is no natural expansion parameter in this region as several relevant mass scales appear in this range (resonance masses, momenta, widths, the characteristic χPT loop scale $\Lambda_\chi \sim 4\pi F$...). Resonance Chiral Theory (RχT) describes the interaction of resonance and pseudo-Goldstones within a general chiral invariant framework [8, 9]. Alternatively to the chiral counting, it uses the $1/N_C$ expansion of QCD in the limit of large number of colours [10] as a guideline to organize the perturbative expansion. At leading order (LO), just tree-level diagrams contribute while loop diagrams yield higher order effects. Integrating out the heavy resonance states leaves at low energies the corresponding chiral invariant effective theory, χPT. Many works have investigated various aspects of RχT: equivalence of formalisms [9,11–13]; Green functions [14–20]; applications to phenomenology [14, 21–27]; determination of chiral low-energy constants (LECs) at NLO in $1/N_C$ [21, 29–32]; determination of the one-loop ultraviolet divergence structures in the generating functional [33]; implications about the renormalizability [34, 35]; possible issues with extra degrees of freedom in the renormalized propagator [36, 37]; renormalization group studies [38].

The infinite tower of mesons contained in large–N_C QCD is often truncated to the lowest states in each channel, usually named as single resonance approximation (SRA). This approximation has led to successful predictions of $\mathcal{O}(p^4)$ and $\mathcal{O}(p^6)$ low-energy constants (LECs) [8, 9, 21, 28, 39]. However, the study of Regge models with an infinite number of mesons has shown that if one keeps just the lightest states with exactly the same couplings and masses of the full model then one finds problems in the short-distance matching and wrong values are obtained for the LECs [40]. Thus, in a high-energy matching with the operator product expansion (OPE) [41] the parameters of the truncated theory will be shifted in order to accommodate the right short-distance dependence. Chiral symmetry ensures the proper low-momentum structure of the RχT amplitudes around $p^2 = 0$ but their high energy behaviour is not fixed by symmetry alone. In that sense, the matched amplitude can be understood with the help of Padé approximants as an rational interpolator between the deep Euclidean $p^2 = -\infty$ and $p^2 = 0$ [43,44].

The Weinberg sum-rules (WSR) [42] yield the most convenient parameters for the interpolation rather than the accurate determinations of the resonance couplings. Furthermore, the RχT couplings for the lightest mesons are expected to be in better agreement, whereas the parameters from the highest excitations may lie far from their right values [43].

The connection of the RχT amplitudes with the operator product expansion (OPE) at high energies seems *a priori* a useful procedure to include extra information from QCD in the resonance theory. It allows to fix combinations of couplings (e.g., through WSR), decreasing the number of unknown parameters in the analysis. However, large–N_C QCD has an infinite number of hadrons and in order to reproduce the full large–N_C theory one must consider the tree-level exchanges of heavier and heavier resonances. In the hadronical ansatz approach, one adds more and more poles to the rational approximant [43,44]. Equivalently, this can be realized within the quantum field theory framework as a generating functional with a lagrangian including interaction operators $J - R_j$ that couple the external current source J and heavier and heavier resonances R_j (e.g. of the form $c_{m,j}\langle\, S_j \chi_+ \,\rangle$ for the SS correlator).

The extension of RχT beyond the tree level approximation still needs to be worked out in detail. Although some theoretical issues on the renormalizability of RχT still need further clarification [34, 35, 45], several chiral LECs have been already computed up to NLO in $1/N_C$ through quantum field theory (QFT) one-loop calculations [29, 30] and dispersion relations [31, 32]. In this article we will focus our attention on the chiral octet $SS - PP$ correlator (for instance, with $I = 1$), which in the chiral limit is determined at low energies by the $\mathcal{O}(p^4)$ and $\mathcal{O}(p^6)$ LECs, respectively, by L_8 [3] and C_{38} [4]. The correlator is computed up to next-to-leading order in $1/N_C$ (NLO) and the chiral limit will be assumed all along the article.

At the one-loop level –NLO in $1/N_C$–, one needs also to devise a procedure to reach the infinite resonance limit of large–N_C QCD. In the case of two–point Green-functions, the imaginary part of the one-loop diagrams is given through the optical theorem by the square of two-meson form-factors computed at tree-level. Thus, based on a dispersive approach, one may add the contribution to the spectral function from higher and higher two-meson absorptive cuts by providing the corresponding form-factors [31, 32]. This would be, in some sense, the natural extension of the minimal hadronical ansatz [44] to the one-loop situation. In a previous computation of the octet $SS - PP$ correlator up to NLO in $1/N_C$, the intermediate two-meson channels were analyzed individually [31]. The corresponding tree-level form-factors were made to vanish appropriately at high energies [32, 46]. This allowed to recover the correlator from its spectral function through an unsubtracted dispersion relation. However, in general, it is not always possible to fulfill the high-energy constraints for all the form-factors at once [1]. Only the two-meson absorptive cuts with at most one resonance ($\pi\pi$ and $R\pi$) were considered in Ref. [31], as the RR' channels have their thresh-

[1] In the case of the scalar and pseudo-scalar form-factors, it is still possible to impose the right high-energy behaviour to all the form-factors if one considers operators with two and three resonance fields $\mathcal{L}_{RR'}$ and $\mathcal{L}_{RR'R''}$ [32, 46]. Nonetheless, there is no consistent set of constraints for all the vector and axial-vector form-factors if only a finite number of resonances is considered [32, 46]. A similar kind of inconsistences was found in the study of three–point Green-functions at large N_C [19].

olds at $(M_R + M_{R'}) \sim 2$ GeV and are suppressed at low energies. Likewise, the short-distance constraints from $VV - AA$ Weinberg sum-rules and the $\pi\pi$ vector and the scalar form-factor were used there in order to fix some of the couplings appearing in the analysis.

In the quantum field theory approach proposed in this work, one has a mesonic lagrangian which at the classical level generates the large–N_C amplitudes and whose quadratic fluctuations around the classical field configuration provide the one-loop corrections [33]. The complete QCD generating functional is approached as one adds more and more hadronic operators to the action. Eventually, one should add the infinite number of possible terms of the given $1/N_C$ order under consideration. For instance, the $S\pi\pi$ interaction (provided by $c_d \langle\, S u_\mu u^\mu \,\rangle$ [8]) is of the same order as in $1/N_C$ as the $SP\pi$ vertex (given by the $\lambda_1^{SP} \langle\, \{\nabla^\mu S, P\} u_\mu \,\rangle$ operator [15, 32, 46]). Notice that one never has a complete description with a finite number of operators. The basic lagrangian $\mathcal{L}_G + \mathcal{L}_R$ with at most one resonance field in each term [8] provides an incomplete description of the $R\pi$ channels, as the possible diagrams with R' resonances exchanged in the s–channel are missing [31, 32]. This requires the incorporation of operators $\mathcal{L}_{RR'}$ with two resonance fields [15, 32, 46]. In the same way, the RR' absorptive cuts are now badly described without the $\mathcal{L}_{RR'R''}$ terms with three resonance fields.

The chiral structure of the lagrangian ensures the right structure at long distances. On the other hand, we will impose that the correlator follows the short-distance behaviour prescribed by the OPE. The one-loop RχT amplitude will be used as an improved interpolator between low and high energies. The resonance couplings become then interpolating parameters that must approach their actual values in the full QCD as more and more operators are added to the RχT action. On the contrary to what was done in former works [31,32], the short-distance matching will be carried out in the present article for the total correlator and spectral function [47], rather than for individual channels. Likewise, we will not use the short-distance constraints from other amplitudes to fix the couplings in the one-loop correlator. We will work within the SRA, including just the chiral Goldstones and the lightest multiplets of scalar, pseudo-scalar, vector and axial-vector resonances. In a first step, the $SS - PP$ correlator will be computed at NLO in $1/N_C$ with the simplest RχT lagrangian, with operators with at most one resonance field (G_V, c_m, d_m...) [8]. This provides the proper structure for the intermediate tree-level exchanges (π, S, P one-particle channels) and the two-Goldstone cut $\pi\pi$. However, this simple lagrangian fails to describe the $R\pi$ and RR' channels as the lagrangian [8] makes their form-factors behave like a constant or like a growing power of the momentum at high energies [30–32, 46, 48]. This will be partly cured by the consideration of $\lambda^{RR'}$ operators with two resonance fields [15, 32, 46, 48], which now allow an appropriate description of the $R\pi$ channels, though the RR' ones still behave badly. Although these cuts with two resonances were neglected in the dispersive approach [31], removing part of the one-loop diagrams is not theoretically well defined and may lead to inconsistences in the renormalization of the QFT. Furthermore, it is not trivial that the effect of the RR' cuts in the short-distance matching is fully negligible. Hence, all the possible diagrams contributing to the correlator up to NLO will be kept in our study.

The amplitude is first computed within the usual subtraction scheme of χPT [2]

(denoted for simplicity as $\widetilde{MS}$ all along the article). However, though equivalent at low energies, some appropriate schemes will be found more convenient: pole masses and other schemes that minimize the uncertainties derived from the short-distance constraints. This will help us to determine the $\mathcal{O}(p^4)$ and $\mathcal{O}(p^6)$ LECs, respectively $L_8(\mu)$ and $C_{38}(\mu)$. The high-energy constraints and their meaning will be discussed and the convergence to full large–N_C QCD will be tested as more and more hadronic operators are added to the RχT action. This work is thought as a complementary and an alternative approach to the dispersive analysis in Ref. [31].

The article is organized as follows. Resonance chiral theory is introduced in detail in Sec. 2.2. The octet $SS-PP$ correlator is defined in Sec. 2.3 and its one-loop RχT computation is provided in Sec. 2.4. The high-energy constraints and low energy expansions are respectively given in Secs. 2.5 and 2.6. The contributions from operators $\mathcal{L}_{RR'}$ with two resonance fields have been singled out in Sec. 2.7 to ease the main argumentation of the article. Finally, the phenomenological analysis is given in Sec. 2.8 and the conclusions are provided in Sec. 2.9. Some technical results are relegated to the Appendices.

2.2 Resonance chiral theory lagrangian

Within the large–N_C approach the mesons will be classified within $U(3)$ multiplets. The chiral Goldstone bosons are introduced by means of the basic building block,

$$u(\phi) = \exp\left(i\frac{\phi}{\sqrt{2}F}\right) \tag{2.1}$$

where $\phi = \frac{1}{\sqrt{2}}\lambda^a\phi^a$ and

$$\phi(x) \;=\; \left(\begin{array}{ccc} \frac{1}{\sqrt{2}}\pi^0+\frac{1}{\sqrt{6}}\eta_8+\frac{1}{\sqrt{3}}\eta_1 & \pi^+ & K^+ \\ \pi^- & -\frac{1}{\sqrt{2}}\pi^0+\frac{1}{\sqrt{6}}\eta_8+\frac{1}{\sqrt{3}}\eta_1 & K^0 \\ K^- & \overline{K}^0 & -\frac{2}{\sqrt{6}}\eta_8+\frac{1}{\sqrt{3}}\eta_1 \end{array}\right). \tag{2.2}$$

This forms the basic covariant tensors,

$$\begin{aligned} u_\mu &= i\left\{u^\dagger(\partial_\mu - ir_\mu)u \,-\, u\,(\partial_\mu - i\ell_\mu)u^\dagger\right\}, \\ \chi_\pm &= u^\dagger\,\chi\,u^\dagger \,\pm\, u\,\chi^\dagger\,u\,, \\ f_\pm^{\mu\nu} &= u\,F_L^{\mu\nu}\,u^\dagger \,\pm\, u^\dagger\,F_R^{\mu\nu}\,u\,, \end{aligned} \tag{2.3}$$

with $\chi = 2B_0(s+ip)$ containing the scalar and pseudo-scalar external sources, s and p respectively, the right and left sources r^μ and ℓ^μ providing the vector and axial-vector external sources, $v^\mu = \frac{1}{2}(r^\mu+\ell^\mu)$ and $a^\mu = \frac{1}{2}(r^\mu-\ell^\mu)$ respectively, and $F_{L,R}^{\mu\nu}$ the corresponding left and right field-strength tensors.

The Goldstone bosons are parametrized by the elements $u(\phi)$ of the coset space $U(3)_L\times U(3)_R/U(3)_V$, transforming as

$$u(\phi)\mapsto V_R u(\phi)h(g,\phi)^{-1} = h(g,\phi)u(\phi)V_R \tag{2.4}$$

under a general chiral rotation $g=(V_L,V_R)\subset G$ in terms of the $U(3)_V$ compensator field $h(g,\phi)$. This makes the tensors $X = u^\mu,\chi_\pm,f_\pm^{\mu\nu}$ to transform

covariantly in the form,

$$X \;\mapsto\; h(g,\phi)\, X\, h(g,\phi)^{-1}\,. \tag{2.5}$$

2.2.1 Leading order lagrangian

For the classification of the vertices entering in the tree-level and one-loop amplitudes it will be useful to organize the operators of the RχT lagrangian according to the number of resonance fields:

$$\mathcal{L} \;=\; \mathcal{L}_G \;+\; \mathcal{L}_R \;+\; \mathcal{L}_{RR'} \;+\; \ldots \tag{2.6}$$

where $\mathcal{L}_G$ only contains Goldstone bosons and external sources, $\mathcal{L}_R$ also includes one resonance, etc. Although in principle one should consider all the terms compatible with symmetry, most of the large–N_C phenomenological calculations consider operators with the minimal number of derivatives [39]. This is usually justified through the argument that higher derivative operators tend to violate the asymptotic high energy QCD behaviour [9,39]. Likewise, its has been proven in several cases that higher derivative resonance operators can be removed from the hadronic action through meson field redefinitions in the generating functional [30,33–35,46,48]. In the present article, the leading lagrangian will only contain operators at most $\mathcal{O}(p^2)$, with the external sources counted as $v^\mu, a^\mu \sim \mathcal{O}(p)$ and $\chi \sim \mathcal{O}(p^2)$ [46,47].

The Lagrangian with only Goldstones has the same form as in χPT but the coupling constants are different. In χPT we have the leading order Lagrangian

$$\mathcal{L}^{(2)}_{\chi\mathrm{PT}} = \frac{F^2}{4}\langle u_\mu u^\mu + \chi_+\rangle\,. \tag{2.7}$$

In RχT beyond leading order the constants standing in front of the operators $\langle\, u^\mu u_\mu \,\rangle$ and $\langle\, \chi_+ \,\rangle$ may not be the same as in χPT. Therefore, generally we can write

$$\mathcal{L}_G = \frac{\widetilde{F}^2}{4}\langle u^\mu u_\mu\rangle + \frac{\hat{F}^2}{4}\langle\chi_+\rangle \tag{2.8}$$

where we explicitly distinguish between $\widetilde{F}$ and $\hat{F}$. These can be split in the way,

$$\widetilde{F} = F + \delta\widetilde{F}, \qquad \hat{F} = F + \delta\hat{F} \tag{2.9}$$

where at large N_C one has the matching condition $\widetilde{F} = \hat{F} = F$ and, hence, $\delta\widetilde{F}$ and $\delta\hat{F}$ are NLO in $1/N_C$. On the contrary to what happens in χPT, where the parameters (F and B_0) which characterize the terms $\langle\, u^\mu u_\mu \,\rangle$ and $\langle\, \chi_+ \,\rangle$ do not become renormalized, in RχT the couplings of these two operators are needed to make the physical amplitude finite. For simplicity, we choose to keep the definitions of the chiral tensors unchanged and to renormalize instead $\widetilde{F}$ and $\hat{F}$, as it was done in Refs. [33,46] with the notation $\alpha_1 = \widetilde{F}^2/4$ and $\alpha_2 = \hat{F}^2/4$.

The Goldstone bosons couple to massive $U(3)$ multiplets of the type $V(1^{--})$, $A(1^{++})$, $S(0^{++})$ and $P(0^{-+})$. The vector multiplet, for instance, is given by

$$V_{\mu\nu} \;=\; \left(\begin{array}{ccc} \frac{1}{\sqrt{2}}\rho^0 + \frac{1}{\sqrt{6}}\omega_8 + \frac{1}{\sqrt{3}}\omega_1 & \rho^+ & K^{*+} \\ \rho^- & -\frac{1}{\sqrt{2}}\rho^0 + \frac{1}{\sqrt{6}}\omega_8 + \frac{1}{\sqrt{3}}\omega_1 & K^{*0} \\ K^{*-} & \overline{K}^{*0} & -\frac{2}{\sqrt{6}}\omega_8 + \frac{1}{\sqrt{3}}\omega_1 \end{array}\right)_{\mu\nu}, \tag{2.10}$$

where we use the antisymmetric tensor formalism for spin–1 fields to describe the vector and axial-vector resonances [8, 9, 13].

The resonance fields R are chosen to transform covariantly under the chiral group as in Eq. (2.5) [8]. The free-field kinetic term is given by the operators

$$\mathcal{L}_{RR}^{\rm Kin} \;=\; -\frac{1}{2}\langle \nabla^\mu R_{\mu\nu} \nabla_\alpha R^{\alpha\nu}\rangle + \frac{1}{4} M_R^2 \langle R_{\mu\nu} R^{\mu\nu}\rangle + \frac{1}{2}\langle \nabla^\alpha R' \nabla_\alpha R'\rangle - \frac{1}{2} M_{R'}^2 \langle R' R'\rangle \, . \tag{2.11}$$

where $R = V, A$ are vector and axial vector resonances and $R' = S, P$ are scalar and pseudoscalar resonances.

The interaction terms which are linear in the resonance fields can be obtained from the seminal work [8]:

$$\begin{aligned} \mathcal{L}_R \;&=\; c_d \langle S u^\mu u_\mu\rangle + c_m \langle S \chi_+\rangle + i d_m \langle P \chi_-\rangle \\ &\quad + \frac{F_V}{2\sqrt{2}}\langle V_{\mu\nu} f_+^{\mu\nu}\rangle + \frac{iG_V}{2\sqrt{2}}\langle V_{\mu\nu}[u^\mu, u^\nu]\rangle + \frac{F_A}{2\sqrt{2}}\langle A_{\mu\nu} f_-^{\mu\nu}\rangle . \end{aligned} \tag{2.12}$$

For our analysis of the $SS - PP$ correlator, the relevant bilinear terms will be [15, 46, 48]

$$\mathcal{L}_{RR'} \;=\; i\lambda_1^{PV} \langle\, [\nabla^\mu P, V_{\mu\nu}]\, u^\nu \,\rangle \;+\; \lambda_1^{SA} \langle\, \{\nabla^\mu S, A_{\mu\nu}\}\, u^\nu \,\rangle \;+\; \lambda_1^{SP} \langle\, \{\nabla^\mu S, P\}\, u_\mu \,\rangle \, . \tag{2.13}$$

Only single flavor–trace operators are considered for the construction of the large–N_C lagrangian. At tree-level, the octet $SS - PP$ correlator only gets contributions from this kind of terms, even at subleading orders in $1/N_C$. Operators with two or more traces might appear in the vertices of one loop diagrams but, since these multi-trace terms are $1/N_C$–suppressed, these contributions would go to next-to-next-to-leading order and they will be neglected in the present work.

The previous operators provide an appropriate description of the form factors with two Goldstones or one resonance and one Goldstone in the final state. We will perform our most elaborate analysis with the lagrangian $\mathcal{L}_G + \mathcal{L}_R + \mathcal{L}_{RR'}$, with at most two resonance fields. As we will see in next sections, the RχT description will progressively approach the actual QCD amplitude as more and more complicated operators are added. However, although we expect the contributions from the operators with three resonance fields to the LECs to be negligible at our level of accuracy, a further refinement is eventually possible by considering these operators $\mathcal{L}_{RR'R''}$.

2.2.2 Subleading Lagrangian

At the loop level, one needs to introduce new subleading operators in order to cancel the ultraviolet divergences, to renormalize RχT and to make the amplitudes finite. As the leading order lagrangian operators are $\mathcal{O}(p^2)$, the naive dimensional analysis tells us that at one loop one expects to find $\mathcal{O}(p^4)$ ultraviolet divergences, requiring the introduction of NLO counter-terms with a higher number of derivatives.

The new operators with just Goldstone bosons required at NLO are, for the

$SS-PP$ correlator under consideration,

$$\begin{aligned}\mathcal{L}_{GB}^{NLO} &= \frac{\widetilde{L}_8}{2}\langle\chi_-^2+\chi_+^2\rangle + i\widetilde{L}_{11}\langle\chi_-(\nabla_\mu u^\mu - \frac{i}{2}\chi_-)\rangle \\ &\quad -\widetilde{L}_{12}\langle(\nabla_\mu u^\mu - \frac{i}{2}\chi_-)^2\rangle + \frac{\widetilde{H}_2}{4}\langle\chi_+^2-\chi_-^2\rangle\,. \end{aligned} \tag{2.14}$$

Though we use the same structure of terms as in χPT, the RχT couplings $\widetilde{L}_i$ are not the same as the chiral LECs L_i. The $\widetilde{L}_i$ will contribute at low energies to $\mathcal{O}(p^4)$ chiral couplings L_i. The latter are dominantly saturated by resonances exchanges, so $\widetilde{L}_i$ are considered to be suppressed and subleading in the $1/N_C$ expansion.

In order to make the resonance propagator finite, one needs to renormalize the mass and wave functions ($M_R^{(B)\,2} = M_R^{r\,2} + \delta M_R^2$, $R^{(B)} = Z_R^{\frac{1}{2}} R^r$) and to introduce at NLO in $1/N_C$ the kinetic operator

$$\mathcal{L}_{\rm Kin}^{NLO} = \frac{X_R}{2}\langle R\nabla^4 R\rangle\,, \tag{2.15}$$

with $R = S, P$. No terms with vector or axial-vectors are needed for the present NLO analysis of the $SS-PP$ correlator.

Likewise, the renormalization of the vertex functions $s(x)\to S$ and $p(x)\to P$ at NLO in $1/N_C$ will require of the linear terms,

$$\mathcal{L}_R^{NLO} = \lambda_{18}^S\langle S\nabla^2\chi_+\rangle + i\lambda_{13}^P\langle P\nabla^2\chi_-\rangle\,. \tag{2.16}$$

At NLO in $1/N_C$, all these subleading counter-terms can only contribute through tree-level diagrams.

2.2.3 Equations of motion and redundant operators

The equations of motion (EOM) of the leading lagrangian are given by [33, 46],

$$\nabla^\mu u_\mu = \frac{i}{2}\chi_- + \frac{ic_m}{F^2}\{\chi_-, S\} - \frac{d_m}{F^2}\{\chi_+, P\} + \ldots \tag{2.17}$$

$$\nabla^2 S = -M_S^2 S + c_d u_\mu u^\mu + c_m\chi_+ + \ldots \tag{2.18}$$

$$\nabla^2 P = -M_P^2 P + id_m\chi_- + \ldots \tag{2.19}$$

where the dots stand for terms with vector or axial-vector resonances or sources, two-meson fields or with one scalar-pseudoscalar external source and one meson field.

Since most of the subleading resonance operators are proportional to the EOM, it is possible to simplify our new NLO resonance operators by means of appropriate meson field redefinitions,:

$$\mathcal{L}_{\rm Kin}^{NLO} \longrightarrow \mathcal{L}_{\rm Kin}^{NLO,\,eff} = -\lambda_{18}^S M_S^2\langle SS\rangle + c_m\lambda_{18}^S\langle\chi_+^2\rangle - i\lambda_{13}^P M_P^2\langle PP\rangle - d_m\lambda_{13}^P\langle\chi_-^2\rangle + \ldots$$

$$\begin{aligned}\mathcal{L}_R^{NLO} \longrightarrow \mathcal{L}_R^{NLO,\,eff} &= \frac{X_S M_S^4}{2}\langle SS\rangle + \frac{c_m^2 X_S}{2}\langle\chi_+^2\rangle - c_m X_S M_S^2\langle S\chi_+\rangle \\ &\quad + \frac{X_P M_P^4}{2}\langle PP\rangle - \frac{d_m^2 X_P}{2}\langle\chi_-^2\rangle - id_m X_P M_P^2\langle P\chi_-\rangle + \ldots \end{aligned} \tag{2.20}$$

where the dots stand for operators that do not contribute to the $SS-PP$ correlator at NLO. After the field redefinition the resonance operators $\mathcal{L}_{\rm Kin}^{NLO}$ and $\mathcal{L}_R^{NLO}$ disappear and the surviving terms in the RχT lagrangian carry in front the effective combinations,

$$\begin{aligned}
\widetilde{L}_8^{eff} &= \widetilde{L}_8 + \frac{1}{2}c_m^2 X_S - \frac{1}{2}d_m^2 X_P + c_m\lambda_{18}^S - d_m\lambda_{13}^P, \\
\widetilde{H}_2^{eff} &= \widetilde{H}_2 + c_m^2 X_S + d_m^2 X_P + 2c_m\lambda_{18}^S + 2d_m\lambda_{13}^P, \\
(M_S^2)^{eff} &= M_S^2 - X_S M_S^4, \\
(M_P^2)^{eff} &= M_P^2 - X_P M_P^4, \\
c_m^{eff} &= c_m - c_m X_S M_S^2 - M_S^2\lambda_{18}^S, \\
d_m^{eff} &= d_m - d_m X_P M_P^2 - M_P^2\lambda_{13}^P.
\end{aligned} \tag{2.21}$$

The $\widetilde{L}_{11}$ and $\widetilde{L}_{12}$ operators do not contribute to terms which can be relevant to our amplitude up to NLO and we will see that they are not present in the final result.

2.3 Chiral octet $SS-PP$ correlator

In the case of $SU(3)$–octet quark bilinears, the two-point Green function $SS-PP$ is defined as

$$\Pi_{S-P}^{ab}(p) \;=\; i\int d^4x e^{ip\cdot x}\langle 0|T[S^a(x)S^b(0) - P^a(x)P^b(0)]|0\rangle = \delta^{ab}\Pi(p^2)\,, \tag{2.22}$$

with $S^a = \bar{q}\frac{\lambda_a}{\sqrt{2}}q$ and $P^a = i\bar{q}\frac{\lambda_a}{\sqrt{2}}\gamma_5 q$, being λ_a the Gellmann matrices ($a = 1,\ldots 8$).

In the chiral limit, assumed all along the article, the low-energy expansion of the octet correlators is determined by χPT in the form [5],

$$\begin{aligned}
\Pi(p^2)_{\chi PT} \;=\; B_0^2\Bigg\{ & \frac{2F^2}{p^2} + \left[32L_8^r(\mu_\chi) + \frac{\Gamma_8}{\pi^2}\left(1 - \ln\frac{-p^2}{\mu_\chi^2}\right)\right] \\
& + \frac{p^2}{F^2}\left[32C_{38}^r(\mu_\chi) - \frac{\Gamma_{38}^{(L)}}{\pi^2}\left(1 - \ln\frac{-p^2}{\mu_\chi^2}\right) + \mathcal{O}(N_C^0)\right] + \mathcal{O}(p^4)\Bigg\}
\end{aligned} \tag{2.23}$$

where in $\Gamma_8 = 5/48$ [3/16] and $\Gamma_{38}^L = -5L_5/6$ [$-3L_5/2$] in $SU(3)$–χPT [$U(3)$–χPT]. Notice that in χPT the correlator is exactly independent of the renormalization scale μ_χ, being its choice completely arbitrary.

In the resonance region, one obtains at leading order in $1/N_C$,

$$\Pi(p^2)_{LO} \;=\; \frac{2B_0^2F^2}{p^2} \;+\; 16B_0^2\sum_i\left(\frac{c_{m,i}^2}{M_{S,i}^2 - p^2} \;-\; \frac{d_{m,i}^2}{M_{P,i}^2 - p^2}\right)\,, \tag{2.24}$$

where one sums over the different resonance multiplets. The subscript $_{,i}$ in $M_{R,i}$, $c_{m,i}$ and $d_{m,i}$ refers to the coupling of the i–th resonance multiplet of the corresponding kind. The requirement of the high energy OPE behaviour

$\Pi(p^2) \overset{p^2\to\infty}{\sim} 1/p^6$ produces the short-distance conditions [2] [39]

$$\sum_i (c_{m,i}^2 - d_{m,i}^2) = \frac{F^2}{8}, \qquad \sum_i c_{m,i}^2 M_{S,i}^2 - d_{m,i}^2 M_{P,i}^2 = 0\,. \tag{2.25}$$

In the single resonance approximation (SRA), it is then possible to express c_m and d_m in terms of F and resonance masses,

$$c_m^2 \;=\; \frac{F^2}{8}\,\frac{M_P^2}{M_P^2 - M_S^2} \qquad\qquad d_m^2 \;=\; \frac{F^2}{8}\,\frac{M_S^2}{M_P^2 - M_S^2}. \tag{2.26}$$

At low energies, we can match the large–N_C expression (2.24) with the χPT expression (2.23), obtaining the LO prediction for the low energy coupling constants L_8 and C_{38},

$$L_8 \;=\; \frac{c_m^2}{2M_S^2} - \frac{d_m^2}{2M_P^2} = \frac{F^2}{16}\left(\frac{1}{M_P^2} + \frac{1}{M_S^2}\right), \tag{2.27}$$

$$C_{38} \;=\; \frac{c_m^2 F^2}{2M_S^4} - \frac{d_m^2 F^2}{2M_P^4} = \frac{F^4}{16 M_P^2 M_S^2}\left(1 + \frac{M_P^2}{M_S^2} + \frac{M_S^2}{M_P^2}\right) \tag{2.28}$$

For the inputs $M_S = M_P/\sqrt{2} \simeq 1$ GeV, one obtains $L_8 \approx 0.7\cdot 10^{-3}$, $C_{38} \approx 7\cdot 10^{-6}$ for $M_S = 1\,\text{GeV}$. However, one does not know to what renormalization scale μ_χ these numerical predictions correspond. In order to pin down this μ–dependence, one must carry the calculation up to the loop level.

2.4 One-loop computation in resonance chiral theory

We follow the renormalization procedure presented in [30]. In general, we will use dimensional regularization and the $\overline{MS}-1$ subtraction scheme, usually employed in χPT calculations [2, 3]. This means we will absorb in the coupling counterterms the ultraviolet divergent piece from the loops, counter-terms,

$$\lambda_\infty(\mu) \;=\; \mu^{d-4}\left[\frac{2}{d-4} \;+\; \gamma_E \;-\; \ln 4\pi \;-\; 1\right]. \tag{2.29}$$

Still, the Goldstone propagator and the Goldstone decay amplitudes will be renormalized in the on-shell scheme, as it is done in χPT, in order to ease the low-energy matching of RχT and χPT at $\mathcal{O}(p^2)$. Everything else will be renormalized in this section in $\overline{MS} - 1$. For simplicity, we will denote this set of schemes as $\widetilde{MS}$ from now on. Afterwards, we will study alternative renormalization schemes for the RχT couplings and their relation with the $\widetilde{MS}$ parameters.

In this section, together with the general structure of the amplitudes, we will provide in this Section just the explicit results for the case when the lagrangian contains the operators $\mathcal{L}_G + \mathcal{L}_R$ with at most one resonance field, derived by Ecker *et al.* [8]. The contributions from operators $\mathcal{L}_{RR'}$ with two resonance fields are provided separately later in Sec. 2.7. For clarity, we provide the individual contributions from each absorptive cut (e.g. $\pi\pi$, $V\pi$...). The precise definitions for the corresponding Feynman integrals are given in Appendix 2.10.3.

[2] The tiny dimension four condensate $\frac{1}{B_0^2}\langle \mathcal{O}_{(4)}^{SS-PP}\rangle \simeq -12\pi\alpha_S F^4$ will be neglected in this work [39, 49].

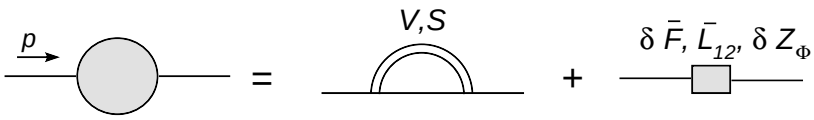

Figure 2.1: Contributions to the Goldstone boson self-energy. The single line represents the Goldstone boson while the double line represents the resonance. The type of resonance is written above it.

2.4.1 Goldstone boson renormalizations

Goldstone self-energy

The general form of the renormalized Goldstone propagator is given by

$$i\Delta_\phi^{-1} \;=\; \frac{\widetilde{F}^2\, Z_\phi}{F^2}p^2 \;-\; \frac{4\widetilde{L}_{12}p^4}{F^2} \;-\; \Sigma_\phi(p^2)\,, \tag{2.30}$$

with Z_ϕ the wave function renormalization of the bare Goldstone field, $\phi^{(B)} = Z_\phi^{\frac{1}{2}}\phi^r$. In order to make the propagator finite, one needs to perform the shifts

$$Z_\phi = 1 + \delta Z_\phi, \qquad \widetilde{F} = F + \delta\widetilde{F}, \qquad \widetilde{L}_{12} = \widetilde{L}_{12}^r + \delta\widetilde{L}_{12}\,, \tag{2.31}$$

where δZ_ϕ and $\delta\widetilde{F}$ are NLO in $1/N_C$. The NLO coupling $\widetilde{L}_{12}$ is split into a finite renormalized part $\widetilde{L}_{12}^r$ and an infinite counter-term $\delta\widetilde{L}_{12}$.

Considering the on-shell renormalization scheme for the Goldstone propagator, i.e. such that $i\Delta_\phi^{-1} = p^2 + \mathcal{O}(p^4)$, leads to the renormalization condition

$$\frac{2\delta\widetilde{F}}{F} \;+\; \delta Z_\phi \;-\; \Sigma_\phi^{'}(0) \;=\; 0\,, \tag{2.32}$$

with $\Sigma_\phi^{'}(0) = \left.\dfrac{d\Sigma_\phi}{dp^2}\right|_{p^2=0}$. The $\mathcal{O}(p^4)$ ultraviolet divergence in Σ_ϕ is absorbed into $\delta\widetilde{L}_{12}$ in the $\widetilde{MS}$ scheme. The renormalized Goldstone propagator is then provided by

$$i\Delta_\phi^{-1} = p^2 \;-\; \frac{4\widetilde{L}_{12}^r p^4}{F^2} \;-\; \Sigma_\phi^r(p^2)\,, \tag{2.33}$$

with its perturbative expansion,

$$\Delta_\phi^r \;=\; \frac{i}{p^2} + \frac{i}{p^4}\left[\frac{4\widetilde{L}_{12}^r p^4}{F^2} + \Sigma_\phi^r(p^2)\right] \;+\; \ldots \tag{2.34}$$

where the dots stand for the next-to-next-to-leading order corrections (NNLO) and $\Sigma_\phi^r(p^2) = \Sigma_\phi(p^2) - p^2\Sigma_\phi'(0) - \Sigma_\phi(p^2)|_{\lambda_\infty\mathcal{O}(p^4)}$ behaving like $\mathcal{O}(p^4)$ when $p^2 \to 0$.

If one considers just the contributions $\mathcal{L}_R$ from interactions linear in the resonance fields [8], the one loop Goldstone self-energy Σ_ϕ is given by the diagrams shown in Fig. 2.1. A priori, tadpole diagrams might appear, either with a Goldstone or a resonance running within the loop. However, they happen to be zero

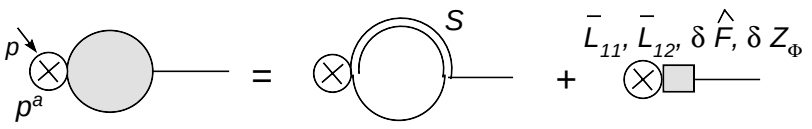

Figure 2.2: Contribution to the vertex $p\phi$. The crossed circle stands for a pseudo-scalar density insertion.

in the chiral limit. All this yields the renormalizations and the renormalized self-energy,

$$\begin{aligned}\frac{2\delta\widetilde{F}}{F} + \delta Z_\phi + \frac{1}{8F^4\pi^2}\left[\frac{9G_V^2M_V^2}{2}\left(\lambda_\infty + \ln\frac{M_V^2}{\mu^2} + \frac{1}{6}\right) - 3c_d^2M_S^2\left(\lambda_\infty + \ln\frac{M_S^2}{\mu^2} - \frac{1}{2}\right)\right] &= 0\,,\\ \delta\widetilde{L}_{12} &= -\frac{3(2c_d^2+G_V^2)}{64\pi^2F^2}\lambda_\infty\,,\end{aligned} \tag{2.35}$$

$$\begin{aligned}\Sigma_\phi^r(p^2)|_{S\phi} &= \frac{3c_d^2p^4}{8\pi^2F^4}\left[\ln\frac{M_S^2}{\mu^2} + \phi\left(\frac{p^2}{M_S^2}\right)\right],\\ \Sigma_\phi^r(p^2)|_{V\phi} &= \frac{3G_V^2p^4}{16\pi^2F^4}\left[\ln\frac{M_V^2}{\mu^2} + \phi\left(\frac{p^2}{M_V^2}\right)\right],\end{aligned} \tag{2.36}$$

with

$$\phi(x) = \left(1-\frac{1}{x}\right)^3\ln(1-x) - \frac{(x-2)\left(x-\frac{1}{2}\right)}{x^2}\,. \tag{2.37}$$

Vertex $p\phi$

The vertex function has the form

$$\Phi_{p\phi}(p^2) = \sqrt{2}\frac{Z_\phi^{\frac{1}{2}}\,\hat{F}^2\,B_0}{F} - \frac{4\sqrt{2}B_0p^2}{F}(\widetilde{L}_{11}+\widetilde{L}_{12}) + \Phi_{p\phi}(p^2)^{1\ell} \tag{2.38}$$

where $\Phi_{p\phi}(p^2)^{1\ell}$ represents the one-particle-irreducible (1PI) contribution from meson loops.

Notice that it is convenient to choose the renormalization scheme for $\delta\hat{F}$ such that the on-shell decay amplitude coincides with the pion decay constant, which by construction we denote as F. Thus, for the renormalizations

$$\hat{F} = F + \delta\hat{F}, \qquad \widetilde{L}_{11} = \widetilde{L}_{11}^r(\mu) + \delta\widetilde{L}_{11}(\mu)\,, \tag{2.39}$$

one has

$$\frac{2\delta\hat{F}}{F} + \frac{1}{2}\delta Z_\phi + \frac{1}{\sqrt{2}B_0F}\Phi_{p\phi}(0)^{1\ell} = 0\,, \tag{2.40}$$

and the counter-term $\delta\widetilde{L}_{11}(\mu)$ is chosen to cancel the $\mathcal{O}(p^2)$ divergent terms in $\Phi_{p\phi}(p^2)^{1\ell}$ in the $\widetilde{MS}$–scheme. The renormalized vertex function is then equal to

$$\Phi_{p\phi}(p^2) = \sqrt{2}B_0F\left\{1 - \frac{4\widetilde{L}_{11}^rp^2}{F^2} - \frac{4\widetilde{L}_{12}^rp^2}{F^2} + \frac{1}{\sqrt{2}B_0F}\,\Phi_{p\phi}^r(p^2)^{1\ell}\right\}, \tag{2.41}$$

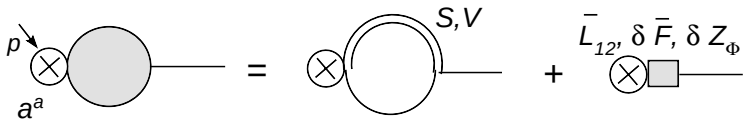

Figure 2.3: Contribution to the vertex $p\phi$. The crossed circle stands for a axial-vector current insertion.

with $\Phi^r_{p\phi}(p^2)^{1\ell}$ being $\mathcal{O}(p^2)$ when $p^2 \to 0$.

In the case with only $\mathcal{L}_R$ interactions, linear in the resonance fields [8], one has the diagrams shown in Fig. 2.2. These lead to the renormalizations and renormalized one-loop contributions,

$$\frac{2\delta\hat{F}}{F} + \frac{1}{2}\delta Z_\phi = 0, \tag{2.42}$$

$$\delta\widetilde{L}_{11}(\mu) + \delta\widetilde{L}_{12}(\mu) = -\frac{3c_d c_m}{16\pi^2 F^2}\lambda_\infty\,, \tag{2.43}$$

$$\frac{1}{\sqrt{2}B_0 F}\Phi^r_{p\phi}(p^2)^{1\ell}|_{S\phi} = \frac{3c_d c_m p^2}{4\pi^2 F^4}\left[1 - \ln\frac{M_S^2}{\mu^2} + \psi\left(\frac{p^2}{M_S^2}\right)\right], \tag{2.44}$$

with

$$\psi(x) = -\frac{1}{x} - \left(1 - \frac{1}{x}\right)^2 \ln(1-x)\,. \tag{2.45}$$

Vertex $a\phi$

Although it is not required for the correlator calculation in this article, we will compute the $a\phi$ vertex function for sake of completeness. From previous calculations we obtained two equations for three unknown objects $\delta\widetilde{F}$, $\delta\hat{F}$ and δZ_ϕ. The third equation can be found by analyzing the $a^\mu \to \phi$ vertex, which, abusing of the notation, has the form

$$\Phi_{a\phi}(p)^\mu = \Phi_{a\phi}\cdot p^\mu \tag{2.46}$$

where

$$\Phi_{a\phi} = \sqrt{2}\frac{\widetilde{F}^2\, Z_\phi^{\frac{1}{2}}}{F} - \frac{4\sqrt{2}\widetilde{L}_{12}p^2}{F} + \Phi_{a\phi}(p^2)^{1\ell}\,. \tag{2.47}$$

As it happened before with $\delta\hat{F}$, it is convenient to choose for $\delta\widetilde{F}$ (as we did here) the scheme that recovers the pion decay constant F when the decay amplitude is set on-shell ($p^2 \to 0$):

$$\frac{2\delta\widetilde{F}}{F} + \frac{1}{2}\delta Z_\phi + \frac{1}{\sqrt{2}F}\Phi_{a\phi}(0)^{1\ell} = 0\,. \tag{2.48}$$

The coupling $\delta\widetilde{L}_{12}(\mu)$ is chosen to cancel the $\mathcal{O}(p^2)$ UV divergent term in $\Phi_{a\phi}(p^2)^{1\ell}$ in the $\widetilde{MS}$ scheme.

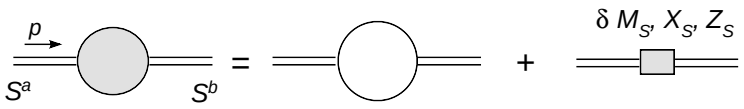

Figure 2.4: Contributions to the scalar resonance self-energy

When only $\mathcal{L}_R$ interactions are taken into account [8], the diagrams shown in Fig. 2.3 yield the renormalizations

$$\frac{2\delta\widetilde{F}}{F}+\frac{1}{2}\delta Z_\phi+\frac{1}{8\pi^2F^4}\left[\frac{9G_V^2M_V^2}{2}\left(\lambda_\infty+\ln\frac{M_V^2}{\mu^2}+\frac{1}{6}\right)-3c_d^2M_S^2\left(\lambda_\infty+\ln\frac{M_S^2}{\mu^2}-\frac{1}{2}\right)\right]\Bigg\}=0 \tag{2.49}$$

$$\delta\widetilde{L}_{12}(\mu)\;=\;-\frac{3(2c_d^2+G_V^2)}{64\pi^2F^2}\lambda_\infty\,. \tag{2.50}$$

In this case, it is possible to see explicitly that the renormalization for $\widetilde{L}_{12}$ is in an agreement with its former result from the Goldstone propagator.

Renormalization of $\hat{F}$, $\widetilde{F}$ and δZ_ϕ

Comparing the three equations for $\delta\hat{F}$, $\delta\widetilde{F}$ and δZ_ϕ, one is finally able to extract each of them separately:

$$\begin{aligned}
\delta Z_\phi &= 2\Sigma_\phi^{'}(0)^{1\ell}+\frac{\sqrt{2}}{F}\Phi_{a\phi}(0)^{1\ell}\,,\\
\frac{\delta\hat{F}}{F} &= -\Sigma_\phi^{'}(0)^{1\ell}-\frac{1}{\sqrt{2}B_0F}\Phi_{p\phi}(0)^{1\ell}-\frac{1}{\sqrt{2}F}\Phi_{a\phi}(0)^{1\ell}\,,\\
\frac{\delta\widetilde{F}}{F} &= -\frac{1}{2}\Sigma_\phi^{'}(0)^{1\ell}-\frac{1}{\sqrt{2}F}\Phi_{a\phi}(0)^{1\ell}\,.
\end{aligned} \tag{2.51}$$

Thus, in the case when only interactions $\mathcal{L}_R$, linear in the resonance fields, are considered [8], one gets $\delta Z_\phi=0$, $\delta\hat{F}=0$ and

$$\delta\widetilde{F}=-\frac{1}{16\pi^2F^4}\left[\frac{9G_V^2M_V^2}{2}\left(\lambda_\infty+\ln\frac{M_V^2}{\mu^2}+\frac{1}{6}\right)-3c_d^2M_S^2\left(\lambda_\infty+\ln\frac{M_S^2}{\mu^2}-\frac{1}{2}\right)\right]\Bigg\}. \tag{2.52}$$

This confirms the results from Ref. [33], where $\widetilde{F}$ was renormalized but $\hat{F}$ was not. On the other hand, the renormalizations of $\hat{F}$ and $\widetilde{F}$ were not considered in Ref. [30] and, consequently, a nonzero δZ_ϕ was found.

2.4.2 Scalar resonance renormalization

Scalar resonance self-energy

The renormalized propagator has the form

$$i\Delta_S^{-1}\;=\;Z_S\,(p^2\,-\,M_S^2)\,+\,X_Sp^4\,-\,\Sigma_S(p^2)\,, \tag{2.53}$$

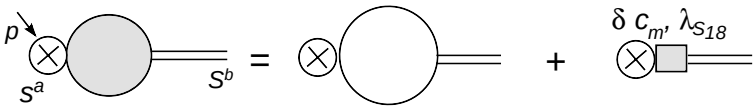

Figure 2.5: Contributions to the vertex sS. The crossed circle stands for a scalar density insertion.

where we have performed the scalar resonance wave-function renormalization $S^{(B)} = Z_S^{\frac{1}{2}} S^r$. In order to cancel the λ_∞ divergent terms of the one-loop self-energy $\Sigma_S(p^2)$, we make the shifts

$$M_S^2 = {M_S^r}^2 + \delta M_S^2, \qquad Z_S = 1 + \delta Z_S, \qquad X_S = X_S^r(\mu) + \delta X_S(\mu). \tag{2.54}$$

The renormalized propagator is then given by,

$$i\Delta_S^{-1} \;=\; p^2 \;-\; {M_S^r}^2 \;+\; X_S^r(\mu) p^4 \;-\; \Sigma_S^r(p^2)\,, \tag{2.55}$$

with its perturbative expansion,

$$\Delta_S \;=\; \frac{i}{p^2 - {M_S^r}^2} \;+\; \frac{i}{(p^2 - {M_S^r}^2)^2} \left\{ \;-\; X_S^r(\mu) p^4 \;+\; \Sigma_S^r(p^2) \right\} + \ldots \tag{2.56}$$

In the case where only the $\mathcal{L}_R$ interactions are considered, one obtains

$$\delta M_S = 0, \qquad \delta Z_S = 0, \qquad \delta X_S(\mu) = \frac{3 c_d^2}{16\pi^2 F^4} \lambda_\infty \,.$$

$$\Sigma_S^r(p^2)|_{\phi\phi} \;=\; -\,\frac{3 c_d^2 p^4}{16\pi^2 F^4} \left[1 - \ln\left(\frac{-p^2}{\mu^2} \right) \right] . \tag{2.57}$$

Vertex sS

The vertex function $s(x) \to S$ has the form

$$\Phi_{sS}(p^2) \;=\; -\,4B_0 \left\{ Z_S^{\frac{1}{2}}\, c_m \;-\; \lambda_{18}^S p^2 \;-\; \frac{1}{4B_0} \Phi_{sS}(p^2)^{1\ell} \right\} . \tag{2.58}$$

The renormalizations of the scalar wave-function $Z_S = 1 + \delta Z_S$, the LO constant $c_m = c_m^r(\mu) + \delta c_m(\mu)$ and the NLO coupling $\lambda_{18}^S = \lambda_{18}^S(\mu) + \delta\lambda_{18}^S(\mu)$ make the amplitude finite:

$$\Phi_{sS}(p^2) \;=\; -\,4B_0 \left\{ c_m^r \;-\; \lambda_{18}^S(\mu) p^2 \;-\; \frac{1}{4B_0} \Phi_{sS}^r(p^2)^{1\ell} \right\} . \tag{2.59}$$

In the case with only $\mathcal{L}_R$ interactions [8], we had $\delta Z_S = 0$. The cancelation of divergences in the $\widetilde{MS}$ scheme leads to the shift and the renormalized one-loop contributions,

$$\delta c_m = 0\,, \qquad \delta\lambda_{18}^S(\mu) = -\frac{3 c_d}{64\pi^2 F^2} \lambda_\infty \tag{2.60}$$

$$-\,\frac{1}{4B_0} \Phi_{sS}^r(p^2)^{1\ell}|_{\phi\phi} \;=\; \frac{3 c_d p^2}{64\pi^2 F^2} \left(1 - \ln\frac{-p^2}{\mu^2} \right) . \tag{2.61}$$

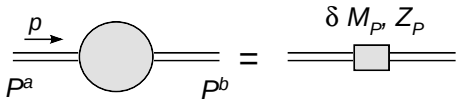

Figure 2.6: Contribution to the pseudoscalar resonance self-energy

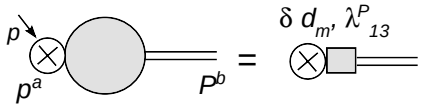

Figure 2.7: Contribution to the renormalization of vertex pP

2.4.3 Pseudo-scalar resonance renormalization

Pseudoscalar resonance self-energy

The renormalized pseudoscalar propagator has the form

$$i\Delta_P^{-1} \;=\; Z_P\,(p^2 \,-\, M_P^2) \,+\, X_P p^4 \,-\, \Sigma_P(p^2)\,, \tag{2.62}$$

with $P^{(B)} = Z_P^{\frac{1}{2}} P^r$. The cancelation of the λ_∞ UV divergent terms in the one-loop self-energy $\Sigma_P(p^2)$ needs the shifts

$$M_P^2 = {M_P^r}^2 + \delta M_P^2, \qquad Z_P = 1 + \delta Z_P, \qquad X_P = X_P^r(\mu) + \delta X_P(\mu), \tag{2.63}$$

leading to the renormalized propagator,

$$i\Delta_P^{-1} \;=\; p^2 \,-\, {M_P^r}^2 \,+\, X_P^r(\mu) p^4 \,-\, \Sigma_P^r(p^2)\,, \tag{2.64}$$

and its perturbative expansion,

$$\Delta_P \;=\; \frac{i}{p^2 - {M_P^r}^2} \,+\, \frac{i}{(p^2 - {M_P^r}^2)^2}\left\{ \,-\, X_P^r(\mu) p^4 \,+\, \Sigma_P^r(p^2) \right\} + \ldots \tag{2.65}$$

In the case where only the $\mathcal{L}_R$ interactions are considered [8], there is no one-loop diagrams contributing and, therefore, $\delta Z_P = \delta M_P^2 = \delta X_P = 0$.

Vertex pP

The vertex function $p(x) \to P$ has the form

$$\Phi_{pP}(p^2) \;=\; -\,4B_0 \left\{ Z_P^{\frac{1}{2}}\, d_m \,-\, \lambda_{13}^P p^2 \,-\, \frac{1}{4B_0}\Phi_{pP}(p^2)^{1\ell} \right\}. \tag{2.66}$$

The renormalizations of the scalar wave-function $Z_P = 1 + \delta Z_P$, the LO constant $d_m = d_m^r(\mu) + \delta d_m(\mu)$ and the NLO coupling $\lambda_{13}^P = \lambda_{13}^P(\mu) + \delta\lambda_{13}^P(\mu)$ make the amplitude finite:

$$\Phi_{pP}(p^2) \;=\; -\,4B_0 \left\{ d_m^r \,-\, \lambda_{13}^P(\mu) p^2 \,-\, \frac{1}{4B_0}\Phi_{pP}^r(p^2)^{1\ell} \right\}. \tag{2.67}$$

In the case with only $\mathcal{L}_R$ interactions [8], $\delta Z_P = 0$ and there is no loop diagram contributing to this vertex, so we have $\delta d_m = \delta\lambda_{13}^P = 0$ and the renormalized vertex function results

$$\Phi_{pP}(p^2) \;=\; -4B_0 \left\{ d_m^r \,-\, \lambda_{13}^P(\mu)\, p^2 \right\}. \tag{2.68}$$

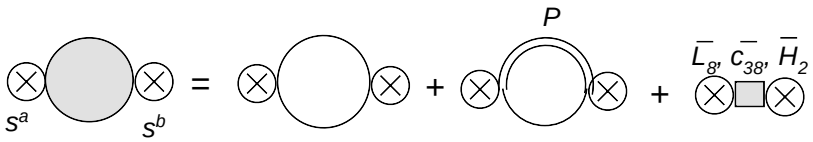

Figure 2.8: Contribution to the 1PI vertex ss

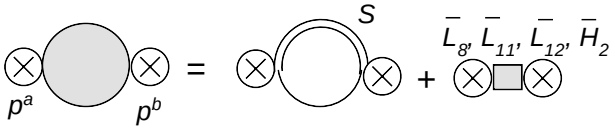

Figure 2.9: Contribution to the 1PI vertex pp

2.4.4 1PI contributions

1PI diagram ss

Now, we analyze 1PI diagrams that appear in the ss–correlator:

$$\Pi_{ss}^{\rm 1PI}(p^2) \;=\; 16B_0^2\widetilde{L}_8 \,+\, 8B_0^2\widetilde{H}_2 \,+\, \Pi_{ss}^{\rm 1PI}(p^2)^{1\ell}\,. \tag{2.69}$$

The shifts $\widetilde{L}_8 = \widetilde{L}_8^r(\mu) + \delta\widetilde{L}_8(\mu)$ and $\widetilde{H}_2 = \widetilde{H}_2^r(\mu) + \delta\widetilde{H}_2(\mu)$ render the amplitude finite by canceling the UV divergences in the $\widetilde{MS}$–scheme, which becomes

$$\Pi_{ss}^{\rm 1PI}(p^2) \;=\; 16B_0^2\widetilde{L}_8^r(\mu) \,+\, 8B_0^2\widetilde{H}_2^r(\mu) \,+\, \Pi_{ss}^{\rm 1PI,\,r}(p^2)^{1\ell}\,. \tag{2.70}$$

In the case with only interactions $\mathcal{L}_R$ linear in the resonance fields [8], the 1PI diagrams contributing to the SS–correlator are shown in Fig. 2.8. Thus, one gets for the shifts and the renormalized amplitude the expressions

$$2\delta\widetilde{L}_8(\mu) + \delta\widetilde{H}_2(\mu) = \frac{3(F^2+16d_m^2)}{128\pi^2F^2}\lambda_\infty\,, \tag{2.71}$$

$$\begin{aligned}
\Pi_{ss}^{\rm 1PI,\,r}(p^2)^{1\ell}|_{\phi\phi} &= B_0^2\,\frac{3}{16\pi^2}\left[1\,-\,\ln\frac{-p^2}{\mu^2}\right],\\
\Pi_{ss}^{\rm 1PI,\,r}(p^2)^{1\ell}|_{P\phi} &= B_0^2\,\frac{3d_m^2}{\pi^2F^2}\left[1\,-\,\ln\frac{M_P^2}{\mu^2}\,-\,\left(1-\frac{M_P^2}{p^2}\right)\ln\left(1-\frac{p^2}{M_P^2}\right)\right]
\end{aligned} \tag{2.72}$$

1PI diagram pp

Similarly, for pp–amplitude one has the structure,

$$\Pi_{pp}^{\rm 1PI}(p^2) \;=\; -\,16B_0^2\widetilde{L}_8 \,-\, 16B_0^2\widetilde{L}_{11} \,-\, 8B_0^2\widetilde{L}_{12} \,+\, 8B_0^2\widetilde{H}_2 \,+\, \Pi_{pp}^{\rm 1PI}(p^2)^{1\ell}\,. \tag{2.73}$$

The UV divergences are absorbed through the renormalization of $\widetilde{L}_8$, $\widetilde{L}_{11}$, $\widetilde{L}_{12}$ and $\widetilde{H}_{12}$, rendering the amplitude finite:

$$\Pi_{pp}^{\rm 1PI}(p^2) \;=\; -\,16B_0^2\widetilde{L}_8^r(\mu) - 16B_0^2\widetilde{L}_{11}^r(\mu) - 8B_0^2\widetilde{L}_{12}^r(\mu) + 8B_0^2\widetilde{H}_2^r(\mu) \,+\, \Pi_{pp}^{\rm 1PI,\,r}(p^2)^{1\ell}\,. \tag{2.74}$$

In the case where only the contributions from $\mathcal{L}_R$ operators are considered [8], the divergences are absorbed by the shift

$$2\delta\widetilde{L}_8(\mu) + 2\delta\widetilde{L}_{11}(\mu) + \delta\widetilde{L}_{12}(\mu) - \delta\widetilde{H}_2 = -\frac{3c_m^2}{8\pi^2 F^2}\lambda_\infty\,, \tag{2.75}$$

leaving the finite one-loop contribution,

$$\Pi_{pp}^{1\mathrm{PI,\,r}}(p^2)^{1\ell}|_{S\phi} \;=\; B_0^2\,\frac{3c_m^2}{\pi^2F^2}\,\left[1\,-\,\ln\frac{M_S^2}{\mu^2}\,-\,\left(1-\frac{p^2}{M_S^2}\right)\ln\left(1+\frac{p^2}{M_S^2}\right)\right]. \tag{2.76}$$

2.4.5 Correlator at NLO

At NLO we can write the general 1PI decomposition of the $SS-PP$ correlator in terms of renormalized correlators and vertex functions,

$$\begin{aligned}\Pi_{ss-pp}(p^2) \;&=\; i\,\Delta_S(p^2)\,\left\{\,\Phi_{sS}(p^2)\,\right\}^2 - i\,\Delta_P(p^2)\,\left\{\,\Phi_{pP}(p^2)\,\right\}^2 - i\,\Delta_\phi(p^2)\,\left\{\,\Phi_{p\phi}(p^2)\,\right\}^2 \\ &\quad + \Pi_{ss}^{1\mathrm{PI}}(p^2) - \Pi_{pp}^{1\mathrm{PI}}(p^2)\,,\end{aligned} \tag{2.77}$$

where we made use of the relation between the vertex functions for incoming and outgoing mesons, $\Phi_{sS}=\Phi_{Ss}$, $\Phi_{pP}=\Phi_{Pp}$, $\Phi_{p\phi}=\Phi_{\phi p}$.

If one now uses the previous perturbative calculation, the $SS-PP$ octet correlator takes up to NLO in $1/N_C$ the form,

$$\begin{aligned}\frac{1}{B_0^2}\,\Pi(p^2) \;&=\; \frac{1}{M_S^2-p^2}\left(16c_m^2 - 32c_m\lambda_{18}^S p^2 + \frac{16c_m^2X_Sp^4}{M_S^2-p^2}\right) \\ &\qquad -\frac{16c_m^2}{(M_S^2-p^2)^2}\Sigma_S^r(p^2)^{1\ell} - \frac{8c_m}{M_S^2-p^2}\,\frac{1}{B_0}\Phi_{sS}^r(p^2)^{1\ell} \\ &\quad -\frac{1}{M_P^2-p^2}\left(16d_m^2 - 32d_m\lambda_{13}^P p^2 + \frac{16d_m^2X_Pp^4}{M_P^2-p^2}\right) \\ &\qquad +\frac{16d_m^2}{(M_P^2-p^2)^2}\Sigma_P^r(p^2)^{1\ell} + \frac{8d_m}{M_P^2-p^2}\,\frac{1}{B_0}\Phi_{pP}^r(p^2)^{1\ell} \\ &\quad +\frac{2F^2}{p^2}\left(1-\frac{8\widetilde{L}_{11}p^2}{F^2}-\frac{4\widetilde{L}_{12}p^2}{F^2}\right) + \frac{2F^2}{p^4}\Sigma_\phi^r(p^2)^{1\ell} + \frac{2F}{p^2}\,\frac{\sqrt{2}}{B_0}\Phi_{p\phi}^r(p^2)^{1\ell} \\ &\quad +32\widetilde{L}_8 + 16\widetilde{L}_{11} + 8\widetilde{L}_{12} \;\;+\;\; \Pi_{ss-pp}^r(p^2)^{1\ell}\,.\end{aligned} \tag{2.78}$$

The couplings shown here (and from now on) are the renormalized ones even if the superscript "r" is not explicitly present. The first two lines are the contribution from the scalar exchanges. The third and fourth ones come from the pseudoscalar resonance exchanges, whereas the fifth one is produced by the Goldstone exchanges. The last line is given by the 1PI diagrams in the $SS-PP$ correlator.

Notice that the correlator results independent of $\widetilde{L}_{11}$ and $\widetilde{L}_{12}$ due to the cancelation between the Goldstone exchanges and the 1PI terms in (2.78). Likewise, it

is possible to check that the correlator only depends on the effective combinations $c_m^{\rm eff}$, $d_m^{\rm eff}$, $M_S^{\rm eff}$, $M_P^{\rm eff}$ $\widetilde{L}_8^{\rm eff}$ from Eq. (2.21):

$$\begin{aligned}\frac{1}{B_0^2}\,\Pi(p^2) &= \frac{16c_m^{\rm eff\ 2}}{M_S^{\rm eff\ 2}-p^2} - \frac{16c_m^2}{(M_S^2-p^2)^2}\Sigma_S^r(p^2)^{1\ell} - \frac{8c_m}{M_S^2-p^2}\,\frac{1}{B_0}\Phi_{sS}^r(p^2)^{1\ell} \\ &\quad - \frac{16d_m^{\rm eff\ 2}}{M_P^{\rm eff\ 2}-p^2} + \frac{16d_m^2}{(M_P^2-p^2)^2}\Sigma_P^r(p^2)^{1\ell} + \frac{8d_m}{M_P^2-p^2}\,\frac{1}{B_0}\Phi_{pP}^r(p^2)^{1\ell} \\ &\quad + \frac{2F^2}{p^2} + \frac{2F^2}{p^4}\Sigma_\phi^r(p^2)^{1\ell} + \frac{2F}{p^2}\,\frac{\sqrt{2}}{B_0}\Phi_{p\phi}^r(p^2)^{1\ell} \\ &\quad + 32\widetilde{L}_8^{\rm eff\ 2} \;+\; \Pi_{ss-pp}^r(p^2)^{1\ell}\,. \end{aligned} \tag{2.79}$$

The couplings X_S, X_P, λ_{18}^S and λ_{13}^P disappear from our NLO calculation and c_m, d_m, M_R and $\widetilde{L}_8$ are replaced everywhere by $c_m^{\rm eff}$, $d_m^{\rm eff}$, $M_R^{\rm eff}$ and $\widetilde{L}_8^{\rm eff}$. The replacement in the subleading terms leaves the expression unaltered up to the order in $1/N_C$ considered in our computation.

This elimination of the renormalized couplings X_S, X_P, λ_{18}^S and λ_{13}^P can be understood in an equivalent way by means of the EOM of the theory and the meson field redefinitions. The effective couplings that are left in front of the operators after the meson field transformations coincide exactly with the combinations that determine the correlator up to NLO.

In the subleading terms in Eq. (2.79), a priori one can use indistinct the original couplings, e.g. c_m, or the effective ones, this is, $c_m^{\rm eff}$, as the difference goes to NNLO. However, for sake of consistence, one should always consider the same renormalized coupling everywhere in the amplitude. Hence, after performing the field redefinition that removes X_S, X_P, λ_{18}^S and λ_{13}^P, all the remaining couplings appearing in $\Pi(p^2)$ are the effective ones. From now on, we will consider that the RχT action has been simplified through meson field redefinitions in the previous way and the superscript "eff" will be implicitly assumed in the couplings in order to make the notation simpler.

2.5 High energy constraints

The NLO expression for the correlator contains plenty of resonance parameters that are not fully well known. A typical procedure to improve the determination of these couplings is the use of the short-distance conditions [9].

The operator product expansion tells us that the $SS-PP$ correlator vanishes like $1/p^4$ for the large Euclidean momentum. Indeed, due to the smallness of its dimension–four condensate ($\frac{1}{B_0^2}\langle\, \mathcal{O}_4^{SS-PP}\,\rangle \simeq 12\pi\alpha_S F^4 \sim 3{\cdot}10^{-4}$ GeV^4 [49]), it is a good approximation to consider that it vanishes like $1/p^6$ when $p^2\to-\infty$ [39,49].

The RχT correlator does not follow this short-distance behaviour for arbitrary values of its couplings. This imposes severe constraints on the coefficients of the high-energy expansion of our NLO correlator,

$$\frac{1}{B_0^2}\,\Pi(p^2) \;=\; \sum_{n=0,1,2\ldots}\frac{1}{(p^2)^k}\left(\alpha_{2n}^{(p)} \,+\, \alpha_{2n}^{(\ell)}\ln\frac{-p^2}{\mu^2}\right). \tag{2.80}$$

The proper OPE short-distance behaviour is therefore recovered by demanding [47]

$$\alpha_k^{(\ell)} = \alpha_k^{(p)} = 0\,, \qquad \text{for} \quad k = 0, 2, 4\,. \tag{2.81}$$

At large N_C, there are no logarithmic terms ($\alpha_k^{(\ell)} = 0$) and for the remaining coefficients one has $\alpha_0^{(p)} = 0$ (no $\widetilde{L}_8$ or higher local couplings at large N_C) and the two Weinberg sum-rules (WSR) [39],

$$\begin{aligned} \alpha_2^{(p)} &= 2F^2 + 16d_m^2 - 16c_m^2 = 0\,, \\ \alpha_4^{(p)} &= 16d_m^2 M_P^2 - 16c_m^2 M_S^2 = 0\,. \end{aligned} \tag{2.82}$$

At NLO, in the case when the interactions only contain operators $\mathcal{L}_R$ with at most one resonance field [8], the high-energy expansion log–term coefficients result

$$\begin{aligned} \frac{8\pi^2F^2}{3}\alpha_0^{(\ell)} &= 8c_m^2 - 8d_m^2 - 4c_dc_m + 2c_d^2 + G_V^2 - \frac{8c_d^2c_m^2}{F^2} - \frac{F^2}{2}\,, \\ \frac{8\pi^2F^2}{3}\alpha_2^{(\ell)} &= 8d_m^2M_P^2 - 8c_m^2M_S^2 - \frac{16M_S^2c_d^2c_m^2}{F^2} + 20c_dc_mM_S^2 - 6c_d^2M_S^2 - 3G_V^2M_V^2\,, \\ \frac{8\pi^2F^2}{3}\alpha_4^{(\ell)} &= -\frac{24c_d^2c_m^2M_S^4}{F^2} - 4c_dc_mM_S^4 + 6c_d^2M_S^4 + 3G_V^2M_V^4\,, \end{aligned} \tag{2.83}$$

and the high-energy coefficients $\alpha_{0,2,4}^{(p)}$ are given by

$$\begin{aligned} \alpha_0^{(p)} &= -\alpha_0^{(l)} + 32\,\widetilde{L}_8\,, \\ \alpha_2^{(p)} &= 2F^2 + 16d_m^2 - 16c_m^2 + A(\mu)\,, \\ \alpha_4^{(p)} &= 16d_m^2M_P^2 - 16c_m^2M_S^2 + B(\mu)\,, \end{aligned} \tag{2.84}$$

with the NLO corrections

$$\begin{aligned} A(\mu) &= -\frac{3d_m^2M_P^2}{\pi^2F^2}\left(\ln\frac{M_P^2}{\mu^2} - 1\right) + \frac{3c_m^2M_S^2}{\pi^2F^2}\left(\ln\frac{M_S^2}{\mu^2} - 1\right) + \frac{6c_d^2c_m^2M_S^2}{\pi^2F^4} \\ &\quad - \frac{6c_dc_mM_S^2}{\pi^2F^2}\left(\ln\frac{M_S^2}{\mu^2} + \frac{1}{4}\right) + \frac{9c_d^2M_S^2}{4\pi^2F^2}\left(\ln\frac{M_S^2}{\mu^2} + \frac{1}{2}\right) + \frac{9G_V^2M_V^2}{8\pi^2F^2}\left(\ln\frac{M_V^2}{\mu^2} + \frac{1}{2}\right)\,, \\ B(\mu) &= -\frac{3d_m^2M_P^4}{2F^2\pi^2} + \frac{9c_d^2c_m^2M_S^4}{F^4\pi^2} + \frac{3c_m^2M_S^4}{2F^2\pi^2} - \frac{6c_dc_mM_S^4}{\pi^2F^2} - \frac{9c_d^2M_S^4}{4\pi^2F^2}\left(\ln\frac{M_S^2}{\mu^2} - \frac{1}{2}\right) \\ &\quad + \frac{3c_dc_mM_S^4}{\pi^2F^2}\ln\frac{M_S^2}{\mu^2} - \frac{9G_V^2M_V^4}{8\pi^2F^2}\left(\ln\frac{M_V^2}{\mu^2} - \frac{1}{2}\right)\,. \end{aligned} \tag{2.85}$$

The large–N_C WSR (2.25) gain the subleading contributions in $1/N_C$, yielding for $\alpha_2^{(p)} = \alpha_4^{(p)} = 0$ the solution [3] [31],

$$\begin{aligned} c_m^2 &= \frac{F^2}{8}\,\frac{M_P^2}{M_P^2 - M_S^2}\left(1 + \frac{A(\mu)}{2F^2} - \frac{B(\mu)}{2F^2M_P^2}\right)\,, \\ d_m^2 &= \frac{F^2}{8}\,\frac{M_S^2}{M_P^2 - M_S^2}\left(1 + \frac{A(\mu)}{2F^2} - \frac{B(\mu)}{2F^2M_S^2}\right)\,. \end{aligned} \tag{2.86}$$

[3] The notation $A(\mu) = 2F^2\delta_{NLO}^{(1)}$, $2F^2M_S^2\delta_{NLO}^{(2)} = B(\mu)$ was used in Ref. [31]

The couplings M_S, M_P, c_m and d_m may also depend on μ. Nonetheless, unless necessary, this dependence will not be explicitly shown. Also, as stated at the end of the previous section, one must keep in mind that these are the results after the meson field redefinition that removes the redundant couplings $X_S, X_P, \lambda_{18}^S, \lambda_{13}^P$, so the surviving couplings carry the superscript "eff" implicit.

The $\alpha_0^{(\ell)} = 0$ constraint implies that $\widetilde{L}_8 = 0$ also at NLO in $1/N_C$ (for any renormalization scale μ). We will see that for all the possible interactions considered in this chapter, now here and later on, there is the same constraint $\alpha_0^{(p)} = -\alpha_0^{(\ell)} + 32\widetilde{L}_8$ and, therefore, in general we find $\widetilde{L}_8 = 0$. The constants $\alpha_k^{(\ell)}$, $A(\mu)$ and $B(\mu)$ only arise at NLO or higher. Hence, when they are used for the computation of the correlator up to NLO, one can indistinctly use for their calculation either renormalized couplings or their large–N_C values, as the difference goes to NNLO.

Although these expressions will be used later in other renormalization schemes, $A(\mu)$ and $B(\mu)$ will always refer to their former definitions in the $\widetilde{MS}$ scheme, like, for instance, the results provided in Eq. (2.85).

2.5.1 Alternative renormalization schemes

During the renormalization procedure we considered the $\widetilde{MS}$–subtraction-scheme for all the resonance couplings. However, in some situations one may get large contributions from $A(\mu)$ and $B(\mu)$. The NLO prediction for c_m and d_m derived from Eq. (2.86) may then become very different from the large–N_C WSR determinations $c_m^2 = \frac{F^2}{8}\frac{M_P^2}{M_P^2 - M_S^2}$, $d_m^2 = \frac{F^2}{8}\frac{M_S^2}{M_P^2 - M_S^2}$.

A way out to minimize possible large radiative corrections to the WSR is the choice of convenient renormalization schemes for couplings (c_m and d_m) and masses (M_S and M_P). In the renormalization procedure we originally chose to cancel the λ_∞ from the one-loop diagrams, but we could have chosen to cancel the λ_∞ term plus an arbitrary subleading constant. This change makes that instead of having in the amplitudes the renormalized coupling $\lambda_{\#1}^r$ in the first scheme, one now has the renormalized coupling in the second scheme plus a constant, $\lambda_{\#2}^r + C^{\#1\to\#2}$. Thus, effectively one can account for a change from the $\widetilde{MS}$–subtraction-scheme (with renormalized couplings $\kappa = c_m, d_m, M_S^2, M_P^2$) to another (with parameters $\hat{\kappa} = \hat{c}_m, \hat{d}_m, \hat{M}_S^2, \hat{M}_P^2$) through the shifts,

$$\kappa \;=\; \hat{\kappa} \;+\; \Delta\kappa\,. \tag{2.87}$$

The difference $\Delta\kappa$ will be, of course, subleading in the $1/N_C$ counting with respect to κ and $\hat{\kappa}$. This will affect the parts of the calculation where these couplings contribute at LO in $1/N_C$. In the contributions that start at NLO (e.g. $\alpha_k^{(\ell)}$, $A(\mu)$ and $B(\mu)$), the variations due to $\Delta\kappa$ go to NNLO and they are therefore neglected. If one applies this change of scheme to Eq. (2.86), one gets for the NLO extension of the WSR,

$$\begin{aligned}
\alpha_2^{(p)} &= 2F^2 + 16\,\hat{d}_m^2 - 16\,\hat{c}_m^2 \;+\; \Big(32\,\hat{d}_m\Delta d_m - 32\,\hat{c}_m\Delta c_m \;+\; A(\mu)\Big)\,, \\
\alpha_4^{(p)} &= 16\,\hat{d}_m^2\hat{M}_P^2 - 16\,\hat{c}_m^2\hat{M}_S^2 \\
&+\; \Big(32\,\hat{M}_P^2\hat{d}_m\Delta d_m + 16\,\hat{d}_m^2\Delta M_P^2 - 32\,\hat{M}_S^2\hat{c}_m\Delta c_m - 16\,\hat{c}_m^2\Delta M_S^2 \;+\; B(\mu)\Big)\,.
\end{aligned} \tag{2.88}$$

The terms within the brackets, $(\cdots)$, would be the finite contributions from the one-loop diagrams in the new scheme.

Pole mass scheme for M_S and M_P

In addition to the $\widetilde{MS}$–scheme for the scalar and pseudo-scalar masses ($\Delta M_R^2 = 0$), we will also study the pole–mass scheme. The problem with the $\widetilde{MS}$ mass is the difficulty to give a direct physical meaning to the μ–dependent mass $M_R(\mu)$, specially when more and more operators are added to the RχT action. On the other hand, the resonance pole mass is a universal property which does not rely on any particular lagrangian realization. Thus, instead of considering the μ–dependent renormalized masses $M_R(\mu)$, we will switch to the renormalization scale independent pole masses $\hat{M}_R = M_R^{\rm pole}$, defined by the pole positions $(M_R^{\rm pole} - i\Gamma_R^{\rm pole}/2)^2$ of the renormalized propagators. Up to NLO in $1/N_C$, one has

$$M_R^{\rm pole\,2} \;=\; M_R^2 + {\rm Re}\Sigma_R^r(M_R^2)\,, \qquad\qquad M_R^{\rm pole}\Gamma_R^{\rm pole} \;=\; -\,{\rm Im}\Sigma_R^r(M_R^2)\,, \quad (2.89)$$

and therefore,

$$\Delta M_R^2 \;=\; M_R^2 - \hat{M}_R^2 \;=\; -{\rm Re}\Sigma_R^r(M_R^2)\,, \quad (2.90)$$

Since ΔM_R^2 is NLO in $1/N_C$, the difference between using the M_R^2 ($\widetilde{MS}$–subtraction-scheme) within $\Sigma(M_R^2)$ or its value $\hat{M}_R$ in another scheme goes to NNLO. Therefore, it is negligible at the perturbative order we are working at.

If only interactions $\mathcal{L}_R$ given by operators linear in the resonance fields are taken into account [8], one has for the pole scheme

$$\Delta M_S^2 \;=\; \frac{3c_d^2 M_S^4}{16\pi^2 F^4}\left[1 - \ln\frac{M_R^2}{\mu^2}\right], \qquad\qquad \Delta M_P^2 \;=\; 0\,, \quad (2.91)$$

where only the two–Goldstone loop $\Sigma_S(p^2)|_{\phi\phi}$ contributes to ΔM_S^2 and $\Sigma_P(p^2) = 0$ if only the $\mathcal{L}_R$ interactions are taken into account [8].

WSR–scheme for c_m and d_m

Since the value of the spin–0 parameters is very poorly known at the experimental level, one finds important uncertainties and variations in the determination of c_m and d_m through the NLO sum-rules (2.86). The choice of a shift that minimizes the finite part of the loop contributions is not straight-forward. For instance, within the $\widetilde{MS}$–subtraction-scheme itself, it is not easy to find a value of μ that minimizes both $A(\mu)$ and $B(\mu)$ at once unless the resonance couplings are appropriately fine-tuned. This makes the short-distance matching rather cumbersome and the extraction of the necessary resonance parameters problematic.

Alternatively, the selection of a shift $\Delta\kappa$ that exactly cancels the one-loop contributions to Eq. (2.86) (provided in the $\widetilde{MS}$–scheme by the constants $A(\mu)$ and $B(\mu)$) seems to be a better option. This converts Eq. (2.86) into

$$\alpha_2^{(p)} \;=\; 2F^2 + 16\,\hat{d}_m^2 - 16\,\hat{c}_m^2 \;=\; 0\,, \qquad\qquad \alpha_4^{(p)} \;=\; 16\,\hat{d}_m^2\hat{M}_P^2 - 16\,\hat{c}_m^2\hat{M}_S^2 \;=\; 0\,, \quad (2.92)$$

with the solutions

$$\hat{c}_m^2 = \frac{F^2}{8}\frac{\hat{M}_P^2}{\hat{M}_P^2 - \hat{M}_S^2}\,, \qquad\qquad \hat{d}_m^2 = \frac{F^2}{8}\frac{\hat{M}_S^2}{\hat{M}_P^2 - \hat{M}_S^2} \quad (2.93)$$

Though this has the same structure as the LO prediction (2.26) of the large–N_C WSR in Eq. (2.82), the couplings appearing here are the renormalized ones. Nonetheless, this result ensures that the difference between $\hat{c}_m/F$ and $\hat{d}_m/F$ at NLO and their large–N_C limits remains small provided $\hat{M}_R \approx M_R^{N_C\to\infty}$. In order to achieve this minimization, the shifts $\Delta\kappa$ must be tuned in such a way that they obey

$$\begin{aligned} 32\hat{d}_m\Delta d_m - 32\hat{c}_m\Delta c_m \; + \; A(\mu) \; &= \; 0\,, \\ 32\hat{M}_P^2\hat{d}_m\Delta d_m + 16\hat{d}_m^2\Delta M_P^2 - 32\hat{M}_S^2\hat{c}_m\Delta c_m - 16\hat{c}_m^2\Delta M_S^2 \; + \; B(\mu) \; &= \; 0\,. \end{aligned} \tag{2.94}$$

If one fixes ΔM_R^2 (for instance, through the pole scheme) the solutions for Δc_m and Δd_m are then given by

$$\begin{aligned} 32\hat{c}_m\Delta c_m \; &= \; \frac{\hat{M}_P^2 A(\mu) - B(\mu) + 16\,\hat{c}_m^2\Delta M_S^2 - 16\,\hat{d}_m^2\Delta M_P^2}{\hat{M}_P^2 - \hat{M}_S^2} \\ 32\hat{d}_m\Delta d_m \; &= \; \frac{\hat{M}_S^2 A(\mu) - B(\mu) + 16\,\hat{c}_m^2\Delta M_S^2 - 16\,\hat{d}_m^2\Delta M_P^2}{\hat{M}_P^2 - \hat{M}_S^2}\,. \end{aligned} \tag{2.95}$$

In the change of scheme we will make the replacement $\kappa = \hat{\kappa} + \Delta\kappa$ in the tree-level LO diagrams, whereas in the subleading contributions we will just consider $\kappa \approx \hat{\kappa}$, as the difference goes to NNLO in $1/N_C$. Thus, we will end up with a matrix element expressed in terms of just renormalized couplings in the new scheme ($\hat{\kappa}$). We will denote the c_m and d_m renormalization scheme prescribed by Eq. (2.95) as WSR–scheme.

2.6 Low-energy expansion

2.6.1 $\widetilde{MS}$–subtraction scheme

At low energies, the expansion of our one-loop RχT correlator yields the structure,

$$\begin{aligned} \Pi_{ss-pp}(p^2) = B_0^2 \, \Bigg\{ \frac{2F^2}{p^2} \; + \; \left[\frac{16c_m^2}{M_S^2} - \frac{16d_m^2}{M_P^2} + 32\widetilde{L}_8 + \frac{G_8}{\pi^2}\left(1 - \ln\frac{-p^2}{\mu^2}\right) + 32\,\xi_{L_8} \right] \\ + \frac{p^2}{F^2}\left[\frac{16\,F^2c_m^2}{M_S^4} - \frac{16\,F^2d_m^2}{M_P^4} - \frac{G_{38}^L}{\pi^2}\left(1 - \ln\frac{-p^2}{\mu^2}\right) + 32\,\xi_{C_{38}} \; + \; \mathcal{O}(N_C^0) \right] + \mathcal{O}(p^4) \Bigg\}\,, \end{aligned} \tag{2.96}$$

where in the $U(3)$ case we obtain $G_8 = \frac{3}{16} = \Gamma_8$ and $G_{38}^L = -3c_dc_m/2M_S^2$, with $G_{38}^L = \Gamma_{38}^L$ after using the LO matching relation $L_5 = c_dc_m/M_S^2$ [8]. The logarithm from the $\pi\pi$ loop in RχT has been singled out in the $\ln(-q^2)$ terms. These RχT logarithms exactly reproduce those in the low-energy χPT expression (2.23), ensuring the possibility of matching both theories [47]. The one-loop contributions from the remaining channels generate only polynomial terms at this chiral order and they are provided here by ξ_{L_8} and $\xi_{C_{38}}$, defined within the $\widetilde{MS}$–renormalization-scheme. The predictions for the low-energy constants at NLO in $1/N_C$ then turn out to be

$$\begin{aligned} L_8(\mu_\chi) \; &= \; \frac{c_m^2}{2\,M_S^2} - \frac{d_m^2}{2\,M_P^2} + \widetilde{L}_8 + \xi_{L_8} \; + \; \frac{\Gamma_8}{\pi^2}\ln\frac{\mu^2}{\mu_\chi^2}\,, \\ C_{38}(\mu_\chi) \; &= \; \frac{F^2c_m^2}{2\,M_S^4} - \frac{F^2d_m^2}{2\,M_P^4} + \xi_{C_{38}} \; - \; \frac{\Gamma_{38}^L}{\pi^2}\ln\frac{\mu^2}{\mu_\chi^2}\,. \end{aligned} \tag{2.97}$$

The dependence of the terms on the right-hand side of the equations (r.h.s.) on the RχT renormalization scale μ have been left partially implicit. Only the last term shows μ explicitly. It comes from the two–Goldstone loop in RχT (Eq. (2.96)) and matches exactly the log from the two–Goldstone loop in χPT (Eq. (2.23), with the chiral renormalization scale μ_χ), producing the $\ln(\mu^2/\mu_\chi^2)$ term. This ensures the right low-energy running with μ_χ for the χPT low-energy constants [47]. On the other hand, the r.h.s. is independent of the RχT scale μ at the given order in $1/N_C$. There can still be some residual μ dependence at NNLO, which would allow the use of renormalization group technics in order to improve the perturbative expansion and to remove possible large radiative corrections [38]. Nonetheless, this is beyond the scope of this article, where we will take the usual prescription $\mu = \mu_\chi$ [30, 46, 47].

If we use the c_m and d_m predictions from the high-energy OPE constraints in Eq. (2.86), the low-energy predictions result [31]

$$\begin{aligned} L_8(\mu) &= \frac{F^2}{16}\left(\frac{1}{M_S^2}+\frac{1}{M_P^2}\right)\left[1 + \frac{A(\mu)}{2F^2} - \frac{B(\mu)}{2F^2(M_S^2+M_P^2)}\right] + \xi_{L_8}\,, \\ C_{38}(\mu) &= \frac{F^4\,(M_S^4+M_S^2M_P^2+M_P^4)}{16\,M_S^4M_P^4}\left[1 + \frac{A(\mu)}{2F^2} - \frac{B(\mu)(M_S^2+M_P^2)}{2F^2(M_S^4+M_S^2M_P^2+M_P^4)}\right] \\ &+ \xi_{C_{38}}\,. \end{aligned} \tag{2.98}$$

In the case, where we only have interactions $\mathcal{L}_R$ in the lagrangian, linear in the resonance fields [8], the low-energy contributions from the one-loop diagrams are given by

$$\begin{aligned} \xi_{L_8} &= -\frac{3c_dc_m}{32\pi^2F^2}\left(\ln\frac{M_S^2}{\mu^2}+\frac{1}{2}\right) + \frac{3c_d^2}{128\pi^2F^2}\left(\ln\frac{M_S^2}{\mu^2}+\frac{5}{6}\right) \\ &+\frac{3G_V^2}{256\pi^2F^2}\left(\ln\frac{M_V^2}{\mu^2}+\frac{5}{6}\right) + \frac{3c_m^2}{32\pi^2F^2}\ln\frac{M_S^2}{\mu^2} - \frac{3d_m^2}{32\pi^2F^2}\ln\frac{M_P^2}{\mu^2}\,, \\ \xi_{C_{38}} &= \frac{3d_m^2}{64\pi^2M_P^2} - \frac{3c_d^2}{512\pi^2M_S^2} - \frac{3G_V^2}{1024\pi^2M_V^2} \\ &-\frac{3c_m^2}{64\pi^2M_S^2} + \frac{3c_dc_m}{96\pi^2M_S^2}\,. \end{aligned} \tag{2.99}$$

The results (2.98) correspond to the predictions for the $U(3)$ chiral perturbation theory couplings, where the η_1 is identified as the ninth chiral Goldstone. In order to recover the traditional $SU(3)$ couplings one needs to make use of the matching equations [31, 50],

$$L_8^{SU(3)}(\mu) = L_8^{U(3)} + \frac{\Gamma_8^{SU(3)}-\Gamma_8^{U(3)}}{32\pi^2}\ln\frac{m_0^2}{\mu^2}\,, \tag{2.100}$$

$$C_{38}^{SU(3)}(\mu) = C_{38}^{U(3)} - \frac{\Gamma_{38}^{(L)\,SU(3)}-\Gamma_{38}^{(L)\,U(3)}}{32\pi^2}\left(\ln\frac{m_0^2}{\mu^2}+\frac{1}{2}\right) - \frac{\Gamma_8^{SU(3)}-\Gamma_8^{U(3)}}{32\pi^2}\,\frac{F^2}{2m_0^2}\,.$$

These outcomes will be used later in the alternative renormalization schemes and the constants $\xi_{L_8}(\mu)$, $\xi_{C_{38}}(\mu)$, $A(\mu)$ and $B(\mu)$ will always refer to their former expressions in the $\widetilde{MS}$ scheme.

2.6.2 Pole masses and WSR–scheme for c_m and d_m

In this case, the renormalization scheme of c_m and d_m is chosen such that the one-loop contributions to the NLO relations in Eq. (2.86) are exactly canceled, yielding $\hat{c}_m^2 = \frac{F^2}{8}\frac{\hat{M}_P^2}{\hat{M}_P^2-\hat{M}_S^2}$ and $\hat{d}_m^2 = \frac{F^2}{8}\frac{\hat{M}_S^2}{\hat{M}_P^2-\hat{M}_S^2}$. The low energy limit of the RχT correlator in the new scheme leads to the LEC determination,

$$L_8(\mu) = \frac{F^2}{16}\left(\frac{1}{\hat{M}_S^2}+\frac{1}{\hat{M}_P^2}\right)\left[1 \; + \; \frac{A(\mu)}{2F^2} - \frac{B(\mu)}{2F^2(\hat{M}_S^2+\hat{M}_P^2)}\right]$$

$$- \; \frac{F^2}{16}\left(\frac{\Delta M_S^2}{\hat{M}_S^4}+\frac{\Delta M_P^2}{\hat{M}_P^4}\right) \; + \; \xi_{L_8}\,,$$

$$C_{38}(\mu) = \frac{F^4\,(\hat{M}_S^4+\hat{M}_S^2\hat{M}_P^2+\hat{M}_P^4)}{16\,\hat{M}_S^4\hat{M}_P^4}\left[1 \; + \; \frac{A(\mu)}{2F^2} - \frac{B(\mu)(\hat{M}_S^2+\hat{M}_P^2)}{2F^2(\hat{M}_S^4+\hat{M}_S^2\hat{M}_P^2+\hat{M}_P^4)}\right]$$

$$- \; \frac{F^4}{16\,\hat{M}_S^2\hat{M}_P^2}\left(\frac{\Delta M_S^2(\hat{M}_S^2+2\hat{M}_P^2)}{\hat{M}_S^4}+\frac{\Delta M_P^2(2\hat{M}_S^2+\hat{M}_P^2)}{\hat{M}_P^4}\right) \; + \; \xi_{C_{38}}\,, \tag{2.101}$$

where $\xi_{L_8,C_{38}}$ are the same one-loop contributions to the LECs computed before in the $\widetilde{MS}$–subtraction scheme. The same applies to $A(\mu)$ and $B(\mu)$, which were defined as the one-loop contributions to the high-energy expansion coefficients in the $\widetilde{MS}$–scheme. In ξ_{L_8}, $\xi_{C_{38}}$, $A(\mu)$ and $B(\mu)$ we will use the couplings and masses in the new scheme $(\hat{c}_m, \hat{d}_m, \hat{M}_R)$ instead of the original ones in the $\widetilde{MS}$–scheme (c_m, d_m, M_R), as the difference goes to NNLO in $1/N_C$. The constants $\Delta M_R^2 = M_R^2 - \hat{M}_R^2$ provide the difference between the mass M_R in the $\widetilde{MS}$–scheme and its value $\hat{M}_R$ in another scheme. In this chapter it will refer in particular to the mass pole, although it accepts further generalizations.

Notice that these expressions are similar to those in the $\widetilde{MS}$–scheme (2.98), up to the ΔM_R^2 terms that arise due to the change of mass prescription. The WSR–scheme does not modify the low-energy prediction, it just serves to reduce the uncertainties in the NLO Weinberg sum-rules.

Finally, in order to obtain the traditional $SU(3)$–χPT LECs, one should use again the matching Eq. (2.100).

2.7 Correlator with the extended RχT lagrangian

Ecker *et al.*'s lagrangian [8] has been found to be very successful for the description of amplitudes with few-Goldstones ($\pi\pi$ form-factors, scatterings...). However, it fails to describe processes with multi-Goldstones states or with a higher number of resonances. The LO meson lagrangian must be then enlarged to improve the description of the new channels. In the case of our observable, the relevant

operators with two resonance fields are [15, 32, 33, 46],

$$\mathcal{L}_{RR'} \,=\, i\lambda_1^{PV}\langle\,[\nabla^\mu P, V_{\mu\nu}]\,u^\nu\,\rangle \,+\, \lambda_1^{SA}\langle\,\{\nabla^\mu S, A_{\mu\nu}\}\,u^\nu\,\rangle \,+\, \lambda_1^{SP}\langle\,\{\nabla^\mu S, P\}\,u_\mu\,\rangle\,. \tag{2.102}$$

The λ_1^{PV} and λ_1^{SP} terms induce a one-loop mixing between the Goldstone and the pseudoscalar resonance. These loops bring ultraviolet divergences which need the presence of the subleading counter-terms,

$$\Delta\mathcal{L}_P \,=\, d'_m\langle\,P\nabla_\mu u^\mu\,\rangle \,+\, d''_m\langle\,(\nabla^2 P)\nabla_\mu u^\mu\,\rangle\,, \tag{2.103}$$

to make the amplitude finite. At LO, in the free field case, the meson kinetic terms are assumed to be defined in the canonical way, i.e., without mixing between particles. This was indeed the case in Ecker *et al.*'s lagrangian [8]. In addition, although these P–ϕ operators may arise at NLO, they happen to be proportional to the EOM. They can be removed from the action through a convenient meson field redefinition, leaving for the relevant couplings in our problem the effective combinations

$$\begin{aligned}
\widetilde{L}_8^{eff} &= \widetilde{L}_8 + \frac{1}{2}c_m^2 X_S - \frac{1}{2}d_m^2 X_P + c_m\lambda_{18}^S - d_m\lambda_{13}^P - \frac{1}{2}d_m d''_m\,,\\
\widetilde{H}_2^{eff} &= \widetilde{H}_2 + c_m^2 X_S + d_m^2 X_P + 2c_m\lambda_{18}^S + 2d_m\lambda_{13}^P + d_m d''_m\,,\\
(M_S^2)^{eff} &= M_S^2 - X_S M_S^4,\\
(M_P^2)^{eff} &= M_P^2 - X_P M_P^4,\\
c_m^{eff} &= c_m - c_m X_S M_S^2 - M_S^2\lambda_{18}^S,\\
d_m^{eff} &= d_m - d_m X_P M_P^2 - M_P^2\lambda_{13}^P + \frac{1}{2}d'_m - \frac{1}{2}M_P^2 d''_m\,.
\end{aligned} \tag{2.104}$$

2.7.1 Meson self-energies

These operators do not modify the previous loop contributions. However, new channels are now open in the different vertex-functions. Thus, the Goldstone self-energy gains the contributions (Fig. 2.10),

$$\begin{aligned}
\Sigma_\phi^r(p^2)|_{PV} &= -\frac{3(\lambda_1^{PV})^2}{F^2}\Bigg\{\left[M_V^4 - 2M_V^2(p^2+M_P^2) + (p^2-M_P^2)^2\right]\bar{J}(p^2,M_P^2,M_V^2)\\
&-\frac{p^2}{16\pi^2(M_P^2-M_V^2)}\left(p^2M_P^2\ln\frac{M_P^2}{\mu^2} - p^2M_V^2\ln\frac{M_V^2}{\mu^2} + M_V^2M_P^2\ln\frac{M_V^2}{M_P^2}\right) - \frac{p^2(M_P^2+M_V^2)}{32\pi^2}\Bigg\},\\
\Sigma_\phi^r(p^2)|_{SA} &= -\frac{3(\lambda_1^{SA})^2}{F^2}\Bigg\{\left[M_A^4 - 2M_A^2(p^2+M_S^2) + (p^2-M_S^2)^2\right]\bar{J}(p^2,M_S^2,M_A^2)\\
&-\frac{p^2}{16\pi^2(M_S^2-M_A^2)}\left(p^2M_S^2\ln\frac{M_S^2}{\mu^2} - p^2M_A^2\ln\frac{M_A^2}{\mu^2} + M_A^2M_S^2\ln\frac{M_A^2}{M_S^2}\right) - \frac{p^2(M_S^2+M_A^2)}{32\pi^2}\Bigg\},\\
\Sigma_\phi^r(p^2)|_{SP} &= -\frac{3(\lambda_1^{SP})^2}{p^4F^2}\Bigg\{(p^2-M_P^2+M_S^2)^2\bar{J}(p^2,M_P^2,M_S^2)\\
&-\frac{p^2}{16\pi^2(M_P^2-M_S^2)}\left(p^2M_P^2\ln\frac{M_P^2}{\mu^2} - p^2M_S^2\ln\frac{M_S^2}{\mu^2} + M_S^2M_P^2\ln\frac{M_S^2}{M_P^2}\right) - \frac{p^2(M_P^2+M_S^2)}{32\pi^2}\Bigg\},
\end{aligned} \tag{2.105}$$

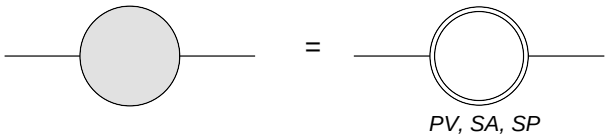

Figure 2.10: Contribution from $\mathcal{L}_{RR'}$ operators to the Goldstone boson self-energy.

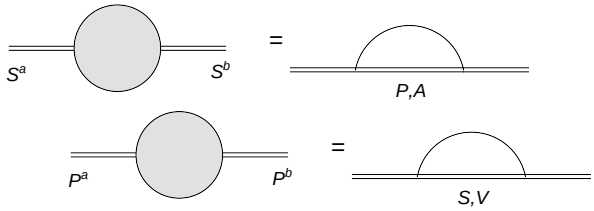

Figure 2.11: Contribution from $\mathcal{L}_{RR'}$ operators to the scalar and the pseudo-scalar resonance self-energies.

in addition to the former $V\phi$ and $S\phi$ cuts from Eq. (2.36). The functions $\bar{J}(p^2, M_a^2, M_b^2)$ is the subtracted two-propagator Feynman integral ($\bar{J}(0, M_a^2, M_b^2) = 0$), given in App. 2.10.3.

The scalar propagators contains now $A\phi$ and $P\phi$ cuts (besides the $\phi\phi$–one from Eq. (2.57)) (Fig. 2.11):

$$\Sigma_S^r(p^2)|_{A\phi} = \frac{3(\lambda_1^{SA})^2}{16\pi^2F^2}\left[\frac{(p^2-M_A^2)^3}{p^2}\ln\left(1-\frac{p^2}{M_A^2}\right) - M_A^4 - 3p^2M_A^2\left(\ln\frac{M_A^2}{\mu^2}-\frac{2}{3}\right) + p^4\left(\ln\frac{M_A^2}{\mu^2}-1\right)\right], \tag{2.106}$$

$$\Sigma_S^r(p^2)|_{P\phi} = \frac{3(\lambda_1^{SP})^2}{16\pi^2F^2}\left[\frac{(p^2-M_P^2)^3}{p^2}\ln\left(1-\frac{p^2}{M_P^2}\right) - M_P^4 + p^2M_P^2\left(\ln\frac{M_P^2}{\mu^2}+2\right) + p^4\left(\frac{M_P^2}{\mu^2}-1\right)\right]. \tag{2.107}$$

Ecker *et al.*'s lagrangian $\mathcal{L}_R$ did not modified the pseudoscalar resonance propagator. However, the new operators $\mathcal{L}_{RR'}$ yield (Fig. 2.11),

$$\begin{aligned}\Sigma_P^r(p^2)|_{V\phi} &= \frac{3(\lambda_1^{PV})^2}{16\pi^2F^2}\left[\frac{(p^2-M_V^2)^3}{p^2}\ln\left(1-\frac{p^2}{M_V^2}\right) - M_V^4\right.\\ &\qquad \left. -3p^2M_V^2\left(\ln\frac{M_V^2}{\mu^2}-\frac{2}{3}\right) + p^4\left(\ln\frac{M_V^2}{\mu^2}-1\right)\right],\\ \Sigma_P^r(p^2)|_{S\phi} &= \frac{3(\lambda_1^{SP})^2}{16\pi^2F^2}\left[\frac{(p^2-M_S^2)^3}{p^2}\ln\left(1-\frac{p^2}{M_S^2}\right) + 4M_S^4\left(\ln\frac{M_S^2}{\mu^2}-\frac{1}{4}\right)\right.\\ &\qquad \left. -3p^2M_S^2\left(\ln\frac{M_S^2}{\mu^2}-\frac{2}{3}\right) + p^4\left(\ln\frac{M_S^2}{\mu^2}-1\right)\right].\end{aligned} \tag{2.108}$$

The renormalized resonance self-energies provide at this order the pole masses through Eq. (2.89), giving the corresponding shifts $\Delta M_R^2 = -\mathrm{Re}\Sigma_R^r(M_R^2)$.

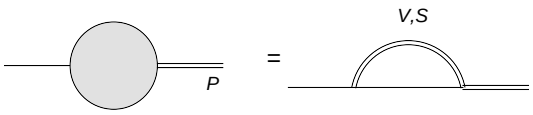

Figure 2.12: Contribution from $\mathcal{L}_{RR'}$ operators to the mixing term between the Goldstone and the pseudo-scalar resonance.

2.7.2 P–ϕ mixing

In addition, these operators λ_1^{PV} and λ_1^{SP} also generate a P–ϕ mixing (Fig. 2.12),

$$\begin{aligned}\Sigma^r_{P-\phi}(p^2)|_{V\phi} &= \frac{3G_V\lambda_1^{PV}}{16\pi^2F^3}\left[\frac{(p^2-M_V^2)^3}{p^2}\ln\left(1-\frac{p^2}{M_V^2}\right) - M_V^4\right.\\ &\qquad \left. -3p^2M_V^2\left(\ln\frac{M_V^2}{\mu^2}-\frac{2}{3}\right)+p^4\left(\ln\frac{M_V^2}{\mu^2}-1\right)\right],\\ \Sigma^r_{P-\phi}(p^2)|_{S\phi} &= \frac{3c_d\lambda_1^{SP}}{8\sqrt{2}\pi^2F^3}\left[\frac{(p^2-M_S^2)^3}{p^2}\ln\left(1-\frac{p^2}{M_S^2}\right) - M_S^4\right.\\ &\qquad \left. -3p^2M_S^2\left(\ln\frac{M_S^2}{\mu^2}-\frac{2}{3}\right)+p^4\left(\ln\frac{M_S^2}{\mu^2}-1\right)\right],\end{aligned} \tag{2.109}$$

leading to an extra perturbative contribution to the PP–correlator that has to be added to the former ones in (2.77):

$$\Pi_{pp}(p^2)^{\mathrm{P}-\phi\text{ mixing}} = \frac{8\sqrt{2}\,Fd_m}{p^2\,(p^2-M_P^2)}\left[-\frac{\sqrt{2}\,d'_m}{F}p^2+\frac{\sqrt{2}\,d''_m}{F}p^4+\Sigma^r_{P-\phi}(p^2)^{1\ell}\right]. \tag{2.110}$$

After a convenient field redefinition d'_m and d''_m disappear from Eq. (2.110), being their information encoded in $d_m^{\rm eff}$, $\widetilde{L}_8^{\rm eff}$ and $\widetilde{H}_2^{\rm eff}$.

It is important to remark that at the NLO under consideration, the mixing does not modify the pseudoscalar resonance mass renormalization. The Goldstone remains massless –as expected– and the resonance pole mass is still provided at this order by $\Delta M_P^2 = -\mathrm{Re}\Sigma_P^r(M_P^2)$ through Eq. (2.89).

2.7.3 New $s\to S$ and $p\to P$ vertex functions

A new $P\phi$ channel is opened in the $s\to S$ vertex function in addition to the $\phi\phi$–cut from Eq. (2.61):

$$-\frac{1}{4B_0}\Phi^r_{sS}(p^2)^{1\ell}|_{P\phi} = \frac{3d_m\lambda_1^{SP}}{16\pi^2F^2}\left[\frac{(p^2-M_P^2)^2}{p^2}\ln\left(1-\frac{p^2}{M_P^2}\right)+M_P^2+p^2\left(\ln\frac{M_P^2}{\mu^2}-1\right)\right]. \tag{2.111}$$

On the other hand, one has now the $S\phi$–absorptive cut in the $p\to P$ vertex-function, which did not get any contribution from $\mathcal{L}_R$ alone:

$$\begin{aligned}-\frac{1}{4B_0}\Phi^r_{pP}(p^2)^{1\ell}|_{S\phi} &= \frac{3c_m\lambda_1^{SP}}{16\pi^2F^2}\left[\frac{(p^2-M_S^2)^2}{p^2}\ln\left(1-\frac{p^2}{M_S^2}\right)\right.\\ &\qquad \left. -2M_S^2\left(\ln\frac{M_S^2}{\mu^2}-\frac{1}{2}\right)+p^2\left(\ln\frac{M_S^2}{\mu^2}-1\right)\right]\end{aligned} \tag{2.112}$$

Figure 2.13: One-loop diagrams with $\mathcal{L}_{RR'}$ operators in the $s(x) \to S$ and $p(x) \to P$ vertex functions.

2.8 Phenomenology

The RχT lagrangian developed by Ecker *et al.* [8], $\mathcal{L} = \mathcal{L}_G + \mathcal{L}_R$, only contained operators with at most one resonance field. This approach has been proven to be very successful at the phenomenological level for the last two decades [39]. Nevertheless, in the few last years it has become clear that the description of more complicated QCD matrix elements (e.g. 3–point Green functions [14–17,19]) demands the introduction of operators with more than one resonance field [15].

Since the $M_R(\mu)$ masses in the $\widetilde{MS}$—scheme are μ dependent, they are difficult to relate with the physical masses provided, for instance, by the *Particle Data Group* (PDG) [51]. This relation is even more cumbersome when one adds more general kinds of vertices (e.g. λ_1^{SP}) within the loops: in the $\widetilde{MS}$–scheme the value of $M_R(\mu)$ will depend on the content of the theory and its lagrangian. Thus, it seems more convenient to use universal properties such as the pole masses, denoted here as $\hat{M}_R$. The octet of the lightest scalar and the pseudoscalar resonances are then related, to the $a_0(980)$ and the $\pi(1300)$, and we will consider from now on the inputs $\hat{M}_S = 980 \pm 20$ MeV and $\hat{M}_P = 1300 \pm 50$ MeV [28, 51].

The procedure that we will follow in order to extract the LECs with higher and higher accuracy is to progressively add more and more physical information to the RχT correlator, starting from lower energies. Since the resonance parameters will be used to accommodate the short-distance OPE behaviour, in general the two-meson thresholds ($S\pi$, $V\pi$, $P\pi$...) may not be at the right place. Likewise, one may find that individual intermediate two-meson channels have a clearly erroneous momentum dependence at high energies (e.g. constant or growing behaviour).

The introduction of the new operators λ_1^{VP}, λ_1^{SP} and λ_1^{SA} will allow us to improve the momentum dependence of the $R\pi$ absorptive channels with one resonance and one Goldstone. However, since these new couplings will be tuned to implement the short-distance OPE constraints, the $R\pi$ channel description may still differ slightly from that provided by the physical values of λ_{SP}, λ_{PV}, λ_{SA}, c_d, G_V... Likewise, the two-resonance RR' absorptive cuts will still remain wrongly described until operators with three resonance fields are taken into account. Nonetheless, we will see that the RχT description progressively approaches the actual QCD amplitude as the hadronic action is completed with more and more complicated operators, bringing along a better and better description of the lower channels.

2.8.1 Phenomenology with Ecker *et al.*'s lagrangian $\mathcal{L}_G$+$\mathcal{L}_R$

First, we will extract the value of the LECs at large N_C within the single resonance approximation. We will use the formerly referred $\hat{M}_S = 980 \pm 20$ MeV and $\hat{M}_P = 1300 \pm 50$ MeV [51], $F = 90 \pm 2$ MeV [28,50] and the standard reference χPT renormalization scale $\mu_0 = 770$ MeV. The short-distance constraints determine c_m and d_m in terms of the scalar and pseudo-scalar masses, producing

$$L_8 \,=\, (0.83 \pm 0.05) \cdot 10^{-3}\,, \qquad\qquad C_{38} \,=\, (8.4 \pm 1.0) \cdot 10^{-6}\,. \tag{2.113}$$

Naively, if the uncertainty on the saturation scale is estimated by observing the variation with μ in the range 0.5–1 GeV, one would expect the former values to be deviated from the actual ones at the order of $\Delta L_8 \sim 0.3 \cdot 10^{-3}$, $\Delta C_{38} \sim 5 \cdot 10^{-6}$.

In order to go beyond the naive estimate of the subleading $1/N_C$ uncertainty, we consider now the one-loop contributions computed in previous sections. In a first approach, we consider just operators in the lagrangian with at most one resonance field [8]. At one-loop, in addition to the tree-level exchanges, one has the two-meson absorptive channels $\pi\pi$, $V\pi$, $S\pi$ and $P\pi$, determined by the scalar parameters c_m and c_d, the pseudo-scalar coupling d_m and the vector ones G_V and M_V. If we work in the WSR–renormalization-scheme for c_m and d_m, the short-distance constraints produce at NLO the same structure found from the large–N_C WSR, $\hat{c}_m^2 = \frac{F^2}{8}\frac{\hat{M}_P^2}{\hat{M}_P^2 - \hat{M}_S^2}$ and $\hat{d}_m^2 = \frac{F^2}{8}\frac{\hat{M}_S^2}{\hat{M}_P^2 - \hat{M}_S^2}$. The other three resonance parameters (c_d, G_V, M_V) are fixed by means of the logarithmic OPE constraints (2.83), $\alpha_0^{(\ell)} = \alpha_2^{(\ell)} = \alpha_4^{(\ell)} = 0$, giving

$$c_d \,=\, 60 \pm 4\,\mathrm{MeV}\,, \qquad\qquad G_V \,=\, 93 \pm 5\,\mathrm{MeV}\,, \qquad\qquad M_V \,=\, 853 \pm 28\,\mathrm{MeV}\,. \tag{2.114}$$

These numbers are found to be quite off the physical ones, $c_d \approx 30$ MeV, $G_V \approx 60$ MeV, $M_V \approx 770$ MeV [8, 9, 23, 24, 26–28, 51]. The LEC prediction for the standard comparison scale $\mu_0 = 770$ MeV then result,

$$L_8(\mu_0) \,=\, (2.28 \,\pm\, 0.19) \cdot 10^{-3}\,, \qquad\qquad C_{38}(\mu_0) \,=\, (26 \,\pm\, 4) \cdot 10^{-6}\,. \tag{2.115}$$

In order to get these $SU(3)$ χPT couplings, we employed in the U(3)–SU(3) matching Eq. (2.100) the chiral singlet pseudoscalar mass $m_0 = 850 \pm 50$ MeV [50]. These estimates are still far from former values in the bibliography for $\mu_0 =$ 770 MeV: $L_8 = 0.9 \cdot 10^{-3}$ and $C_{38} = 10 \cdot 10^{-6}$ from $\mathcal{O}(p^6)$ χPT and resonance estimates [5], later refined into $L_8 = (0.61 \pm 0.20) \cdot 10^{-3}$ [6] and recently updated into $L_8 = (0.37 \pm 0.17) \cdot 10^{-3}$ [7]; $L_8 = (0.6 \pm 0.4) \cdot 10^{-3}$ and $C_{38} = (2 \pm 6) \cdot 10^{-6}$ from a previous NLO calculation in RχT [31]; $L_8 = (1.02 \pm 0.06) \cdot 10^{-3}$ and $C_{38} = (3.3 \pm 0.6) \cdot 10^{-6}$ from Dyson-Schwinger equation analysis [52]; $L_8 = (0.36 \pm 0.05 \pm 0.07) \cdot 10^{-3}$ from Lattice simulations [53].

Although the calculation with just the $\mathcal{L}_R$ operators is able produce an appropriate description of the $\pi\pi$ channel (thanks to the $c_d \langle\, S u_\mu u^\mu \,\rangle$ operator), its coupling c_d gets a extremely shifted value as this parameter has been used to accommodate the OPE at short distances. This does not represent by itself an important drawback in our analysis, where the goals are the LECs and RχT is devised as a convenient interpolator between high and low energies. However, the problem in our case is the erroneous description that one obtains for the $R\pi$ channels with only the $\mathcal{L}_R$ operators [32,46]: The $S\pi$ contribution to the spectral

function behaves like a constant and the $V\pi$ one grows with the energy. moreover, as M_V is also determined from the OPE matching, the position of the first two-meson threshold after the $\pi\pi$ one (i.e., the $V\pi$ channel) is shifted from its physical place.

2.8.2 Improving one $R\pi$ channel: extending the lagrangian

The straight forward procedure to ameliorate our one-loop amplitude is the inclusion of the required operators for the proper description of the lowest absorptive cuts, this is, $\pi\pi$ and $V\pi$. The first one is ruled by the already included c_d operator but the latter demands the λ_1^{PV} term from Eq. (2.102), which now induces $PV\pi$ interactions and allows to cure the infinitely growing behaviour of the $V\pi$ contribution to the spectral function.

Now we use the former inputs $\hat{M}_S$, $\hat{M}_P$, F, m_0 and the physical coupling $c_d = 30 \pm 10$ MeV [8, 26–28, 39]. The remaining parameters $(G_V, M_V, \lambda_1^{PV})$ are extracted from the three logarithmic OPE constraints $\alpha_0^{(\ell)} = \alpha_2^{(\ell)} = \alpha_4^{(\ell)} = 0$. Indeed, this system only has real solutions in the very corner of the parameter space, for low pseudo-scalar mass ($\hat{M}_P \approx 1.25$ GeV) and high c_d and scalar mass ($c_d \approx 40$ MeV, $\hat{M}_S \approx 1.00$ GeV). This does not improve the value of the vector coupling and mass with respect to the former section, which become $G_V \approx 120$ MeV and $M_V \approx 400$ MeV. The LEC predictions result,

$$L_8(\mu_0) \approx 0.5 \cdot 10^{-3}\,, \qquad C_{38}(\mu_0) \approx -8 \cdot 10^{-6}\,, \tag{2.116}$$

where L_8 may look acceptable but the presence of such a low distorted $V\pi$ threshold is reflected in a value of C_{38} which looks still a bit off. Nonetheless, these values are closer to those formerly obtained in the bibliography [5–7, 31, 52, 53].

The problem is that the $V\pi$ is not the only relevant channel that appears after the $\pi\pi$ one. The $S\pi$ channel opens up at an energy not far from the $V\pi$ threshold. Thus, even if the $V\pi$ channel can be now correctly described, the $S\pi$ contribution to the spectral function still shows a wrong constant behaviour [32, 46]. The λ_1^{SP} operator in (2.102) is then crucial to cure that behaviour. Furthermore, this operator mends as well the similar bad short-distance behaviour found in the $P\pi$ cut contribution to the SS spectral function.

Nonetheless, the presence of λ_1^{PV} in the lagrangian is still essential. If one repeats the NLO computation adding only the λ_1^{SP} operator (but not λ_1^{PV}) the vector parameters become of the order of $G_V \sim 20$ MeV and $M_V \sim 2$ GeV. On the other hand, the LEC predictions $L_8 \sim 1.3 \cdot 10^{-3}$ and $C_{38} \sim 12 \cdot 10^{-6}$ seem to improve with respect to the case with only $\mathcal{L}_R$ operators in the RχT lagrangian [8], with at most one resonance field.

The inclusion of the λ_1^{SA} operator alone seems to move the results also in the right direction. Although it does not affect the previous channels, it opens the $A\pi$ absorptive cut. Even if its effect at low energies is small, it helps to fulfill the OPE constraints. Taking now the extra needed input $M_V = 770 \pm 20$ MeV together with the former ones, it is possible to extract the remaining ones $(\lambda_1^{SA}, G_V, M_A)$ through the three log OPE conditions. The value for the vector coupling turns out to be now more natural ($G_V = 67 \pm 18$ MeV) but the $a_1(1230)$ mass falls down to very low values ($M_A = 610 \pm 50$ MeV). The predictions for the chiral couplings show a clear improvement, $L_8 = (0.7 \pm 0.4) \cdot 10^{-3}$, $C_{38} = (4 \pm 5) \cdot 10^{-6}$.

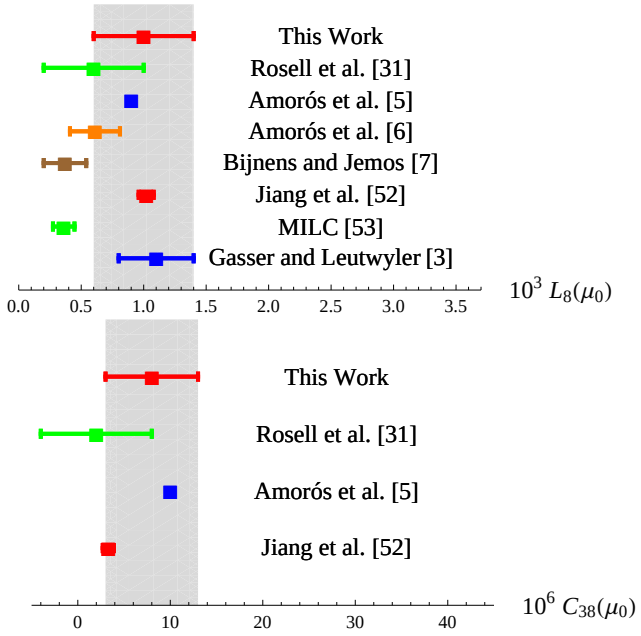

Figure 2.14: Comparison of the LEC predictions in this work with previous results in the bibliography.

2.8.3 Improving the $V\pi$, $S\pi$, $A\pi$ and $P\pi$ channels

In order to have a proper description of all the $R\pi$ absorptive cuts, the λ_1^{SA}, λ_1^{PV} and λ_1^{SP} operators from Eq. (2.102) are now included in the RχT action. We take the same inputs as before, $\hat{M}_S = 980 \pm 20$ MeV, $\hat{M}_P = 1300 \pm 50$ MeV, $F = 90 \pm 2$ MeV, $m_0 = 850 \pm 50$ MeV, $c_d = 30 \pm 10$ MeV, $M_A = 1230 \pm 200$ MeV, $M_V = 770 \pm 20$ MeV and $G_V = 60 \pm 20$ MeV. Both c_d and G_V have been taken with a naive 33% error, as they appear only in the NLO part of the correlator. This will account for the possible NNLO variations in the one-loop correlator depending on whether it is evaluated with these physical couplings or their large–N_C values. The remaining unknown parameters $(\lambda_1^{PV}, \lambda_1^{SP}, \lambda_1^{SA})$ are extracted from the three logarithmic OPE constraints, leading to our final LEC estimates,

$$L_8(\mu_0) \,=\, (1.0 \pm 0.4) \,\cdot\, 10^{-3}\,, \qquad\qquad C_{38}(\mu_0) \,=\, (8 \pm 5) \,\cdot\, 10^{-6}\,. \qquad (2.117)$$

These numbers are compared to previous determinations in Fig. 2.14. Although there is still a clear dispersion between the various measurements, at the present error level we remain essentially compatible. Further efforts should be focused on the extraction of the scalar and pseudo-scalar pole masses in order to sizably reduce the uncertainties in the RχT calculations.

In general, the three logarithmic OPE constraints $\alpha_0^{(\ell)} = \alpha_2^{(\ell)} = \alpha_4^{(\ell)} = 0$ produce complex solutions for the λ_1^{SP}, λ_1^{PV}, λ_1^{SA}. In order to remain within the quantum field theory description, only the real values are kept. The regions with at least one real solution are shown in Fig. 2.15. There, we plot the allowed ranges for c_d and G_V, with the other inputs taken at their central values. Indeed, there is no real solution for the central values $c_d = 30$ MeV and $G_V = 60$ MeV. On the contrary to other phenomenological analysis which seem to prefer a c_d coupling below 30 MeV [23, 27, 28], the log OPE constraints require slightly larger values,

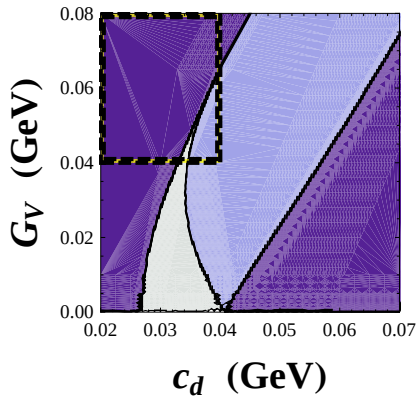

Figure 2.15: Allowed regions with one (light blue) or two (white) real solutions from the logarithmic OPE constraints $\alpha_0^{(\ell)} = \alpha_2^{(\ell)} = \alpha_4^{(\ell)} = 0$. No real solution exists in the darker purple regions. In the upper left corner one can see the dashed rectangle provided by the ranges $c_d = 30 \pm 10$ MeV, $G_V = 60 \pm 20$ MeV.

$cd \gtrsim 30$ MeV. However, in general for c_d around 30 MeV is always impossible to have real solutions for the value of the coupling $G_V \simeq 64$ MeV obtained from V decays [8, 9, 28]. Actually, if one demanded the $\pi\pi$ scalar form-factor (and the corresponding $\pi\pi$ contribution to the SS spectral function) to vanish at high energies one would obtain $c_d = F^2/4c_m \simeq 42$ MeV. However, in this work we do not perform a channel by channel analysis as in Ref. [31]. Indeed, in our field theory approach one could fix separately the short-distance behaviour of the $\pi\pi$ and all the $R\pi$ channels through the $\lambda^{RR'}$ operators, but the latter also generate RR' absorptive cuts with the wrong properties at high momentum. The only option is the global adjustment of parameters considered in this work, where the lowest channels arrange the short-distance behaviour of the highest cuts at the price of slight modifications on their couplings.

The allowed (c_d, G_V) region of Fig. 2.15 actually changes if one varies the other inputs. Thus, we observed the whole range of the LECs allowed for the possible variations of the inputs and used this interval as our estimate of the central value and error. The maximum (minimum) value of the LECs was obtained at the largest (smallest) c_d and G_V. Likewise, the most extreme LEC values were obtain when $\hat{M}_P$ and M_A became smaller and $\hat{M}_S$ larger. These three parameters are responsible for most of the uncertainties. The impact of the M_V, F and m_0 errors in the global precision is negligible.

The RχT computation progressively approaches the physical value as one incorporates more and more physical information. This is quite non-trivial, as the introduction of a new chiral invariant operator leads to the opening of the new absorptive cuts in addition to those channels we are in principle interested in. For instance, the $c_m \langle\, S\chi_+ \,\rangle$ rules the decay into one scalar resonance and also contributes to the S-meson exchange in the $\pi\pi$ channel. But at the same time it also induces the decay into $S\pi$ (though other operators like λ_1^{SP} are also relevant). Thus, the $\mathcal{L}_{RR'}$ terms were used in our calculation to improve the description of the $R\pi$ channels, which were incompletely described by the linear lagrangian $\mathcal{L}_R$ [8]. The price to pay was that new RR' channels with two intermediate resonances showed up in our NLO computation of the correlator. Although the

impact of these higher thresholds is suppressed at low energies if one chooses a convenient renormalization scheme [32, 46], their impact in the high-energy matching and OPE constraints is a priori non-trivial. In this chapter we find that, indeed, the most relevant information in order to extract the low energy chiral couplings seems to be provided by the lightest cuts. On the other hand, one realizes that the values of the couplings differ from those in the full large–N_C theory [40] and that the description of the heaviest absorptive channels may be very distorted [43]. Indeed, we obtain the resonance couplings $\lambda_1^{SP} = -0.22 \pm 0.08$, $\lambda_1^{PV} = 0.14 \pm 0.07$ and $|\lambda_1^{SA}| = 0.16 \pm 0.14$. Even though these numbers have the right signs and order of the magnitude as the theoretical expectations $\lambda_1^{SP} = -\frac{d_m}{c_m} = \frac{c_d - 2c_m}{2d_m} \sim -0.7$, $\lambda_1^{PV} = \frac{G_V}{2\sqrt{2}d_m} \sim 0.7$ and $\lambda_1^{SA} = 0$ (in our analysis, for convention, we have took c_m, d_m and G_V as positive), their values are still far from being accurate determinations of these parameters.

2.8.4 Impact of the RR' channels

In this section we will make a digression on the importance of the RR' intermediate cuts that are opened after including the $\mathcal{L}_{RR'}$ operators in the LO action. We will remove by hand the contributions with two–resonance cuts. Although this procedure is not well justified from the QFT point of view, we will perform this exercise in order make a rough comparison with the previous dispersive calculation of the octet $SS-PP$ correlator [31]. The RR' channels were neglected there, as their contribution in the dispersive integral was suppressed at low energies by inverse powers of $(M_R + M_{R'})^2$.

Thus, we redid the calculation and removed by hand the diagrams with two–resonance cuts. This expression was then matched to the OPE at short distances, producing finally the low–energy constants,

$$L_8(\mu_0) = (0.1 \pm 0.7) \cdot 10^{-3}\,, \qquad C_{38}(\mu_0) = (-3 \pm 9) \cdot 10^{-6}\,, \quad (2.118)$$

where we used the same inputs as in the previous subsection. The errors are now found to be larger and, though compatible with our final result (2.117), the elimination of the RR' cuts decreases slightly the range for the LEC determinations, approaching them to the lower values preferred by recent $\mathcal{O}(p^6)$ analysis [7] and lattice simulations [53]. However, discarding these heavier channels from the one-loop computation in this way does not seem very sound from the theoretical point of view and it is shown here just as an exercise.

2.9 Conclusions

In this chapter, we have performed the one loop QFT calculation of the two-point $SS - PP$ correlator within RχT. We started with Ecker *et al.*'s lagrangian [8], containing only operators with at most one resonance field, and renormalized step by step all the relevant vertex-functions and propagators. Then we imposed OPE constraints on the full one-loop correlator, not on separate individual channels as it was performed in a previous NLO calculation [31]. Likewise, no short-distance constraint from other observables [39] was used in the present article.

After fixing part of our RχT couplings through these high-energy conditions, we expanded our result at low energies. Due to the chiral invariant structure

of RχT, we were able to match the chiral logarithms and found predictions for the χPT coupling constants $L_8(\mu)$ and $C_{38}(\mu)$. The large discrepancy of these first numerical determinations with respect to the numbers found in the literature indicated that the simple Lagrangian $\mathcal{L}_R$ (with operators with at most one resonance field [8]) pointed out the need for a more complicated structure of the RχT action. The $\mathcal{L}_R$ terms could not fully describe the dynamics of all the two-meson intermediate channels: just the $\pi\pi$ channel description was adequately provided by the operators with at most one resonance field; all other channels ($V\pi$, $S\pi\ldots$) did not have the right short-distance behavior. Thus, beyond any numerical discrepancy in the LECs, the absence of operators with two an three resonance fields produces a severe theoretical issue at high energies [30].

In order to arrange the $R\pi$ cuts with one resonance and one Goldstone we add all the operators $\mathcal{L}_{RR'}$ with two resonance fields relevant for the $SS-PP$ correlator to the leading RχT lagrangian. These are the λ_1^{SP}, λ_1^{PV} and λ_1^{SA} terms given in Eq. (2.102). The introduction of these operators produce a dramatic improvement. When only one of them is added to the action, the LEC predictions move in the right direction, i.e., towards the range of values found in previous studies. After considering all the three $\mathcal{L}_{RR'}$ operators, we obtain the final values for $\mu_0 = 770$ MeV,

$$L_8(\mu_0) \;=\; (1.0 \pm 0.4)\cdot 10^{-3}\,, \qquad\qquad C_{38}(\mu_0) \;=\; (8 \pm 5)\cdot 10^{-6}\,, \quad (2.119)$$

in reasonable agreement with the values obtained through other approaches [5–7, 31,52,53]. We want to remark, that this result is progressively approached as more and more complicated operators are added to the hadronic action. The terms of the lagrangian that rule the lightest channels result crucial and, thus, those determining heavier cuts not included in the analysis are expected to produce little influence.

The essential difference with the previous dispersive calculation of the $SS-PP$ correlator at NLO [31] is the presence of RR' cuts in the present work. These intermediate channels automatically show up at the very moment we place the $\mathcal{L}_{RR'}$ operators in the RχT action. Although it is possible to demonstrate that the contribution from these heavy RR' cuts is suppressed at low energies [32, 46], their impact in high-energy conditions such as the NLO Weinber sum-rules is pretty non-trivial. The difference between the present article and Ref. [31] could be taken as a crude estimate of the impact of neglecting those higher channels.

In addition to the estimation of LECs, we also discussed some general issues about renormalization schemes within RχT. The use of the running $\widetilde{MS}$ masses $M_R(\mu)$ was not very convenient as their meaning changed as one added new operators to the RχT action. Thus, they were reexpressed in terms of pole masses $\hat{M}_R$. Likewise, we found that, with respect to the large–N_C WSR, the NLO Weinberg sum-rules (2.86) led to large uncertainties and variations for the values of c_m and d_m derived from them in the $\widetilde{MS}$–scheme. A more convenient subtraction scheme was found to minimize these uncertainties that stemmed from the high-energy matching whereas, on the other hand, it was found to leave the low energy prediction (2.98) unchanged (except for the improved accuracy in the resonance coupling determination from short-distance constraints).

2.10 Appendix

2.10.1 Running of the renormalized parameters with $\mathcal{L}_G + \mathcal{L}_R$

When only operators with at most one resonance fields are considered in the RχT action [8], one finds before performing the meson field redefinition the running,

$$\begin{aligned}
\frac{\partial \widetilde{L}_8}{\partial \ln \mu^2} &= \frac{3}{512\pi^2 F^2}\left[16(c_m^2 - d_m^2) - F^2 - 16 c_d c_m + 4c_d^2 + 2G_V^2\right] , \\
\frac{\partial M_S^2}{\partial \ln \mu^2} &= \frac{\partial M_P^2}{\partial \ln \mu^2} = \frac{\partial c_m}{\partial \ln \mu^2} = \frac{\partial d_m}{\partial \ln \mu^2} = 0 , \\
\frac{\partial X_S}{\partial \ln \mu^2} &= -\frac{3c_d^2}{16\pi^2 F^4} , \qquad \frac{\partial X_P}{\partial \ln \mu^2} = 0 , \\
\frac{\partial \lambda_{18}^S}{\partial \ln \mu^2} &= \frac{3c_d}{64\pi^2 F^2} , \qquad \frac{\partial \lambda_{13}^P}{\partial \ln \mu^2} = 0 .
\end{aligned} \tag{2.120}$$

After the renormalization one may then consider a convenient field redefinition that removes precisely the renormalized $X_{S,P}$, λ_{13}^P and λ_{18}^S. They (and their running) seem to disappear from the theory although their information is actually encoded in the renormalized effective couplings that remain in the action. Their running turns out to be then

$$\begin{aligned}
\frac{\partial \widetilde{L}_8^{\rm eff}}{\partial \ln \mu^2} &= \frac{3}{512\pi^2 F^2}\left[16\, c_m^2 - 16\, d_m^2 - F^2 - 8\, c_d c_m + 2\, c_d^2 + 2\, G_V^2 - 16\, c_d^2 c_m^2\right] , \\
\frac{\partial M_S^{\rm eff\ 2}}{\partial \ln \mu^2} &= \frac{3c_d^2 M_S^4}{16\pi^2 F^4} , \qquad \frac{\partial M_P^{\rm eff\ 2}}{\partial \ln \mu^2} = 0 , \\
\frac{\partial c_m^{\rm eff}}{\partial \ln \mu^2} &= \frac{3c_d M_S^2}{64\pi^2 F^4}(4c_d c_m - F^2) , \qquad \frac{\partial d_m^{\rm eff}}{\partial \ln \mu^2} = 0 .
\end{aligned} \tag{2.121}$$

2.10.2 On-shell scheme for c_m and d_m

This would be a continuation of the pole-mass scheme. In addition to this, the renormalized on-shell couplings $\hat{c}_m$ and $\hat{d}_m$ are prescribed, respectively, by the real part of the residue of the correlator at the scalar and the pseudoscalar resonance poles [31, 32]. This was the scheme considered in the dispersive approach from Refs. [31, 32]. The shift $\Delta\kappa$ with respect to the $\widetilde{MS}$–subtraction prescription is given up to NLO in $1/N_C$ by

$$\begin{aligned}
2\, c_m \Delta c_m &= c_m^2 - \hat{c}_m^2 = \frac{c_m}{2B_0}\,{\rm Re}\Phi_{sS}^r(M_S^2)^{1\ell} \; - \; c_m^2\,{\rm Re}\Sigma_S^{r\,\prime}(M_S^2)^{1\ell} , \\
2\, d_m \Delta d_m &= d_m^2 - \hat{d}_m^2 = \frac{d_m}{2B_0}\,{\rm Re}\Phi_{pP}^r(M_P^2)^{1\ell} \; - \; d_m^2\,{\rm Re}\Sigma_P^{r\,\prime}(M_P^2)^{1\ell} .
\end{aligned} \tag{2.122}$$

In the case where only $\mathcal{L}_R$ interactions are considered, one has

$$\begin{aligned}
2\, c_m \Delta c_m &= \frac{4\, c_d c_m}{F^2}\,\frac{3\, M_S^2}{128\pi^2}\left[-1 + \left(1 - \frac{4\, c_d c_m}{F^2}\right)\ln\frac{M_S^2}{\mu^2}\right] , \\
2\, d_m \Delta d_m &= 0 .
\end{aligned} \tag{2.123}$$

2.10.3 Feynman integrals

The scalar integrals are

$$\begin{aligned} A_0(M^2) &= \int \frac{dk^d}{i(2\pi)^d} \frac{1}{k^2 - M^2 + i\epsilon}, \\ B_0(p^2, M_a^2, M_b^2) &= \int \frac{dk^d}{i(2\pi)^d} \frac{1}{(k^2 - M_a^2 + i\epsilon)[(p-k)^2 - M_b^2 + i\epsilon]} \end{aligned} \quad (2.124)$$

Using the formula in [30] we use the following expansions

$$\begin{aligned} A_0(M^2) &= \frac{-M^2}{16\pi^2}\left\{\lambda_\infty + \ln\frac{M^2}{\mu^2}\right\}, \\ B_0(p^2, 0, 0) &= -\frac{1}{16\pi^2}\left\{\lambda_\infty - 1 + \ln\left(\frac{-p^2}{\mu^2}\right)\right\}, \\ B_0(p^2, 0, M^2) &= -\frac{1}{16\pi^2}\left\{\lambda_\infty + \ln\frac{M^2}{\mu^2} - 1 + \left(1 - \frac{M^2}{p^2}\right)\ln\left(1 - \frac{p^2}{M^2}\right)\right\}, \\ B_0(p^2, M^2, M^2) &= -\frac{1}{16\pi^2}\left\{\lambda_\infty + \ln\frac{M^2}{\mu^2} - 1 + \sigma_M \ln\left(\frac{\sigma_M + 1}{\sigma_M - 1}\right)\right\} \\ \overline{J}(p^2, M_a^2, M_b^2) &= \frac{1}{32\pi^2}\left\{2 + \left[\frac{M_a^2 - M_b^2}{p^2} - \frac{M_a^2 + M_b^2}{M_a^2 - M_b^2}\right]\ln\frac{M_b^2}{M_a^2}\right. \\ &\quad \left. - \frac{\lambda^{1/2}(p^2, M_a^2, M_b^2)}{p^2}\ln\left(\frac{\left[p^2 + \lambda^{1/2}(p^2, M_a^2, M_b^2)\right]^2 - (M_a^2 - M_b^2)^2}{\left[p^2 - \lambda^{1/2}(p^2, M_a^2, M_b^2)\right]^2 - (M_a^2 - M_b^2)^2}\right)\right\}, \end{aligned} \quad (2.125)$$

where $\sigma_M = \sqrt{1 - 4M^2/p^2}$ and $\lambda(x, y, z) = (x - y - z)^2 - 4yz$.

2.10.4 Useful expansions

Using expansions for $x \to \infty$

$$\begin{aligned} \phi(x) &= \ln(-x) - 1 - \frac{3\ln(-x)}{x} + \frac{3}{2x} + \frac{3\ln(-x)}{x^2} + \frac{3}{2x^2} + \ldots, \\ \psi(x) &= -\ln(-x) + \frac{2\ln(-x)}{x} - \frac{\ln(-x)}{x^2} - \frac{3}{2x^2} + \ldots, \\ (1 - \frac{1}{x})\ln(1 - x) &= \ln(-x) - \frac{\ln(-x)}{x} - \frac{1}{x} + \frac{1}{2x^2} + \ldots \end{aligned}$$

3. Renormalization in the effective theory for spin-1 resonances

3.1 Introduction

As is well known, in the low energy region the dynamical degrees of freedom of QCD are not quarks and gluons but the low lying hadronic states and, as a consequence, a non-perturbative description of the their dynamics is inevitable. An approach using effective Lagrangians appears to be very efficient for this purpose and it has made a considerable progress recently. In the very low energy region ($E \ll \Lambda_H \sim 1\text{GeV}$), the octet of the lightest pseudoscalar mesons (π, K, η) represents the only relevant part of the QCD spectrum. The Chiral Perturbation Theory (χPT) [1–3] based on the spontaneously broken chiral symmetry $SU(3)_L \times SU(3)_R$ grew into a very successful model-independent tool for the description of the Green functions (GF) of the quark currents and related low-energy phenomenology. The pseudoscalar octet is treated as the octet of pseudo-Goldstone bosons (PGB) and χPT is organized according to the Weinberg power-counting formula [1] as a rigorously defined simultaneous perturbative expansion in small momenta and the light quark masses. Recently, the calculations are performed at the next-to-next-to-leading order $O(p^6)$ (for a comprehensive review and further references see [54]).

In the intermediate energy region ($\Lambda_H \leq E < 2\text{GeV}$), where the set of relevant degrees of freedom includes also the low lying resonances, the situation is less satisfactory. This region is not separated by a mass gap from the rest of the spectrum and, as a consequence, there is no appropriate scale playing the role analogous to that of Λ_H in χPT. Therefore, the effective theory in this region cannot be constructed as a straightforward extension of the χPT low energy expansion by means of introducing resonances *e.g.* as homogenously (but non-linearly) transformed matter fields in the sense of [55], [56] and pushing the scale Λ_H to 2GeV.

In order to introduce another type of effective Lagrangian description, the considerations based on the large N_C expansion together with the high-energy constraints derived from perturbative QCD and OPE appear to be particularly useful. In the limit $N_C \to \infty$, the chiral symmetry is enlarged to $U(3)_L \times U(3)_R$ and the spectrum relevant for the correlators of the quark bilinears consists of an infinite tower of free stable mesonic resonaces exchanged in each channel and classified according to the symmetry group $U(3)_V$. An appropriate description should therefore require an infinite number of resonance fields entering the $U(3)_L \times U(3)_R$ symmetric effective Lagrangian. Because the quasi-classical expansion is correlated with the large N_C expansion, the interaction vertices are suppressed by an appropriate power of $N_C^{-1/2}$ according to the number of the meson legs. At the leading order only the tree graphs have to be taken into account . An approximation to this general picture where we limit the number of the resonance fields to one in each channel and matching the resulting theory in the high energy region

with OPE is known as the Resonance Chiral Theory (RχT) (it was introduced in seminal papers [8, 9]). Integrating out the resonance fields from the Lagrangian of RχT in the low energy region and the subsequent matching with χPT has become very successful tool for the estimates of the resonance contribution to the values of the $O(p^4)$ [8] and $O(p^6)$ [57,58] low energy constants (LEC) entering the χPT Lagrangian. Therefore, studying RχT can help us to understand not only the dynamics of resonances but also the origin of LECs in χPT.

However, even when restricting to the case of the matter field formalism, it is known from the very beginning [9] that the form of the RχT Lagrangian is not determined uniquely. The reason is that the resonances with a given spin can be described in many ways using fields with different Lorentz structure. For example, for the spin-one resonances one can use *i.a.* the Proca vector field or the antisymmetric tensor field or both (within the first order formalism [59, 60]). Though the theories based on different types of fields with Lagrangians which contain only finite number of operators are not strictly equivalent already on the tree level (in general, it is necessary to include nonlocal interaction or infinite number of operators and contact terms to ensure the complete equivalence, see [60]), we can always ensure a weak equivalence of all three formalisms up to a given fixed chiral order (this was established to $O(p^4)$ in [9] and enlarged to $O(p^6)$ in [60]).

As we have mentioned above, the lack of the mass gap (which could provide us with a scale playing the role analogous to Λ_H) prevents us from using a straightforward extension of the Weinberg power-counting formula [1] taking the resonance masses and momenta of the order $O(p)$ on the same footing as for PGB. Also the usual chiral power counting which takes the resonance masses as an additional heavy scale (which is counted as $O(1)$) fails within the RχT in a way analogous to the χPT with baryons [61]. Nevertheless, it seems to be fully legitimate to go beyond the tree level RχT and calculate the loops [62–70].

Being suppressed by one power of $1/N_C$, the loops allow to encompass such NLO effects in the $1/N_C$ expansion as resonance widths, resonance cuts and the final state interaction and (by means matching with χPT) to determine the NLO resonance contribution to LEC (and their running with renormalization scale).

However, we can expect both technical and conceptual complications connected with the renormalization of the effective theory for which no natural organization of the expansion (other than the $1/N_C$ counting) exists. Especially, because there is no natural analog of the Weinberg power counting in RχT, we can expect mixing of the naive chiral orders in the process of the renormalization (*e.g* the loops renormalize the $O(p^2)$ LEC and also counterterms of unusually high chiral orders are needed). Also a straightforward construction of the propagator from the self-energy using the Dyson re-summation can bring about the appearance of new poles in the GF. Because the spin-one particles are described using fields transforming under the reducible representation of the rotation group and due to the lack of an appropriate protective symmetry, some of these additional poles can correspond to new degrees of freedom, which are frozen at the tree level. The latter might be felt as a pathological artefact of the not carefully enough formulated theory, particularly because these extra poles might be negative norm ghosts or tachyons [71]. On the other hand, however, we could also try to take an advantage of this feature and to adjust the poles in such a way that they

correspond to the well established resonance states [72].

Let us note, that similar problems are generic for the description of the higher spin particles in terms of quantum field theory. As an example we can mention e.g. the problem with the renormalization of quantum gravity which is trying to be cured by imposing additional symmetry or by introducing a non-perturbative quantization believing that UV divergences are only artefact of a perturbative theory. In the context of the extensions of the χPT, this has been studied in connection with introducing of the spin-3/2 isospin-3/2 $\Delta(1232)$ resonance in the baryonic sector (for a review see [73] and references therein). The Rarita-Schwinger field commonly used for its description contains along with the spin-3/2 sector also spin-1/2 sector, which is frozen at the tree level due to the form of the free equations of motion. These provides the necessary constraints reducing the number of propagating spin degrees of freedom to four corresponding to spin 3/2 particles. However, these constraints are generally not present in the interacting theory and negative norm ghost [74] and/or tachyonic [75] poles might appear beyond the tree level. The appearance of these extra unphysical degrees of freedom can be avoided by means of the requirement of additional protective gauge symmetry under which the interaction Lagrangian has to be invariant. Such a symmetry, which is also a symmetry of the kinetic term (but not of the mass term), is an analog of the $U(1)$ gauge symmetry of the electromagnetic field and its role is also similar. As it has been shown by means of path integral formalism, it leads to the same constraints as in the noninteracting theory and prevent therefore the extra spin-1/2 states from propagating.

On the other hand, it has been proved, that the most general interaction Lagrangian at most bilinear in Rarita-Schwinger field (*i.e.* without the protective gauge symmetry) is on shell equivalent to the gauge invariant one [76] . The latter is, however, nonlocal (or equivalently it contains an infinite number of terms). Also the above protective gauge symmetry is, as a rule, in a conflict with chiral symmetry, and has therefore to be implemented with a care. Though there are efficient methods how to handle this obstacles in concrete loop calculations [73], [76], the problem still has not been solved completely.

In the following, we would like to discuss these problems in more detail. As an explicit example we use the one-loop renormalization of the propagator corresponding to the fields which originally describe 1^{--} vector resonance (ρ meson) at the tree level within the Proca field, the antisymmetric tensor field and within the first order formalism in the chiral limit. The situation here is quite similar to the case of spin-3/2 resonances discussed above. In addition, to the spin-1 degrees of freedom, there are extra sectors that are frozen at the tree level. There exists a protective gauge symmetry which prevents these modes from propagation. The kinetic term is invariant with respect to this symmetry while the mass term is not.

By means of an explicit calculation we will show that (unlike the ordinary χPT) the one-loop corrections to the self-energy need counterterms with a number of derivatives ranging from zero up to six and also that a new kinetic counterterm with two derivatives (which was not present in the tree level Lagrangian) is necessary. We will also demonstrate that the corresponding propagator obtained by means of Dyson re-summation of the one-particle irreducible self-energy insertions has unavoidably additional poles. Due to the unusual higher order growth

of the self-energy in the UV region some of them are inevitably pathological (with a negative norm or a negative mass squared). Though these additional poles are decoupled in the limit $N_C \to \infty$, for reasonable concrete values of the parameters of the Lagrangian they might appear near or even inside the region for which $R\chi T$ was originally designed. We also discuss briefly within the antisymmetric tensor formalism a possible interpretation of some of the non-pathological poles as a manifestation of the dynamical generation of various types of additional 1+-states. We will also show that the appropriate adjustment of coupling constants in the antisymmetric tensor case allows us (at least in principle) to generate in this way the one which could be identified *e.g.* with the $b_1(1235)$ meson [72]. Such a mechanism is analogous to the model [77] for the dynamical generation of the scalar resonances from the bare quark-antiquark "seed", the propagator of which develops (after dressing with pseudoscalar meson loops) additional poles identified *e.g.* as $a_0(980)$ (cf. also [78], [79]).

The chapter organized as follows. In Section 3.2 we remind the basic facts about the propagators and briefly discuss the issue of the additional degrees of freedom in all three formalisms for the description of spin-one resonances. We use the path integral formulation where the protective symmetry analogous to the Rarita-Schwinger case is manifest. In Section 3.3 we discuss the power counting. We try to formulate here a formal self-consistent organization of the counterterms and one-particle irreducible graphs, which sorts the operators in the Lagrangian according to the number of derivatives as well as number of the resonance fields and which is useful for the proof of renormalizability of the $R\chi T$ as an effective theory. In Section 3.4 we present the results of the explicit calculation of the self-energies. Then we give a list of counterterms and briefly discuss the renormalization prescription. Section 3.5 is devoted to the construction of the propagators and to the discussion of their poles. Because the basic ideas are similar within all three formalisms, we concentrate here on the antisymmetric tensor case. Section 3.6 contains summary and conclusions. Some of the long formulae are postponed to the appendices: the explicit form of the renormalization scale independent parameters of the self-energies are collected in Appendix 3.7.4, namely for the Proca field in 3.7.4, for the antisymmetric tensor field in 3.7.4 and for the first order formalism in 3.7.4. In Appendix 3.7.5 we give a proof of the positivity of the spectral functions for the antisymmetric tensor propagator.

3.2 Propagators and poles

In this section, we collect the basic properties of the propagators and the corresponding self-energies within the Proca field, the antisymmetric tensor field and the first order formalisms. The discussion will be as general as possible without explicit references to $R\chi T$, which can be assumed as the special example of the general case.

3.2.1 Proca formalism

General properties of the propagator

We start our discussion with a standard textbook example of the interacting Proca field. Let us write the Lagrangian in the form

$$\mathcal{L} = \mathcal{L}_0 + \mathcal{L}_{int}, \tag{3.1}$$

where the free part of the Lagrangian is

$$\mathcal{L}_0 = -\frac{1}{4}\widehat{V}_{\mu\nu}\widehat{V}^{\mu\nu} + \frac{1}{2}M^2 V_\mu V^\mu \tag{3.2}$$

with

$$\widehat{V}_{\mu\nu} = \partial_\mu V_\nu - \partial_\nu V_\mu. \tag{3.3}$$

Without any additional assumptions on the form and symmetries of the interaction part of the Lagrangian $\mathcal{L}_{int}$, we can expect the following general structure of the full two-point one-particle irreducible (1PI) Green function

$$\Gamma^{(2)}_{\mu\nu}(p) = (M^2 - p^2 + \Sigma^T(p^2))P^T_{\mu\nu} + (M^2 + \Sigma^L(p^2))P^L_{\mu\nu}. \tag{3.4}$$

Here

$$P^L_{\mu\nu} = \frac{p_\mu p_\nu}{p^2} \tag{3.5}$$

$$P^T_{\mu\nu} = g_{\mu\nu} - \frac{p_\mu p_\nu}{p^2} \tag{3.6}$$

are the usual longitudinal and transverse projectors and $\Sigma^{T,L}$ are the corresponding transverse and longitudinal self-energies, which vanish in the free field limit. Inverting (3.4) we get for the full propagator

$$\Delta_{\mu\nu}(p) = -\frac{1}{p^2 - M^2 - \Sigma^T(p^2)}P^T_{\mu\nu} + \frac{1}{M^2 + \Sigma^L(p^2)}P^L_{\mu\nu}. \tag{3.7}$$

The possible (generally complex) poles of such a propagator are of two types; either at $p^2 = s_V$, where s_V is given by the solutions of

$$s_V - M^2 - \Sigma^T(s_V) = 0, \tag{3.8}$$

or at $p^2 = s_S$ where s_S is the solution of

$$M^2 + \Sigma^L(s_S) = 0. \tag{3.9}$$

Let us first discuss the poles of the first type. Assuming that (3.8) is satisfied for $s_V = M_V^2 > 0$, then for $p^2 \to M_V^2$

$$\begin{aligned}\Delta_{\mu\nu}(p) &= \frac{Z_V}{p^2 - M_V^2}\left(-g_{\mu\nu} + \frac{p_\mu p_\nu}{M^2}\right) + O(1) \\ &= \frac{Z_V}{p^2 - M_V^2}\sum_\lambda \varepsilon^{(\lambda)}_\mu(p)\varepsilon^{(\lambda)*}_\nu(p) + O(1)\end{aligned} \tag{3.10}$$

where

$$Z_V = \frac{1}{1 - \Sigma'^T(M_V^2)} \tag{3.11}$$

and where $\varepsilon_\mu^{(\lambda)}(p)$ are the usual spin-one polarization vectors. Under the condition $Z_V > 0$ the poles of this type correspond to spin-one one particle states $|p, \lambda, V\rangle$ which couple to the Proca field as

$$\langle 0|V_\mu(0)|p, \lambda, V\rangle = {Z_V}^{1/2}\varepsilon_\mu^{(\lambda)}(p). \tag{3.12}$$

At least one of these states is expected to be perturbative in the sense that its mass and coupling to V_μ can be written as

$$M_V^2 = M^2 + \delta M_V^2 \tag{3.13}$$

$$Z_V = 1 + \delta Z_V, \tag{3.14}$$

where δM_V^2 and δZ_V are small corrections vanishing in the free field limit. This solution corresponds to the original degree of freedom described by the free part of the Lagrangian $\mathcal{L}_0$. The additional one particle states corresponding to the other possible (non-perturbative) solutions of (3.8) decouple in the free field limit.

The second type of poles is given by (intrinsically nonperturbative) solutions of (3.9). Suppose that this condition is satisfied by $s_S = M_S^2 > 0$. For $p^2 \to M_S^2$

$$\Delta_{\mu\nu}(p) = \frac{Z_S}{p^2 - M_S^2}\frac{p_\mu p_\nu}{M_S^2} + O(1) \tag{3.15}$$

where

$$Z_S = \frac{1}{\Sigma'^L(M_S^2)}. \tag{3.16}$$

Assuming $Z_S > 0$ this pole corresponds to the spin-zero one particle state $|p, S\rangle$ which couples to V_μ as

$$\langle 0|V_\mu(0)|p, S\rangle = \mathrm{i}p_\mu\frac{{Z_S}^{1/2}}{M_S}. \tag{3.17}$$

For the free field this scalar mode is frozen and does not propagate according to the special form of the Proca field Lagrangian. Therefore, in the limit of vanishing interaction the extra scalar state decouples.

Without any additional assumptions on the symmetries of the interaction Lagrangian we can therefore expect the appearance of additional dynamically generated degrees of freedom.

The general picture is, however, more subtle. Note that, the interpretation of the above additional spin-one and spin-zero poles as physical one-particle asymptotic states depends on the proper positive sign of the corresponding residues Z_V, $Z_S > 0$, otherwise the norm of these states is negative and the poles correspond to the negative norm ghosts. Similarly, also poles with $M_{V,S}^2 < 0$ can be generated, which correspond to the tachyonic states. Let us illustrate this feature using a toy example. Suppose, that the only interaction terms are of the form

$$\mathcal{L}_{int} \equiv \mathcal{L}_{ct} = -\frac{\alpha}{4}\widehat{V}_{\mu\nu}\widehat{V}^{\mu\nu} - \frac{\beta}{2}(\partial_\mu V^\mu)^2 + \frac{\gamma}{2M^2}(\partial_\mu\widehat{V}^{\mu\nu})(\partial^\rho\widehat{V}_{\rho\nu}) + \frac{\delta}{2M^2}(\partial_\mu\partial_\rho V^\rho)(\partial^\mu\partial_\sigma V^\sigma). \tag{3.18}$$

Such a Lagrangian can be typically produced by radiative corrections in an effective field theory with Proca field, which does not couple to other fields in a $U(1)$ gauge invariant way, and can provide us with counterterms necessary to renormalize the loops contributing to the V field self-energy. $\mathcal{L}_{ct}$ gives rise to the following contributions to $\Sigma^T(p^2)$ and $\Sigma^L(p^2)$

$$\Sigma^T(p^2) = -\alpha p^2 + \gamma \frac{p^4}{M^2} \tag{3.19}$$

$$\Sigma^L(p^2) = -\beta p^2 + \delta \frac{p^4}{M^2}. \tag{3.20}$$

As a result, we have two spin-one and two spin-zero one-particle states. The masses and residue of the spin-one states are then

$$M^2_{V\pm} = M^2 \left(1 + \frac{1+\alpha-2\gamma \mp \sqrt{(1+\alpha)^2-4\gamma}}{2\gamma}\right) \tag{3.21}$$

$$1 - \Sigma'^T(M^2_{V\pm}) = \pm\sqrt{(1+\alpha)^2-4\gamma}, \tag{3.22}$$

which are real for for $(1+\alpha)^2 - 4\gamma > 0$. In the limit $\alpha, \gamma \to 0$, $\alpha/\gamma = const$ we get either the perturbative solution with mass M_{V+} or (for $\gamma > 0$) an additional spin-one ghost with mass M_{V-} (for $1+\alpha > 0$ and $\gamma < 0$ this pole is tachyonic). Similarly for the spin-zero states

$$M^2_{S\pm} = M^2 \left(\frac{\beta \mp \sqrt{\beta^2 - 4\delta}}{2\delta}\right) \tag{3.23}$$

$$\Sigma'^L(M^2_{S\pm}) = \mp\sqrt{\beta^2 - 4\delta}. \tag{3.24}$$

The poles are real for $\beta^2 > 4\delta$ and *e.g.* for $\beta, \delta > 0$ one of the poles is spin-zero ghost. In both cases for appropriate values of the parameters we can get also two tachyons or even the complex Lee-Wick pair of ghosts. These features are of course well known in the connection with the higher derivative regularization (as well as with the properties of the gauge-fixing term).

Additional degrees of freedom in the path integral formalism

The additional degrees of freedom discussed in the previous subsection can be made manifest in the path integral formalism. Let us start with the generating functional for the interacting Proca field

$$Z[J] = \int \mathcal{D}V \exp \left(\mathrm{i} \int \mathrm{d}^4x \left(-\frac{1}{4}\widehat{V}_{\mu\nu}\widehat{V}^{\mu\nu} + \frac{1}{2}M^2 V_\mu V^\mu + \mathcal{L}_{int}(V, J, \ldots)\right)\right), \tag{3.25}$$

where the external sources are denoted collectively by J. In order to separate the transverse and longitudinal degrees of freedom of the field V_μ within the path integral we can use the standard Faddeev-Popov trick with respect to the $U(1)$ gauge transformation of the field V_μ

$$V_\mu \to V_\mu + \partial_\mu \Lambda. \tag{3.26}$$

As a result, we get the generating functional in the form

$$Z[J] = \int \mathcal{D}V_\perp \mathcal{D}\Lambda \exp\left(\mathrm{i}\int \mathrm{d}^4x \left(\frac{1}{2}V_\perp^\mu \Box V_{\perp\mu} + \frac{1}{2}M^2 V_\perp^\mu V_{\perp\mu} + \frac{1}{2}M^2\partial_\mu\Lambda\partial^\mu\Lambda + \mathcal{L}_{int}\right)\right). \tag{3.27}$$

where $\mathcal{L}_{int} = \mathcal{L}_{int}(V_\perp - \partial\Lambda, J, \ldots)$. Here $\mathcal{D}V_\perp = \mathcal{D}V\delta(\partial_\mu V^\mu)$ and

$$V_\perp^\mu = \left(g^{\mu\nu} - \frac{\partial^\mu\partial^\nu}{\Box}\right)V_\nu$$

is the transverse part of the vector field V^μ, the longitudinal part of which corresponds to the scalar field Λ, *i.e.*

$$V^\mu = V_\perp^\mu + \partial^\mu\Lambda. \tag{3.28}$$

The free propagators of the fields $V_\perp^\mu$ and Λ are

$$\Delta_\perp^{\mu\nu}(p) = -\frac{P^{T\,\mu\nu}}{p^2 - M^2} \tag{3.29}$$

$$\Delta_\Lambda(p) = \frac{1}{M^2}\frac{1}{p^2}. \tag{3.30}$$

Both these propagators have spurious poles at $p^2 = 0$, however, the only necessary combination which matters in the Feynman graphs is

$$\Delta_0^{\mu\nu}(p) = \Delta_\perp^{\mu\nu}(p) + p^\mu p^\nu \Delta_\Lambda(p), \tag{3.31}$$

which coincides with the original free propagator of the field V^μ and the spurious poles cancel each other.

Note that, provided the interaction Lagrangian $\mathcal{L}_{int}$ is symmetric under the $U(1)$ gauge transformation (3.26), the spin-zero field Λ completely decouples and can be integrated out . The theory can then be formulated solely in terms of the field $V_\perp^\mu$. The $U(1)$ invariant form of the interaction allows to simplify the propagator $\Delta_\perp^{\mu\nu}(p)$

$$\Delta_\perp^{\mu\nu}(p) \to -\frac{g_{\mu\nu}}{p^2 - M^2} \tag{3.32}$$

within the Feynman graphs and the spurious pole $p^2 = 0$ in (3.29) becomes harmless. In this case, the scalar one-particle states cannot be dynamically generated. On the other hand, in the case when $\mathcal{L}_{int}$ is not invariant with respect to (3.26), we cannot forget the longitudinal component of V^μ which has now nontrivial interactions and, as a result, contributions to Σ^L can be generated.

Let us now return to the illustrative example discussed in the previous subsection. Suppose that the interaction Lagrangian has the form

$$\mathcal{L}_{int} = \mathcal{L}_{ct} + \mathcal{L}'_{int} \tag{3.33}$$

where $\mathcal{L}_{ct}$ is the toy interaction Lagrangian (3.18) and we assume $\alpha > -1$ and $\delta > 0$ in what follows. Then it is possible to transform $Z[J]$ to the form of the path integral with all the additional degrees of freedom represented explicitly

in the Lagrangian and the integration measure. In terms of the transverse and longitudinal degrees of freedom we get

$$\begin{aligned}\mathcal{L}_{int}(V_\perp - \partial\Lambda, J, \ldots) &= \mathcal{L}_{ct}(V_\perp - \partial\Lambda, J, \ldots) + \mathcal{L}'_{int}(V_\perp - \partial\Lambda, J, \ldots) \\ &= \frac{\alpha}{2}V_\perp^\mu \Box V_{\perp\mu} - \frac{\beta}{2}(\Box\Lambda)^2 + \frac{\gamma}{2M^2}(\Box V_\perp^\mu)(\Box V_{\perp\mu}) + \frac{\delta}{2M^2}(\partial_\mu\Box\Lambda)(\partial^\mu\Box\Lambda) \\ &+ \mathcal{L}'_{int}(V_\perp - \partial\Lambda, J\ldots). \end{aligned} \tag{3.34}$$

In order to lower the number of derivatives in the kinetic terms we integrate in auxiliary scalar fields χ, ρ, π, σ and auxiliary transverse vector field $B_{\perp\mu}$ writing *e.g.*

$$\exp\left(-i\int \mathrm{d}^4x \frac{\beta}{2}(\Box\Lambda)^2\right) = \int \mathcal{D}\chi \exp\left(i\int \mathrm{d}^4x \left(\frac{1}{2\beta}\chi^2 - \partial_\mu\chi\partial^\mu\Lambda\right)\right) \tag{3.35}$$

and similarly for other higher derivative terms. After the superfluous degrees of freedom are identified and integrated out, the fields are re-scaled and then the resulting mass matrix can be diagonalized by means of two symplectic rotations with angles θ_V and θ_S (the technical details are postponed to the Appendix 3.7.1). Finally we get (under the conditions $(1+\alpha)^2 > 4\gamma$ and $\beta^2 > 4\delta$)

$$Z[J] = \int \mathcal{D}V_\perp \mathcal{D}B_\perp \mathcal{D}\Lambda \mathcal{D}\chi \mathcal{D}\sigma \exp\left(i\int \mathrm{d}^4x \mathcal{L}(V_\perp, B_\perp, \Lambda, \chi, \sigma, J, \ldots)\right) \tag{3.36}$$

where

$$\begin{aligned}\mathcal{L}(V_\perp, B_\perp, \Lambda, \chi, \sigma, J, \ldots) &= \frac{1}{2}V_\perp^\mu \Box V_{\perp\mu} + \frac{1}{2}M_{V+}^2 V_\perp^\mu V_{\perp\mu} - \frac{1}{2}B_\perp^\mu \Box B_{\perp\mu} + \frac{1}{2}M_{V-}^2 B_\perp^\mu B_{\perp\mu} \\ &+ \frac{1}{2}\partial_\mu\sigma\partial^\mu\sigma - \frac{1}{2}M_{S+}^2\sigma^2 - \frac{1}{2}\partial_\mu\chi\partial^\mu\chi - \frac{1}{2}M_{S-}^2\chi^2 + \frac{1}{2}M^2\partial_\mu\Lambda\partial^\mu\Lambda \\ &+ \mathcal{L}'_{int}(\overline{V}^{(\theta)}, J, \ldots). \end{aligned} \tag{3.37}$$

and

$$\overline{V}^{(\theta)} = \frac{\exp\theta_V}{(1+\alpha)^{1/2}}(V_\perp + B_\perp) - \partial\chi\cosh\theta_S - \partial\sigma\sinh\theta_S - \partial\Lambda \tag{3.38}$$

and where $M_{V\pm}^2$, $M_{S\pm}^2$ are the mass eigenvalues (3.21) and (3.23). The theory is now formulated in terms of two spin one and two spin zero fields, whereas two of them, namely $B_\perp^\mu$ and χ have a wrong sign of the kinetic terms and are therefore negative norm ghosts. As above, the field Λ does not correspond to any dynamical degree of freedom, its role is merely to cancel the spurious poles of the free propagators of the transverse fields $V_\perp$ and $B_\perp$ at $p^2 = 0$.

3.2.2 Antisymmetric tensor formalism

For the antisymmetric tensor field in the formalism [8, 9] the situation is quite analogous to the Proca field case so our discussion will be parallel to the previous subsection. Let us write the Lagrangian in the form

$$\mathcal{L} = \mathcal{L}_0 + \mathcal{L}_{int}. \tag{3.39}$$

where the free part is

$$\mathcal{L}_0 = -\frac{1}{2}(\partial_\mu R^{\mu\nu})(\partial^\rho R_{\rho\nu}) + \frac{1}{4}M^2 R_{\mu\nu}R^{\mu\nu}, \tag{3.40}$$

and introduce the transverse and longitudinal projectors

$$\Pi^T_{\mu\nu\alpha\beta} = \frac{1}{2}\left(P^T_{\mu\alpha}P^T_{\nu\beta} - P^T_{\nu\alpha}P^T_{\mu\beta}\right) \tag{3.41}$$

$$\Pi^L_{\mu\nu\alpha\beta} = \frac{1}{2}\left(g_{\mu\alpha}g_{\nu\beta} - g_{\nu\alpha}g_{\mu\beta}\right) - \Pi^T_{\mu\nu\alpha\beta} \tag{3.42}$$

with $P^T_{\mu\alpha}$ given by (3.6). Again, in analogy with (3.4), for completely general $\mathcal{L}_{int}$ we can expect the following general form of the full two-point 1PI Green function

$$\Gamma^{(2)}_{\mu\nu\alpha\beta}(p) = \frac{1}{2}(M^2 + \Sigma^T(p^2))\Pi^T_{\mu\nu\alpha\beta} + \frac{1}{2}(M^2 - p^2 + \Sigma^L(p^2))\Pi^L_{\mu\nu\alpha\beta} \tag{3.43}$$

where $\Sigma^{T,L}$ are the corresponding self-energies. The full propagator is then obtained by means of the inversion of $\Gamma^{(2)}_{\mu\nu\alpha\beta}$ in the form

$$\Delta_{\mu\nu\alpha\beta}(p) = -\frac{2}{p^2 - M^2 - \Sigma^L(p^2)}\Pi^L_{\mu\nu\alpha\beta} + \frac{2}{M^2 + \Sigma^T(p^2)}\Pi^T_{\mu\nu\alpha\beta}. \tag{3.44}$$

This propagator has two types of poles analogous to (3.8) and (3.9), either at $p^2 = s_V$, satisfying

$$s_V - M^2 - \Sigma^L(s_V) = 0, \tag{3.45}$$

or at $p^2 = s_{\widetilde{V}}$ where

$$M^2 + \Sigma^T(s_{\widetilde{V}}) = 0. \tag{3.46}$$

Assuming that the solution of (3.45) satisfies $s_V = M_V^2 > 0$, the propagator behaves at this pole as

$$\begin{aligned}\Delta_{\mu\nu\alpha\beta}(p) &= \frac{Z_V}{p^2 - M_V^2}\frac{p_\mu g_{\nu\alpha}p_\beta - p_\nu g_{\mu\alpha}p_\beta - (\alpha \leftrightarrow \beta)}{M_V^2} + O(1) \\ &= \frac{Z_V}{p^2 - M_V^2}\sum_\lambda u^{(\lambda)}_{\mu\nu}(p)u^{(\lambda)}_{\alpha\beta}(p)^* + O(1)\end{aligned} \tag{3.47}$$

where

$$Z_V = \frac{1}{1 - \Sigma'^L(M_V^2)} \tag{3.48}$$

and the wave function $u^{(\lambda)}_{\mu\nu}(p)$ can be expressed in terms of the spin-one polarization vectors $\varepsilon^{(\lambda)}_\nu(p)$ as

$$u^{(\lambda)}_{\mu\nu}(p) = \frac{\mathrm{i}}{M_V}\left(p_\mu \varepsilon^{(\lambda)}_\nu(p) - p_\nu \varepsilon^{(\lambda)}_\mu(p)\right). \tag{3.49}$$

For $Z_V > 0$ the pole of this type corresponds therefore to the spin-one state $|p, \lambda, V\rangle$ which couples to $R_{\mu\nu}$ as

$$\langle 0|R_{\mu\nu}(0)|p, \lambda, V\rangle = {Z_V}^{1/2} u^{(\lambda)}_{\mu\nu}(p). \tag{3.50}$$

Analogously to the Proca case, at least one of these poles is expected to be perturbative and corresponds to the original degree of freedom described by the free Lagrangian $\mathcal{L}_0$. This means

$$M_V^2 = M^2 + \delta M_V^2 \tag{3.51}$$
$$Z_V = 1 + \delta Z_V \tag{3.52}$$

with small corrections δM_V^2 and δZ_V vanishing in the free field limit. The other possible nonperturbative solutions of (3.45) decouple in this limit.

Provided there exists a solution of (3.46) for which $s_{\widetilde{V}} = M_{\widetilde{V}}^2 > 0$, we get at this pole

$$\begin{aligned}\Delta_{\mu\nu\alpha\beta}(p) &= \frac{Z_{\widetilde{V}}}{p^2 - M_{\widetilde{V}}^2}\left(g_{\mu\alpha}g_{\nu\beta} + \frac{p_\mu g_{\nu\alpha}p_\beta - p_\mu g_{\nu\beta}p_\alpha}{M_A^2} - (\mu \leftrightarrow \nu)\right) + O(1) \\ &= \frac{Z_{\widetilde{V}}}{p^2 - M_{\widetilde{V}}^2}\sum_\lambda w_{\mu\nu}^{(\lambda)}(p) w_{\alpha\beta}^{(\lambda)}(p)^* + O(1) \end{aligned} \tag{3.53}$$

where

$$Z_{\widetilde{V}} = \frac{1}{\Sigma'^T(M_{\widetilde{V}}^2)} \tag{3.54}$$

and the wave function is dual to the wave function (3.49)

$$w_{\mu\nu}^{(\lambda)}(p) = \widetilde{u}_{\mu\nu}^{(\lambda)}(p) = \frac{1}{2}\varepsilon_{\mu\nu\alpha\beta}u^{(\lambda)\alpha\beta}(p). \tag{3.55}$$

Provided $Z_{\widetilde{V}} > 0$, the poles of this type correspond to the spin-one particle states $|p, \lambda, \widetilde{V}\rangle$ with the opposite intrinsic parity in comparison with $|p, \lambda, V\rangle$, which couple to the antisymmetric tensor field as

$$\langle 0|R_{\mu\nu}(0)|p, \lambda, \widetilde{V}\rangle = {Z_{\widetilde{V}}}^{1/2} w_{\mu\nu}^{(\lambda)}(p). \tag{3.56}$$

This degree of freedom is frozen in the free propagator due to the specific form of the free Lagrangian and it decouples in the limit of the vanishing interaction.

As in the Proca field case, we can therefore generally expect dynamically generated additional degrees of freedom, which can be either regular asymptotic states ($M_{V,\widetilde{V}}^2$, $Z_{V,\widetilde{V}} > 0$) or negative norm ghosts ($M_{V,\widetilde{V}}^2 > 0$, $Z_{V,\widetilde{V}} < 0$) or tachyons ($M_{V,\widetilde{V}}^2 < 0$). Complex poles on the unphysical sheets can be then interpreted as resonances.

As the toy illustration of these possibilities, let us take the interaction Lagrangian similar to (3.18) in the Proca field case *e.g.* in the form

$$\begin{aligned}\mathcal{L}_{int} \equiv \mathcal{L}_{ct} = &-\frac{\alpha - \beta}{2}(\partial_\mu R^{\mu\nu})(\partial^\rho R_{\rho\nu}) - \frac{\beta}{4}(\partial_\mu R^{\alpha\beta})(\partial^\mu R_{\alpha\beta}) \\ &+\frac{\gamma - \delta}{2M^2}(\partial_\alpha\partial_\mu R^{\mu\nu})(\partial^\alpha\partial^\rho R_{\rho\nu}) + \frac{\delta}{4M^2}(\partial_\rho\partial_\mu R^{\alpha\beta})(\partial^\rho\partial^\mu R_{\alpha\beta}).\end{aligned} \tag{3.57}$$

We get then the following contributions to the longitudinal and transverse self-energies

$$\Sigma^L(p^2) = -\alpha p^2 + \gamma\frac{p^4}{M^2} \tag{3.58}$$
$$\Sigma^T(p^2) = -\beta p^2 + \delta\frac{p^4}{M^2}. \tag{3.59}$$

These are exactly the same as (3.20) and (3.19) (with the identification $\Sigma^{T,L} \leftrightarrow \Sigma^{L,T}$). Therefore, provided we further identify $M^2_{S\pm} \leftrightarrow M^2_{\widetilde{V}\pm}$, the properties of the poles and residues are the same as in the previous subsection (see the discussion after (3.20) and (3.19)), with the only exception that instead of the extra spin-zero states with the mass (3.23) we have now extra spin-one states with the same mass (3.23) but with the opposite parity in comparison with the original degrees of freedom described by the free lagrangian $\mathcal{L}_0$.

Path integral formulation

We can again made the additional degrees of freedom manifest within the path integral approach in the way parallel to subsection 3.2.1. An analog of the $U(1)$ gauge symmetry used in the case of the Proca field formalism in order to separate the transverse and longitudinal components of the field V_μ is here the following transformation with a pseudovector[1] parameter Λ_α

$$R^{\mu\nu} \to R^{\mu\nu} + \frac{1}{2}\varepsilon^{\mu\nu\alpha\beta}\widehat{\Lambda}_{\alpha\beta}, \tag{3.60}$$

where

$$\widehat{\Lambda}_{\alpha\beta} = \partial_\alpha\Lambda_\beta - \partial_\beta\Lambda_\alpha. \tag{3.61}$$

This leaves the kinetic term invariant, while the mass term is changed. Note, that the transformation with the parameters Λ_α and Λ^λ_α where

$$\Lambda^\lambda_\alpha = \Lambda_\alpha + \partial_\alpha\lambda \tag{3.62}$$

are the same. This residual gauge invariance has to be taken into account when using the Faddeev-Popov trick in order to isolate the longitudinal and transverse degrees of freedom of the field $R_{\mu\nu}$. Analog of the formula (3.28) is now

$$R^{\mu\nu} = R^{\mu\nu}_\parallel + \frac{1}{2}\varepsilon^{\mu\nu\alpha\beta}\widehat{\Lambda}_{\alpha\beta} \tag{3.63}$$

where $R^{\mu\nu}_\parallel$ is the longitudinal component of $R_{\mu\nu}$. Its transverse component is described with the transverse component $\Lambda^\mu_\perp$ of the field Λ^μ where

$$\Lambda^\mu = \Lambda^\mu_\perp + \partial^\mu\lambda. \tag{3.64}$$

Starting with the path integral representation of the generating functional[2]

$$Z[J] = \int \mathcal{D}R \exp\left(\mathrm{i}\int \mathrm{d}^4x \left(-\frac{1}{2}(\partial_\mu R^{\mu\nu})(\partial^\rho R_{\rho\nu}) + \frac{1}{4}M^2 R_{\mu\nu}R^{\mu\nu} + \mathcal{L}_{int}(R^{\mu\nu}, J, \ldots)\right)\right) \tag{3.65}$$

and using the Faddeev-Popov trick twice with respect to the transformations (3.60) and (3.62) we finally find for $Z[J]$ the following representation

$$Z[J] = \int \mathcal{D}R_\parallel \mathcal{D}\Lambda_\perp \exp\left(\mathrm{i}\int \mathrm{d}^4x \mathcal{L}(R^{\mu\nu}_\parallel, \Lambda^\mu_\perp, \ldots)\right) \tag{3.66}$$

[1] This is of course true only in the case of the proper tensor field $R_{\mu\nu}$. Provided $R_{\mu\nu}$ is a pseudotensor, the parameter of the transformation is vectorial.

[2] Here J are the external sources, cf. previous subsecrion.

where the integral measure is

$$\mathcal{D}R_{\parallel}\mathcal{D}\Lambda_{\perp} = \mathcal{D}R\mathcal{D}\Lambda\delta(\partial_{\alpha}R_{\mu\nu} + \partial_{\nu}R_{\alpha\mu} + \partial_{\mu}R_{\nu\alpha})\delta(\partial_{\mu}\Lambda^{\mu}) \tag{3.67}$$

and

$$R^{\mu\nu}_{\parallel} = -\frac{1}{2\Box}(\partial^{\mu}g^{\nu\alpha}\partial^{\beta} + \partial^{\nu}g^{\mu\beta}\partial^{\alpha} - (\mu \leftrightarrow \nu))R_{\alpha\beta} \tag{3.68}$$

$$\Lambda^{\mu}_{\perp} = \left(g^{\mu\nu} - \frac{\partial^{\mu}\partial^{\nu}}{\Box}\right)\Lambda_{\nu}. \tag{3.69}$$

are the longitudinal part of the tensor field $R^{\mu\nu}$and the transverse part of the vector field Λ^{μ} (describing the transverse part of the tensor field $R^{\mu\nu}$) respectively[3]. The Lagrangian expressed in these variables reads

$$\mathcal{L}(R^{\mu\nu}_{\parallel}, \Lambda^{\mu}_{\perp}, J, \ldots) = \tag{3.70}$$
$$\frac{1}{4}R^{\mu\nu}_{\parallel}\Box R_{\parallel\,\mu\nu} + \frac{1}{4}M^2R^{\mu\nu}_{\parallel}R_{\parallel\,\mu\nu} + \frac{1}{2}M^2\Lambda^{\mu}_{\perp}\Box\Lambda_{\perp\mu} + \mathcal{L}_{int}(R^{\mu\nu}_{\parallel} - \frac{1}{2}\varepsilon^{\mu\nu\alpha\beta}\widehat{\Lambda}_{\alpha\beta}, J, \ldots).$$

The free propagators of the fields $R^{\mu\nu}_{\parallel}$ and $\Lambda^{\mu}_{\perp}$ are therefore

$$\Delta^{\mu\nu\alpha\beta}_{\parallel}(p) = -\frac{2}{p^2 - M^2}\Pi^{L\,\mu\nu\alpha\beta} \tag{3.71}$$

$$\Delta^{\mu\nu}_{\perp}(p) = -\frac{1}{M^2}\frac{1}{p^2}P^{T\,\mu\nu} \tag{3.72}$$

and, similarly to the case of the Proca field, they have spurious poles at $p^2 = 0$. Due to the form of the interaction, however, only the combination

$$\begin{aligned}\Delta^{\mu\nu\alpha\beta}_{0}(p) &= \Delta^{\mu\nu\alpha\beta}_{\parallel}(p) + \varepsilon^{\mu\nu\rho\sigma}\varepsilon^{\alpha\beta\kappa\lambda}p_{\rho}p_{\kappa}\Delta_{\perp\,\sigma\lambda}(p) \\ &= -\frac{2}{p^2 - M^2}\Pi^{L\,\mu\nu\alpha\beta} + \frac{2}{M^2}\Pi^{T\,\mu\nu\alpha\beta}\end{aligned} \tag{3.73}$$

corresponding to the free propagator of the original tensor field $R^{\mu\nu}$ is relevant within the Feynman graphs and the spurious poles cancel. By analogy with the Proca field case, for the interaction Lagrangian invariant with respect to the transformation (3.60) the field $\Lambda^{\mu}_{\perp}$ completely decouples and can be integrated out. Such a form of the interaction also allows to modify the propagator $\Delta^{\mu\nu\alpha\beta}_{\parallel}(p)$ within the Feynman graphs

$$\Delta^{\mu\nu\alpha\beta}_{\parallel}(p) \to -\frac{g_{\mu\alpha}g_{\nu\beta} - g_{\mu\beta}g_{\nu\alpha}}{p^2 - M^2} \tag{3.74}$$

and no spurious pole at $p^2 = 0$ effectively appears. In this case the opposite parity spin-one states discussed in the previous subsection cannot be dynamically generated.

In order to illustrate the appearance of the additional degrees of freedom connected with the interaction Lagrangian (3.57) within the path integral formalism, we can make the same exercise with the interaction Lagrangian (3.57) as we did

[3]Note again that, the field Λ_{μ} has opposite parity than the field $R_{\mu\nu}$ (being pseudovector for proper tensor field $R_{\mu\nu}$ and vice versa).

in the previous subsection with (3.18). Our aim is again to make the additional degrees of freedom explicit in the path integral representation of $Z[J]$. The procedure is almost one-to-one to the case of the Proca fields so that we will be more concise. The technical details can be found in the Appendix 3.7.2.

We assume the interaction Lagrangian to be of the form

$$\mathcal{L}_{int} = \mathcal{L}_{ct} + \mathcal{L}'_{int}, \tag{3.75}$$

where $\mathcal{L}_{ct}$ is given by (3.57) and we assume $\alpha > -1$ and $\delta > 0$ as above. $\mathcal{L}_{int}$ can be then re-express it in terms of the longitudinal and transverse components of the original field $R_{\mu\nu}$

$$\mathcal{L}_{int}(R^{\mu\nu}_{\parallel} - \frac{1}{2}\varepsilon^{\mu\nu\alpha\beta}\widehat{\Lambda}_{\alpha\beta}, J, \ldots) = \mathcal{L}_{ct}(R^{\mu\nu}_{\parallel} - \frac{1}{2}\varepsilon^{\mu\nu\alpha\beta}\widehat{\Lambda}_{\alpha\beta}, J, \ldots) + \mathcal{L}'_{int}(R^{\mu\nu}_{\parallel} - \frac{1}{2}\varepsilon^{\mu\nu\alpha\beta}\widehat{\Lambda}_{\alpha\beta}, J, \ldots) \tag{3.76}$$

where

$$\begin{aligned}\mathcal{L}_{ct}(R^{\mu\nu} - \frac{1}{2}\varepsilon^{\mu\nu\alpha\beta}\widehat{\Lambda}_{\alpha\beta}J, \ldots) &= \frac{\alpha}{4}R^{\mu\nu}_{\parallel}\Box R_{\parallel\,\mu\nu} + \frac{\gamma}{4M^2}(\Box R^{\mu\nu}_{\parallel})(\Box R_{\parallel\,\mu\nu}) \\ &+ \frac{\beta}{2}(\Box\Lambda^{\mu}_{\perp})(\Box\Lambda_{\perp\mu}) - \frac{\delta}{2M^2}(\partial^{\alpha}\Box\Lambda^{\mu}_{\perp})(\partial_{\alpha}\Box\Lambda_{\perp\mu}).\end{aligned} \tag{3.77}$$

We then introduce the auxiliary (longitudinal) antisymmetric tensor field $B^{\mu\nu}_{\parallel}$ and (transverse) vector fields $\chi^{\mu}_{\perp}$, $\rho^{\mu}_{\perp}$, $\sigma^{\mu}_{\perp}$ and $\pi^{\mu}_{\perp}$ in order to avoid the higher derivative terms in a complete analogy with the Proca field case. Again, not all the fields correspond to propagating degrees of freedom and such redundant fields can be integrated out. After rescaling the fields and diagonalization of the resulting mass terms by means of two symplectic rotations with angles θ_V and $\theta_{\widetilde{V}}$ exactly as in the case of the Proca fields (see the Appendix 3.7.2 for details) we end up with

$$\begin{aligned}Z[J] = \int \mathcal{D}R_{\parallel}\mathcal{D}B_{\parallel}\mathcal{D}\Lambda_{\perp}\mathcal{D}\chi_{\perp}\mathcal{D}\rho_{\perp}\mathcal{D}\sigma_{\perp}\mathcal{D}\pi_{\perp}\exp \\ \left(\mathrm{i}\int \mathrm{d}^4x\mathcal{L}(R_{\parallel}, B_{\parallel}, \Lambda_{\perp}, \chi_{\perp}, \rho_{\perp}, \sigma_{\perp}, \pi_{\perp}, J, \ldots)\right)\end{aligned} \tag{3.78}$$

with (cf. (3.191))

$$\begin{aligned}\mathcal{L} &= \frac{1}{4}R^{\mu\nu}_{\parallel}\Box R_{\parallel\,\mu\nu} + \frac{1}{4}M^2_{V+}R^{\mu\nu}_{\parallel}R_{\parallel\,\mu\nu} \\ &- \frac{1}{4}B^{\mu\nu}_{\parallel}\Box B_{\parallel\,\mu\nu} + \frac{1}{4}M^2_{V-}B^{\mu\nu}_{\parallel}B_{\parallel\,\mu\nu} \\ &+ \frac{1}{2}M^2\Lambda^{\mu}_{\perp}\Box\Lambda_{\perp\mu} \\ &- \frac{1}{2}\chi^{\mu}_{\perp}\Box\chi_{\perp\mu} + \frac{1}{2}M^2_{\widetilde{V}-}\chi^{\mu}_{\perp}\chi_{\perp\mu} + \frac{1}{2}\sigma^{\mu}_{\perp}\Box\sigma_{\perp\mu} + \frac{1}{2}M^2_{\widetilde{V}+}\sigma^{\mu}_{\perp}\sigma_{\perp\mu} \\ &+ \mathcal{L}_{int}(\overline{R}^{(\theta)}, J, \ldots)\end{aligned} \tag{3.79}$$

where

$$\overline{R}^{(\theta)\mu\nu} = \frac{\exp\theta_V}{(1+\alpha)^{1/2}}(R^{\mu\nu}_{\parallel} + B^{\mu\nu}_{\parallel}) - \frac{1}{2}\varepsilon^{\mu\nu\alpha\beta}\left(\widehat{\Lambda}_{\alpha\beta} + \widehat{\sigma}_{\perp\alpha\beta}\sinh\theta_{\widetilde{V}} + \widehat{\chi}_{\perp\alpha\beta}\cosh\theta_{\widetilde{V}}\right)$$

and with the diagonal mass terms corresponding to the eigenvalues (3.21, 3.23) (with identification $M^2_{\widetilde{V}\pm} \to M^2_{S\pm}$). Again we have two pairs of fields with the opposite signs of the kinetic terms, namely $(R^{\mu\nu}_{\parallel}, B^{\mu\nu}_{\parallel})$ and $(\chi^{\mu}_{\perp}, \sigma^{\mu}_{\perp})$ respectively. As a result we have found four spin-one states, two of them being negative norm ghosts, namely $B^{\mu\nu}_{\parallel}$ and $\sigma^{\mu}_{\perp}$ and two of them with the opposite parity, namely $\chi^{\mu}_{\perp}$ and $\sigma^{\mu}_{\perp}$. As in the Proca field case, the field $\Lambda^{\mu}_{\perp}$ effectively compensates the spurious $p^2 = 0$ poles in the $R^{\mu\nu}_{\parallel}$ and $B^{\mu\nu}_{\parallel}$ propagators within Feynman graphs.

3.2.3 First order formalism

The first order formalism is a natural alternative to the previous two (for the motivation and details of the quantization see [60], cf. also [59]). It introduces both vector and antisymmetric tensor fields into the Lagrangian, therefore the analysis is a little bit more complex in comparison with previous two cases. In this case, the Lagrangian is of the form

$$\mathcal{L} = \mathcal{L}_0 + \mathcal{L}_{int} \tag{3.80}$$

where now the free part is

$$\mathcal{L}_0 = MV_\nu \partial_\mu R^{\mu\nu} + \frac{1}{2}M^2 V_\mu V^\mu + \frac{1}{4}M^2 R_{\mu\nu}R^{\mu\nu}. \tag{3.81}$$

Instead of just one one-particle irreducible two point Green function we have a matrix

$$\Gamma^{(2)}(p) = \begin{pmatrix} \Gamma^{(2)}_{VV}(p)_{\mu\nu} & \Gamma^{(2)}_{VR}(p)_{\alpha\mu\nu} \\ \Gamma^{(2)}_{RV}(p)_{\mu\nu\alpha} & \Gamma^{(2)}_{RR}(p)_{\mu\nu\alpha\beta} \end{pmatrix} \tag{3.82}$$

where (without any additional assumptions on the form of $\mathcal{L}_{int}$) the matrix elements have the following general form (cf. (3.4) and (3.43))

$$\Gamma^{(2)}_{RR}(p)_{\mu\nu\alpha\beta} = \frac{1}{2}(M^2 + \Sigma^T_{RR}(p^2))\Pi^T_{\mu\nu\alpha\beta} + \frac{1}{2}(M^2 + \Sigma^L_{RR}(p^2))\Pi^L_{\mu\nu\alpha\beta} \tag{3.83}$$

$$\Gamma^{(2)}_{VV}(p)_{\mu\nu} = (M^2 + \Sigma^T_{VV}(p^2))P^T_{\mu\nu} + (M^2 + \Sigma^L_{VV}(p^2))P^L_{\mu\nu} \tag{3.84}$$

$$\Gamma^{(2)}_{RV}(p)_{\mu\nu\alpha} = \frac{\mathrm{i}}{2}\left(M + \Sigma_{RV}(p^2)\right)\Lambda_{\mu\nu\alpha} \tag{3.85}$$

$$\Gamma^{(2)}_{VR}(p)_{\alpha\mu\nu} = \frac{\mathrm{i}}{2}\left(M + \Sigma_{VR}(p^2)\right)\Lambda^t_{\alpha\mu\nu}. \tag{3.86}$$

Here $\Sigma^{T,L}_{RR}(p^2)$, $\Sigma^{T,L}_{VV}(p^2)$ and $\Sigma_{RV}(p^2) = \Sigma_{VR}(p^2)$ are corresponding self-energies and the off-diagonal tensor structures are

$$\Lambda_{\mu\nu\alpha} = -\Lambda^t_{\alpha\mu\nu} = p_\mu g_{\nu\alpha} - p_\nu g_{\mu\alpha}. \tag{3.87}$$

This matrix of propagators

$$\Delta(p) = \begin{pmatrix} \Delta_{VV}(p)_{\mu\nu} & \Delta_{VR}(p)_{\alpha\mu\nu} \\ \Delta_{RV}(p)_{\mu\nu\alpha} & \Delta_{RR}(p)_{\mu\nu\alpha\beta} \end{pmatrix} \tag{3.88}$$

can be obtained by means of the inversion of the matrix (3.82) with the result

$$\Delta_{RR}(p)_{\mu\nu\alpha\beta} = \frac{2}{M^2+\Sigma^T_{RR}(p^2)}\Pi^T_{\mu\nu\alpha\beta} + 2\frac{M^2+\Sigma^T_{VV}(p^2)}{D(p^2)}\Pi^L_{\mu\nu\alpha\beta} \quad (3.89)$$

$$\Delta_{VV}(p)_{\mu\nu} = \frac{1}{M^2+\Sigma^L_{VV}(p^2)}P^L_{\mu\nu} + \frac{M^2+\Sigma^L_{RR}(p^2)}{D(p^2)}P^T_{\mu\nu} \quad (3.90)$$

$$\Delta_{RV}(p)_{\mu\nu\alpha} = -\mathrm{i}\frac{M+\Sigma_{RV}(p^2)}{D(p^2)}\Lambda_{\mu\nu\alpha} \quad (3.91)$$

$$\Delta_{VR}(p)_{\alpha\mu\nu} = -\mathrm{i}\frac{M+\Sigma_{VR}(p^2)}{D(p^2)}\Lambda^t_{\alpha\mu\nu}, \quad (3.92)$$

where

$$D(p^2) = (M^2+\Sigma^L_{RR}(p^2))(M^2+\Sigma^T_{VV}(p^2)) - p^2(M+\Sigma_{RV}(p^2))(M+\Sigma_{VR}(p^2)). \quad (3.93)$$

Let us now discuss the structure of the poles, which is now richer than in previous two cases. We have three possible types of poles, namely s_V, $s_{\widetilde{V}}$ and s_S, being solutions of

$$\begin{aligned} D(s_V) &= 0 \\ M^2+\Sigma^T_{RR}(s_{\widetilde{V}}) &= 0 \\ M^2+\Sigma^L_{VV}(s_S) &= 0 \end{aligned} \quad (3.94)$$

respectively. As far as the pole s_V is concerned, let us assume $s_V = M_V^2 > 0$. We get then at this pole (see also previous two subsections)

$$\Delta_{RR}(p)_{\mu\nu\alpha\beta} = \frac{Z_{RR}}{p^2-M_V^2}\sum_\lambda u^{(\lambda)}_{\mu\nu}(p)u^{(\lambda)}_{\alpha\beta}(p)^* + O(1) \quad (3.95)$$

$$\Delta_{VV}(p)_{\mu\nu} = \frac{Z_{VV}}{p^2-M_V^2}\sum_\lambda \varepsilon^{(\lambda)}_{\mu}(p)\varepsilon^{(\lambda)*}_{\nu}(p) + O(1) \quad (3.96)$$

$$\Delta_{RV}(p)_{\mu\nu\alpha} = \frac{Z_{RV}}{p^2-M_V^2}\sum_\lambda u^{(\lambda)}_{\mu\nu}(p)\varepsilon^{(\lambda)}_{\alpha}(p)^* + O(1) \quad (3.97)$$

$$\Delta_{VR}(p)_{\alpha\mu\nu} = \frac{Z_{VR}}{p^2-M_V^2}\sum_\lambda \varepsilon^{(\lambda)}_{\alpha}(p)u^{(\lambda)*}_{\mu\nu}(p) + O(1) \quad (3.98)$$

where $u^{(\lambda)}_{\mu\nu}(p)$ is given by (3.49) and the residue are

$$Z_{RR} = \frac{M^2+\Sigma^T_{VV}(M_V^2)}{D'(M_V^2)} \quad (3.99)$$

$$Z_{VV} = \frac{M^2+\Sigma^L_{RR}(M_V^2)}{D'(M_V^2)} \quad (3.100)$$

$$Z_{RV} = \frac{M+\Sigma_{RV}(M_V^2)}{D'(M_V^2)}M_V = Z_{VR} = \frac{M+\Sigma_{VR}(M_V^2)}{D'(M_V^2)}M_V. \quad (3.101)$$

Note that, as a consequence of (3.94) we get the following relation

$$Z_{RR}Z_{VV} = Z^2_{RV} = Z^2_{VR}, \quad (3.102)$$

(remember $\Sigma_{RV}(p^2) = \Sigma_{VR}(p^2)$), therefore assuming $Z_{RR}, Z_{VV} > 0$ the pole $p^2 = M_V^2 > 0$ corresponds to the spin-one one-particle state $|p, \lambda, V\rangle$ which couples to the fields as

$$\begin{aligned} \langle 0|R_{\mu\nu}(0)|p,\lambda,V\rangle &= {Z_{RR}}^{1/2} u^{(\lambda)}_{\mu\nu}(p) \quad (3.103) \\ \langle 0|V_{\mu}(0)|p,\lambda,V\rangle &= {Z_{VV}}^{1/2} \varepsilon^{(\lambda)}_{\mu}(p). \quad (3.104) \end{aligned}$$

Again at least one of such states is expected to be perturbative as above and it correspond to the original degree of freedom described by $\mathcal{L}_0$; the others decouple when the interactions is switched off. The other possible poles, $s_S = M_S^2$ and $s_{\widetilde{V}} = M_{\widetilde{V}}^2$ are analogical to the spin-zero and spin-one (opposite parity) states discussed in detail in the previous two subsections; they correspond to the modes which are frozen at the leading order and decouple in the free field limit. As we have already discussed, without further restriction on the form of the interaction, all the additional states can be also negative norm ghosts or tachyons.

Let us illustrate the general case using a toy interaction Lagrangian of the form

$$\begin{aligned} \mathcal{L}_{ct} &= -\frac{\alpha_V}{4}\widehat{V}_{\mu\nu}\widehat{V}^{\mu\nu} - \frac{\beta_V}{2}(\partial_\mu V^\mu)^2 \\ &\quad -\frac{\alpha_R - \beta_R}{2}(\partial_\mu R^{\mu\nu})(\partial^\rho R_{\rho\nu}) - \frac{\beta_R}{4}(\partial_\mu R^{\alpha\beta})(\partial^\mu R_{\alpha\beta}). \quad (3.105) \end{aligned}$$

This gives

$$\begin{aligned} \Sigma^L_{RR}(p^2) &= -\alpha_R p^2 \\ \Sigma^T_{RR}(p^2) &= -\beta_R p^2 \\ \Sigma^T_{VV}(p^2) &= -\alpha_V p^2 \\ \Sigma^L_{VV}(p^2) &= -\beta_V p^2 \\ \Sigma_{RV}(p^2) &= \Sigma_{VR}(p^2) = 0 \quad (3.106) \end{aligned}$$

and for $\beta_{V,R} > 0$ the spectrum of one-particle states consists of one spin-zero ghost, one spin-one ghost with opposite parity. Their masses and residue are

$$\begin{aligned} M_S^2 &= \frac{M^2}{\beta_V}, \quad Z_S = -\frac{1}{\beta_V} \quad (3.107) \\ M_{\widetilde{V}}^2 &= \frac{M^2}{\beta_R}, \quad Z_{\widetilde{V}} = -\frac{1}{\beta_R} \quad (3.108) \end{aligned}$$

(provided $\beta_R < 0$ or $\beta_V < 0$ the corresponding states are tachyons) and two spin-one states with masses

$$\begin{aligned} M^2_{V\pm} &= M^2 \frac{1 + \alpha_R + \alpha_V \pm \sqrt{\mathcal{D}}}{2\alpha_R\alpha_V} \\ \mathcal{D} &= (1 + \alpha_R + \alpha_V)^2 - 4\alpha_R\alpha_V. \quad (3.109) \end{aligned}$$

To get both $M^2_{V\pm} > 0$ we need $\mathcal{D} > 0$, $\alpha_V\alpha_R > 0$ and $1 + \alpha_R + \alpha_V > 0$; in this case we get for the residue $Z^{(\pm)}_{RR}$ and $Z^{(\pm)}_{VV}$ at poles $M^2_{V\pm}$

$$\alpha_R Z^{(+)}_{RR} Z^{(-)}_{RR} = \alpha_V Z^{(+)}_{VV} Z^{(-)}_{VV} = \frac{1}{\mathcal{D}} > 0 \quad (3.110)$$

Assuming $Z_{RR}^{(-)},\ Z_{VV}^{(-)} > 0$ (note that, for small couplings $M_{V-}^2 = M^2(1+O(\alpha_R, \alpha_V))$ with $Z_{RR}^{(-)}, Z_{VV}^{(-)} = 1 + O(\alpha_R, \alpha_V)$ corresponds to the perturbative solution), the additional spin one-state is either positive norm state for $\alpha_{V,R} > 0$ or ghost for $\alpha_{V,R} < 0$ (in this latter case the extra kinetic terms in $\mathcal{L}_{ct}$ have wrong signs).

Also in this case the propagating degrees of freedom can be made manifest within the path integral formalism. The corresponding discussion is in a sense synthesis of subsections 3.2.1 and 3.2.2 and is postponed to Appendix 3.7.3.

3.3 Organization of the counterterms

Let us now return to the concrete case of $R\chi T$. Our aim is to calculate the one loop self-energies defined in the previous section in all three formalisms discussed there. In the process of the loop calculation we are lead to the problem of performing a classification of the countertems, which have to be introduced in order to renormalize infinities. For this purpose, it is convenient to have a scheme, which allows us to assign to each operator in the Lagrangian and to each Feynman graph an appropriate expansion index. Indices of the counterterms, which are necessary in order to cancel the divergences of the given Feynman graph, should be then correlated with the indices of the vertices of the graph as well as with the number of the loops. When we restrict ourselves to the (one-particle irreducible) graphs with a given index, the number of the allowed operators contributing to the graph as well as that of necessary counterterms should be finite.

There are several possibilities how to do it, some of them being quite efficient but purely formal and unphysical, some of them having good physical meaning, but not very useful in practise. In the literature, several attempts to organize the individual terms of the $R\chi T$ Lagrangian can be found. Let us briefly comment on some of them from the point of view of its applicability to our purpose.

The first one is intimately connected with the effective chiral Lagrangian $\mathcal{L}_{\chi,\mathrm{res}}$ which appears as a result of the (tree-level) integrating out of the resonances from the $R\chi T$. Such a counting assigns to each operator of the resonance part of the $R\chi T$ Lagrangian $\mathcal{L}_{\mathrm{res}}$ a chiral order according to the minimal chiral order of the coupling (LEC) of the effective chiral Lagrangian $\mathcal{L}_{\chi,\mathrm{res}}$ to which the corresponding operator contributes [58], [57]. More generally, in this scheme the chiral order of the operators from $\mathcal{L}_{\mathrm{res}}$ refers to the minimal chiral order of its contribution to the generating functional of the currents $Z[v,a,p,s] = \sum_n Z^{(2n)}[v,a,p,s]$. The loop expansion of $Z[v,a,p,s]$ formally corresponds to the expansion around the classical fields which are solutions of the classical equation of motion. The formal chiral order of the resonance fields corresponds then to the chiral order of the leading term of the expansion of the classical resonance fields in powers of p and external sources according to the standard chiral power counting, *i.e.*

$$V^\mu = O(p^3), \quad R^{\mu\nu} = O(p^2). \tag{3.111}$$

At the same time, for the resonance mass (which plays a role of the hadronic scale within the standard power counting) we take

$$M = O(1), \tag{3.112}$$

and for the external sources as usual

$$v^\mu, a^\mu = O(p), \quad \chi, \chi^+ = O(p^2). \tag{3.113}$$

The resonance propagators are then of the (minimal) order $O(1)$ and the order of the operators which contain the resonance fields is at least $O(p^4)$. This formal power counting therefore restricts both the number of the resonance fields in the generic operator as well as the number of the derivatives. When combined with the large N_C arguments, it allows for the construction of the complete operator basis necessary for the saturation of the LEC's in the chiral Lagrangian at a given chiral order and a leading order in the $1/N_C$ expansion [57].

Originally this type of power counting was designed for the leading order (tree-level) matching of $R\chi T$ and χPT within the large N_C expansion and there is no straightforward extension to the general graph Γ with L loops. The reason is that the above power counting of the resonance propagators inside the loops does not reproduce correctly the standard chiral order of the graph. As a result, the loop graphs violate the naive chiral power counting in a way analogous to the χPT with baryons [61] .

The second possibility applicable to loops is to generalize the Weinberg [1] power counting scheme and *formally* arrange the computation as an expansion in the power of the momenta *and* the resonance masses [80] (though there is no mass gap and no natural scale which would give to such a formal power counting a reasonable physical meaning[4]). Nevertheless, provided we make a following assignment to the resonance field and to the resonance mass M

$$V^\mu, R^{\mu\nu} = O(1), \quad M = O(p) \tag{3.114}$$

we get for the kinetic and mass term of the resonance field

$$\mathcal{L}_{kin}, \mathcal{L}_{mass} = O(p^2) \tag{3.115}$$

i.e. the same order as for the lowest order chiral Lagrangian, which allows the same power counting of the resonance propagators as for PGB within the pure χPT. As a result, the Weinberg formula for the order D_Γ of a given graph Γ with L loops built from the vertices with the order D_V,

$$D_\Gamma = 2 + 2L + \sum_V (D_V - 2), \tag{3.116}$$

remains valid also within $R\chi T$. Note however, that now $p^2/M^2 = O(1)$ and therefore the counterterms needed for renormalization of the graph with chiral order D_Γ might contain more than D_Γ derivatives (this feature is typical for graphs with resonances inside the loops because of the nontrivial numerator of the resonance propagator). Therefore this type of power counting is less useful for the classification of the counterterms than in the case of the pure χPT, where D_Γ gives an upper bound on the number of derivatives of the counterterms needed to renormalize Γ.

[4]Sometimes it is argued [80], [81], that such a counting can be used within the large N_C limit, due to the fact that the natural χPT scale $\Lambda_{\chi PT} = 4\pi F = O(\sqrt{N_C})$ grows with N_C while the masses of the resonances behave as $O(1)$. In fact this results only in the suppression of the loops but generally not in the suppression of the counterterm contributions. In the latter case the expansion is rather controlled by the scale $\Lambda_H \sim M_R = O(1)$, where M_R is the typical mass of the higher resonance in the considered channel not included in truncated Lagrangian corresponding to minimal hadronic ansatz.

There are also some other complications, which depreciate this counting in the case of $R\chi T$. First note that the interaction vertices with the resonance fields can carry a chiral order smaller than two. This applies *e.g.* to the trilinear vertex in the antisymmetric tensor representation

$$\mathcal{O}^{RRR} = \mathrm{i}g_{\rho\sigma}\langle R_{\mu\nu}R^{\mu\rho}R^{\nu\sigma}\rangle \tag{3.117}$$

or to the odd intrinsic parity vertex mixing the vector and rge antisymmetric tensor field in the first order formalism

$$\mathcal{O}^{RV} = \varepsilon_{\alpha\beta\mu\nu}\langle\{V^{\alpha}, R^{\mu\nu}\}u^{\beta}\rangle. \tag{3.118}$$

Therefore, increasing number of such vertices will decrease the formal chiral order causing again a mismatch between the chiral counting and the loop expansion. Furthermore, such a naive scheme unlike the previous one does not restrict the number of the resonance fields in a general operator because only the number of derivatives, the resonance masses and the external sources score.

The former drawback can be *formally* cured by adding an artificial power of M in front of such operators[5] (or equivalently counting the corresponding couplings as $O(p^2)$ and $O(p)$ respectively) in order to increase artificially their chiral order and preserve the validity of the Weinberg formula, which now can serve as a *formal* tool for the classification of the counterterms. How to treat the latter drawback we will discuss further bellow. Let us, however, stress once again, that there is *no* physical content in such a classification scheme, though it might be technically useful.

Third possibility how to assign an index to the given interaction terms and to the general graphs, independent of the previous two, is offered by the large N_C expansion. In the $N_C \to \infty$ limit, the amplitude of the interaction of the n mesonic resonances is suppressed at least by the factor $O(N_C^{1-n/2})$ and, more generally, the matrix element of arbitrary number of quark currents and n mesons in the initial and final states has the same leading order behavior; *e.g.* for the GB decay constant we get $F = O(N_C^{1/2})$. Because within the chiral building blocks the GB fields always go with the factor $1/F$, we can treat the coupling $c_{\mathcal{O}}$ corresponding to the operator $\mathcal{O}$ of the $R\chi T$ Lagrangian as $c_{\mathcal{O}} = O(N_C^{\omega_{\mathcal{O}}})$, where

$$\omega_{\mathcal{O}} = 1 - \frac{n_R^{\mathcal{O}}}{2} - s_{\mathcal{O}}, \tag{3.119}$$

$n_R^{\mathcal{O}}$ is the number of the resonance fields contained in $\mathcal{O}$ and $s_{\mathcal{O}}$ is a possible additional suppression coming *e.g.* from multiple flavor traces or from the fact, that this coupling appears as a counterterm renomalizing the loop divergences[6]. From such an operator, generally the infinite number of vertices V with increasing number n_{GB}^V of GB legs can be derived, each accompanied with a factor $c_{\mathcal{O}}F^{-n_{GB}/2}$ and therefore, suppressed as $O(N_C^{\omega_V})$, where the index ω_V is given by[7]

$$\omega_V = 1 - \frac{n_R^{\mathcal{O}}}{2} - \frac{n_{GB}^V}{2} - s_{\mathcal{O}}. \tag{3.120}$$

[5] In the case of $\mathcal{O}^{RV}$ it seems to be natural from the dimensional reason.

[6] Note that, each additional mesonic loop yields a further suppression $1/N_C$, see also bellow.

[7] Here and in what follows we use subscript $\mathcal{O}$ when referring to the operator, while the superscript V corresponds to the concrete vertex derived from the operator $\mathcal{O}$.

For a given graph, we have the large N_C behavior $O(N_C^{\omega_\Gamma})$ where[8]

$$\omega_\Gamma = \sum_V \omega_V = 1 - \frac{1}{2}E - L - \sum_{\mathcal{O}} s_{\mathcal{O}}, \tag{3.121}$$

where L is number of the loops, E is the number of external mesonic lines and we have used the identities

$$\begin{aligned} \sum_V (n_R^V + n_{GB}^V) &= 2I_R + 2I_{GB} + E \\ I_R + I_{GB} &= L + V - 1 \end{aligned} \tag{3.122}$$

relating L and E with the number of resonance and GB internal lines I_R and I_{GB}. The loop expansion is therefore correlated with the large N_C expansion; higher loops need additionally N_C-suppressed counterterms $\mathcal{O}_{ct}$ with higher $s_{\mathcal{O}_{ct}}$:

$$s_{\mathcal{O}_{ct}} = \left(1 - \frac{1}{2}E\right) - \omega_\Gamma = L + \sum_{\mathcal{O}} s_{\mathcal{O}} \tag{3.123}$$

Though the formula (3.121) refers seemingly to individual vertices, reformulated in in the form (3.123) it points to the members of the chiral symmetric operator basis of the $R\chi T$ Lagrangian. However, as it stays, it does not suit for our purpose because the large N_C counting rules give no restriction for the number of derivatives as well as to the number of resonance fields (once the couplings respect the leading order large N_C behavior described above). The formula (3.123) expresses merely the the fact that the large N_C expansion coincide with the loop one.

Let us now describe another useful technical way how to classify the couterterms, which could overcome the problems with the above schemes and is in a sense a combination of them. Let us start with the familiar formula for the degree of superficial divergence d_Γ of a given *one particle irreducible* graph Γ, which provides us with the upper bound on the number of derivatives $d_{\mathcal{O}_{ct}}$ in a counterterm $\mathcal{O}_{ct}$ needed for the renormalization of Γ. Because in the Proca and antisymmetric tensor formalisms the spin 1 resonance propagator behaves as[9] $O(1)$ for $p \to \infty$, we get

$$d_{\mathcal{O}_{ct}} \leq d_\Gamma = 4L - 2I_{GB} + \sum_{\mathcal{O}} d_{\mathcal{O}} \tag{3.124}$$

where $d_{\mathcal{O}}$ means the number of derivatives of the vertex V derived from the operator $\mathcal{O}$. Eliminating I_{GB} in favour of L and I_R and using the identity

$$\sum_{\mathcal{O}} n_R^{\mathcal{O}} = 2I_R + E_R,$$

relating I_R with the number of external resonance lines E_R, we get eventually

$$d_{\mathcal{O}_{ct}} \leq d_\Gamma = 2 + 2L + \sum_{\mathcal{O}} (d_{\mathcal{O}} + n_R^{\mathcal{O}} - 2) - E_R.$$

[8]Here and in what follows, the sum over $\mathcal{O}$ include all the operators from which the individual vertices entering the graph Γ are derived with necessary multiplicity.

[9]In the case of the first order formalism, the mixed propagator behaves as $O(p^{-1})$. In this case, $d_\Gamma = 4L - 2I_{GB} - I_{RV} + \sum_{\mathcal{O}} d_{\mathcal{O}}$ where I_{RV} is number of the internal mixed lines. In the following considerations we can take the r.h.s. of (3.124) as an upper bound on d_Γ with the conclusions unchanged.

Adding further to both sides $\sum_{\mathcal{O}}(2n_s^{\mathcal{O}} + 2n_p^{\mathcal{O}} + n_v^{\mathcal{O}} + n_a^{\mathcal{O}})$, the total number of insertions of the external v, a, p and s sources weighted with its chiral order, we have

$$D_{\mathcal{O}_{ct}} + n_R^{ct} - 2 \leq 2L + \sum_{\mathcal{O}}(D_{\mathcal{O}} + n_R^{\mathcal{O}} - 2)$$

where $D_{\mathcal{O}}$ is the usual chiral order (as in pure χPT) of generic operator $\mathcal{O}$. Therefore, introducing an index $i_{\mathcal{O}}$ of a general operator $\mathcal{O}$ as follows[10]

$$i_{\mathcal{O}} = D_{\mathcal{O}} + n_R^{\mathcal{O}} - 2 \tag{3.125}$$

we get analog of the Weinberg formula[11], now in the form of an upper bound

$$i_{\mathcal{O}_{ct}} \leq i_\Gamma = 2L + \sum_{\mathcal{O}} i_{\mathcal{O}}. \tag{3.126}$$

Let us now discuss its properties more closely. First, the number of operators with given $i_{\mathcal{O}} \leq i_{\max}$ is finite, because this requirement limits both the number of derivatives as well as the number of resonance fields. Second, note that, for general operator $\mathcal{O}$ the index $i_{\mathcal{O}} \geq 0$. We have $i_{\mathcal{O}} = 0$ for the leading order χPT Lagrangian, for the resonance mass (counter)terms as well as for the resonance-GB mixing term $\langle A^\mu u_\mu \rangle$ possible for 1^{+-} resonances in the Proca field formalism[12]. The usual interaction terms with one resonance field and $O(p^2)$ building blocks correspond to the sector $i_{\mathcal{O}} = 1$, the same is true for the trilinear resonance vertex (3.117) as well as for the "mixed" vertex (3.118), while the two resonance vertices with $O(p^2)$ building blocks correspond to the sector $i_{\mathcal{O}} = 2$, *etc.*

Therefore, according to the formula (3.126), the loop expansion is correlated with the organization of the operators and loop graphs according to the indices $i_{\mathcal{O}}$ and i_Γ respectively analogously to the pure χPT, with the only exception that also lower sectors of the Lagrangian w.r.t. $i_{\mathcal{O}}$ are renormalized at each step. Therefore, we get the renormalizability provided we limit ourselves to the graphs composed from one-particle ireducible building blocs for which the RHS of (3.126) is smaller or equal to $i_{\max}$.

The counting rules can be summarized as follows

$$R_{\mu\nu},\, V_\mu = O(p),\, M = O(1) \tag{3.127}$$

and for the external sources as usual

$$v^\mu, a^\mu = O(p),\ \chi, \chi^+ = O(p^2). \tag{3.128}$$

Note also that, the index $i_{\mathcal{O}}$ can be rewritten as

$$i_{\mathcal{O}} = D_{\mathcal{O}} - 2\left(1 - \frac{n_R^{\mathcal{O}}}{2}\right) \tag{3.129}$$

[10] Analogous assignment of the chiral order to the interaction terms with at least two resonance fields is proposed in [80], note however, that in this reference it is used by means of substitution $D_V \to i_{\mathcal{O}}$ in the Weinberg formula (3.116) with counting $M = O(p)$.

[11] This can be recovered for $n_R^{\mathcal{O}} = 0$, when the inequality changes to the equality.

[12] Note however, that this term can be removed by means of the field redefinition.

and in the last bracket we recognize the exponent controlling the leading large N_C behavior of the coupling constant in front of the operator $\mathcal{O}$. Remember, however, that the loop induced counterterms have an additional $1/N_C$ suppression for each loop (cf. (3.121)). Therefore it is natural to modify the index $i_{\mathcal{O}}$ and i_Γ as follows (the coefficient 1/2 is a matter of convenience, see bellow)

$$\begin{aligned}\widehat{i}_{\mathcal{O}} &= \frac{i_{\mathcal{O}}}{2} + s_{\mathcal{O}} = \frac{1}{2}D_{\mathcal{O}} - \left(1 - \frac{n_R^{\mathcal{O}}}{2} - s_{\mathcal{O}}\right) = \frac{1}{2}D_{\mathcal{O}} - \omega_{\mathcal{O}} \\ \widehat{i}_\Gamma &= \frac{i_\Gamma}{2} + s_\Gamma = L + \sum_{\mathcal{O}} \frac{i_{\mathcal{O}}}{2} + s_\Gamma = 2L + \sum_{\mathcal{O}} \widehat{i}_{\mathcal{O}}\end{aligned} \tag{3.130}$$

where $\omega_{\mathcal{O}}$ is given by (3.119) and we have used (3.123) in the last line. With such a modified indices $\widehat{i}_{\mathcal{O}}$, $\widehat{i}_\Gamma$ the formula (3.126) has the form

$$\widehat{i}_{\mathcal{O}_{ct}} \leq \widehat{i}_\Gamma = 2L + \sum_{\mathcal{O}} \widehat{i}_{\mathcal{O}} \tag{3.131}$$

The content of this redefinition of $i_{\mathcal{O}}$ is evident: the operators are now classified according to the combined derivative and large N_C expansion according to the counting rules (for pure χPT introduced in [82], [83], [84])

$$p = O(\delta^{1/2}),\ v, a = O(\delta^{1/2}),\ \chi, \chi^+ = O(\delta),\ \frac{1}{N_C} = O(\delta) \tag{3.132}$$

In what follows we shall use for the classification of the counterterms and for the organization of our calculation the index $i_{\mathcal{O}}$ given by (3.125) and (3.126). Note however, that these formulae similarly to the previous cases, do not have much of physical content and serve only as a *formal* tool for the proof of the renormalizability and for the ordering of the counterterms. Namely, the index i_Γ which is by construction related to the superficial degree of the divergence (and which applies to one-particle irreducible graphs only) does not reflect the infrared behavior of the (one-particle irreducible) graph Γ, rather it refers to its ultraviolet properties.

Note also, that the hierarchy of the contributions to the GF by means of fixing i_Γ for *one-particle irreducible building blocks*[13] might appear to be unusual. For instance, let us assume the antisymmetric tensor formalism. Taking then $i_\Gamma = 0$ allows only the tree graphs with vertices from pure $O(p^2)$ chiral Lagrangian with resonaces completely decoupled (the only $i_{\mathcal{O}} = 0$ relevant term with resonance fields is the resonance mass terms) and such a case is therefore equivalent to the LO χPT. When fixing $i_\Gamma \leq 1$, also the terms linear in the resonance fields (at least in the antisymmetric tensor formalism, where the linear sources start at $O(p^2)$) can be used as the one-particle irreducible building blocks and again only the tree graphs are in the game. However, the resonance propagator is still derived from the mass terms only. Therefore, summing up all the tree graphs with resonance internal lines leads then effectively to the contributions equivalent to those of the pure $O(p^4)$ χPT operators with $O(p^4)$ LEC saturated with the resonances in the

[13] That means at a given level $i_{\max}$ we allow for all the graphs with one-particle irreducible building blocks satisfying $i_\Gamma \leq i_{\max}$. This point of view is crucial in order to preserve the symmetric properties of the corresponding GF.

usual way[14]. Because the resonance kinetic term has $i_{\mathcal{O}} = 2$, the resonances start to propagate only when we take $i_\Gamma \leq 2$. At this level we recover the complete NLO χPT as a part of the theory (including the loop graphs) supplemented with tree graphs built from the free resonance propagators and vertices with $i_{\mathcal{O}} \leq 2$. As far as the resonance part of the Lagrangian is concerned, these vertices coincide with the $O(p^6)$ vertices in the first type of power counting we have considered in the beginning of this section (where we assumed $R_{\mu\nu} = O(p^2)$, see (3.111)) but also the four resonance term without derivatives is allowed. The resonance loops start to contribute at $i_\Gamma \leq 3$ (with the resonance tadpoles) and $i_\Gamma \leq 4$ (with the pure resonance bubbles). In order to renormalize the corresponding divergences, plethora of new counterterms with increasing number of resonances as well as increasing order of the chiral building blocks is needed. In what follows we will encounter graphs with $i_\Gamma = 6$ (the mixed GB and resonance bubbles) for which we will need counterterms up to the index $i_{\mathcal{O}} \leq 6$.

3.4 The self-energies at one loop

In this section we present the main result of our chapter, namely the one-loop self-energies within all three formalisms discussed in the Section 3.2 in the chiral limit. In what follows, the loops are calculated within the dimensional regularization scheme. In order to avoid complications with the $d-$dimensional Levi-Civita tensor, we use its simplest variant known as Dimensional reduction, *i.e.* we perform the four-dimensional tensor algebra first in order to reduce the tensor integrals to scalar ones and only then we continue to d dimensions.

3.4.1 The Proca field case

Our starting point is the following Lagrangian for 1^{--} resonances [85] (see also [86])

$$\begin{aligned}\mathcal{L}_V &= -\frac{1}{4}\langle \widehat{V}_{\mu\nu}\widehat{V}^{\mu\nu}\rangle + \frac{1}{2}M^2\langle V_\mu V^\mu\rangle \\ &\quad -\frac{\mathrm{i}}{2\sqrt{2}}g_V\langle \widehat{V}^{\mu\nu}[u_\mu,u_\nu]\rangle + \frac{1}{2}\sigma_V\varepsilon_{\alpha\beta\mu\nu}\langle\{V^\alpha,\widehat{V}^{\mu\nu}\}u^\beta\rangle + \dots \quad (3.133)\end{aligned}$$

where we have written down explicitly only the terms contributing to the self-energy. Originally it was constructed to encompass terms up to the order $O(p^6)$ within the chiral power-counting (3.111, 3.112). In the large N_C limit the couplings behave as $g_V = O(N_C^{1/2})$ and $\sigma_V = O(N_C^{-1/2})$. This suggests that the odd intrinsic parity terms are of higher order, however the vertices relevant for our calculations have the same order $O(N_C^{-1})$ in both cases due to the presence of the factor $1/F = O(N_C^{-1/2})$ which accompanies each Goldstone bosons field. In the above Lagrangian the operators shown explicitly have no more than two derivatives and two resonance fields. Therefore, because the interaction terms are $O(p^2)$ we would expect (by analogy with the χPT power counting) the counterterms necessary to cancel the divergencies of the one-loop graphs to have four

[14]Here we tacitly assume that the trilinear term without derivatives has been removed by means of field redefinition, cf. [57, 58].

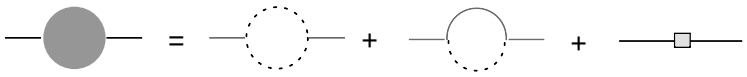

Figure 3.1: The one-loop graphs contributing to the self-energy of the Proca field. The dotted and full lines corresponds to the Goldstone boson and resonance propagators respectively. Both one-loop graphs have $i_\Gamma = 6$

derivatives at most. However, the nontrivial structure of the free resonance propagator (namely the presence of the P_L part) results in the failure of this naive expectation. In fact, according to (3.125) and (3.126), the operators in (3.133) have index up to $i_\mathcal{O} \leq 2$, whereas the Feynman graphs corresponding to the self-energies $\Sigma_{L,T}$ (depicted in Fig. 3.1) $i_\Gamma = 6$. In order to cancel the infinite part of the loops we have therefore to introduce a set of counterterms with two resonance fields and indices[15] $i_\mathcal{O} \leq 6$, namely

$$\begin{aligned}\mathcal{L}_V^{ct} &= \frac{1}{2}M^2 Z_M \langle V_\mu V^\mu\rangle + \frac{Z_V}{4}\langle \hat{V}_{\mu\nu}\hat{V}^{\mu\nu}\rangle - \frac{Y_V}{2}\langle (D_\mu V^\mu)^2\rangle \\ &+ \frac{X_{V1}}{4}\langle \{D_\alpha, D_\beta\}V_\mu \{D^\alpha, D^\beta\}V^\mu\rangle + \frac{X_{V2}}{4}\langle \{D_\alpha, D_\beta\}V_\mu \{D^\alpha, D^\mu\}V^\beta\rangle \\ &+ \frac{X_{V3}}{4}\langle \{D_\alpha, D_\beta\}V^\beta \{D^\alpha, D^\mu\}V_\mu\rangle + \frac{X_{V4}}{2}\langle D^2 V_\mu \{D^\mu, D^\beta\}V_\beta\rangle + X_{V5}\langle D^2 V_\mu D^2 V^\mu\rangle \\ &+ \mathcal{L}_V^{ct(6)}. \end{aligned} \tag{3.134}$$

Here the last term accumulates the operators with six derivatives ($i_\mathcal{O} = 6$), which we do not write down explicitly. The bare couplings are split into a finite part renormalized at a scale μ and a divergent part. The infinite parts of the bare couplings are fixed according to

$$\begin{aligned} Z_M &= Z_M^r(\mu) \\ Z_V &= Z_V^r(\mu) + \frac{80}{3}\left(\frac{M}{F}\right)^2 \sigma_V^2 \lambda_\infty \\ X_V &= X_V^r(\mu) - \frac{80}{9}\left(\frac{M}{F}\right)^2 \sigma_V^2 \frac{1}{M^2}\lambda_\infty \\ Y_V &= Y_V^r(\mu) \\ X_V' &= X_V'^r(\mu) \end{aligned}$$

where

$$\begin{aligned} X_V^r(\mu) &= X_{V1}^r(\mu) + X_{V5}^r(\mu) \\ X_V'^r(\mu) &= X_{V1}^r(\mu) + X_{V2}^r(\mu) + X_{V3}^r(\mu) + X_{V4}^r(\mu) + X_{V5}^r(\mu), \end{aligned}$$

and

$$\lambda_\infty = \frac{\mu^{d-4}}{(4\pi)^2}\left(\frac{1}{d-4} - \frac{1}{2}(\ln 4\pi - \gamma + 1)\right).$$

[15]Note that, for these counterterms the index $i_\mathcal{O}$ coincides with the usual chiral order $D_\mathcal{O}$.

The result can be written in the form (in the following formulae $x = s/M^2$)

$$\begin{aligned}
\Sigma_T^r(s) &= M^2\left(\frac{M}{4\pi F}\right)^2\left[\sum_{i=0}^{3}\alpha_i x^i - \frac{1}{2}g_V^2\left(\frac{M}{F}\right)^2 x^3\widehat{B}(x) - \frac{40}{9}\sigma_V^2(x-1)^2 x\widehat{J}(x)\right] \\
\Sigma_L^r(s) &= M^2\left(\frac{M}{4\pi F}\right)^2\sum_{i=0}^{3}\beta_i x^i
\end{aligned}$$

In the above formulae α_i and β_i can be expressed in terms of the renormalization scale independent combinations of the counterterm couplings and χlogs. The explicit formulae are collected in the Appendix 3.7.4. The functions $\widehat{B}(x)$ and $\widehat{J}(x)$ correspond to the vacuum bubbles with two Goldstone boson lines or with one Goldstone boson and one resonance line respectively. On the first (physical) sheet,

$$\begin{aligned}
\widehat{B}(x) &= \widehat{B}^I(x) = 1 - \ln(-x) \\
\widehat{J}(x) &= \widehat{J}^I(x) = \frac{1}{x}\left[1 - \left(1 - \frac{1}{x}\right)\ln(1-x)\right],
\end{aligned} \tag{3.135}$$

where we take the principal branch of the logarithm ($-\pi < \mathrm{Im}\ln \mathrm{x} \leq \pi$) with cut for $x < 0$. On the second sheet we have then $\widehat{B}^{II}(x - \mathrm{i}0) = \widehat{B}^I(x + \mathrm{i}0) = \widehat{B}^I(x - \mathrm{i}0) + 2\pi\mathrm{i}$ and similarly for $\widehat{J}(x)$, therefore

$$\begin{aligned}
\widehat{B}^{II}(x) &= \widehat{B}^I(x) + 2\pi\mathrm{i} \\
\widehat{J}^{II}(x) &= \widehat{J}^I(x) + \frac{2\pi\mathrm{i}}{x}\left(1 - \frac{1}{x}\right).
\end{aligned} \tag{3.136}$$

The equation for the pole in the 1^{--} channel

$$s - M^2 - \Sigma_T(s) = 0$$

has a perturbative solution corresponding to the original 1^{--} vector resonance, which develops a mass correction and a finite width of the order $O(1/N_C)$ due to the loops. This solution can be written in the form $\overline{s} = M_{\mathrm{phys}}^2 - \mathrm{i}M_{\mathrm{phys}}\Gamma_{\mathrm{phys}}$ where

$$\begin{aligned}
M_{\mathrm{phys}}^2 &= M^2 + \mathrm{Re}\Sigma_T(M^2) = M^2\left[1 + \left(\frac{M}{4\pi F}\right)^2\left(\sum_{i=0}^{3}\alpha_i - \frac{1}{2}g_V^2\left(\frac{M}{F}\right)^2\right)\right] \\
M_{\mathrm{phys}}\Gamma_{\mathrm{phys}} &= -\mathrm{Im}\Sigma_T(M^2) = M^2\left(\frac{M}{4\pi F}\right)^2\frac{1}{2}g_V^2\left(\frac{M}{F}\right)^2\pi
\end{aligned}$$

which gives a constraint on the values of α_i's

$$M_{\mathrm{phys}}^2 + \frac{1}{\pi}M_{\mathrm{phys}}\Gamma_{\mathrm{phys}} = M^2\left[1 + \left(\frac{M}{4\pi F}\right)^2\sum_{i=0}^{3}\alpha_i\right]$$

and in terms of the physical mass and the width we have then

$$\begin{aligned}
\Sigma_T^r(s) &= M_{\mathrm{phys}}^2\left(\frac{M_{\mathrm{phys}}}{4\pi F}\right)^2\left[\sum_{i=0}^{3}\alpha_i x^i - \frac{40}{9}\sigma_V^2(x-1)^2 x\widehat{J}(x)\right] - \frac{1}{\pi}M_{\mathrm{phys}}\Gamma_{\mathrm{phys}}x^3\widehat{B}(x) \\
\Sigma_L^r(s) &= M_{\mathrm{phys}}^2\left(\frac{M_{\mathrm{phys}}}{4\pi F}\right)^2\sum_{i=0}^{3}\beta_i x^i.
\end{aligned}$$

For further numerical estimates it is convenient to adopt the on shell renormalization prescription demanding $M^2 = M^2_{\rm phys}$ and also to identify F with F_π (because $F = F_\pi$ at the leading order). This gives

$$\frac{1}{\pi}\frac{\Gamma_{\rm phys}}{M_{\rm phys}} = \left(\frac{M}{4\pi F}\right)^2 \sum_{i=0}^{3} \alpha_i$$

and, introducing parameters a_i, b_i with natural size $O(1)$

$$\begin{aligned} a_i &= \pi \frac{M_{\rm phys}}{\Gamma_{\rm phys}} \left(\frac{M_{\rm phys}}{4\pi F_\pi}\right)^2 \alpha_i \sim O(1) \\ b_i &= \pi \frac{M_{\rm phys}}{\Gamma_{\rm phys}} \left(\frac{M_{\rm phys}}{4\pi F_\pi}\right)^2 \beta_i \sim O(1) \end{aligned}$$

we get in this scheme for $\sigma^r_{T,L}(x) = M^{-2}_{\rm phys}\Sigma^r_{T,L}(M^2_{\rm phys}x)$

$$\begin{aligned} \sigma^r_T(x) &= \frac{1}{\pi}\frac{\Gamma_{\rm phys}}{M_{\rm phys}} \left(1 + \sum_{i=1}^{3} a_i(x^i - 1) - x^3 \widehat{B}(x)\right) - \frac{40}{9}\left(\frac{M_{\rm phys}}{4\pi F_\pi}\right)^2 \sigma_V^2 (x-1)^2 x \widehat{J}(x) \\ \sigma^r_L(x) &= \frac{1}{\pi}\frac{\Gamma_{\rm phys}}{M_{\rm phys}} \sum_{i=0}^{3} b_i x^i. \end{aligned}$$

3.4.2 The antisymmetric tensor case

We start with the following Lagrangian for 1^{--} resonances (here only the terms relevant for the one-loop selfenergy are shown explicitly)

$$\begin{aligned} \mathcal{L}_R &= -\frac{1}{2}\langle D_\mu R^{\mu\nu} D^\alpha R_{\alpha\nu}\rangle + \frac{1}{4} M^2 \langle R^{\mu\nu} R_{\mu\nu}\rangle \\ &+ \frac{iG_V}{2\sqrt{2}}\langle R^{\mu\nu}[u_\mu, u_\nu]\rangle + d_1 \varepsilon_{\mu\nu\alpha\sigma}\langle D_\beta u^\sigma \{R^{\mu\nu}, R^{\alpha\beta}\}\rangle \\ &+ d_3 \varepsilon_{\rho\sigma\mu\lambda}\langle u^\lambda \{D_\nu R^{\mu\nu}, R^{\rho\sigma}\}\rangle + d_4 \varepsilon_{\rho\sigma\mu\alpha}\langle u_\nu \{D^\alpha R^{\mu\nu}, R^{\rho\sigma}\}\rangle \\ &+ \mathrm{i}\lambda^{VVV}\langle R_{\mu\nu} R^{\mu\rho} R^{\nu\sigma}\rangle + \ldots \end{aligned} \tag{3.137}$$

Note that, in the large N_C limit the coupling G_V behaves as $G_V = O(N_C^{1/2})$, whereas $d_i = O(1)$ and $\lambda^{VVV} = O(N_C^{-1/2})$. Apparently the intrinsic parity odd part and the trilinear resonance coupling are thus of higher order. However, the trilinear vertices contributing to the one-loop self-energies are $O(N_C^{-1/2})$ in both cases due to the appropriate power of $1/F = O(N_C^{-1/2})$ accompanying u_α. Therefore, the operators with two and three resonance fields cannot be got rid of using the large N_C arguments. Also nonzero d_i are required in order to satisfy the OPE constraints for VVP GF at the LO; especially for d_3 we get [87]

$$d_3 = -\frac{N_C}{64\pi^2}\left(\frac{M}{F_V}\right)^2 + \frac{1}{8}\left(\frac{F}{F_V}\right)^2 \tag{3.138}$$

where F_V is the strength of the resonance coupling to the vector current.

The Lagrangian (3.137) includes terms up to the index $i_{\mathcal{O}} \leq 2$. The one-loop Feynman graphs contributing to the self-energy are depicted in Fig. 3.2. The

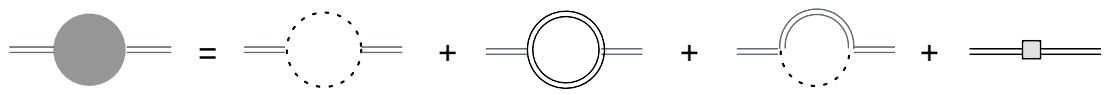

Figure 3.2: The one-loop graphs contributing to the self-energy of the antisymmetric tensor field. The dotted and double lines correspond to the Goldstone boson and resonance propagators respectively. The GB and pure resonance bubbles have $i_\Gamma = 4$, while the "mixed" one has $i_\Gamma = 6$

first two bubbles include only interaction vertices with $i_\mathcal{O} = 1$ and therefore they have indices $i_\Gamma = 4$ while the third one is built from vertices with $i_\mathcal{O} = 2$ and has the index $i_\Gamma = 6$. In order to cancel the infinite part of the loops we have then to add counterterms with indices $i_\mathcal{O} \leq 6$, namely the following set

$$\begin{aligned}
\mathcal{L}_R^{ct} &= \frac{1}{4}M^2 Z_M \langle R^{\mu\nu} R_{\mu\nu}\rangle + \frac{1}{2} Z_R \langle D_\alpha R^{\alpha\mu} D^\beta R_{\beta\mu}\rangle + \frac{1}{4} Y_R \langle D_\alpha R^{\mu\nu} D^\alpha R_{\mu\nu}\rangle \\
&+\frac{1}{4} X_{R1} \langle D^2 R^{\mu\nu} \{D_\nu, D^\sigma\} R_{\mu\sigma}\rangle + \frac{1}{8} X_{R2} \langle \{D_\nu, D_\alpha\} R^{\mu\nu} \{D^\sigma, D^\alpha\} R_{\mu\sigma}\rangle \\
&+\frac{1}{8} X_{R3} \langle \{D^\sigma, D^\alpha\} R^{\mu\nu} \{D_\nu, D_\alpha\} R_{\mu\sigma}\rangle \\
&+\frac{1}{4} W_{R1} \langle D^2 R^{\mu\nu} D^2 R_{\mu\nu}\rangle + \frac{1}{16} W_{R2} \langle \{D^\alpha, D^\beta\} R^{\mu\nu} \{D_\alpha, D_\beta\} R_{\mu\nu}\rangle \\
&+\mathcal{L}_R^{ct(6)},
\end{aligned} \tag{3.139}$$

where the last term accumulates the operators with six derivatives ($i_\mathcal{O} = 6$), which we do not write down explicitly. The infinite parts of the bare couplings are fixed as

$$\begin{aligned}
Z_M &= Z_M^r(\mu) + \frac{80}{3}\left(\frac{M}{F}\right)^2 d_1^2 \lambda_\infty - 60\left(\frac{\lambda^{VVV}}{M}\right)^2 \lambda_\infty \\
Z_R &= Z_R^r(\mu) + \frac{40}{9}\left(\frac{M}{F}\right)^2 \frac{1}{M^2}(12 d_1(d_3+d_4) - d_3^2 - 9d_4^2 + 6 d_3 d_4)\lambda_\infty \\
&\quad +80\left(\frac{\lambda^{VVV}}{M}\right)^2 \frac{1}{M^2}\lambda_\infty \\
Y_R &= Y_R^r(\mu) + \frac{40}{9}\left(\frac{M}{F}\right)^2 \frac{1}{M^2}(6d_1^2 - 12 d_1(d_3+d_4) + 5d_3^2 + 9d_4^2 - 6 d_3 d_4)\lambda_\infty \\
&\quad -40\left(\frac{\lambda^{VVV}}{M}\right)^2 \frac{1}{M^2}\lambda_\infty \\
X_R &= X_R^r(\mu) + \frac{40}{9}\left(\frac{M}{F}\right)^2 \frac{1}{M^2}(d_3^2 - 6 d_3 d_4 + 5 d_4^2)\lambda_\infty - \left(\frac{G_V}{F}\right)^2 \frac{1}{M^2}\lambda_\infty \\
W_R &= W_R^r(\mu) + \frac{40}{9}\left(\frac{M}{F}\right)^2 \frac{1}{M^4}(d_3^2 + 6 d_3 d_4 - 5 d_4^2)\lambda_\infty - 10\left(\frac{\lambda^{VVV}}{M}\right)^2 \frac{1}{M^4}\lambda_\infty
\end{aligned}$$

where

$$\begin{aligned}
X_R^r(\mu) &= X_{R1}^r(\mu) + X_{R2}^r(\mu) + X_{R3}^r(\mu) \\
W_R^r(\mu) &= W_{R1}^r(\mu) + W_{R2}^r(\mu).
\end{aligned}$$

An explicit calculation gives for the renormalized self-energies (in the following formulae $x = s/M^2$)

$$\begin{aligned}
\Sigma_L^r(s) &= M^2\left(\frac{M}{4\pi F}\right)^2\left[\sum_{i=0}^{3}\alpha_i x^i - \left(\frac{1}{2}\left(\frac{G_V}{F}\right)^2 x^2\widehat{B}(x) + \frac{40}{9}d_3^2(x^2-1)^2\widehat{J}(x)\right)\right] \\
&\quad -5\left(\frac{\lambda^{VVV}}{4\pi}\right)^2(x-4)(x+2)\overline{J}(x) \\
\Sigma_T^r(s) &= M^2\left(\frac{M}{4\pi F}\right)^2\left[\sum_{i=0}^{3}\beta_i x^i + \frac{20}{9}\left(2d_3^2 + (d_3^2 + 6d_3d_4 + d_4^2)x + 2d_4^2x^2\right)(x-1)^2\widehat{J}(x)\right] \\
&\quad +5\left(\frac{\lambda^{VVV}}{4\pi}\right)^2(x^2-2x+4)\overline{J}(x).
\end{aligned}$$

Here the functions $\widehat{B}(x)$ and $\widehat{J}(x)$ are same as in the previous subsection and $\overline{J}(x)$ is given on the physical sheet by

$$\overline{J}(x) = \overline{J}^I(x) = 2 + \sqrt{1-\frac{4}{x}}\ln\frac{\sqrt{1-\frac{4}{x}}-1}{\sqrt{1-\frac{4}{x}}+1}.$$

with the same branch of the logarithm as before. On the second sheet we have $\overline{J}^{II}(x-\mathrm{i}0) = \overline{J}^I(x+\mathrm{i}0) = \overline{J}^I(x-\mathrm{i}0) + 2\mathrm{i}\pi\sqrt{1-4/x}$ and therefore

$$\overline{J}^{II}(x) = \overline{J}^I(x) + 2\mathrm{i}\pi\sqrt{1-\frac{4}{x}}.$$

The explicit dependence of the renormalization scale invariant polynomial parameters α_i and β_i on the counterterm couplings and χlogs are given in the Appendix 3.7.4.

In order to simplify the following discussion we put $\lambda^{VVV} = 0$ in the rest of this subsection. This is in accord with the fact, that the corresponding trilinear interaction term can be effectively removed by resonance field redefinition [57]. Also, the two-resonance cut starts at $x = 4$ which is far from the region we are interested in. Here the effect of the resonance bubble can be effectively absorbed to the polynomial part of the self-energies.

The equation for the propagator poles in the 1^{--} channel

$$s - M^2 - \Sigma_L(s) = 0$$

has an approximative perturbative solution corresponding to the original 1^{--} vector resonance, which develops a mass correction and a finite width of the order $O(1/N_C)$ due to the loops. This solution can be written in the form $\overline{s} = M_{\rm phys}^2 - \mathrm{i}M_{\rm phys}\Gamma_{\rm phys}$ where

$$\begin{aligned}
M_{\rm phys}^2 &= M^2 + \mathrm{Re}\Sigma_L(M^2) = M^2\left[1 + \left(\frac{M}{4\pi F}\right)^2\left(\sum_{i=0}^{3}\alpha_i - \frac{1}{2}\left(\frac{G_V}{F}\right)^2\right)\right] \\
M_{\rm phys}\Gamma_{\rm phys} &= -\mathrm{Im}\Sigma_L(M^2) = M^2\left(\frac{M}{4\pi F}\right)^2\frac{1}{2}\left(\frac{G_V}{F}\right)^2\pi,
\end{aligned}$$

which gives a constraint on the values of α_i's

$$M^2_{\rm phys} + \frac{1}{\pi} M_{\rm phys}\Gamma_{\rm phys} = M^2 \left(1 + \frac{1}{(4\pi)^2}\left(\frac{M}{F}\right)^2 \sum_{i=0}^{3} \alpha_i\right).$$

This allows us to re-parameterize perturbatively $\Sigma_L(s)$ in terms of $M_{\rm phys}$ and $\Gamma_{\rm phys}$ as

$$\begin{aligned}
\Sigma^r_L(s) &= M^2_{\rm phys}\left(\frac{M_{\rm phys}}{4\pi F}\right)^2 \left[\sum_{i=0}^{3} \alpha_i x^i - \frac{40}{9} d_3^2 (x^2-1)^2 \widehat{J}(x)\right] - \frac{1}{\pi}\Gamma_{\rm phys} M_{\rm phys} x^2 \widehat{B}(x) \\
\Sigma^r_T(s) &= M^2_{\rm phys}\left(\frac{M_{\rm phys}}{4\pi F}\right)^2 \times \\
&\quad \left[\sum_{i=0}^{3} \beta_i x^i + \frac{20}{9}\left(2d_3^2 + (d_3^2 + 6d_3 d_4 + d_4^2)x + 2d_4^2 x^2\right)(x-1)^2 \widehat{J}(x)\right].
\end{aligned}$$

As for the Proca field case, within the on shell renormalization prescription $M^2 = M^2_{\rm phys}$ and we get a constraint

$$\frac{1}{\pi}\frac{\Gamma_{\rm phys}}{M_{\rm phys}} = \left(\frac{M_{\rm phys}}{4\pi F_\pi}\right)^2 \sum_{i=0}^{3} \alpha_i. \tag{3.140}$$

As a result, we can re-write the self-energy (in the units of $M^2_{\rm phys}$, *i.e.* as in the previous section $\sigma^r_{T,L}(x) = M^{-2}_{\rm phys}\Sigma^r_{T,L}(M^2_{\rm phys}x)$ in what follows) in the form

$$\sigma^r_L(x) = \frac{1}{\pi}\frac{\Gamma_{\rm phys}}{M_{\rm phys}}\left[1 - x^2\widehat{B}(x) + \sum_{i=1}^{3} a_i (x^i - 1)\right] - \frac{40}{9}\left(\frac{M_{\rm phys}}{4\pi F_\pi}\right)^2 d_3^2 (x^2-1)^2 \widehat{J}(x)$$

using the re-scaled parameters a_i with a natural size $O(1)$

$$a_i = \pi \frac{M_{\rm phys}}{\Gamma_{\rm phys}}\left(\frac{M_{\rm phys}}{4\pi F_\pi}\right)^2 \alpha_i \sim O(1).$$

So that the $\Sigma^r_L(s)$ has four independent parameters α_i, $i = 1, 2, 3$ and d_3. Similarly, $\Sigma^r_T(s)$ can be written in this scheme in terms of six independent dimensionless parameters b_i , d_3 and γ

$$\begin{aligned}
b_i &= \pi \frac{M_{\rm phys}}{\Gamma_{\rm phys}}\left(\frac{M_{\rm phys}}{4\pi F_\pi}\right)^2 \beta_i \sim O(1) \\
\gamma &= d_4/d_3 \sim O(1)
\end{aligned}$$

as

$$\sigma^r_T(x) = \frac{1}{\pi}\frac{\Gamma_{\rm phys}}{M_{\rm phys}}\sum_{i=0}^{3} b_i x^i + \frac{20}{9}\left(\frac{M_{\rm phys}}{4\pi F_\pi}\right)^2 d_3^2 \left(2 + (1 + 6\gamma + \gamma^2)x + 2\gamma^2 x^2\right)(x-1)^2 \widehat{J}(x).$$

In order to satisfy the OPE constraints for VVP correlator [87], we have to put further (according to (3.138))

$$d_3 = -\frac{3}{4}\left(\frac{M_{\rm phys}}{4\pi F_\pi}\right)^2 \left(\frac{F_\pi}{F_V}\right)^2 \left[1 - \frac{1}{6}\left(\frac{4\pi F_\pi}{M_{\rm phys}}\right)^2\right] \tag{3.141}$$

which reduces the number of the independent parameters for $\sigma^r_L(x)$ and $\sigma^r_T(x)$ to three and five respectively.

Figure 3.3: The extra one-loop graphs contributing to the vector field self-energy of in the first order formalism. The dotted and double lines corresponds to the Goldstone boson and antisymmetric tensor field propagators respectively, the thick line stay symbolically for the "mixed" propagator.

3.4.3 The first order formalism

In this case, the interaction part of the Lagrangian describing 1^{--} resonances collects all the terms from the previous two formalisms. It contains also one extra term which mixes the the fields $R_{\mu\nu}$ and V_α

$$\begin{aligned}
\mathcal{L}_{RV} &= \frac{1}{2}M^2\langle V_\mu V^\mu\rangle + \frac{1}{4}M^2\langle R^{\mu\nu}R_{\mu\nu}\rangle - \frac{1}{2}\langle R^{\mu\nu}\widehat{V}_{\mu\nu}\rangle \\
&\quad -\frac{\mathrm{i}}{2\sqrt{2}}g_V\langle\widehat{V}^{\mu\nu}[u_\mu,u_\nu]\rangle + \frac{1}{2}\sigma_V\varepsilon_{\alpha\beta\mu\nu}\langle\{V^\alpha,\widehat{V}^{\mu\nu}\}u^\beta\rangle \\
&\quad +\frac{iG_V}{2\sqrt{2}}\langle R^{\mu\nu}[u_\mu,u_\nu]\rangle + d_1\varepsilon_{\mu\nu\alpha\sigma}\langle D_\beta u^\sigma\{R^{\mu\nu},R^{\alpha\beta}\}\rangle \\
&\quad +d_3\varepsilon_{\rho\sigma\mu\lambda}\langle u^\lambda\{D_\nu R^{\mu\nu},R^{\rho\sigma}\}\rangle + d_4\varepsilon_{\rho\sigma\mu\alpha}\langle u_\nu\{D^\alpha R^{\mu\nu},R^{\rho\sigma}\}\rangle \\
&\quad +\frac{1}{2}M\sigma_{RV}\varepsilon_{\alpha\beta\mu\nu}\langle\{V^\alpha,R^{\mu\nu}\}u^\beta\rangle + \mathrm{i}\lambda^{VVV}\langle R_{\mu\nu}R^{\mu\rho}R^{\nu\sigma}\rangle + \dots
\end{aligned}$$

Because the free diagonal propagators are the same as in the pure Proca or antisymmetric tensor cases, all the graphs depicted in the Figs. 3.1, 3.2 contribute also here to the diagonal self-energies Σ_{RR} and Σ_{VV}. The mixed vertex and mixed propagator generate additional graphs contributing to Σ_{RR}, Σ_{VV} and Σ_{RV} which are depicted in the Figs. 3.3, 3.4 and 3.5 respectively (in the latter case also the GB bubble contributes).

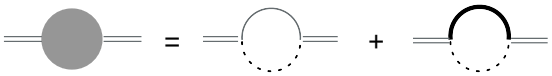

Figure 3.4: The extra one-loop graphs contributing to the antisymmetric tensor field self-energy in the first order formalism. The meaning of the various types of lines is the same as in the previous figures.

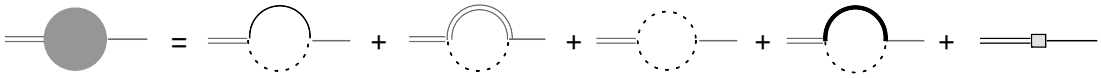

Figure 3.5: The one-loop graphs contributing to the "mixed" self-energy in the first order formalism.

Similarly, the set of counterterms necessary to renormalize the infinities in-

cludes all the terms (3.134) and (3.139) and additional mixed terms

$$
\begin{aligned}
\mathcal{L}^{ct}_{RV} &= \frac{1}{2}M^2 Z_{MV}\langle V_\mu V^\mu\rangle + \frac{Z_V}{4}\langle \hat{V}_{\mu\nu}\hat{V}^{\mu\nu}\rangle - \frac{Y_V}{2}\langle (D_\mu V^\mu)^2\rangle \\
&+ \frac{X_{V1}}{4}\langle \{D_\alpha, D_\beta\}V_\mu \{D^\alpha, D^\beta\}V^\mu\rangle + \frac{X_{V2}}{4}\langle \{D_\alpha, D_\beta\}V_\mu \{D^\alpha, D^\mu\}V^\beta\rangle \\
&+ \frac{X_{V3}}{4}\langle \{D_\alpha, D_\beta\}V^\beta \{D^\alpha, D^\mu\}V_\mu\rangle + \frac{X_{V4}}{2}\langle D^2 V_\mu \{D^\mu, D^\beta\}V_\beta\rangle + X_{V5}\langle D^2 V_\mu D^2 V^\mu\rangle \\
&+ \frac{1}{4}M^2 Z_{MR}\langle R^{\mu\nu}R_{\mu\nu}\rangle + \frac{1}{2}Z_R\langle D_\alpha R^{\alpha\mu}D^\beta R_{\beta\mu}\rangle + \frac{1}{4}Y_R\langle D_\alpha R^{\mu\nu}D^\alpha R_{\mu\nu}\rangle \\
&+ \frac{1}{4}X_{R1}\langle D^2 R^{\mu\nu}\{D_\nu, D^\sigma\}R_{\mu\sigma}\rangle + \frac{1}{8}X_{R2}\langle \{D_\nu, D_\alpha\}R^{\mu\nu}\{D^\sigma, D^\alpha\}R_{\mu\sigma}\rangle \\
&+ \frac{1}{8}X_{R3}\langle \{D^\sigma, D^\alpha\}R^{\mu\nu}\{D_\nu, D_\alpha\}R_{\mu\sigma}\rangle \\
&+ \frac{1}{4}W_{R1}\langle D^2 R^{\mu\nu}D^2 R_{\mu\nu}\rangle + \frac{1}{16}W_{R2}\langle \{D^\alpha, D^\beta\}R^{\mu\nu}\{D_\alpha, D_\beta\}R_{\mu\nu} \\
&- \frac{1}{2}Z_{RV}M\langle R^{\mu\nu}\widehat{V}_{\mu\nu}\rangle + \frac{1}{2}X_{RV1}M\langle D^\alpha R^{\mu\nu}D_\alpha \widehat{V}_{\mu\nu}\rangle + \frac{1}{2}X_{RV2}M\langle D_\mu R^{\mu\nu}D^\sigma \widehat{V}_{\sigma\nu} \\
&+ \mathcal{L}^{ct(6)}_{RV}
\end{aligned}
$$

Now the infinite parts of the bare couplings have to be fixed as follows

$$
\begin{aligned}
Z_{RV} &= Z^r_{RV}(\mu) - \frac{20}{3}\left(\frac{M}{F}\right)^2(\sigma_{RV}+2\sigma_V)(2d_1-\sigma_{RV})\lambda_\infty \\
X_{RV} &= X^r_{RV}(\mu) - \frac{20}{9}\left(\frac{M}{F}\right)^2\frac{1}{M^2}(\sigma_{RV}+2\sigma_V)(4d_3+\sigma_{RV})\lambda_\infty \\
Z_{MV} &= Z^r_{MV}(\mu) \\
Z_V &= Z^r_V(\mu) + \frac{20}{3}\left(\frac{M}{F}\right)^2\left(\sigma_{RV}(\sigma_{RV}+2\sigma_V)+4\sigma_V^2\right)\lambda_\infty \\
X_V &= X^r_V(\mu) - \frac{20}{9}\left(\frac{M}{F}\right)^2\frac{1}{M^2}\left(\sigma_{RV}(\sigma_{RV}+2\sigma_V)+4\sigma_V^2\right)\lambda_\infty \\
Y_V &= Y^r_V(\mu) \\
X'_V &= X'^r_V(\mu) \\
Z_{MR} &= Z^r_{MR}(\mu) + \frac{20}{3}\left(\frac{M}{F}\right)^2(4d_1^2-\sigma_{RV}(\sigma_{RV}-2d_1))\lambda_\infty \\
Z_R &= Z^r_R(\mu) + \frac{40}{9}\left(\frac{M}{F}\right)^2(12d_1(d_3+d_4)-d_3^2-9d_4^2+6d_3d_4)\lambda_\infty \\
&\quad +\frac{10}{9}\sigma_{RV}(10d_3+18d_4+\sigma_{RV})\lambda_\infty \\
Y_R &= Y^r_R(\mu) + \frac{10}{9}\left(\frac{M}{F}\right)^2\frac{1}{M^2}(24d_1^2-48d_1(d_3+d_4)+20d_3^2+36d_4^2 \\
&\quad -24d_3d_4-\sigma_{RV}^2+2\sigma_{RV}(d_3+3d_4))\lambda_\infty \\
X_R &= X^r_R(\mu) + \frac{40}{9}\left(\frac{M}{F}\right)^2\frac{1}{M^2}(d_3^2-6d_3d_4+5d_4^2)\lambda_\infty \\
&\quad -\frac{10}{9}\frac{1}{M^2}\sigma_{RV}(6(d_3+d_4)-\sigma_{RV})\lambda_\infty - \left(\frac{G_V}{F}\right)^2\frac{1}{M^2}\lambda_\infty \\
W_R &= W^r_R(\mu) + \frac{40}{9}\left(\frac{M}{F}\right)^2\frac{1}{M^4}(d_3^2+6d_3d_4-5d_4^2)\lambda_\infty + \frac{10}{9}\sigma_{RV}(\sigma_{RV}-2(d_3+3d_4))\lambda_\infty
\end{aligned}
$$

where

$$
\begin{aligned}
X^r_V(\mu) &= X^r_{V1}(\mu) + X^r_{V5}(\mu) \\
X'^r_V(\mu) &= X^r_{V1}(\mu) + X^r_{V2}(\mu) + X^r_{V3}(\mu) + X^r_{V4}(\mu) + X^r_{V5}(\mu) \\
X^r_R(\mu) &= X^r_{R1}(\mu) + X^r_{R2}(\mu) + X^r_{R3}(\mu) \\
W^r_R(\mu) &= W^r_{R1}(\mu) + W^r_{R2}(\mu) \\
X^r_{RV}(\mu) &= X^r_{RV1}(\mu) + X^r_{RV2}(\mu)
\end{aligned}
$$

The renormalized self-energies can be then written in the form

$$\begin{aligned}
\Sigma_{RV}(s)^r &= M\left(\frac{M}{4\pi F}\right)^2\left[\sum_{i=0}^{2}\alpha_i^{RV}x^i+\frac{1}{2}\frac{g_V G_V}{M}\left(\frac{M}{F}\right)^2 x^2\widehat{B}(x)\right.\\
&\left.+\frac{10}{9}(\sigma_{RV}+2\sigma_V)(2d_3x+2d_3-\sigma_{RV})(x-1)^2\widehat{J}(x)\right]=\Sigma_{VR}(s)^r\\
\Sigma_{VV}^T(s)^r &= M^2\left(\frac{M}{4\pi F}\right)^2\left[\sum_{i=0}^{3}\alpha_i^{VV}x^i-\frac{1}{2}g_V^2\left(\frac{M}{F}\right)^2 x^3\widehat{B}(x)\right.\\
&\left.-\frac{10}{9}\left(\sigma_{RV}(\sigma_{RV}+2\sigma_V)+4\sigma_V^2\right)(x-1)^2x\widehat{J}(x)\right]\\
\Sigma_{VV}^L(s)^r &= M^2\left(\frac{M}{4\pi F}\right)^2\sum_{i=0}^{3}\beta_i^{VV}x^i\\
\Sigma_{RR}^L(s)^r &= M^2\left(\frac{M}{4\pi F}\right)^2\left[\sum_{i=0}^{3}\alpha_i^{RR}x^i-\frac{1}{2}\left(\frac{G_V}{F}\right)^2 x^2\widehat{B}(x)\right.\\
&\left.-\frac{10}{9}(4d_3^2(x+1)^2-2d_3\sigma_{RV}(x+1)+\sigma_{RV}^2)(x-1)^2\widehat{J}(x)\right]\\
\Sigma_{RR}^T(s)^r &= M^2\left(\frac{M}{4\pi F}\right)^2\left[\sum_{i=0}^{3}\beta_i^{RR}x^i+\frac{5}{9}(8d_3^2-4\sigma_{RV}d_3+2\sigma_{RV}^2\right.\\
&\left.+(4d_3^2-2\sigma_{RV}d_3+\sigma_{RV}^2+24d_3d_4+4d_4^2-6\sigma_{RV}d_4)x+8d_4^2x^2)(x-1)^2\widehat{J}(x)\right].
\end{aligned}$$

Here again the renormalization scale independent coefficients of the polynomial parts of the self-energies are expressed in terms of the couplings and chiral logs; the explicit formulae can be found in the Appendix 3.7.4.

The equation for the poles in the 1^{--} channel

$$D(s)=(M^2+\Sigma_{RR}^L(s))(M^2+\Sigma_{VV}^T(s))-s(M+\Sigma_{RV}(s))(M+\Sigma_{VR}(s))=0$$

can be solved perturbatively writing the solution in the form $\overline{s}=M_{\rm phys}^2-\mathrm{i}M_{\rm phys}\Gamma_{\rm phys}=M^2+\Delta$. To the first order in Δ and the self-energies we get then

$$\overline{s}=M^2+\Sigma_{RR}^L(M^2)+\Sigma_{VV}^T(M^2)-M(\Sigma_{RV}(M^2)+\Sigma_{VR}(M^2))$$

and therefore

$$\begin{aligned}
M_{\rm phys}^2 &= M^2+\mathrm{Re}\left[\Sigma_{RR}^L(M^2)+\Sigma_{VV}^T(M^2)-M(\Sigma_{RV}(M^2)+\Sigma_{VR}(M^2))\right]\\
&= M^2\left[1+\left(\frac{M}{4\pi F}\right)^2\left(\sum_{i=0}^{3}(\alpha_i^{RR}+\alpha_i^{VV})-2\sum_{i=0}^{2}\alpha_i^{RV}-\frac{1}{2}\left(\frac{M}{F}\right)^2\left(g_V+\frac{G_V}{M}\right)^2\right)\right]\\
M_{\rm phys}\Gamma_{\rm phys} &= -\mathrm{Im}\left[\Sigma_{RR}^L(M^2)+\Sigma_{VV}^T(M^2)-M(\Sigma_{RV}(M^2)+\Sigma_{VR}(M^2))\right]\\
&= \pi M^2\left(\frac{M}{4\pi F}\right)^2\frac{1}{2}\left(\frac{M}{F}\right)^2\left(g_V+\frac{G_V}{M}\right)^2
\end{aligned}$$

which yield the constraint

$$M_{\rm phys}^2+\frac{1}{\pi}M_{\rm phys}\Gamma_{\rm phys}=M^2\left(1+\left(\frac{M}{4\pi F}\right)^2\left(\sum_{i=0}^{3}(\alpha_i^{RR}+\alpha_i^{VV})-2\sum_{i=0}^{2}\alpha_i^{RV}\right)\right).$$

In the on-shell scheme $M^2 = M^2_{\rm phys}$we get further

$$\frac{1}{\pi}\frac{\Gamma_{\rm phys}}{M_{\rm phys}} = \left(\frac{M_{\rm phys}}{4\pi F_\pi}\right)^2 \left(\sum_{i=0}^{3}(\alpha_i^{RR}+\alpha_i^{VV}) - 2\sum_{i=0}^{2}\alpha_i^{RV}\right)$$

On the contrary to the previous two cases, this allows to exclude both the constants g_V and G_V in favor of the physical observables only for the combination

$$\begin{aligned}\sigma(x) &\equiv x\sigma^L_{RR}(x) + \sigma^T_{VV}(x) - x(\sigma_{RV}(x)+\sigma_{VR}(x)) \\ &= \frac{1}{\pi}\frac{\Gamma_{\rm phys}}{M_{\rm phys}}\left(1+\sum_{i=0}^{4}a_i(x-1)^i - x^3\widehat{B}(x)\right) \\ &-\frac{20}{9}\left(\frac{M_{\rm phys}}{4\pi F_\pi}\right)^2 x(x-1)^2\widehat{J}(x)\left[d_3(x+1)(2d_3(x+1)+\sigma_{RV}+4\sigma_V)+\sigma_V(\sigma_{RV}-2\sigma_V)\right]\end{aligned}$$

(here $\Sigma^{Lr}_{RR} = M^2\sigma^L_{RR}$, $\Sigma^r_{RV} = M\sigma_{RV}$ etc.), where

$$a_i = \pi\frac{M_{\rm phys}}{\Gamma_{\rm phys}}\left(\frac{M_{\rm phys}}{4\pi F_\pi}\right)^2\left(\alpha^{RR}_{i-1}+\alpha^{VV}_i - 2\alpha^{RV}_{i-1}\right)$$

with $\alpha^{RR}_{-1} = \alpha^{RV}_{-1} = 0$ are parameters of order $O(1)$,

From the OPE constraints applied to VVP correlator within the first order formalism we get further

$$\begin{aligned}d_3 &= -\frac{N_C}{64\pi^2}\left(\frac{M}{F_V}\right)^2 + \frac{1}{8}\left(\frac{F}{F_V}\right)^2 + \frac{1}{2}(\sigma_{RV}+\sigma_V) \\ &= -\frac{3}{4}\left(\frac{M_{\rm phys}}{4\pi F_\pi}\right)^2\left(\frac{F_\pi}{F_V}\right)^2\left[1-\frac{1}{6}\left(\frac{4\pi F_\pi}{M_{\rm phys}}\right)^2\right] + \frac{1}{2}(\sigma_{RV}+\sigma_V)\end{aligned}$$

Using dimensionless variables, we can write the condition for the poles in the form

$$(1+\sigma^L_{RR}(x))(1+\sigma^T_{VV}(x)) - x(1+\sigma_{RV}(x))(1+\sigma_{VR}(x)) = 0$$

in the 1^{--} channel and

$$\begin{aligned}1+\sigma^T_{RR}(x) &= 0 \\ 1+\sigma^L_{VV}(x) &= 0\end{aligned}$$

in the 1^{+-} and 0^{+-} channels respectively. Within the on-shell scheme

$$\begin{aligned}
\sigma_{RV}(s)^r &= \frac{1}{\pi}\frac{\Gamma_{\rm phys}}{M_{\rm phys}}\left(\sum_{i=0}^{2} a_i^{RV} x^i - (1-C)Cx^2\widehat{B}(x)\right) \\
&\quad +\frac{10}{9}\left(\frac{M_{\rm phys}}{4\pi F_\pi}\right)^2\Big[(\sigma_{RV}+2\sigma_V)(2d_3x+2d_3-\sigma_{RV})(x-1)^2\widehat{J}(x)\Big] \\
\sigma^T_{VV}(s)^r &= \frac{1}{\pi}\frac{\Gamma_{\rm phys}}{M_{\rm phys}}\left(\sum_{i=0}^{3} a_i^{VV} x^i + C^2x^3\widehat{B}(x)\right) \\
&\quad -\frac{10}{9}\left(\frac{M_{\rm phys}}{4\pi F_\pi}\right)^2\Big[\left(\sigma_{RV}(\sigma_{RV}+2\sigma_V)+4\sigma_V^2\right)(x-1)^2x\widehat{J}(x)\Big] \\
\sigma^L_{VV}(s)^r &= \frac{1}{\pi}\frac{\Gamma_{\rm phys}}{M_{\rm phys}}\sum_{i=0}^{3} b_i^{VV} x^i \\
\sigma^L_{RR}(s)^r &= \frac{1}{\pi}\frac{\Gamma_{\rm phys}}{M_{\rm phys}}\left(\sum_{i=0}^{3} a_i^{VV} x^i + (1-C)^2x^3\widehat{B}(x)\right) \\
&\quad -\frac{10}{9}\left(\frac{M_{\rm phys}}{4\pi F_\pi}\right)^2\Big[(4d_3^2(x+1)^2-2d_3\sigma_{RV}(x+1)+\sigma_{RV}^2)(x-1)^2\widehat{J}(x)\Big] \\
\sigma^T_{RR}(s)^r &= \frac{1}{\pi}\frac{\Gamma_{\rm phys}}{M_{\rm phys}}\sum_{i=0}^{3} b_i^{RR} x^i + \frac{5}{9}\left(\frac{M_{\rm phys}}{4\pi F_\pi}\right)^2\big[(8d_3^2-4\sigma_{RV}d_3+2\sigma_{RV}^2 \\
&\quad +(4d_3^2-2\sigma_{RV}d_3+\sigma_{RV}^2+24d_3d_4+4d_4^2-6\sigma_{RV}d_4)x+8d_4^2x^2)(x-1)^2\widehat{J}(x)\Big].
\end{aligned}$$

and

$$\frac{1}{\pi}\frac{\Gamma_{\rm phys}}{M_{\rm phys}}C^2 = \frac{1}{2}g_V^2\left(\frac{M_{\rm phys}}{F_\pi}\right)^2 M_{\rm phys}\left(\frac{M_{\rm phys}}{4\pi F_\pi}\right)^2$$

and the other parameters are of natural size $O(1)$ with the constraint

$$\sum_{i=0}^{3}(a_i^{RR}+a_i^{VV}) - 2\sum_{i=0}^{2} a_i^{RV} = \sum_{i=0}^{4} a_i = 1.$$

3.4.4 Note on the counterterms

Let us note, that the counterterm Lagrangians (3.134), (3.139) and (3.142) might be further simplified using the leading order equations of motion (EOM) in order to eliminate the terms with more then two derivatives as it has been done *e.g.* in [64]. However, this does not mean, that we do not need to introduce such counterterms at all. As we have proved by means of the above explicit calculations, without the higher derivative counterterms (or equivalently without the couterterms proportional to the EOM) we would not have the off-shell self-energies finite.

In fact, the infinities originating in the missing EOM-proportional counterterms are not always dangerous. Note *e.g.*, that such infinities are in fact harmless, provided we restrict our treatment to strict one-loop contribution to the GF of quark bilinears or to the corresponding on-shell S-matrix elements. Namely, in this case, the one-loop generating functional of the GF is obtained by means

of the Gaussian functional integration of the quantum fluctuations around the solution of the lowest order EOM. As a result, the EOM can be safely used to simplify the infinite part of the one-loop generating functional. On the strict one-loop level the infinite parts of the self-energy subgraphs corresponding to the missing EOM-proportional counterterms cancel with similar infinities stemming from the vertex corrections.

Nevertheless, already at the one-loop level these counterterms might be necessary under some conditions. Namely, near the resonance poles we can (and in fact have to) go beyond the strict one-loop expansion *e.g.* by means of the Dyson resumation of the one-loop self-energy contributions to the propagator. This will generally destroy such a compensation of infinities. This is the reason why we keep the counterterm Lagrangian in the general form (3.134), (3.139) and (3.142).

3.5 From self-energies to propagators

In the previous sections we have given the explicit form of the self-energies in a given approximation within all three formalisms for the description of the spin-1 resonances. Here we would like to discuss interpretation of these results and the construction of the corresponding propagators. We will concentrate on the most frequently used antisymmetric tensor representation, where all the characteristic features of other approaches are visible without unsubstantial technical complications. The remaining two cases can be discussed along the same lines with similar results.

Let us remind the form of the self-energies for the antisymmetric tensor case

$$\sigma_L^r(x) = \frac{1}{\pi}\frac{\Gamma_{\rm phys}}{M_{\rm phys}}\left[1 - x^2\widehat{B}(x) + \sum_{i=1}^{3} a_i(x^i - 1)\right] - \frac{40}{9}\left(\frac{M_{\rm phys}}{4\pi F_\pi}\right)^2 d_3^2(x^2-1)^2\widehat{J}(x) \tag{3.142}$$

$$\sigma_T^r(x) = \frac{1}{\pi}\frac{\Gamma_{\rm phys}}{M_{\rm phys}}\sum_{i=0}^{3} b_i x^i + \frac{20}{9}\left(\frac{M_{\rm phys}}{4\pi F_\pi}\right)^2 d_3^2\left(2 + (1+6\gamma+\gamma^2)x + 2\gamma^2x^2\right)(x-1)^2\widehat{J}(x), \tag{3.143}$$

where d_3 is given by (3.138) and where we have already re-parametrized the general result in terms of the parameters of the perturbative solution of the pole equation in the 1^{--} channel (which we have identified with the original degree of freedom). In doing that we have tacitly assumed the validity of the general relation between the self-energies and the propagator (3.44). The equations determining the additional poles of the propagators are then

$$f_L(x) \equiv x - 1 - \sigma_L^r(x) = 0 \tag{3.144}$$

$$f_T(x) \equiv 1 + \sigma_T^r(x) = 0. \tag{3.145}$$

In what follows we shall discuss these equations in more detail. We will find a lower and upper bound on the number of their solutions and give a proof, that the corresponding lover bounds are greater than one on both sheets. We will also briefly discuss the compatibility of the relation (3.44) with the Källén-Lehman representation and show, that at least one of the roots of (3.6) and (3.145) corresponds inevitably either to the negative norm ghost or the tachyon.

3.5.1 The number of poles using Argument principle

Let us first briefly discuss a determination of the number of solution of the equations (3.6) and (3.145). This can be made using the theorem known as Argument principle (see *e.g.* [88]). According to this theorem, for a meromorphic function $f(z)$ with no zeros or poles on a simple closed contour C, the difference between the number of zeros N and poles P (counted according to their multiplicity) inside C is given as

$$N - P = \frac{1}{2\pi}[\arg f(z)]_C. \tag{3.146}$$

Here $[\arg f(z)]_C$ is the change of the argument of $f(z)$ along C. Using this theorem we will show, that in both cases (3.6) and (3.145) there is a nonzero lower bound on the number of solutions on the first and the second sheet, which correspond to the poles of the propagator (3.44). We will also give conditions for the saturation of these lower bounds.

Let us start with (3.145). The left hand side of the pole equation $f_T(z) = 1 + \sigma_T^r(z)$ is analytic on the first sheet (and meromorphic on the second sheet) of the cut complex plane with cut from $z = 1$ to $z = +\infty$. Let us choose contour $C = C_+ + C_R - C_- + C_\varepsilon$ which is usually used for the proof of the dispersive representation for the self-energy, namely the one consisting of the infinitesimal circle C_ε encircling the point $z = 1$ clockwise, two straight lines $C_\pm$ infinitesimally above and bellow the real axis going from $z = 1$ to $z = R$ and a circle C_R corresponding to $z = R\,\mathrm{e}^{\mathrm{i}\theta}$, $0 < \theta < 2\pi$, and take the limit with $\varepsilon \to 0$, $R \to \infty$ in the end. According to the argument principle, the total change of the phase of the function $f_T^{I,II}(z)$ along this contour gives the number of zeros (with their multiplicities) n^I of $f(z)$ on the first sheet and $n^{II} - 2$, where n^{II} is the number of zeros of $f(z)$ on the second sheet (note that $f_T^{II}(z)$ has pole of the second order at $z = 0$) lying inside the contour C, i.e.

$$\begin{aligned} n^I &= \frac{1}{2\pi}[\arg f_T^I(z)]_C \\ n^{II} &= \frac{1}{2\pi}[\arg f_T^{II}(z)]_C + 2. \end{aligned}$$

Let us assume the contour C_ε first. Suppose that $x = 1$ is not a solution of the equation $f_T(z) = 0$. As a consequence, $[\arg f_T^{I,II}(z)]_{C_\varepsilon}$ vanishes [16].

On the contour C_R, *i.e.* for $z = R\,\mathrm{e}^{\mathrm{i}\theta}$ we get for $b_3 \neq 0$

$$f_T^{I,II}(R\,\mathrm{e}^{\mathrm{i}\theta}) = R^3\mathrm{e}^{3\mathrm{i}\theta}\left(\frac{1}{\pi}\frac{\Gamma_{\mathrm{phys}}}{M_{\mathrm{phys}}}b_3 + \frac{20}{9}\left(\frac{M_{\mathrm{phys}}}{4\pi F_\pi}\right)^2 d_3^2 2\gamma^2\left[1 - \ln R + \mathrm{i}(2\pi - \theta \mp \pi)\right]\right. \tag{3.147}$$

$$\left. + O\left(\frac{1}{R}, \frac{\ln R}{R}\right)\right) \tag{3.148}$$

[16] In the case $f_T^{I,II}(x) \to 0$ for $x \to 1$ when $f_T^{I,II}(x) = (x-1)^k\, g_T^{I,II}(x)$ where $k \leq 3$ and when $g_T^{I,II}(x)$ (which has the branching point at $x = 1$) has a finite nonzero limit at $x = 1$) we get $[\arg f_T^{I,II}(z)]_{C_\varepsilon} = -2\pi k$.

and therefore, for $R \to \infty$, $[\arg f_T^{I,II}(z)]_{C_R} \to 6\pi$. The same is valid also for $b_3 = 0$ with $\gamma \neq 0$. However, for $b_3 = \gamma = 0$ we get

$$f_T^{I,II}(R\,\mathrm{e}^{\mathrm{i}\theta}) = R^2\mathrm{e}^{2\mathrm{i}\theta}\left(\frac{1}{\pi}\frac{\Gamma_{\rm phys}}{M_{\rm phys}}b_2 + \frac{20}{9}\left(\frac{M_{\rm phys}}{4\pi F_\pi}\right)^2 d_3^2\,[1 - \ln R + \mathrm{i}(2\pi - \theta \mp \pi)]\right. \tag{3.149}$$

$$\left. + O\left(\frac{1}{R}, \frac{\ln R}{R}\right)\right). \tag{3.150}$$

In this case $[\arg f_T^{I,II}(z)]_{C_R} \to 4\pi$ and because $d_3 \neq 0$ (unless we are in a conflict with OPE for the tree level VVP correlator[17]), this gives also the lower bound for $[\arg f_T^{I,II}(z)]_{C_R}$.

Finally let us discuss the lines $C_\pm$. Because $\mathrm{Im}\, f_T^I(x \pm \mathrm{i}0) = \mathrm{Im}\sigma_T^r(x \pm \mathrm{i}0) \gtrless 0$ (and f_T^I is real analytic), $\mathrm{Im}\, f_T^{II}(x \pm \mathrm{i}0) > 0$ for $x > 1$, and $\mathrm{Re} f_T^{I,II}(R \pm \mathrm{i}0\,) \to -\infty$ for $R \to \infty$, we can easily conclude that in this limit $[\arg f_T^{I,II}(z)]_{C_+} = 0$ unless $f_T^{I,II}(1) > 0$, in the latter case $[\arg f_T^{I,II}(z)]_{C_+} = \pi$ and in both cases $[\arg f_T^{I,II}(z)]_{C_-} = \pm[\arg f_T^{I,II}(z)]_{C_+}$.

Putting all pieces together we get under the assumption $f_T^{I,II}(1) \neq 0$ the following bound

$$[\arg f_T^{I,II}(z)]_C \geq 4\pi$$

and therefore for the number of zeros in the cut complex plane we get

$$2 \leq n^I \leq 4 \tag{3.151}$$

$$4 \leq n^{II} \leq 5 \tag{3.152}$$

where the lower bound is saturated for $f_T^{I,II}(1) < 0$, $b_3 = \gamma = 0$ and the upper bound for $f_T^{I,II}(1) > 0$ and either $b_3 \neq 0$ or $\gamma \neq 0$. For $f_T^{I,II}(1) = 0$ (provided we include also this zero with its multiplicity into $n^{I,II}$) the these bounds are valid too[18].

An analogous simple analysis for $f_L(z) = z - 1 - \sigma_L^r(z)$ in the cut complex plane with the cut from $z = 0$ to $z = +\infty$ gives [19] for $f_L^{I,II}(0) \neq 0$

$$3 \leq n^I \leq 4 \tag{3.153}$$

$$n^{II} = 5 \tag{3.154}$$

where the lower bounds are saturated for $f_L^{I,II}(0) < 0$ otherwise n^I equals to the upper bound.

---

[17] Note however, that the requirement that the tree level conditions for OPE are satisfied might be modified by loop corrections.

[18] In this case the point $x = 1$ is solution of $f_T^{I,II}(x) = 0$ and provided $f_T^{I,II}(x) = (x-1)^k\, g_T^{I,II}(x)$ (zero with multiplicity $k \leq 3$) we have according to the footnote 16 the phase deficit $-2\pi k$ (*i.e.* the number of the poles different from $z = 1$ is then reduced by k) in comparison with the case $f_T^{I,II}(x) \neq 0$.

[19] Note, that in this case,

$$f_L^{I,II}(R\,\mathrm{e}^{\mathrm{i}\theta}) = R^3\mathrm{e}^{3\mathrm{i}\theta}\left(-\frac{1}{\pi}\frac{\Gamma_{\rm phys}}{M_{\rm phys}}a_3 + \frac{40}{9}\left(\frac{M_{\rm phys}}{4\pi F_\pi}\right)^2 d_3^2\,[1 - \ln R + \mathrm{i}(2\pi - \theta \mp \pi)] + O\left(\frac{1}{R}, \frac{\ln R}{R}\right)\right)$$

and therefore $[\arg f_L^{I,II}(z)]_{C_R} = 6\pi$.

We can not therefore avoid in any way the generation of the additional poles (some of them might even be of the higher order) in both 1^{--} and 1^{+-} channels of the propagator only by means of an appropriate choice of the free parameters a_i, b_i and γ. The minimal number of the additional poles (with their orders) on the second sheet is the same for both channels (note that, one pole in 1^{--} channel has to correspond to the perturbative solution describing the original degrees of freedom we have started with). The conditions for the saturation of the lower bounds in the 1^{--} and 1^{+-} channels are

$$-\frac{1}{\pi}\frac{\Gamma_{\rm phys}}{M_{\rm phys}}\left[1-\sum_{i=1}^{3}a_i\right]+\frac{20}{9}\left(\frac{M_{\rm phys}}{4\pi F_\pi}\right)^2 d_3^2<1 \tag{3.155}$$

and

$$b_3 = \gamma = 0 \tag{3.156}$$

$$-\frac{1}{\pi}\frac{\Gamma_{\rm phys}}{M_{\rm phys}}\sum_{i=0}^{3}b_i > 1 \tag{3.157}$$

respectively. Note that, while the first condition is in accord with the large N_C counting, the last one is not. Let us now discuss the physical relevance of such additional poles.

3.5.2 The Källén-Lehman representation and nature of the poles

In this subsection, we will show that the the propagator (3.44) with self-energies (3.142) and (3.143) is incompatible with the Källén-Lehman representation with the positive spectral function. Moreover, at least one of the solutions of both equations (3.6) and (3.145) is pathological and corresponds to the negative norm ghost or the tachyonic pole.

Let us first briefly remind the Källén-Lehman representation of the antisymmetric tensor field propagator. According to the Lorentz structure we can write the following spectral representation of the full propagator (modulo generally non-covariant contact terms)

$$\Delta_{\mu\nu\alpha\beta}(p)=p^2\Pi^T_{\mu\nu\alpha\beta}(p)\Delta_T(p^2)-p^2\Pi^L_{\mu\nu\alpha\beta}(p)\Delta_L(p^2)+\Delta^{\rm contact}_{\mu\nu\alpha\beta}(p)$$

where (up to the necessary subtractions)

$$\Delta_{L,T}(p^2)=\int_0^\infty {\rm d}\mu^2\frac{\rho_{L,T}(\mu^2)}{p^2-\mu^2+{\rm i}0} \tag{3.158}$$

and where the spectral functions $\rho_{T,L}(p^2)$ are given in terms of the sum over the intermediate states as

$$\begin{aligned}&(2\pi)^{-3}\theta(p^0)\left[\rho_T(p^2)p^2\Pi^T_{\mu\nu\alpha\beta}(p)-\rho_L(p^2)p^2\Pi^L_{\mu\nu\alpha\beta}(p)\right] \\ &=\sum_N\delta^{(4)}(p-p_N)\langle 0|R_{\mu\nu}(0)|N\rangle\langle N|R_{\alpha\beta}(0)|0\rangle.\end{aligned} \tag{3.159}$$

Note that, in the above formula we assume all the states $|N\rangle$ to have a positive norm; the spectral functions $\rho_{L,T}(p^2)$ are then positive (for the proof see the Appendix 3.7.5). For the one particle spin-one bound stated states $|p,\lambda\rangle$ with mass M either

$$\langle 0|R_{\mu\nu}(0)|p,\lambda\rangle = Z_L^{1/2} u_{\mu\nu}^{(\lambda)}(p) \tag{3.160}$$

or

$$\langle 0|R_{\mu\nu}(0)|p,\lambda\rangle = Z_T^{1/2} w_{\mu\nu}^{(\lambda)}(p) \tag{3.161}$$

according to its parity (cf. (3.50) and (3.56)). Therefore (using the formulae from the Appendix 3.7.5), the corresponding one particle contribution to $\rho_{L,T}(\mu^2)$ is

$$\rho_{L,T}^{\text{one-particle}}(\mu^2) = \frac{2}{M^2} Z_{L,T} \delta(\mu^2 - M^2). \tag{3.162}$$

Positivity $\rho_{L,T}(\mu^2)$ implies $Z_{L,T} > 0$ in the above one-particle contributions.

For free fields with mass M we get

$$\begin{aligned} \rho_L^{free}(\mu^2) &= \frac{2}{M^2}\left(\delta(\mu^2 - M^2) - \delta(\mu^2)\right) \\ \rho_T^{free}(\mu^2) &= \frac{2}{M^2}\delta(\mu^2). \end{aligned} \tag{3.163}$$

Note the kinematical poles in $\Delta_{L,T}(p^2)$ at $p^2 = 0$, which do not correspond to any one-particle intermediate state and which sum up to the contact terms of the form

$$\Delta_{\mu\nu\alpha\beta}^{free,\text{contact}}(p) = \frac{1}{M^2}\left(g_{\mu\alpha}g_{\beta\nu} - g_{\mu\beta}g_{\nu\alpha}\right). \tag{3.164}$$

Let us now define for complex z by means of the analytic continuation (up to the possible subtractions)

$$\Delta_{L,T}(z) = \int_0^\infty \mathrm{d}s \frac{\rho_{L,T}(s)}{s - z}\ , \tag{3.165}$$

Within the perturbation theory however, the primary quantities are the self-energies, which we define as (cf. (3.44))

$$\begin{aligned} \Delta_T(s) &= \frac{1}{s}\frac{2}{M^2 + \Sigma_T(s)} \\ \Delta_L(s) &= \frac{1}{s}\frac{2}{s - M^2 - \Sigma_L(s^2)}. \end{aligned} \tag{3.166}$$

The poles at $s = 0$ are of the kinematical origin and in analogy with the free propagator they sum up into the contact terms provided $\Sigma_T(0) = \Sigma_L(0)$. The formulae (3.166) can be understood as the Dyson re-summation of the $1PI$ self-energy insertions to the propagator or as an inversion of the $1PI$ two-point function. Due to the positivity of $\rho_{L,T}(s)$, we get for the imaginary parts of $\Sigma_{L,T}$ the following positivity (negativity) constraints:

$$\begin{aligned} \mathrm{Im}\Sigma_L(s+i0) &= \frac{1}{2}\theta(s)s\ \mathrm{Im}\Delta_L(s+i0)|s - M^2 - \Sigma_L(s+i0)|^2 \le 0 \\ \mathrm{Im}\Sigma_T(s+i0) &= -\frac{1}{2}\theta(s)s\ \mathrm{Im}\Delta_T(s+i0)|M^2 + \Sigma_L(s+i0)|^2 \ge 0. \end{aligned} \tag{3.167}$$

Let us now turn to the $R\chi T$ -like effective theories and try to demonstrate their possible limitations. In such a framework the self-energies $\Sigma_{L,T}$ are given by a sum of the 1PI graphs organized according to some counting rule (for $R\chi T$ *e.g.* by the index i_Γ , cf. (3.126)). Up to a fixed given order (which we assume to be fixed from now on) we have the asymptotic behavior $\Sigma_{L,T}(z) = O(z^n \ln^k z))$ for $z \to -\infty$ according to the Weinberg theorem. Here n corresponds to the maximal degree of divergence of the contributing (sub)graphs and therefore, it grows with the number of loops as well as with the index of the vertices (cf. (3.125)).

Such a grow of the inverse propagator is known to lead to problems. Suppose *e.g.*, that we can organize the result of the calculation of the 1PI graphs in the form of a dispersive representation for the functions $\Sigma_{L,T}(z)$ on the first sheet[20]

$$\Sigma^I_{L,T}(z) = P^{L,T}_n(z) + \frac{Q^{L,T}_{n+1}(z)}{\pi}\int_{x_t}^{\infty}\frac{dx}{Q^{L,T}_{n+1}(x)}\frac{\mathrm{Im}\Sigma_{L,T}(x+i0)}{x-z} \tag{3.168}$$

where $x_t \geq 0$ is the lowest multi-particle threshold, $P^{L,T}_n(z)$ and $Q^{L,T}_{n+1}(z)$ (we suppose $Q^{L,T}_{n+1}(x) > 0$ for $x > 0$) are renormalization scale independent real polynomials of the order n and $n+1$ respectively and $\mathrm{Im}\Sigma_{L,T}(x+i0)$ can be obtained using the Cutkosky rules. The contributions to $P^{L,T}_n(z)$ stem from the counterterms necessary to renormalize the superficial divergences of the contributing 1PI graphs as well as from the loops (χlogs)[21].

As a consequence, the functions $z^k\Delta_{L,T}(z)$ where $0 \leq k \leq n$ and where $\Delta_{L,T}(s)$ is naively defined by (3.166) are analytic (up to the finite number of complex poles z_j generally different for Δ_L and Δ_T and a kinematical pole at $z = 0$ - see bellow) in the cut complex plane. As far as the number of poles z_j are concerned, provided $\mathrm{Im}\Sigma_{L,T}(x+i0) \lesseqgtr 0$ as suggested by (3.167), we can almost literally repeat the analysis from the previous subsection based on the argument principle. The change of a phase of the inverse propagator along the path C_R is now $[\arg\Delta^{-1}_{L,T}(z)]_{C_R} \to 2\pi n$ (for $R \to \infty$), while the absolute value of the $[\arg\Delta^{-1}_{L,T}(z)]_{C_\pm}$ is bounded by π due to the positivity (negativity) of $\mathrm{Im}\Sigma_{L,T}(x \pm i0)$. Provided $\Delta^{-1}_{L,T}(x_t) \neq 0$, we can therefore conclude

$$n-1 \leq n^I \tag{3.169}$$

$$n \leq n^{II} - p^{II} \tag{3.170}$$

where $n^{I,II}$ is the number of the solutions of the equation $\Delta^{-1}_{L,T}(z) = 0$ on the first and second sheet respectively and p^{II} is the number of the poles (weighted with their order) of $\Sigma_{L,T}(z)$ on the second sheet[22].

[20]Here we do not assume the existence of any CDD poles [89] for simplicity. In general case, provided the spectral representation of $\Delta_{L,T}$ is valid in the form (3.165), and $\mathrm{Im}\Delta^{-1}_{L,T}(s) = O(s^n)$ for $s \to \infty$ we formally get

$$\Delta^{-1}_{L,T}(z) = P_n(z) + Q^{L,T}_{n+1}(z)\left(\frac{1}{\pi}\int_{x_t}^{\infty}\frac{dx}{Q^{L,T}_{n+1}(x)}\frac{\mathrm{Im}\Delta^{-1}_{L,T}(x)}{x-z} - \sum_i \frac{C_i}{z-z_{0i}}\right)$$

where $C_i > 0$ and $0 < z_{0i} < x_t$ correspond to the CDD poles.

[21]In what follows we give such an representation of our one-loop $i_\Gamma \leq 6$ result explicitly.

[22]Note that, the case $n = 1$ is in some sense exceptional. In this case it is possible to get a

Therefore, because $z^k\Delta_{L,T}(z) = O(z^{k-n-1})$, we can write for $0 < k \leq n$ an unsubtracted dispersion relation (cf. (3.165), we will omit the subscript L, T in the following formulae for brevity and write simply $\Delta(z)$, $\rho(s)$ *etc.*)

$$z^k\Delta(z) = \sum_{j>0} \frac{R_j z_j^k}{z - z_j} + \frac{1}{\pi}\int_{x_t}^{\infty} \mathrm{d}x \frac{x^k \mathrm{disc}\Delta(x)}{x - z}$$

or

$$\Delta(z) = \frac{1}{z^k}\sum_{j>0} \frac{R_j z_j^k}{z - z_j} + \frac{1}{\pi z^k}\int_{x_t}^{\infty} \mathrm{d}x \frac{x^k \mathrm{disc}\Delta(x)}{x - z}. \tag{3.171}$$

and for $k = 0$ (note the kinematical pole at $z = 0$)

$$\Delta(z) = \frac{R_0}{z} + \sum_{j>0} \frac{R_j}{z - z_j} + \frac{1}{\pi}\int_{x_t}^{\infty} \mathrm{d}x \frac{\mathrm{disc}\Delta(x)}{x - z} \tag{3.172}$$

Due to the asymptotic fall off $\Delta(z) = O(z^{-n-1})$ the discontinuity $\mathrm{disc}\Delta(x)$ has to satisfy the following sum rules

$$-\frac{1}{\pi}\int_{x_t}^{\infty} \mathrm{d}x x^k \mathrm{disc}\Delta(x) + \sum_j R_j z_j^k = 0, \quad 0 < k \leq n-1. \tag{3.173}$$

$$-\frac{1}{\pi}\int_{x_t}^{\infty} \mathrm{d}x \mathrm{disc}\Delta(x) + \sum_j R_j + R_0 = 0 \tag{3.174}$$

Suppose on the other hand validity of the dispersive representation (3.165). Then all the poles have to be real, and we can identify

$$\rho(s) = -\frac{1}{\pi}\mathrm{disc}\Delta(s) + \sum_j R_j \delta(s - z_j) + R_0\delta(s). \tag{3.175}$$

However, the sum rules (3.173) are generally inconsistent with the spectral representation (3.165). The validity of some of them might require either an appearance of the states with the negative norm in the spectrum, *i.e.* we are in a conflict with the positivity of the spectral function $\rho(s) \geq 0$ or an appearance of physically non-acceptable tachyon poles leading to the acausality. For instance, suppose $\mathrm{disc}\Delta(s) \leq 0$, then for $R_0 \geq 0$ at least one of the poles has to correspond to a negative norm one-particle state (ghost). On the other hand, for $\mathrm{disc}\Delta(s) \leq 0$, $R_j > 0$ we can still satisfy the $k = 0$ sum rule with negative R_0, however, from the $k = 1$ sum rule we need at least one pole to be negative (tachyon) (in this case, however, the sum rules with even k cannot be satisfied)[23]. These considerations illustrate the known fact that the representation of the propagator based on the formulas (3.166) has limited range of validity within the fixed order of the perturbation theory and has to be taken with some care.

realistic resonance propagator compatible with the Källén-Lehman representation with no pole on the first sheet and one pole on the unphysical sheet. Such a propagator has been obtained in [90] for scalar resonances. Cf. also [91].

[23] An analogous discussion can be done for the second sheet. Concrete examples of various types of poles will be given in the next section.

One point of view might be that the range of applicability of the formulae (3.166) is $|z| < \Lambda_{\max} = \min\{|z_j|\}$ where $\{z_j\}$ is the set of unwanted poles. Provided there exists a genuine expansion parameter α applicable to the organization of the perturbative series, according to which $\Sigma_{L,T} = \sum_{i>0} \alpha^i \Sigma^{(i)}_{L,T}$ (*e.g.* expanding in powers of $\alpha = 1/N_C$ in $R\chi T$), one can expect the additional (generally pathological) poles of $\Delta_{L,T}(z)$ to decouple (*i.e.* $\Lambda_{\max} \to \infty$ for $\alpha \to 0$). In such a case we could argue that they are in fact harmless. However, the size of $\Lambda_{\max}$ for actual value of α need not to be far from M which could invalidate this approach to the theory in the region for which it was originally designed.

Alternatively, instead of using the (partial) Dyson re-summation, we can expand directly $\Delta_{\mu\nu\alpha\beta}(p)$ to the fixed finite order n which leads to

$$\begin{aligned}
\Delta_L(s) &= \frac{2}{s}\left(\frac{1}{s-M^2} + \alpha\frac{1}{s-M^2}\Sigma_L^{(1)}(s^2)\frac{1}{s-M^2} + \ldots + \alpha^n\frac{1}{s-M^2}\Sigma_L^{(n)}(s^2)\frac{1}{s-M^2}\right)\\
\Delta_T(s) &= \frac{2}{s}\left(\frac{1}{M^2} + \alpha\frac{1}{M^2}\Sigma_T^{(1)}(s^2)\frac{1}{M^2} + \ldots + \alpha^n\frac{1}{M^2}\Sigma_T^{(n)}(s^2)\frac{1}{M^2}\right).
\end{aligned}$$

This expansion (which does not give rise to the additional poles of the propagator) might be useful for $s \ll M^2$, however, in this case a higher-order pole at $s = M^2$ is generated, which is not correct physically in the resonance region $s \sim M^2$. Here we instead expect a single pole on the second sheet of $\Delta_L(z)$, where $z = M^2_{\rm phys} - iM_{\rm phys}\Gamma_{\rm phys}$ (where the mass $M^2_{\rm phys} = M^2 + O(\alpha)$ and the width $\Gamma_{\rm phys} = O(\alpha)$) corresponding to the original degree of freedom of the free Lagrangian. Therefore, the Dyson re-summation (*i.e.* the application of the formulae (3.166)) suplemented with some other more sophisticated approaches (*e.g.* the Redmond and Bogolyubov method [92, 93] consisting of the subtraction[24] of the additional unwanted poles from the propagator, or diagonal Padé approximation method [94]) seems to be inevitable for $s \sim M^2$.

However, in the concrete case of our calculations of the antisymmetric tensor field propagator, the plain Dyson re-summation might produce various types of poles some of which we illustrate in the next subsection.

3.5.3 Examples of the poles

The additional poles of the propagator can have different nature. Let us assume the 1^{--} channel first. By construction for any values of the constants a_i we have one pole on the second sheet (which is directly accessible from the physical sheet by means of the crossing of the cut for $0 < z < 1$) which corresponds to the physical resonance (ρ meson) we have started with at the tree level. On the first sheet we get then a typical resonance peak. These two structures are illustrated in the Fig. 3.6, where the square of the modulus of the propagator function, namely *i.e.* $|z - 1 - \sigma_L(z)|^{-2}$, is plotted[25] on the first and the second sheet for $a_i = 0$. In this case, no additional pole appears in the region of assumed applicability of

[24] Note that, in order to perform this on the lagrangian level, nonperturbative and nonlocal counterterms would have to be added to the theory. However the status of such a counterterms is not clear, cf. [95].

[25] We have used the following numerical inputs: $M_{\rm phys} = 770MeV$, $\Gamma_{\rm phys} = 150MeV$, $F = 93.2MeV$, $F_V = 154MeV$.

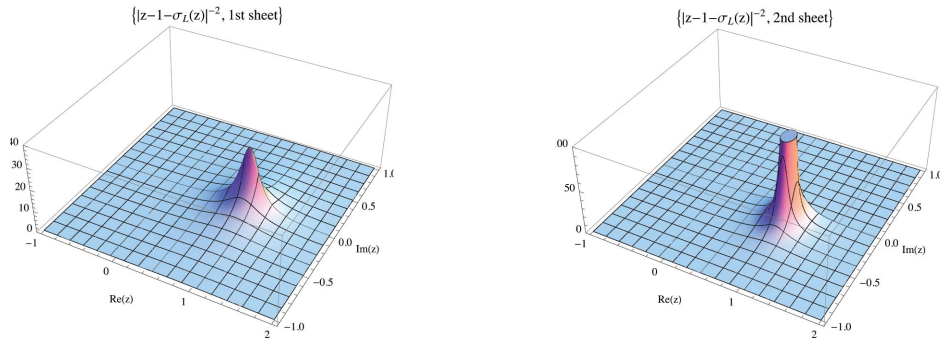

Figure 3.6: The plot of the the square of the modulus of the propagator function $|z-1-\sigma_L(z)|^{-2}$ on the first and the second sheet for $a_i = 0$. The pole on the second sheet and the peak on the first sheet correspond to the $\rho(770)$.

$R\chi T$. However, for another set of parameters we can get also pathological poles not far from this region (*e.g.* tachyon as it is illustrated in analogous Fig. 3.7, now for $a_0 = a_1 = a_2 = 10$, $a_3 = 0$).

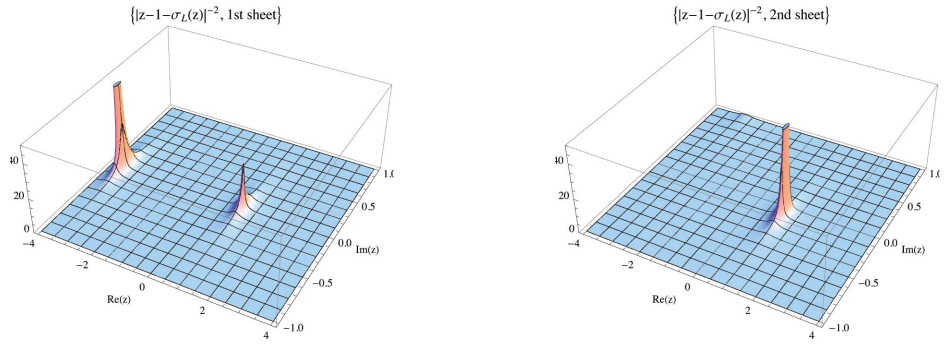

Figure 3.7: The plot of the the square of the modulus of the propagator function $|z-1-\sigma_L(z)|^{-2}$ on the first and the second sheet for $a_0 = a_1 = a_2 = 10$, $a_3 = 0$. The additional pole on the first sheet is a tachyon.

In the 1^{+-} channel, there is no tree-level pole in the propagator. The structure of the poles of the Dyson resumed propagator is strongly dependent on the parameters b_i and γ in this case. Let us illustrate this briefly. Note *e.g.* that, the equation (3.145) can have (exact) solution $x = 1$ on the first sheet provided the parameters b_i satisfy the following constraint

$$\sum_{i=0}^{3} b_i = -\pi \frac{M_{\rm phys}}{\Gamma_{\rm phys}} \sim -16 \tag{3.176}$$

where the numerical estimate corresponds to $(M_{\rm phys}, \Gamma_{\rm phys}) \sim (M_\rho, \Gamma_\rho)$. In order to interpret this solution as a 1^{+-} bound state pole we need the residuum Z_A at this pole to be positive, *i.e.*

$$Z_A^{-1} = \sigma_T^r(x)'|_{x=1} = \frac{1}{\pi} \frac{\Gamma_{\rm phys}}{M_{\rm phys}} \sum_{j=1}^{3} j b_j > 0 \tag{3.177}$$

otherwise the pole is a negative norm ghost state. Of course, from the phenomenological point of view, both these possibilities are meaningless. Note also that, the constraints (3.176) and (3.177) require unnatural large values of the parameters b_i and it is also in a conflict with the large N_C counting[26].

For $\gamma = 0$, a pathological tachyonic solution of (3.145) exists for $x = -2$ provided

$$\sum_{i=0}^{3}(-2)^i b_i = -\pi\frac{M_{\rm phys}}{\Gamma_{\rm phys}}$$

which might be satisfied with more reasonable values of the parameters b_i than in the previous case. More generally, we can have pathological poles $x = x_\gamma$ where x_γ is a solution of

$$2 + (1 + 6\gamma + \gamma^2)x_\gamma + 2\gamma^2 x_\gamma^2 = 0.$$

This x_γ is a pole of the propagator on both physical and unphysical sheets under the conditions that the following constraint on the parameters b_i

$$\sum_{i=0}^{3} x_\gamma^i b_i = -\pi\frac{M_{\rm phys}}{\Gamma_{\rm phys}}$$

is satisfied. Here x_γ is real (and negative) for $|\gamma + 5| > 2\sqrt{6}$ and it represents therefore a physically unacceptable tachyonic pole. Outside of this region of γ we get pair of complex conjugate poles on the physical sheet with ${\rm Re}x_\gamma > 0$ when $-3 + 2\sqrt{2} > \gamma > -3 - 2\sqrt{2}$.

However, we can easily get a more realistic situation and ensure that the position of the complex pole $z_R = x_R - {\rm i}y_R$ on the second sheet in the 1^{+-} channel corresponds *e.g.* to a resonance $b_1(1235)$. In this case, two conditions for b_i, and γ have to be satisfied, which correspond to the real and imaginary part of the pole equation $1 + \sigma_T^r(z_R) = 0$. This allows us to eliminate two of the five independent parameters in favor of the mass and the width of the desired resonance[27]. However, it might be difficult to eliminate additional pathological poles in the assumed region of applicability of $R\chi T$. We illustrate this in the Fig. 3.8, where the the square of the modulus of the propagator function $|1+\sigma_T(z)|^{-2}$ on the first and the second sheet for $b_0 = -2.16$, $b_1 = -3.66$, $b_2 = -4.45$, $b_3 = 1.47$ and $\gamma = 0$ is plotted on the first and the second sheet. In addition to the desired $b_1(1235)$ pole on the second sheet we get also four additional poles on the second sheet which is difficult to interpret physically as well as two additional structures the first sheet one of which can be interpreted as an tachyonic pole.

In general it is not so straightforward to formulate the conditions for a_i, b_i, and γ under which there are *no* additional poles on the real axis in the antisymmetric tensor field propagator. Because ${\rm Im}\sigma_L^r(x+i0)$ is negative for $x > 0$ (and similarly ${\rm Im}\sigma_T^r(x + i0)$ is positive for $x > 1$), we can clearly conclude, that there is no real pole in these regions on the first and the second sheet. As far as the regions of $x < 0$ (for σ_L^r) and $x < 1$ (for σ_T^r) are concerned, we can proceed as follows. Note, that we can write for the functions $\widehat{J}(x)$ and $\widehat{B}(x)$ the following dispersive

[26]While $b_i = O(1)$ in the large N_C limit, the right hand side of (3.176) begaves as $O(N_C)$.

[27]Similar conditions we get in the 1^{--} channel, provided we demand to generate *e.g.* $\rho(1450)$ dynamically.

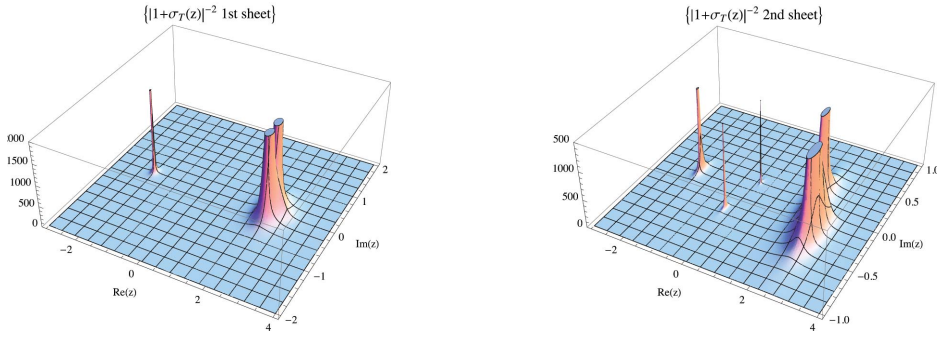

Figure 3.8: The plot of the the square of the modulus of the propagator function $|1+\sigma_T(z)|^{-2}$ on the first and the second sheet for $b_0 = -2.16$, $b_1 = -3.66$, $b_2 = -4.45$, $b_3 = 1.47$ and $\gamma = 0$. Along the desired $b_1(1235)$ pole on the 2nd sheet ($z = 2.552 - 0.295$i) and peak on the 1st sheet, additional structures appear.

representation

$$\begin{aligned}\widehat{B}(x) &= 2 + x + (x+1)^2 \int_0^\infty \frac{dx'}{(x'+1)^2}\frac{1}{x'-x} \\ &\equiv 2 + x + b(x) \\ \widehat{J}(x) &= \int_1^\infty \frac{dx'}{x'}\left(1 - \frac{1}{x'}\right)\frac{1}{x'-x},\end{aligned}$$

from which the representation (3.168) for Σ_L with desired properties easily follows. From this we can see that on the first sheet $b(x)$, $\widehat{J}(x) > 0$ for $x < 0$ and $x < 1$ respectively. Similarly, for Σ_T we can write

$$\left(2 + (1 + 6\gamma + \gamma^2)x + 2\gamma^2 x^2\right)\widehat{J}(x) = 1 + \frac{1}{6}\left(3\gamma^2 + 18\gamma + 5\right)x + j(x)$$

where

$$j(x) = x^2 \int_1^\infty \frac{dx'}{x'^3}\left(1 - \frac{1}{x'}\right)\left(2 + (1 + 6\gamma + \gamma^2)x' + 2\gamma^2 x'^2\right)\frac{1}{x'-x}$$

and $j(x) > 0$ for $x < 1$. The equations (3.5) and (3.145) have therefore the following structure

$$p_L(x) = -\frac{1}{\pi}\frac{\Gamma_{\rm phys}}{M_{\rm phys}}x^2\left(b(x)+2\right) - \frac{40}{9}\left(\frac{M_{\rm phys}}{4\pi F_\pi}\right)^2 d_3^2(x^2-1)^2\widehat{J}(x) \quad (3.178)$$

$$p_T(x) = -\frac{20}{9}\left(\frac{M_{\rm phys}}{4\pi F_\pi}\right)^2 d_3^2(x-1)^2\left(j(x)+1\right), \quad (3.179)$$

where $p_{L,T}(x)$ are the following polynomials of the third order

$$\begin{aligned}p_L(x) &= x - 1 - \frac{1}{\pi}\frac{\Gamma_{\rm phys}}{M_{\rm phys}}\left[1 - x^3 + \sum_{i=1}^3 a_i(x^i - 1)\right] = (x-1)q_L(x) \\ p_T(x) &= 1 + \frac{1}{\pi}\frac{\Gamma_{\rm phys}}{M_{\rm phys}}\sum_{i=0}^3 b_i x^i + \frac{10}{27}\left(\frac{M_{\rm phys}}{4\pi F_\pi}\right)^2 d_3^2\left(3\gamma^2 + 18\gamma + 5\right)x(x-1)^2.\end{aligned}$$

where

$$q_L(x) = 1 - \frac{1}{\pi}\frac{\Gamma_{\rm phys}}{M_{\rm phys}}\left((1+x+x^2)(a_3-1)+a_1+a_2(x+1)\right)$$

Because the right hand sides of the equations (3.178) and (3.179) are negative in the regions of interest, the sufficient (but not necessary) condition of the absence of the poles in these regions is $q_L(x) < 0$ for $x < 0$ and $p_T(x) > 0$ for $x < 1$. For $q_L(x)$ this can be achieved in many ways, *e.g.* for

$$\begin{aligned} a_3 &\geq 1 \\ q_L(0) &= 1 - \frac{1}{\pi}\frac{\Gamma_{\rm phys}}{M_{\rm phys}}(a_1+a_2+a_3-1) < 0 \\ q_L^{'}(0) &= -\frac{1}{\pi}\frac{\Gamma_{\rm phys}}{M_{\rm phys}}(a_3+a_2-1) > 0 \end{aligned}$$

i.e.

$$a_1 > \pi\frac{M_{\rm phys}}{\Gamma_{\rm phys}},\ a_2 < 0,\ a_3 \geq 1.$$

Note however, that such a condition for a_1 requires unnatural value for this parameter and is in a conflict with the large N_C counting. Similarly, the condition $p_T(x) > 0$ can be ensured *e.g.* when the coefficients at the third power of x vanish identically, *i.e.*

$$b_3 = -\frac{10}{27}\left(\frac{M_{\rm phys}}{4\pi F_\pi}\right)^2 \pi\frac{M_{\rm phys}}{\Gamma_{\rm phys}} d_3^2\left(3\gamma^2+18\gamma+5\right),$$

the coefficients at the second power of x are positive, *i.e*

$$b_2 > \frac{20}{27}\left(\frac{M_{\rm phys}}{4\pi F_\pi}\right)^2 \pi\frac{M_{\rm phys}}{\Gamma_{\rm phys}} d_3^2\left(3\gamma^2+18\gamma+5\right),$$

and

$$\begin{aligned} p_T(1) &= 1 + \frac{1}{\pi}\frac{\Gamma_{\rm phys}}{M_{\rm phys}}\sum_{i=0}^{3} b_i > 0 \\ p_T^{'}(1) &= \frac{1}{\pi}\frac{\Gamma_{\rm phys}}{M_{\rm phys}}\sum_{j=0}^{3} b_j j > 0. \end{aligned}$$

On the contrary to the previous case, these conditions respect the large N_C counting. Therefore without any detailed information about the actual value of the a_i and b_i it seems to be quite natural to have tachyonic pole in the 1^{--} channel and no bound states or tachyon poles in the 1^{+-} channel of the propagator.

3.6 Summary and discussion

In this chapter we have studied and illustrated various aspects of the renormalization procedure of the Resonance Chiral Theory using the spin-one resonance self-energy and the corresponding propagator as a concrete example. The explicit calculation of the one-loop self-energies within three possible formalisms for

the description of the spin-one resonances, namely the Proca filed, antisymmetric tensor field and the first order formalism is the main result of our article. Because the theory is non-renormalizable and the loop corrections break the ordinary chiral power counting, we had presumed an accurence of problems of several types which have proved to be true within our explicit example.

The first sort of problems concerned the technical aspects of the process of renormalization, namely the organization of the loop corrections and the counterterms and the mixing of the ordinary chiral orders by the loops. In order to organize our calculations we have proposed a self-consistent scheme for classification of the one-particle irreducible graphs Γ and corresponding counterterms $\mathcal{O}_i$ which renormalize its superficial divergences. The classification is according to the indices i_Γ and $i_{\mathcal{O}_i}$ assigned to graph Γ and operator $\mathcal{O}_i$ respectively. Though the scheme based on $i_{\mathcal{O}}$ restricts both the chiral order of the chiral building blocs (number of derivatives and external sources) as well as the number of resonance fields in the operators in the $R\chi T$ Lagrangian at each fixed order and can be understood as a combination of the chiral and $1/N_C$ counting, it is however not possible to assign to i_Γ a clear physical meaning connected with the infrared characteristics of the graphs Γ. Nevertheless the scheme works at least formally and can be used for the proof of the renormalizability of $R\chi T$ to given order $i_\Gamma, i_{\mathcal{O}_i} \leq i_{\max}$. We have used it at the level $i_{\max} \leq 6$ and proved that the complete set of counterterms from zero up to six derivatives is necessary to renormalize the divergences of the one-loop self-energies in the contrary to the naive expectations based on the usual chiral powercounting.

The last aspect, namely that the complete set of counterterms including also those with two derivatives (*i.e.* the kinetic terms) is necessary, is connected to the second sort of problems. The tree level Lagrangian is constructed using just one of such a kinetic term in order to ensure the propagation of just three degrees of freedom corresponding to the spin-one particle state. If we would include all possible kinetic terms with two derivatives into the free Lagrangian, we would get (according to the formalism used) additional poles in the free propagator corresponding to the additional one-particle states some of them being necessarily either negative norm ghost or tachyon. This was the first signal of the problems with unphysical degrees of freedom connected with the one-loop corrections to the self-energies. The higher derivative kinetic terms further increase the number of these extra degrees of freedom. We have studied this feature also using the path integral representation and integrated in additional fields which appear to be responsible for the additional propagator poles.

The problems with additional degrees of freedom are also connected with the well known fact that the propagator obtained by means of the Dyson resummation of the perturbative one-particle irreducible self-enery insertions might be incompatible with the Källén-Lehman spectral representation even in the case of the renormalizable theories [96]. As is well known, in this case tachyonic or negative norm ghost state can appear as an additional pole. Such an extra pole is usually harmless because it is very far from the energy range where the theory is applicable. In the power-counting non-renormalizable effective theories like $R\chi T$ such problems are much stronger either because of the worse UV behavior of the self-energies (which increases the number of additional poles) or because the additional pathological poles might lie near the region where the theory was

assumed to be valid. The nontrivial Lorentz structure of the fields describing spin-one resonances further complicates this delineation because some of the additional poles might have different quantum numbers than the original tree-level degrees of freedom. As far as this type of poles is concerned, we have demonstrated using the path integral formalism that it can be eliminated by means of the requirement of additional protective symmetry of the interaction Lagrangian, which is an analog of $U(1)$ gauge transformation known for the Proca and Rarita-Schwinger fields. However, these symmetries are in general in conflict with chiral symmetry, though individual interaction vertices can posses such a symmetry accidentally.

The results of our calculations proved to fit this general picture. Using the explicit example of the one-loop antisymmetric tensor self-energy we have shown that the Dyson re-summed propagator has always (ie. irrespectively to the actual values of the couterterm couplings) at least three additional poles on the first sheet in the 1^{--} channel, just five such poles on the second sheet (one of them corresponding to the original degree of freedom) and at least two additional poles on the first sheet in the 1^{+-} channel and at least four such poles on the second sheet. As we have seen in explicit analysis of the pole equations, without any additional information about the size of the counterterm couplings and consequently about the actual values of the renormalization scale invariant parameters entering the polynomial part of the self-energies, a rich variety of poles in the propagator is possible. Some of the poles might be unphysical (complex conjugated pairs of poles on the first sheet and tachyonic or negative norm ghosts on both sheets) and some of them even can be situated near or inside the assumed applicability region of $R\chi T$.

It might be argued that the additional poles are just artifacts of the inappropriate treatment of the theory and that the one-loop one-particle irreducible self-energy insertion cannot be re-summed in order to construct a reliable approximation of the full resonance propagator. However, the mere truncation of the Dyson series keeping only first two terms (corresponding to tree-level contribution and to the strict one-loop correction to the propagator respectively) generates double poles at $s = M^2$ on both sheets and is therefore in contradiction with the expected analytic structure of the full propagator. Though this might be an useful approximation of the full propagator for $s \ll M^2$, it cannot be correct in the resonance region. Therefore provided we would like to use $R\chi T$ at one-loop also for $s \sim M^2$, the construction the propagator using some sort of re-summation (*i.e.* the Dyson one or its modifications like *e.g.* the Redmond and Bogolyubov procedure or Padé approximation) might be inevitable. The actual position of the additional poles (if there are any within the chosen procedure) might be then understood as a bound limiting the range of applicability of the theory. In the most optimistic scenario all the additional poles are far form the region of interest and $R\chi T$ can be treated as a consistent effective theory describing just the degrees of freedom we start with at the tree level. The less satisfactory case when only the pathological poles are far-distant, we can either abandon the theory as inconsistent or alternatively we can try to interpret the non-pathological poles as a prediction of the theory corresponding to the dynamical generation of higher resonances. Such a treatment was used in the case of scalar resonances in [77] (see also [78, 79]). Eventually in the case when all the additional poles lie near $s \sim M^2$, either the approximative construction of the propagator or one-loop

$R\chi T$ itself might be problematic. Which scenario actually turns up depends on the values of the couplings in the $R\chi T$ Lagrangian.

3.7 Appendix

3.7.1 Additional degrees of freedom in the path integral - the Proca field

Suppose that the interaction Lagrangian has the form

$$\mathcal{L}_{int} = \mathcal{L}_{ct} + \mathcal{L}'_{int} \tag{3.180}$$

where $\mathcal{L}_{ct}$ is the toy interaction Lagrangian (3.18). Our aim will be to transform $Z[J]$ to the form of the path integral with all the additional degrees of freedom represented explicitly in the Lagrangian and the integration measure. In terms of the transverse and longitudinal degrees of freedom we get

$$\begin{aligned}\mathcal{L}_{int}(V_\perp - \partial\Lambda, J, \ldots) &= \mathcal{L}_{ct}(V_\perp - \partial\Lambda, J, \ldots) + \mathcal{L}'_{int}(V_\perp - \partial\Lambda, J, \ldots) \\ &= \frac{\alpha}{2}V_\perp^\mu \Box V_{\perp\mu} - \frac{\beta}{2}(\Box\Lambda)^2 + \frac{\gamma}{2M^2}(\Box V_\perp^\mu)(\Box V_{\perp\mu}) + \frac{\delta}{2M^2}(\partial_\mu\Box\Lambda)(\partial^\mu\Box\Lambda) \\ &+\mathcal{L}'_{int}(V_\perp - \partial\Lambda, J\ldots).\end{aligned} \tag{3.181}$$

In order to lower the number of derivatives in the kinetic terms we integrate in auxiliary scalar fields χ, ρ, π, σ and auxiliary transverse vector field $B_{\perp\mu}$. Writing

$$\exp\left(-i\int \mathrm{d}^4x \frac{\beta}{2}(\Box\Lambda)^2\right) = \int \mathcal{D}\chi \exp\left(i\int \mathrm{d}^4x \left(\frac{1}{2\beta}\chi^2 - \partial_\mu\chi\partial^\mu\Lambda\right)\right) \tag{3.182}$$

and similarly for other higher derivative terms we can finally formulate the theory as

$$Z[J] = \int \mathcal{D}V_\perp \mathcal{D}B_\perp \mathcal{D}\Lambda\mathcal{D}\chi\mathcal{D}\rho\mathcal{D}\sigma\mathcal{D}\pi \exp\left(i\int \mathrm{d}^4x \mathcal{L}(V_\perp, B_\perp, \Lambda, \chi, \rho, \sigma, \pi, J, \ldots)\right) \tag{3.183}$$

with

$$\mathcal{D}B_\perp = \mathcal{D}B\delta(\partial_\mu B^\mu) \tag{3.184}$$

$$B_\perp^\mu = \left(g^{\mu\nu} - \frac{\partial^\mu\partial^\nu}{\Box}\right)B_\nu. \tag{3.185}$$

and

$$\begin{aligned}\mathcal{L}(V_\perp, B_\perp, \Lambda, \chi, \rho, \sigma, \pi, J, \ldots) &= \\ &\frac{1}{2}(1+\alpha)V_\perp^\mu \Box V_{\perp\mu} + \frac{1}{2}M^2 V_\perp^\mu V_{\perp\mu} - \frac{1}{2\gamma}M^2 B_\perp^\mu B_{\perp\mu} - B_\perp^\mu \Box V_\perp^\mu \\ &+\frac{1}{2}M^2\partial_\mu\Lambda\partial^\mu\Lambda + \frac{1}{2\beta}\chi^2 - \partial_\mu\chi\partial^\mu\Lambda \\ &-\frac{1}{2\delta}M^2\partial_\mu\rho\partial^\mu\rho - \partial_\mu\rho\partial^\mu\sigma - \partial_\mu\pi\partial^\mu\Lambda - \pi\sigma \\ &+\mathcal{L}'_{int}(V_\perp - \partial\Lambda, J, \ldots)\end{aligned} \tag{3.186}$$

In this formulation the kinetic terms have no more than two derivatives, however, the number of fields is higher than the actual number of degrees of freedom. We therefore have to integrate out the redundant variables. As a first step we diagonalize the kinetic terms performing the shifts

$$\begin{aligned} V_\perp^\mu &\to V_\perp^\mu + \frac{1}{1+\alpha} B_\perp^\mu \\ \Lambda &\to \Lambda + \frac{1}{M^2}\chi + \frac{1}{M^2}\pi \\ \rho &\to \rho - \frac{\delta}{M^2}\sigma \\ \chi &\to \chi - \pi \end{aligned} \tag{3.187}$$

respectively to the form

$$\begin{aligned} \mathcal{L}(V_\perp, B_\perp, \Lambda, \chi, \rho, \sigma, \pi, J, \ldots) &= \frac{1}{2}(1+\alpha) V_\perp^\mu \Box V_{\perp\mu} + \frac{1}{2} M^2 V_\perp^\mu V_{\perp\mu} \\ &\quad -\frac{1}{2}(1+\alpha)^{-1} B_\perp^\mu \Box B_\perp^\mu + \frac{1}{2} M^2 \left((1+\alpha)^{-2} - \gamma^{-1}\right) B_\perp^\mu B_{\perp\mu} \\ &\quad + M^2 (1+\alpha)^{-1} V_\perp^\mu B_{\perp\mu} \\ &\quad + \frac{1}{2} M^2 \partial_\mu \Lambda \partial^\mu \Lambda - \frac{1}{2M^2} \partial_\mu \chi \partial^\mu \chi + \frac{1}{2\beta}(\chi - \pi)^2 \\ &\quad - \frac{1}{2\delta} M^2 \partial_\mu \rho \partial^\mu \rho + \frac{\delta}{2M^2} \partial_\mu \sigma \partial^\mu \sigma - \pi\sigma \\ &\quad + \mathcal{L}'_{int}(\overline{V}, J, \ldots). \end{aligned} \tag{3.188}$$

where

$$\overline{V} = V_\perp + \frac{1}{1+\alpha} B_\perp - \partial\Lambda - \frac{1}{M^2}\partial\chi \tag{3.189}$$

Now the superfluous degrees of freedom are easily identified. Namely, the fields ρ and σ decouple and moreover π has no kinetic term. Both of them can be therefore easily integrated out. As a result of the gaussian integration we get

$$Z[J] = \int \mathcal{D}V_\perp \mathcal{D}B_\perp \mathcal{D}\Lambda \mathcal{D}\chi \mathcal{D}\sigma \exp\left(i \int \mathrm{d}^4 x \mathcal{L}(V_\perp, B_\perp, \Lambda, \chi, \sigma, J, \ldots) \right) \tag{3.190}$$

where

$$\begin{aligned} \mathcal{L}(V_\perp, B_\perp, \Lambda, \chi, \sigma, J, \ldots) &= \frac{1}{2}(1+\alpha) V_\perp^\mu \Box V_{\perp\mu} + \frac{1}{2} M^2 V_\perp^\mu V_{\perp\mu} \\ &\quad -\frac{1}{2}(1+\alpha)^{-1} B_\perp^\mu \Box B_\perp^\mu + \frac{1}{2} M^2 \left((1+\alpha)^{-2} - \gamma^{-1}\right) B_\perp^\mu B_{\perp\mu} \\ &\quad + M^2 (1+\alpha)^{-1} V_\perp^\mu B_{\perp\mu} \\ &\quad - \frac{1}{2M^2} \partial_\mu \chi \partial^\mu \chi + \frac{\delta}{2M^2} \partial_\mu \sigma \partial^\mu \sigma - \frac{1}{2}\beta\sigma^2 - \chi\sigma \\ &\quad + \frac{1}{2} M^2 \partial_\mu \Lambda \partial^\mu \Lambda \\ &\quad + \mathcal{L}'_{int}(\overline{V}, J, \ldots). \end{aligned} \tag{3.191}$$

Let us assume $\alpha > -1$ and $\delta > 0$ in what follows. Note that, in this case the fields $B_\perp^\mu$ and χ have opposite minus sign at their kinetic terms. This is a signal

of the appearence of the negative norm ghosts in the spectrum of the theory. The "dangerous" fields $B^\mu_\perp$ and χ mix with the fields $V^\mu_\perp$ and σ respectively. In order to identify the mass eigenstates we further rescale the fields

$$\begin{aligned} V^\mu_\perp &\to (1+\alpha)^{-1/2} V^\mu_\perp \\ B^\mu_\perp &\to (1+\alpha)^{1/2} B^\mu_\perp \\ \chi &\to M\chi \\ \sigma &\to \delta^{-1/2} M\sigma \end{aligned} \tag{3.192}$$

and afterwards we diagonalize the mass terms

$$\begin{aligned} \mathcal{L}_{mass} &= \frac{1}{2}\frac{M^2}{1+\alpha}\left(V^\mu_\perp V_{\perp\mu} + \left(1 - \frac{(1+\alpha)^2}{\gamma}\right) B^\mu_\perp B_{\perp\mu}\right) \\ &\quad -\frac{1}{2}M^2\left(\beta\sigma^2 + \delta^{-1/2}\chi\sigma\right) \end{aligned} \tag{3.193}$$

by means of an appropriate $Sp(2)$ symplectic rotation of the fields $V^\mu_\perp$, $B^\mu_\perp$ and χ, σ

$$\begin{aligned} V^\mu_\perp &\to V^\mu_\perp \cosh\theta_V + B^\mu_\perp \sinh\theta_V \\ B^\mu_\perp &\to V^\mu_\perp \sinh\theta_V + B^\mu_\perp \cosh\theta_V \\ \chi &\to \chi\cosh\theta_S + \sigma\sinh\theta_S \\ \sigma &\to \chi\sinh\theta_S + \sigma\cosh\theta_S. \end{aligned} \tag{3.194}$$

This is possible for $(1+\alpha)^2 > 4\gamma$ and $\beta^2 > 4\delta$, when the off-diagonal elements of the mass matrix vanish for

$$\begin{aligned} \tanh\theta_V &= \frac{(1+\alpha)^2 - 2\gamma - (1+\alpha)\sqrt{(1+\alpha)^2 - 4\gamma}}{2\gamma} \\ \tanh\theta_S &= \frac{\sqrt{\beta^2 - 4\delta} - \beta}{2\delta^{1/2}}. \end{aligned} \tag{3.195}$$

We get finally for the generating functional

$$Z[J] = \int \mathcal{D}V_\perp \mathcal{D}B_\perp \mathcal{D}\Lambda \mathcal{D}\chi \mathcal{D}\sigma \exp\left(i\int \mathrm{d}^4x \mathcal{L}(V_\perp, B_\perp, \Lambda, \chi, \sigma, J, \ldots)\right) \tag{3.196}$$

where

$$\begin{aligned} \mathcal{L}(V_\perp, B_\perp, \Lambda, \chi, \sigma, J, \ldots) &= \frac{1}{2}V^\mu_\perp \Box V_{\perp\mu} + \frac{1}{2}M^2_{V+}V^\mu_\perp V_{\perp\mu} - \frac{1}{2}B^\mu_\perp \Box B^\mu_\perp + \frac{1}{2}M^2_{V-}B^\mu_\perp B_{\perp\mu} \\ &\quad + \frac{1}{2}\partial_\mu\sigma\partial^\mu\sigma - \frac{1}{2}M^2_{S+}\sigma^2 - \frac{1}{2}\partial_\mu\chi\partial^\mu\chi - \frac{1}{2}M^2_{S-}\chi^2 + \frac{1}{2}M^2\partial_\mu\Lambda\partial^\mu\Lambda \\ &\quad + \mathcal{L}'_{int}(\overline{V}^{(\theta)}, J, \ldots). \end{aligned} \tag{3.197}$$

where now

$$\overline{V}^{(\theta)} = \frac{\exp\theta_V}{(1+\alpha)^{1/2}}(V_\perp + B_\perp) - \partial\chi\cosh\theta_S - \partial\sigma\sinh\theta_S - \partial\Lambda \tag{3.198}$$

and where $M^2_{V\pm}$, $M^2_{S\pm}$ are the mass eigenvalues (3.21) and (3.23). The theory is now formulated in terms of two spin one and two spin zero fields, whereas two of them, namely $B^\mu_\perp$ and χ, are negative norm ghosts. The field Λ do not correspond to any dynamical degree of freedom, its role is merely to cancel the spurious poles of the free propagators of the transverse fields $V_\perp$ and $B_\perp$ at $p^2 = 0$.

3.7.2 The additional degrees of freedom in the path integral- the antisymmetric tensor case

We assume the interaction Lagrangian to be of the form

$$\mathcal{L}_{int} = \mathcal{L}_{ct} + \mathcal{L}'_{int}, \tag{3.199}$$

where $\mathcal{L}_{ct}$ is given by (3.57) and re-express it in the terms of the longitudinal and transverse components of the original field $R_{\mu\nu}$

$$\mathcal{L}_{int}(R^{\mu\nu}_{\parallel} - \frac{1}{2}\varepsilon^{\mu\nu\alpha\beta}\widehat{\Lambda}_{\alpha\beta}, J, \ldots) = \mathcal{L}_{ct}(R^{\mu\nu}_{\parallel} - \frac{1}{2}\varepsilon^{\mu\nu\alpha\beta}\widehat{\Lambda}_{\alpha\beta}, J, \ldots) + \mathcal{L}'_{int}(R^{\mu\nu}_{\parallel} - \frac{1}{2}\varepsilon^{\mu\nu\alpha\beta}\widehat{\Lambda}_{\alpha\beta}, J, \ldots) \tag{3.200}$$

where

$$\begin{aligned}\mathcal{L}_{ct}(R^{\mu\nu} - \frac{1}{2}\varepsilon^{\mu\nu\alpha\beta}\widehat{\Lambda}_{\alpha\beta}J, \ldots) &= \frac{\alpha}{4}R^{\mu\nu}_{\parallel}\Box R_{\parallel\,\mu\nu} + \frac{\gamma}{4M^2}(\Box R^{\mu\nu}_{\parallel})(\Box R_{\parallel\,\mu\nu}) \\ &+\frac{\beta}{2}(\Box\Lambda^{\mu}_{\perp})(\Box\Lambda_{\perp\mu}) - \frac{\delta}{2M^2}(\partial^{\alpha}\Box\Lambda^{\mu}_{\perp})(\partial_{\alpha}\Box\Lambda_{\perp\mu})\end{aligned} \tag{3.201}$$

We can introduce the auxiliary (longitudinal) antisymmetric tensor field $B^{\mu\nu}_{\parallel}$ and (transverse) vector fields $\chi^{\mu}_{\perp}$, $\rho^{\mu}_{\perp}$, $\sigma^{\mu}_{\perp}$ and $\pi^{\mu}_{\perp}$ in order to avoid the higher derivative terms and write in complete analogy with the Proca field case

$$\begin{aligned}Z[J] = \int &\mathcal{D}R_{\parallel}\mathcal{D}B_{\parallel}\mathcal{D}\Lambda_{\perp}\mathcal{D}\chi_{\perp}\mathcal{D}\rho_{\perp}\mathcal{D}\sigma_{\perp}\mathcal{D}\pi_{\perp} \\ &\exp\left(\mathrm{i}\int \mathrm{d}^4x\mathcal{L}(R_{\parallel}, B_{\parallel}, \Lambda_{\perp}, \chi_{\perp}, \rho_{\perp}, \sigma_{\perp}, \pi_{\perp}, J, \ldots)\right)\end{aligned} \tag{3.202}$$

where the measures and fields are

$$\mathcal{D}B_{\parallel} = \mathcal{D}B\delta(\partial_{\alpha}B_{\mu\nu} + \partial_{\nu}B_{\alpha\mu} + \partial_{\mu}B_{\nu\alpha}) \tag{3.203}$$

$$B^{\mu\nu}_{\parallel} = -\frac{1}{2\Box}(\partial^{\mu}g^{\nu\alpha}\partial^{\beta} + \partial^{\nu}g^{\mu\beta}\partial^{\alpha} - (\mu \leftrightarrow \nu))B_{\alpha\beta} \tag{3.204}$$

and for $\phi^{\mu} = \chi^{\mu}$, ρ^{μ}, σ^{μ} and π^{μ}

$$\mathcal{D}\phi_{\perp} = \mathcal{D}\phi\delta(\partial_{\mu}\phi^{\mu}) \tag{3.205}$$

$$\phi^{\mu}_{\perp} = \left(g^{\mu\nu} - \frac{\partial^{\mu}\partial^{\nu}}{\Box}\right)\phi_{\perp\nu}. \tag{3.206}$$

The Lagrangian is then

$$\begin{aligned}\mathcal{L} &= \frac{1+\alpha}{4}R^{\mu\nu}_{\parallel}\Box R_{\parallel\,\mu\nu} + \frac{1}{4}M^2R^{\mu\nu}_{\parallel}R_{\parallel\,\mu\nu} \\ &-\frac{1}{\gamma}M^2B^{\mu\nu}_{\parallel}B_{\parallel\,\mu\nu} + B^{\mu\nu}_{\parallel}\Box R_{\parallel\,\mu\nu} \\ &+\frac{1}{2}M^2\Lambda^{\mu}_{\perp}\Box\Lambda_{\perp\mu} - \frac{1}{2\beta}\chi^{\mu}_{\perp}\chi_{\perp\mu} - \chi^{\mu}_{\perp}\Box\Lambda_{\perp\mu} \\ &+\frac{1}{2\delta}M^2\partial^{\alpha}\rho^{\mu}_{\perp}\partial_{\alpha}\rho_{\perp\mu} - \partial^{\alpha}\rho^{\mu}_{\perp}\partial_{\alpha}\sigma_{\perp\mu} - \partial^{\alpha}\Lambda^{\mu}_{\perp}\partial_{\alpha}\pi_{\perp\mu} - \pi^{\mu}_{\perp}\sigma_{\perp\mu} \\ &+\mathcal{L}_{int}\left(R^{\mu\nu} - \frac{1}{2}\varepsilon^{\mu\nu\alpha\beta}\widehat{\Lambda}_{\alpha\beta}, J, \ldots\right).\end{aligned} \tag{3.207}$$

Note that, the fields χ^μ, ρ^μ, σ^μ and π^μ mix with Λ^μ and are therefore pseudovectors. The Lagrangian (3.207) is completely analogical to (3.186) up to the more Lorentz indices, so will be brief in the next steps. First we identify the redundant degrees of freedom diagonalizing the kinetic terms by means of the following sequence of shifts (cf. (3.187))

$$\begin{aligned} R_\parallel^{\mu\nu} &\to R_\parallel^{\mu\nu} - 2(1+\alpha)^{-1} B_\parallel^{\mu\nu} \\ \Lambda_\perp^\mu &\to \Lambda_\perp^\mu + \frac{1}{M^2}\chi_\perp^\mu - \frac{1}{M^2}\pi_\perp^\mu \\ \rho_\perp^\mu &\to \rho_\perp^\mu + \frac{\delta}{M^2}\sigma_\perp^\mu \\ \chi_\perp^\mu &\to \chi_\perp^\mu + \pi_\perp^\mu . \end{aligned} \tag{3.208}$$

As a result we get the Lagrangian in the form (cf. (3.188))

$$\begin{aligned} \mathcal{L} &= \frac{1}{4}(1+\alpha) R_\parallel^{\mu\nu} \Box R_{\parallel\,\mu\nu} + \frac{1}{4} M^2 R_\parallel^{\mu\nu} R_{\parallel\,\mu\nu} \\ &\quad -(1+\alpha)^{-1} B_\parallel^{\mu\nu} \Box B_{\parallel\,\mu\nu} + (1+\alpha)^{-2} M^2 B_\parallel^{\mu\nu} B_{\parallel\,\mu\nu} - \frac{1}{\gamma} M^2 B_\parallel^{\mu\nu} B_{\parallel\,\mu\nu} \\ &\quad -(1+\alpha)^{-1} M^2 R_\parallel^{\mu\nu} B_{\parallel\,\mu\nu} \\ &\quad +\frac{1}{2} M^2 \Lambda_\perp^\mu \Box \Lambda_{\perp\mu} - \frac{1}{2M^2}\chi_\perp^\mu \Box \chi_{\perp\mu} - \frac{1}{2\beta}(\chi_\perp^\mu + \pi_\perp^\mu)(\chi_{\perp\mu} + \pi_{\perp\mu}) \\ &\quad +\frac{1}{2\delta} M^2 \partial^\alpha \rho_\perp^\mu \partial_\alpha \rho_{\perp\mu} - \frac{\delta}{2M^2}\partial^\alpha \sigma_\perp^\mu \partial_\alpha \sigma_{\perp\mu} - \pi_\perp^\mu \sigma_{\perp\mu} \\ &\quad +\mathcal{L}_{int}\left(\overline{R}, J, \ldots\right), \end{aligned} \tag{3.209}$$

where

$$\overline{R}^{\mu\nu} = R_\parallel^{\mu\nu} - 2(1+\alpha)^{-1} B_\parallel^{\mu\nu} - \frac{1}{2}\varepsilon^{\mu\nu\alpha\beta}(\widehat{\Lambda}_{\alpha\beta} + \frac{1}{M^2}\widehat{\chi}_{\perp\alpha\beta}). \tag{3.210}$$

Integrating out the superfluous fields $\rho_{\perp\mu}$ and $\pi_{\perp\mu}$ which are decoupled from the interaction we get

$$\begin{aligned} Z[J] = \int &\mathcal{D}R_\parallel \mathcal{D}B_\parallel \mathcal{D}\Lambda_\perp \mathcal{D}\chi_\perp \mathcal{D}\rho_\perp \mathcal{D}\sigma_\perp \mathcal{D}\pi_\perp \\ &\exp\left(\mathrm{i}\int \mathrm{d}^4x \mathcal{L}(R_\parallel, B_\parallel, \Lambda_\perp, \chi_\perp, \rho_\perp, \sigma_\perp, \pi_\perp, J, \ldots)\right) \end{aligned} \tag{3.211}$$

with (cf. (3.191))

$$\begin{aligned} \mathcal{L} &= \frac{1}{4}(1+\alpha) R_\parallel^{\mu\nu} \Box R_{\parallel\,\mu\nu} + \frac{1}{4} M^2 R_\parallel^{\mu\nu} R_{\parallel\,\mu\nu} \\ &\quad -(1+\alpha)^{-1} B_\parallel^{\mu\nu} \Box B_{\parallel\,\mu\nu} + (1+\alpha)^{-2} M^2 B_\parallel^{\mu\nu} B_{\parallel\,\mu\nu} - \frac{1}{\gamma} M^2 B_\parallel^{\mu\nu} B_{\parallel\,\mu\nu} \\ &\quad -(1+\alpha)^{-1} M^2 R_\parallel^{\mu\nu} B_{\parallel\,\mu\nu} \\ &\quad +\frac{1}{2} M^2 \Lambda_\perp^\mu \Box \Lambda_{\perp\mu} \\ &\quad -\frac{1}{2M^2}\chi_\perp^\mu \Box \chi_{\perp\mu} + \frac{\delta}{2M^2}\sigma_\perp^\mu \Box \sigma_{\perp\mu} + \frac{1}{2}\beta \sigma_\perp^\mu \sigma_{\perp\mu} + \chi_\perp^\mu \sigma_{\perp\mu} \\ &\quad +\mathcal{L}_{int}(S, J, \ldots) \end{aligned} \tag{3.212}$$

Again, assuming $\alpha > -1$ and $\delta > 0$ we have two pairs of fields with opposite signs of the kinetic terms, namely $(R^{\mu\nu}_{\parallel}, B^{\mu\nu}_{\parallel})$ and $(\chi^{\mu}_{\perp}, \sigma^{\mu}_{\perp})$ respectively.The fields within both of these these pairs mix. After re-scaling

$$\begin{aligned} R^{\mu\nu}_{\parallel} &\rightarrow (1+\alpha)^{-1/2} R^{\mu\nu}_{\parallel} \\ B^{\mu\nu}_{\parallel} &\rightarrow \frac{1}{2}(1+\alpha)^{1/2} B^{\mu\nu}_{\parallel} \\ \chi^{\mu}_{\perp} &\rightarrow M\chi^{\mu}_{\perp} \\ \sigma^{\mu}_{\perp} &\rightarrow \frac{M}{\sqrt{\delta}}\sigma^{\mu}_{\perp} \end{aligned} \tag{3.213}$$

the form of the mass matrix becomes identical to that of (3.193) (with obvious identifications) and we can therefore perform the same symplectic rotations as in the Proca field case and under the same assumptions to get diagonal mass terms corresponding to the eigenvalues (3.21, 3.23). As a result we have found four spin-one states, two of them being negative norm ghosts, namely $B^{\mu\nu}_{\parallel}$ and $\sigma^{\mu}_{\perp}$ and two of them with opposite parity, namely $\chi^{\mu}_{\perp}$ and $\sigma^{\mu}_{\perp}$. As in the Proca field case, the field $\Lambda^{\mu}_{\perp}$ effectively compensates for the spurious $p^2 = 0$ poles in the $R^{\mu\nu}_{\parallel}$ and $B^{\mu\nu}_{\parallel}$ propagators within Feynman graphs.

3.7.3 Path integral formulation of the first order formalism

Within the first order formalism, the path integral formulation is merely a generalization of the previous two cases, so we will be as brief as possible in what follows. Note that, now the kinetic term is invariant with respect to the both transformations (3.26) and (3.60), therefore the manifestation of the degrees of freedom within the the path integral formalism can be done in analogy with the previous two cases. Using triple Faddeev-Popov trick in the path integral

$$Z[J] = \int \mathcal{D}R \exp\left(\mathrm{i}\int \mathrm{d}^4x \left(MV_\nu \partial_\mu R^{\mu\nu} + \frac{1}{2}M^2 V_\mu V^\mu + \frac{1}{4}M^2 R_{\mu\nu}R^{\mu\nu} + \mathcal{L}_{int}\right)\right) \tag{3.214}$$

where $\mathcal{L}_{int} = \mathcal{L}_{int}(V^\alpha, R^{\mu\nu}, J, \ldots)$. We get

$$Z[J] = \int \mathcal{D}R_{\parallel}\mathcal{D}\Lambda_{\perp}\mathcal{D}V_{\perp}\mathcal{D}\Lambda \exp\left(\mathrm{i}\int \mathrm{d}^4x \mathcal{L}(R^{\mu\nu}_{\parallel}, \Lambda^{\rho}_{\perp}, V^{\alpha}_{\perp} \ldots, \Lambda, J, \ldots)\right) \tag{3.215}$$

where

$$\begin{aligned} \mathcal{L}(R^{\mu\nu}_{\parallel}, \Lambda^{\rho}_{\perp}, V^{\alpha}_{\perp} \ldots, \Lambda, J, \ldots) &= MV_{\perp\nu}\partial_\mu R^{\mu\nu}_{\parallel} + \frac{1}{2}M^2 V_{\perp\mu}V^{\mu}_{\perp} + \frac{1}{4}M^2 R_{\parallel\mu\nu}R^{\mu\nu}_{\parallel} \\ &+\frac{1}{2}M^2\Lambda^{\mu}_{\perp}\Box\Lambda_{\perp\mu} + \frac{1}{2}M^2\partial_\mu\Lambda\partial^\mu\Lambda \\ &+\mathcal{L}_{int}(R^{\mu\nu}_{\parallel} - \frac{1}{2}\varepsilon^{\mu\nu\alpha\beta}\widehat{\Lambda}_{\alpha\beta}, V^{\alpha}_{\perp} - \partial^\alpha\Lambda, J, \ldots) \end{aligned} \tag{3.216}$$

and, as in the previous subsections

$$\begin{aligned}
\mathcal{D}R_{\parallel} &= \mathcal{D}R\delta(\partial_\alpha R_{\mu\nu}+\partial_\nu R_{\alpha\mu}+\partial_\mu R_{\nu\alpha}) \\
\mathcal{D}\Lambda_{\perp} &= \mathcal{D}\Lambda\delta(\partial_\mu\Lambda^\mu) \\
\mathcal{D}V_{\perp} &= \mathcal{D}V\delta(\partial_\mu\Lambda^\mu) \\
R_{\parallel}^{\mu\nu} &= -\frac{1}{2\Box}(\partial^\mu g^{\nu\alpha}\partial^\beta+\partial^\nu g^{\mu\beta}\partial^\alpha-(\mu\leftrightarrow\nu))R_{\alpha\beta} \\
\Lambda_{\perp}^{\mu} &= \left(g^{\mu\nu}-\frac{\partial^\mu\partial^\nu}{\Box}\right)\Lambda_\nu \\
V_{\perp}^{\mu} &= \left(g^{\mu\nu}-\frac{\partial^\mu\partial^\nu}{\Box}\right)V_\nu.
\end{aligned} \tag{3.217}$$

In order to diagonalize the kinetic terms we perform a shift

$$V_{\perp}^{\mu}\to V_{\perp}^{\mu}-\frac{1}{M}\partial_\nu R_{\parallel}^{\nu\mu} \tag{3.218}$$

and get

$$\begin{aligned}
\mathcal{L}(R_{\parallel}^{\mu\nu},\Lambda_{\perp}^{\rho},V_{\perp}^{\alpha}\ldots,\Lambda,J,\ldots) &= \frac{1}{4}R_{\parallel}^{\mu\nu}\Box R_{\parallel\,\mu\nu}+\frac{1}{4}M^2R_{\parallel\mu\nu}R_{\parallel}^{\mu\nu}+\frac{1}{2}M^2V_{\perp\mu}V_{\perp}^{\mu} \\
&\quad+\frac{1}{2}M^2\Lambda_{\perp}^{\mu}\Box\Lambda_{\perp\mu}+\frac{1}{2}M^2\partial_\mu\Lambda\partial^\mu\Lambda \\
&\quad+\mathcal{L}_{int}(R_{\parallel}^{\mu\nu}-\frac{1}{2}\varepsilon^{\mu\nu\alpha\beta}\widehat{\Lambda}_{\alpha\beta},V_{\perp}^{\alpha}-\frac{1}{M}\partial_\nu R_{\parallel}^{\nu\mu}-\partial^\alpha\Lambda,J,).
\end{aligned} \tag{3.219}$$

The discussion of the role of the field $R_{\parallel}^{\mu\nu}$ and the $\Lambda_{\perp}^{\mu}$ is the same as in the antisymmetric tensor case. The extra fields $V_{\perp}^{\mu}$ and Λ do not correspond to the original degree of freedom, their free propagators are

$$\Delta_{V\perp}^{\mu\nu}(p) = \frac{P^{T\,\mu\nu}}{M^2} \tag{3.220}$$

$$\Delta_{\Lambda}(p) = \frac{1}{M^2}\frac{1}{p^2} \tag{3.221}$$

with spurious poles at $p^2=0$. According to the form of the interaction, only the combination with spurious poles cancelled, namely

$$\Delta_{V\perp}^{\mu\nu}(p)+p^\mu p^\nu\Delta_{\Lambda}(p)+\frac{1}{M^2}p_\alpha p_\beta\Delta_{\parallel}^{\alpha\mu\beta\nu}(p)=-\frac{P^{T\,\mu\nu}}{p^2-M^2}+\frac{P^{L\,\mu\nu}}{M^2} \tag{3.222}$$

enters the Feynman graphs.

Alternatively, we could make in (3.216) the following shift

$$R_{\parallel}^{\mu\nu}\to R_{\parallel}^{\mu\nu}+\frac{1}{M}\left(\partial^\mu V_{\perp}^{\nu}-\partial^\nu V_{\perp}^{\mu}\right) \tag{3.223}$$

leading to

$$\begin{aligned}
\mathcal{L}(R_{\parallel}^{\mu\nu},\Lambda_{\perp}^{\rho},V_{\perp}^{\alpha}\ldots,\Lambda,J,\ldots) &= \frac{1}{2}V_{\perp\mu}\Box V_{\perp}^{\mu}+\frac{1}{2}M^2V_{\perp\mu}V_{\perp}^{\mu}+\frac{1}{4}M^2R_{\parallel\mu\nu}R_{\parallel}^{\mu\nu} \\
&\quad+\frac{1}{2}M^2\Lambda_{\perp}^{\mu}\Box\Lambda_{\perp\mu}+\frac{1}{2}M^2\partial_\mu\Lambda\partial^\mu\Lambda \\
&\quad+\mathcal{L}_{int}(R_{\parallel}^{\mu\nu}+\frac{1}{M}\left(\partial^\mu V_{\perp}^{\nu}-\partial^\nu V_{\perp}^{\mu}\right)-\frac{1}{2}\varepsilon^{\mu\nu\alpha\beta}\widehat{\Lambda}_{\alpha\beta},V_{\perp}^{\alpha}-\partial^\alpha\Lambda,J,\ldots).
\end{aligned} \tag{3.224}$$

In this formulation, the role of the fields $V_\perp^\mu$ and the field Λ is the same as in the Proca field case. $R_\parallel^{\mu\nu}$ does not correspond to the original degree of freedom and, as in the previous formulation, it serves together with $\Lambda_{\perp\mu}$ to cancel the spurious $p^2 = 0$ poles.

Let us end up this subsection with the path integral treatment of the toy quadratic interaction Lagrangian (3.105). Using the same transformations as before we get

$$\begin{aligned}\mathcal{L}(R_\parallel^{\mu\nu}, \Lambda_\perp^\rho, V_\perp^\alpha \ldots, \Lambda, J, \ldots) &= MV_{\perp\nu}\partial_\mu R_\parallel^{\mu\nu} + \frac{1}{2}M^2 V_{\perp\mu}V_\perp^\mu + \frac{1}{4}M^2 R_{\parallel\mu\nu}R_\parallel^{\mu\nu} \\ &+\frac{1}{2}M^2\Lambda_\perp^\mu\Box\Lambda_{\perp\mu} + \frac{1}{2}M^2\partial_\mu\Lambda\partial^\mu\Lambda \\ &+\frac{\alpha_V}{2}V_{\perp\mu}\Box V_\perp^\mu - \frac{\beta_V}{2}(\Box\Lambda)^2 + \frac{\alpha_R}{4}R_{\parallel\mu\nu}\Box R_\parallel^{\mu\nu} + \frac{\beta_R}{4}\Box\Lambda_\perp^\mu\Box\Lambda_{\perp\mu} \\ &+\mathcal{L}'_{int}(R_\parallel^{\mu\nu} - \frac{1}{2}\varepsilon^{\mu\nu\alpha\beta}\widehat{\Lambda}_{\perp\alpha\beta}, V_\perp^\alpha - \partial^\alpha\Lambda, J, \ldots) \qquad (3.225)\end{aligned}$$

Introducing the auxiliary fields analogous to the previous two examples, we have

$$\begin{aligned}\mathcal{L}(R_\parallel^{\mu\nu}, \Lambda_\perp^\mu, \chi, \chi_\perp^\mu, \sigma_\perp^\mu, \pi_\perp^\mu, J, \ldots) &= \frac{\alpha_V}{2}V_{\perp\mu}\Box V_\perp^\mu + \frac{1}{2}M^2 V_{\perp\mu}V_\perp^\mu \qquad (3.226) \\ &+\frac{\alpha_R}{4}R_{\parallel\mu\nu}\Box R_\parallel^{\mu\nu} + \frac{1}{4}M^2 R_{\parallel\mu\nu}R_\parallel^{\mu\nu} \\ &+MV_{\perp\nu}\partial_\mu R_\parallel^{\mu\nu} \\ &+\frac{1}{2}M^2\Lambda_\perp^\mu\Box\Lambda_{\perp\mu} - \frac{1}{2}M^2\Lambda\Box\Lambda \\ &+\frac{1}{2\beta_V}\chi^2 + \chi\Box\Lambda - \frac{1}{2\beta_R}\chi_\perp^\mu\chi_{\perp\mu} - \chi_\perp^\mu\Box\Lambda_{\perp\mu} \\ &+\mathcal{L}'_{int}(R_\parallel^{\mu\nu} - \frac{1}{2}\varepsilon^{\mu\nu\alpha\beta}\widehat{\Lambda}_{\perp\alpha\beta}, V_\perp^\alpha - \partial^\alpha\Lambda, J, \ldots)\end{aligned}$$

The kinetic terms can be diagonalized now by means of the shifts

$$\Lambda_\perp^\mu \rightarrow \Lambda_\perp^\mu + \frac{1}{M^2}\chi_\perp^\mu \qquad (3.227)$$

$$\Lambda \rightarrow \Lambda + \frac{1}{M^2}\chi \qquad (3.228)$$

to the form

$$\begin{aligned}\mathcal{L}(R_\parallel^{\mu\nu}, \Lambda_\perp^\mu, \chi, \chi_\perp^\mu, J, \ldots) &= \frac{\alpha_V}{2}V_{\perp\mu}\Box V_\perp^\mu + \frac{1}{2}M^2 V_{\perp\mu}V_\perp^\mu \\ &+\frac{\alpha_R}{4}R_{\parallel\mu\nu}\Box R_\parallel^{\mu\nu} + \frac{1}{4}M^2 R_{\parallel\mu\nu}R_\parallel^{\mu\nu} \\ &+MV_{\perp\nu}\partial_\mu R_\parallel^{\mu\nu} \\ &+\frac{1}{2}M^2\Lambda_\perp^\mu\Box\Lambda_{\perp\mu} - \frac{1}{2}M^2\Lambda\Box\Lambda \\ &-\frac{1}{2M^2}\chi_\perp^\mu\Box\chi_{\perp\mu} - \frac{1}{2\beta_R}\chi_\perp^\mu\chi_{\perp\mu} \\ &+\frac{1}{2M^2}\chi\Box\chi + \frac{1}{2\beta_V}\chi^2 \\ &+\mathcal{L}'_{int}(S, W, J, \ldots), \qquad (3.229)\end{aligned}$$

where

$$\begin{aligned}\overline{R}^{\mu\nu} &= R_{\parallel}^{\mu\nu} - \frac{1}{2}\varepsilon^{\mu\nu\alpha\beta}\widehat{\Lambda}_{\perp\alpha\beta} - \frac{1}{2M^2}\varepsilon^{\mu\nu\alpha\beta}\widehat{\chi}_{\perp\alpha\beta} \\ \overline{V}^{\mu} &= V_{\perp}^{\alpha} - \partial^{\alpha}\Lambda - \frac{1}{M^2}\partial^{\alpha}\chi.\end{aligned}$$

In the formula (3.229) the scalar and axial-vector ghost field as well as two propagating dynamically mixed spin-1 degrees of freedom are explicit.

3.7.4 The parameters α_i and β_i in terms of LECs

In this appendix we present the expressions for the renormalization scale independent polynomial parameters entering the self-energies (cf. Section 3.4).

The Proca field case

$$\begin{aligned}\alpha_0 &= \left(\frac{4\pi F}{M}\right)^2 Z_M^r(\mu) \\ \alpha_1 &= \left(\frac{4\pi F}{M}\right)^2 Z_V^r(\mu) - \frac{40}{3}\sigma_V^2\left(\ln\frac{M^2}{\mu^2} + \frac{1}{3}\right) \\ \alpha_2 &= \left(\frac{4\pi F}{M}\right)^2 M^2 X_V^r(\mu) + \frac{40}{9}\sigma_V^2\left(\ln\frac{M^2}{\mu^2} + \frac{1}{3}\right) \\ \alpha_3 &= \left(\frac{4\pi F}{M}\right)^2 M^4 U_V^r(\mu) + g_V^2\left(\frac{M}{F}\right)^2\left(\ln\frac{M^2}{\mu^2} - \frac{2}{3}\right) \\ \beta_0 &= \left(\frac{4\pi F}{M}\right)^2 Z_M^r(\mu) = \alpha_0 \\ \beta_1 &= \left(\frac{4\pi F}{M}\right)^2 Y_V^r(\mu) \\ \beta_2 &= \left(\frac{4\pi F}{M}\right)^2 M^2 X_V^{\prime r}(\mu) \\ \beta_3 &= \left(\frac{4\pi F}{M}\right)^2 M^4 V_V^r(\mu).\end{aligned}$$

Here U_V and V_V are certain linear combinations of the couplings of $\mathcal{L}_V^{ct(6)}$ renormalized as

$$\begin{aligned}U_V &= U_V^r(\mu) - 2g_V^2\left(\frac{M}{F}\right)^4\frac{1}{M^4}\lambda_\infty \\ V_V &= V_V^r(\mu)\end{aligned}$$

The antisymmetric tensor case

$$
\begin{aligned}
\alpha_0 &= \left(\frac{4\pi F}{M}\right)^2 Z_M^r(\mu) - \frac{40}{3}d_1^2 \ln\frac{M^2}{\mu^2} - \frac{20}{9}(3d_1^2 - d_3^2) \\
&\quad -5\left(\frac{\lambda^{VVV}}{M}\right)^2\left(\frac{F}{M}\right)^2\left(7 - 6\ln\frac{M^2}{\mu^2}\right) \\
\alpha_1 &= \left(\frac{4\pi F}{M}\right)^2 (Z_R^r(\mu) + Y_R^r(\mu)) - \frac{40}{9}(3d_1^2 + 2d_3^2)\ln\frac{M^2}{\mu^2} - \frac{20}{3}\left(d_1^2 + \frac{1}{9}d_2^2\right) \\
&\quad +\frac{10}{3}\left(\frac{\lambda^{VVV}}{M}\right)^2\left(\frac{F}{M}\right)^2\left(7 - 6\ln\frac{M^2}{\mu^2}\right) \\
\alpha_2 &= \left(\frac{4\pi F}{M}\right)^2 M^2(X_R^r(\mu) + W_R^r(\mu)) - \frac{40}{9}d_3^2\left(\ln\frac{M^2}{\mu^2} + \frac{1}{3}\right) \\
&\quad +\frac{1}{2}\left(\frac{G_V}{F}\right)^2\left(\ln\frac{M^2}{\mu^2} - \frac{2}{3}\right) - \frac{5}{3}\left(\frac{\lambda^{VVV}}{M}\right)^2\left(\frac{F}{M}\right)^2\left(2 - 3\ln\frac{M^2}{\mu^2}\right) \\
\alpha_3 &= \left(\frac{4\pi F}{M}\right)^2 M^4 U_R^r(\mu) + \frac{40}{9}d_3^2\left(\ln\frac{M^2}{\mu^2} + \frac{1}{3}\right) \\
\beta_0 &= \left(\frac{4\pi F}{M}\right)^2 Z_M^r(\mu) - \frac{40}{3}d_1^2\ln\frac{M^2}{\mu^2} - \frac{20}{9}(3d_1^2 + d_3^2) \\
&\quad -\frac{5}{3}\left(\frac{\lambda^{VVV}}{M}\right)^2\left(\frac{F}{M}\right)^2\left(11 - 6\ln\frac{M^2}{\mu^2}\right) \\
\beta_1 &= \left(\frac{4\pi F}{M}\right)^2 Y_R^r(\mu) - \frac{20}{9}(6d_1^2 - 12d_1(d_3+d_4) + 5d_3^2 + 9d_4^2 - 6d_3d_4)\ln\frac{M^2}{\mu^2} \\
&\quad -\frac{20}{27}(9d_1^2 - 18d_1(d_3+d_4) - 7d_3^2 - 12d_4^2 + 18d_3d_4) \\
&\quad \frac{20}{3}\left(\frac{\lambda^{VVV}}{M}\right)^2\left(\frac{F}{M}\right)^2\left(7 + 3\ln\frac{M^2}{\mu^2}\right) \\
\beta_2 &= \left(\frac{4\pi F}{M}\right)^2 M^2 W_R^r(\mu) - \frac{20}{9}(d_3^2 + 6d_3d_4 - 5d_4^2)\ln\frac{M^2}{\mu^2} - \frac{80}{27}(d_3^2 + 4d_4^2) \\
&\quad -\frac{5}{3}\left(\frac{\lambda^{VVV}}{M}\right)^2\left(\frac{F}{M}\right)^2\left(4 - 3\ln\frac{M^2}{\mu^2}\right) \\
\beta_3 &= \left(\frac{4\pi F}{M}\right)^2 M^4 V_R^r(\mu) - \frac{40}{9}d_4^2\left(\ln\frac{M^2}{\mu^2} - \frac{2}{3}\right).
\end{aligned}
$$

Here U_R and V_R are certain linear combinations of the couplings of $\mathcal{L}_R^{ct(6)}$ with the infinite parts fixed as

$$
\begin{aligned}
U_R &= U_R^r(\mu) - \frac{80}{9}\left(\frac{M}{F}\right)^2\frac{1}{M^4}d_3^2\lambda_\infty \\
V_R &= V_R^r(\mu) + \frac{80}{9}\left(\frac{M}{F}\right)^2\frac{1}{M^4}d_4^2\lambda_\infty.
\end{aligned}
$$

$$
\begin{aligned}
\alpha_0^{RV} &= \left(\frac{4\pi F}{M}\right)^2 Z_{RV}^r(\mu) + \frac{10}{9}(\sigma_{RV}+2\sigma_V)\left[(d_1-d_3)+3(2d_1-\sigma_{RV})\left(\ln\frac{M^2}{\mu^2}+\frac{1}{3}\right)\right] \\
\alpha_1^{RV} &= \left(\frac{4\pi F}{M}\right)^2 M^2 X_{RV}^r(\mu) + \frac{10}{9}(\sigma_{RV}+2\sigma_V)(4d_3+\sigma_{RV})\left(\ln\frac{M^2}{\mu^2}+\frac{1}{3}\right) \\
\alpha_2^{RV} &= \left(\frac{4\pi F}{M}\right)^2 M^4 Y_{RV}^r(\mu) - \frac{20}{9}(\sigma_{RV}+2\sigma_V)d_3\left(\ln\frac{M^2}{\mu^2}+\frac{1}{3}\right) \\
&\quad -\frac{1}{2}\frac{g_V G_V}{M}\left(\frac{M}{F}\right)^2\left(\ln\frac{M^2}{\mu^2}-\frac{2}{3}\right) \\
\alpha_0^{VV} &= \left(\frac{4\pi F}{M}\right)^2 Z_{MV}^r(\mu) \\
\alpha_1^{VV} &= \left(\frac{4\pi F}{M}\right)^{22} Z_V^r(\mu) - \frac{10}{3}\left(\sigma_{RV}(\sigma_{RV}+2\sigma_V)+4\sigma_V^2\right)\left(\ln\frac{M^2}{\mu^2}+\frac{1}{3}\right) \\
\alpha_2^{VV} &= \left(\frac{4\pi F}{M}\right)^2 M^2 X_V^r(\mu) + \frac{10}{9}\left(\sigma_{RV}(\sigma_{RV}+2\sigma_V)+4\sigma_V^2\right)\left(\ln\frac{M^2}{\mu^2}+\frac{1}{3}\right) \\
\alpha_3^{VV} &= \left(\frac{4\pi F}{M}\right)^2 M^4 U_V^r(\mu) + g_V^2\left(\frac{M}{F}\right)^2\left(\ln\frac{M^2}{\mu^2}-\frac{2}{3}\right) \\
\beta_0^{VV} &= \left(\frac{4\pi F}{M}\right)^2 Z_{MV}^r(\mu) = \alpha_0^{VV} \\
\beta_1^{VV} &= \left(\frac{4\pi F}{M}\right)^2 Y_V^r(\mu) \\
\beta_2^{VV} &= \left(\frac{4\pi F}{M}\right)^2 M^2 X_V'^r(\mu) \\
\beta_3^{VV} &= \left(\frac{4\pi F}{M}\right)^2 M^4 V_V^r(\mu) \\
\alpha_0^{RR} &= \left(\frac{4\pi F}{M}\right)^2 Z_{MR}^r(\mu) + \frac{10}{3}\left(\sigma_{RV}(2d_1-\sigma_{RV})-4d_1^2\right)\left(\ln\frac{M^2}{\mu^2}+\frac{1}{3}\right) \\
&\quad -\frac{10}{9}(d_1-d_3)(2d_1+2d_3-\sigma_{RV}) \\
\alpha_1^{RR} &= \left(\frac{4\pi F}{M}\right)^2 (Z_R^r(\mu)+Y_R^r(\mu)) - \frac{40}{9}(3d_1^2+2d_3^2)\ln\frac{M^2}{\mu^2} - \frac{20}{3}\left(d_1^2+\frac{1}{9}d_2^2\right) \\
&\quad +\frac{10}{9}\left(\ln\frac{M^2}{\mu^2}+\frac{1}{3}\right)\sigma_{RV}(4d_3+\sigma_{RV}) \\
\alpha_2^{RR} &= \left(\frac{4\pi F}{M}\right)^2 M^2(X_R^r(\mu)+W_R^r(\mu)) - \frac{20}{9}d_3(2d_3+\sigma_{RV})\left(\ln\frac{M^2}{\mu^2}+\frac{1}{3}\right) \\
&\quad +\frac{1}{2}\left(\frac{G_V}{F}\right)^2\left(\ln\frac{M^2}{\mu^2}-\frac{2}{3}\right) \\
\alpha_3^{RR} &= \left(\frac{4\pi F}{M}\right)^2 M^4 U_R^r(\mu) + \frac{40}{9}d_3^2\left(\ln\frac{M^2}{\mu^2}+\frac{1}{3}\right)
\end{aligned}
$$

$$
\begin{aligned}
\beta_0^{RR} &= \left(\frac{4\pi F}{M}\right)^2 Z_{MR}^r(\mu) + \frac{10}{3}(\sigma_{RV}(2d_1-\sigma_{RV})-4d_1^2)\left(\ln\frac{M^2}{\mu^2}+\frac{1}{3}\right)\\
&\quad -\frac{20}{9}(d_1^2+d_3^2)+\frac{10}{9}\sigma_{RV}\,(d_1+d_3-\sigma_{RV})\\
&= \alpha_0^{RR}-\frac{40}{9}d_3^2+\frac{10}{9}\sigma_{RV}\,(2d_3-\sigma_{RV})\\
\beta_1^{RR} &= \left(\frac{4\pi F}{M}\right)^2 Y_R^r(\mu)-\frac{20}{9}(6d_1^2-12d_1(d_3+d_4)+5d_3^2+9d_4^2-6d_3d_4)\ln\frac{M^2}{\mu^2}\\
&\quad -\frac{20}{27}(9d_1^2-18d_1(d_3+d_4)-7d_3^2-12d_4^2+18d_3d_4)\\
&\quad -\frac{5}{27}\sigma_{RV}\left(32d_3+6(d_3+9d_4)\ln\frac{M^2}{\mu^2}-3\sigma_{RV}\left(\ln\frac{M^2}{\mu^2}-\frac{2}{3}\right)\right)\\
\beta_2^{RR} &= \left(\frac{4\pi F}{M}\right)^2 M^2 W_R^r(\mu)-\frac{20}{9}(d_3^2+6d_3d_4-5d_4^2)\ln\frac{M^2}{\mu^2}-\frac{80}{27}(d_3^2+4d_4^2)\\
&\quad +\frac{5}{27}\sigma_{RV}\left(8d_3+6(d_3+3d_4)\ln\frac{M^2}{\mu^2}-3\sigma_{RV}\left(\ln\frac{M^2}{\mu^2}-\frac{2}{3}\right)\right)\\
\beta_3^{RR} &= \left(\frac{4\pi F}{M}\right)^2 M^4 V_R^r(\mu)-\frac{40}{9}d_4^2\left(\ln\frac{M^2}{\mu^2}-\frac{2}{3}\right).
\end{aligned}
$$

Here U_V, V_V, U_R, V_R and Y_{RV} are certain linear combination of the couplings from $\mathcal{L}_{RV}^{ct(6)}$ with infinite parts fixed according to

$$
\begin{aligned}
U_V &= U_V^r(\mu)-2g_V^2\left(\frac{M}{F}\right)^4\frac{1}{M^4}\lambda_\infty\\
V_V &= V_V^r(\mu)\\
U_R &= U_R^r(\mu)-\frac{80}{9}\left(\frac{M}{F}\right)^2\frac{1}{M^4}d_3^2\lambda_\infty\\
V_R &= V_R^r(\mu)+\frac{80}{9}\left(\frac{M}{F}\right)^2\frac{1}{M^4}d_4^2\lambda_\infty\\
Y_{RV} &= Y_{RV}^r(\mu)+\frac{40}{9}\left(\frac{M}{F}\right)^2\frac{1}{M^4}(\sigma_{RV}+2\sigma_V)d_3\lambda_\infty+\frac{g_VG_V}{M}\left(\frac{M}{F}\right)^2\frac{1}{M^4}\lambda_\infty
\end{aligned}
$$

3.7.5 Proof of the positivity of the spectral functions

Here we prove the positivity of the spectral functios $\rho_{L,T}(\mu^2)$ defined as

$$
\begin{aligned}
&(2\pi)^{-3}\theta(p^0)\left[\rho_T(p^2)p^2\Pi^T_{\mu\nu\alpha\beta}(p)-\rho_L(p^2)p^2\Pi^L_{\mu\nu\alpha\beta}(p)\right]\\
&=\sum_N\delta^{(4)}(p-p_N)\langle 0|R_{\mu\nu}(0)|N\rangle\langle N|R_{\alpha\beta}(0)|0\rangle. \qquad (3.230)
\end{aligned}
$$

Let us define for $p^2>0$

$$
\begin{aligned}
u^{(\lambda)}_{\mu\nu}(p) &= \frac{\mathrm{i}}{\sqrt{p^2}}\left(p_\mu\varepsilon^{(\lambda)}_\nu(p)-p_\nu\varepsilon^{(\lambda)}_\mu(p)\right)\\
w^{(\lambda)}_{\mu\nu}(p) &= \frac{1}{2}\varepsilon_{\mu\nu}{}^{\alpha\beta}u^{(\lambda)}_{\alpha\beta}(p)
\end{aligned}
$$

where $\varepsilon_{\mu}^{(\lambda)}(p)$ are the usual spin-one polarization vectors corresponding to the mass $\sqrt{p^2}$. Then for $p^2 > 0$ we get the following orthogonality relations

$$\begin{aligned} u_{\mu\nu}^{(\lambda)}(p) u^{(\lambda')\mu\nu}(p)^* &= -2\delta^{\lambda\lambda'} \\ w_{\mu\nu}^{(\lambda)}(p) w^{(\lambda')\mu\nu}(p)^* &= 2\delta^{\lambda\lambda'} \\ u_{\mu\nu}^{(\lambda)}(p) w^{(\lambda')\mu\nu}(p)^* &= 0 \end{aligned}$$

and the projectors can be written for $p^2 > 0$ in terms of the polarization sums as

$$\begin{aligned} \Pi^L_{\mu\nu\alpha\beta}(p) &= -\frac{1}{2} \sum_{\lambda} u_{\mu\nu}^{(\lambda)}(p) u_{\alpha\beta}^{(\lambda)}(p)^* \\ \Pi^T_{\mu\nu\alpha\beta}(p) &= \frac{1}{2} \sum_{\lambda} w_{\mu\nu}^{(\lambda)}(p) w_{\alpha\beta}^{(\lambda)}(p)^*. \end{aligned}$$

Multiplying (**??**) by $u_{\mu\nu}^{(\lambda)}(p)^* u_{\alpha\beta}^{(\lambda)}(p)$ and $w_{\mu\nu}^{(\lambda)}(p)^* w_{\alpha\beta}^{(\lambda)}(p)$ respectively we get the positivity constraints for the spectral functions

$$\begin{aligned} 0 &\leq \sum_N \delta^{(4)}(p - p_N) |\langle 0|R_{\mu\nu}(0)|N\rangle u^{(\lambda')\mu\nu}(p)^*|^2 = 2(2\pi)^{-3} \theta(p^0) \rho_L(p^2) p^2 \\ 0 &\leq \sum_N \delta^{(4)}(p - p_N) |\langle 0|R_{\mu\nu}(0)|N\rangle w^{(\lambda')\mu\nu}(p)^*|^2 = 2(2\pi)^{-3} \theta(p^0) \rho_T(p^2) p^2. \end{aligned}$$

4. Amplitudes in the Non-linear sigma model

4.1 Introduction

The chiral nonlinear sigma model is a widely used tool for description of many phenomena in theoretical particle physics. It is based on a simple Lie Group G and the spontaneous symmetry breaking $G \times G \to G$ gives rise to massless excitations - Goldstone bosons. For instance, in the theory of strong interactions, the group G is $SU(N_f)$ where $N_f = 2, 3$ is a number of light quark flavors and Goldstone bosons are associated with the triplet of pions (for $N_f = 2$) or octet of pseudoscalar mesons π, K and η (for $N_f = 3$). The interactions of these degrees of freedom dominate the hadronic world at low energies. In this context, the leading order nonlinear $U(3) \times U(3)$ chiral invariant effective Lagrangian, the kinetic part of which corresponds to the chiral nonlinear $U(3)$ sigma model, was constructed in the late sixties by Cronin [97] while the $SU(2)$ case was studied by Weinberg [98, 99], Brown [100] and Chang and Gürsey [101]. Further generalization lead to the invention of Chiral Perturbation Theory as a low energy effective theory of Quantum Chromodynamics by Weinberg [1] and by Gasser and Leutwyler [2], [3]. Chiral Perturbation Theory became a very useful tool for the investigation of the low energy hadron physics.

The focus of this chapter is on scattering amplitudes of Goldstone bosons within the $SU(N)$ nonlinear sigma model described by the leading order Lagrangian. In principle, the standard Feynman diagram approach allows us to calculate arbitrary amplitude. Because the model is effective, and the Lagrangian contains an infinite tower of terms the calculation becomes very complicated for amplitudes of many external Goldstone bosons even at tree-level. It would be therefore desirable to find alternative non-diagrammatic methods which could save the computational effort and provide us with a tool to get the amplitudes more efficiently. In the past an attempt to formulate the calculation of the tree-level without any reference to the Lagrangian was made by Susskind and Frye [102]. They postulated recursive procedure for pion amplitudes based on certain algebraic duality assumptions supplemented with the requirement of Adler zero condition which should have to be satisfied separately for group-factor free kinematical functions recently known as the partial or stripped amplitudes. Such a condition had been proven in the special case of pion amplitudes described by the $SU(2)$ nonlinear sigma model by Osborn [103]. In [102] the authors successively calculated the amplitudes up to eight pions and showed that these results are equivalent to the diagrammatic calculation based on the $SU(2)$ nonlinear sigma model. The full equivalence for all amplitudes has been proven by Ellis and Renner in [104].

Over the past two decades there has been a huge progress in understanding scattering amplitudes using *on-shell methods* (for a review see e.g. [105–108]). They do not use explicitly the Lagrangian description of the theory and all on-shell quantities are calculated using on-shell data only with no access to off-shell physics (unlike virtual particles in Feynman diagrams). This has lead to many new theoretical tools (e.g. unitary methods [109, 110], BCFW recursion

relations for tree-level amplitudes [111, 112] and the loop integrand [113]) as well as practical applications of on-shell methods to LHC processes (for recent results of the next-to-leading order QCD corrections for W + 4-jets see [114]). Most of the recent theoretical developments have been driven by an intensive exploration of $\mathcal{N} = 4$ super Yang-Mills theory in the planar limit both at weak and strong couplings (see e.g. [115–126]).

There have been several attempts to extend some of these methods to other theories. The most natural starting point are the recursion relations for on-shell tree-level amplitudes, originally found by Britto, Cachazo, Feng and Witten for Yang-Mills theory [111], [112] and later also for gravity [127], [128] . The main idea is to perform a complex shift on external momenta and reconstruct the amplitude recursively using analytic properties of the S-matrix. More recently, this recursive approach was extended to Yang-Mills and gravity theories coupled to matter, as well as more general class of renormalizable theories [129].

In this chapter, we find the new recursion relations for all on-shell tree-level amplitudes of Goldstone bosons within $SU(N)$ nonlinear sigma model. This shows that on-shell methods can be applied also for effective field theories and it gives new computational tool in this model. Using these recursion relations we are also able to prove more properties of tree-level amplitudes that are invisible in the Feynman diagram approach.

The chapter is organized as follows: In section 2 we discuss $SU(N)$ nonlinear sigma model, introduce *stripped amplitudes* and using *minimal* parametrization (the convenient properties of which has been discussed in [104]) we calculate tree-level amplitudes up to 10 points. In section 3 we review BCFW recursion relations and their generalization to theories that do not vanish at infinity at large momentum shift. Section 4 is the main part of the chapter, we first introduce semi-on-shell amplitudes, ie. amplitudes with $n - 1$ on-shell and one off-shell external legs. Then we prove scaling properties under particular momentum shifts which allows us to construct BCFW-like recursion relations. Finally, we show explicit 6pt example. In section 5 we use previous results to prove Adler zeroes and double-soft limit formula for stripped amplitudes. Additional results and technical details are postponed to appendices: In Appendix 4.7.1, we describe the general parametrization of the $SU(N)$ nonlinear sigma model. In Appendix 4.7.2 we give the results of the amplitudes up to 10p. Appendix 4.7.3 is devoted to the counting of flavor-ordered Feynman graphs needed for the calculations of the amplitudes in nonlinear sigma models and other theories. In Appendix 4.7.4 we present additional scaling properties of the semi-on-shell amplitudes. In Appendix 4.7.5, we study the double soft-limit for more general class of spontaneously broken theories for complete (not stripped) amplitudes.

4.2 Nonlinear sigma model

4.2.1 Leading order Lagrangian

Let us first assume a most general case of the principal chiral nonlinear sigma model based on a simple compact Lie group G. Such a model corresponds to the spontaneous symmetry breaking of the chiral group $G_L \times G_R$ where $G_{L,R} = G$ to its diagonal subgroup $G_V = G$, i.e. to the subgroup of the elements $h =$

(g_L, g_R) where $g_L = g_R$. The vacuum little group G_V is invariant with respect to the involutive automorphism $(g_L, g_R) \to (g_R, g_L)$ and the homogeneous space $G_L \times G_R/G_V$ is a symmetric space which is isomorphic to the group space G. A canonical realization of such an isomorphism is via restriction of the mapping

$$(g_L, g_R) \to g_R g_L^{-1} \equiv U \tag{4.1}$$

(which is constant on the right cosets of G_V in $G_L \times G_R$) to $G_L \times G_R/G_V$. Provided we induce the action of the chiral group on $G_L \times G_R/G_V$ by means of the left multiplication, the transformation of U under general element (V_L, V_R) of the chiral group is linear

$$U \to V_R U V_L^{-1}. \tag{4.2}$$

This can be used to construct the most general chiral invariant leading order effective Lagrangian in general number d of space-time dimensions describing the dynamics of the Goldstone bosons corresponding to the spontaneous symmetry breaking $G_L \times G_R \to G_V$ as

$$\mathcal{L}^{(2)} = \frac{F^2}{4}\langle \partial_\mu U \partial^\mu U^{-1}\rangle = -\frac{F^2}{4}\langle (U^{-1}\partial_\mu U)(U^{-1}\partial^\mu U)\rangle, \tag{4.3}$$

where F is a constant[1] with the canonical dimension $d/2 - 1$. Here and in what follows we use the notation $\langle\cdot\rangle = \mathrm{Tr}(\cdot)$ and the trace is taken in the defining representation of G. The overall normalization factor is dictated by the form of the parametrization of the matrix U in terms of the Goldstone boson fields ϕ^a which we write for the purposes of this subsection[2] as

$$U = \exp\left(\sqrt{2}\frac{\mathrm{i}}{F}\phi\right) \tag{4.4}$$

where $\phi = \phi^a t^a$ and t^a, $a = 1, \ldots, \dim G$ are generators of G satisfying

$$\langle t^a t^b\rangle = \delta^{ab} \tag{4.5}$$

$$[t^a, t^b] = \mathrm{i}\sqrt{2} f^{abc} t^c. \tag{4.6}$$

Here f^{abc} are totally antisymmetric structure constants of the group G. According to (4.2), the fields ϕ^a transform linearly under the little group G_V as the vector in the adjoint representation of G while the general chiral transformations of ϕ^a are nonlinear.

The Lagrangian $\mathcal{L}^{(2)}$ can be rewritten in terms of the Goldstone boson fields as follows. We have

$$U^{-1}\partial_\mu U = -\frac{\exp\left(-\sqrt{2}\frac{\mathrm{i}}{F}\mathrm{Ad}(\phi)\right) - 1}{\mathrm{Ad}(\phi)}\partial_\mu\phi = -\frac{1}{\sqrt{2}} t \cdot \frac{\exp\left(-\frac{2\mathrm{i}}{F}D_\phi\right) - 1}{D_\phi} \cdot \partial\phi \tag{4.7}$$

where

$$\mathrm{Ad}(\phi)\partial_\mu\phi = [\phi, \partial_\mu\phi] = \sqrt{2} t^a D_\phi^{ab} \partial_\mu \phi^b \equiv \sqrt{2} t \cdot D_\phi \cdot \partial\phi, \tag{4.8}$$

the matrix D_ϕ^{ab} is given as

$$D_\phi^{ab} = -\mathrm{i} f^{cab}\phi^c \tag{4.9}$$

[1] The decay constant of the Goldstone bosons.

[2] In what follows we will use also more general parametrization of U.

and the dot means contraction of the indices in the adjoint representation. Inserting this in (4.3) we get finally

$$\mathcal{L}^{(2)} = \frac{F^2}{4}\partial\phi^T \cdot \frac{1-\cos\left(\frac{2}{F}D_\phi\right)}{D_\phi^2}\cdot\partial\phi = -\partial\phi^T\cdot\left(\sum_{n=1}^{\infty}\frac{(-1)^n}{(2n)!}\left(\frac{2}{F}\right)^{2n-2}D_\phi^{2n-2}\right)\cdot\partial\phi. \tag{4.10}$$

4.2.2 General properties of the tree-level scattering amplitudes

Note that, the only group factors which enter the interaction vertices are the structure constants f^{abc}. In any tree Feynman diagram each f^{abc} is contracted either with another structure constant within the same vertex or via propagator factor δ^{ab} with some structure constant entering next vertex. Therefore, using the standard argumentation for a general tree graph [105], i.e. expressing any f^{abc} as a trace $f^{abc} = -\langle \mathrm{i}[t^a, t^b]t^c\rangle/\sqrt{2}$ and then successively using the relations like $f^{cde}t^c = -\mathrm{i}[t^d, t^e]/\sqrt{2}$ in order to replace the contracted structure constants with the commutators of the generators inside the single trace, we can prove that any tree level on-shell amplitude has a simple group structure, namely

$$\mathcal{M}^{a_1a_2\ldots a_n}(p_1,p_2,\ldots,p_n) = \sum_{\sigma\in S_n/Z_n}\langle t^{a_{\sigma(1)}}t^{a_{\sigma(2)}}\ldots t^{a_{\sigma(n)}}\rangle\mathcal{M}_\sigma(p_1,\ldots,p_n). \tag{4.11}$$

Here all the momenta treated as incoming and the sum is taken over the permutation of the n indices $1,2,\ldots,n$ modulo cyclic permutations. As a consequence of the cyclicity of the trace we get

$$\mathcal{M}_\sigma(p_1,p_2\ldots,p_n) = \mathcal{M}_\sigma(p_2,\ldots,p_n,p_1) \tag{4.12}$$

Due to the Bose symmetry, the kinematical factors $\mathcal{M}_\sigma(p_1,,\ldots,p_n)$ has to satisfy

$$\mathcal{M}_{\sigma\circ\rho}(p_1,,\ldots,p_n) = \mathcal{M}_\sigma(p_{\rho(1)},p_{\rho(2)},\ldots,p_{\rho(n)}) \tag{4.13}$$

(where $\sigma\circ\rho$ is a composition of permutations) and therefore

$$\mathcal{M}_\sigma(p_1,\ldots,p_n) = \mathcal{M}(p_{\sigma(1)},p_{\sigma(2)},\ldots,p_{\sigma(n)}) \tag{4.14}$$

where we have denoted $\mathcal{M}\equiv\mathcal{M}_{\mathrm{id}}$ (here id is identical permutation). The amplitudes $\mathcal{M}(p_1,\ldots,p_n)$ are called the *stripped* or *partial* amplitudes. Note that the same arguments can be used also for the Feynman rules for the interaction vertices, the general form of which can be written as

$$V_n^{a_1a_2\ldots a_n}(p_1,p_2,\ldots,p_n) = \sum_{\sigma\in S_n/Z_n}\langle t^{a_{\sigma(1)}}t^{a_{\sigma(2)}}\ldots t^{a_{\sigma(n)}}\rangle V_n(p_{\sigma(1)},p_{\sigma(2)},\ldots,p_{\sigma(n)}). \tag{4.15}$$

After some algebra we get explicitly (see Appendix 4.7.1 for details) $V_{2n+1}(p_1,\ldots,p_{2n+1}) = 0$ and

$$V_{2n}(p_1,\ldots,p_{2n}) = \frac{(-1)^n}{(2n)!}\left(\frac{2}{F^2}\right)^{n-1}\sum_{k=1}^{2n-1}(-1)^{k-1}\left(\begin{array}{c}2n-2\\k-1\end{array}\right)\sum_{i=1}^{2n}(p_i\cdot p_{i+k}). \tag{4.16}$$

Let us note that besides (4.3), (4.4) we need not to use any algebraic relations specific for the concrete group G when deriving this formula and it is therefore valid for general G. In the general case we can therefore define the stripped amplitudes and stripped vertices, however, their relation is not straightforward and may depend on the group G. In what follows we will concentrate on the case $G = SU(N)$.

4.2.3 Tree-level amplitudes for $G = SU(N)$

Flavor ordered Feynman rules

The standard way of calculation of the tree-level amplitudes $\mathcal{M}^{a_1\cdots a_n}(p_1,\ldots,p_n)$ is to evaluate the contributions of all tree Feynman graphs with n external legs build form the complete vertices (4.15) and propagators $\Delta_{ab} = \mathrm{i}\delta_{ab}/p^2$. This includes rather tedious group algebra which is specific for each group G. In the special case of $G = SU(N)$ the calculations can be further simplified. Because we have the completeness relations for the generators t^a in the form

$$\sum_{a=1}^{N^2-1} \langle Xt^a\rangle\langle t^aY\rangle = \langle XY\rangle - \frac{1}{N}\langle X\rangle\langle Y\rangle, \tag{4.17}$$

we can simply merge the traces from the vertices of any tree Feynman graphs in one single trace preserving at the same time the order of the generators t^{a_j} inside the trace. Note that the "disconencted" $1/N$ terms have to cancel in the sum in order to produce the single trace in (4.11)[3]. This enables us to formulate simple "flavor ordered Feynman rules" directly for the stripped amplitudes $\mathcal{M}$ completely in terms of the stripped vertices V_n. The general recipe is exactly the same as in the more familiar case of $SU(N)$ Yang-Mills theory, i.e. the tree graphs built form the stripped vertices and propagators are decorated with cyclically ordered external momenta and the corresponding ordering of the momenta inside the stripped vertices are kept.

Let us note that such a simple way of the calculation of the stripped amplitudes might not be possible for general group G. For instance for $G = SO(N)$ we have the following completeness relations

$$\sum_{a=1}^{N(N-1)/2} \langle Xt^a\rangle\langle t^aY\rangle = \frac{1}{2}\left(\langle XY\rangle - \langle XY^T\rangle\right) \tag{4.18}$$

the second term of which reverses the order of the generators in the merged vertex and the aforementioned simple argumentation leading to the flavor ordered Feynman rules has to be modified.

The $SU(N)$ case has also another useful feature. As a consequence of the completeness relations (4.17) for the group generators of $SU(N)$ and the analogous relation

$$\sum_{a=1}^{N^2-1} \langle Xt^aYt^a\rangle = \langle X\rangle\langle Y\rangle - \frac{1}{N}\langle XY\rangle \tag{4.19}$$

[3]As we shall see in what follows, this fact can be understood as a consequence of the decoupling of the $U(1)$ Goldstone boson in the nonlinear $U(N)$ sigma model.

it can be proved [105] that the traces $\langle t^{a_{\sigma(1)}} t^{a_{\sigma(2)}} \dots t^{a_{\sigma(n)}} \rangle$ and $\langle t^{a_{\rho(1)}} t^{a_{\rho(2)}} \dots t^{a_{\rho(n)}} \rangle$ are orthogonal in the leading order of N in the sense that

$$\sum_{a_1,a_2,\dots,a_n} \langle t^{a_{\sigma(1)}} t^{a_{\sigma(2)}} \dots t^{a_{\sigma(n)}} \rangle \langle t^{a_{\rho(1)}} t^{a_{\rho(2)}} \dots t^{a_{\rho(n)}} \rangle^* = N^{n-2}(N^2-1) \left(\delta_{\sigma\rho} + O\left(\frac{1}{N^2}\right)\right) \tag{4.20}$$

where $\delta_{\sigma\rho} = 1$ for $\rho = \sigma$ modulo cyclic permutation and zero otherwise. This relation is enough to uniquely determine the coefficients $\mathcal{T}_\sigma$ in the general expansion of the form

$$\mathcal{T}^{a_1 a_2 \dots a_n} = \sum_{\sigma \in S_n/Z_n} \langle t^{a_{\sigma(1)}} t^{a_{\sigma(2)}} \dots t^{a_{\sigma(n)}} \rangle \mathcal{T}_\sigma, \tag{4.21}$$

(provided the coefficients $\mathcal{T}_\sigma$ are $N-$independent) as the leading in N terms of the "scalar product"

$$\sum_{a_1,a_2,\dots,a_n} \mathcal{T}^{a_1 a_2 \dots a_n} \langle t^{a_{\sigma(1)}} t^{a_{\sigma(2)}} \dots t^{a_{\sigma(n)}} \rangle^* = N^{n-2}(N^2-1) \left(\mathcal{T}_\sigma + O\left(\frac{1}{N^2}\right)\right) \tag{4.22}$$

Because the stripped amplitudes and vertices by construction do not depend on N, the coefficients at the individual traces in the representation (4.11) are unique a therefore the stripped amplitudes and vertices are unique.

Dependence on the parametrization

Up to now we have identified the Goldstone boson fields ϕ^a using the exponential parametrization (4.4) of the group elements $U(\phi^a)$. However, according the equivalence theorem, the amplitudes $\mathcal{M}^{a_1 a_2 \dots a_n}(p_1, p_2, \dots, p_n)$ are the same for any other parametrization $U(\widetilde{\phi}^a)$ where

$$\widetilde{\phi}^a = \phi^a + F^a(\phi) \tag{4.23}$$

where $F^a(\phi) = O(\phi^2)$ is at least quadratic in the fields ϕ. Therefore, according to the aforementioned uniqueness, the stripped amplitudes for the nonlinear $SU(N)$ sigma model do not depend on the parametrization. Note, however, that this is not true for the stripped vertices which do depend on the parametrization because the complete vertices $V_n^{a_1 a_2 \dots a_n}(p_1, p_2, \dots, p_n)$ do.

As far as the on-shell tree-level amplitudes are concerned, in various calculations we are thus free to use the most suitable parametrization and consequently the most useful form of the corresponding stripped vertices for a given purpose. We shall often take advantage of this freedom in what follows.

A wide class of parameterizations for the chiral nonlinear sigma model with $G = U(N)$ and $G = SU(N)$ has been discussed in [97]. The general form of such a parameterizations reads

$$U = \sum_{k=0}^{\infty} a_k \left(\sqrt{2} \frac{\mathrm{i}}{F} \phi \right)^k \tag{4.24}$$

where $a_0 = a_1 = 1$ and the remaining real coefficients a_k are constrained by the requirement $UU^+ = 1$. The exponential parametrization (4.4) corresponds to the choice $a_n = 1/n!$. In fact, as was proved in [97], for $SU(N)$ nonlinear

sigma model with $N > 2$, the exponential parametrization is the only admissible choice within the above class of parameterizations (4.24) compatible with the nonlinearly realized symmetry with respect to the $SU(N)$ chiral transformations (4.2). On the other hand, for $SU(2)$ and for the extended chiral group $G = U(N)$ with arbitrary N, the parameterizations of the form (4.24) represent an infinite-parametric class. The more detailed discussion can be found in Appendix 4.7.1.

Interrelation of the cases $G = U(N)$ and $G = SU(N)$

Let us note, that the $SU(N)$ and $U(N)$ chiral nonlinear sigma models are tightly related. Within the exponential parametrization we can write in the $U(N)$ case

$$U = \exp\left(\frac{\mathrm{i}}{F}\sqrt{\frac{2}{N}}\phi^0\right)\widehat{U} \tag{4.25}$$

where $\widehat{U} \in SU(N)$ and ϕ^0 is the additional $U(1)$ Goldstone boson corresponding to the $U(1)$ generator $t^0 = \mathbf{1}/\sqrt{N}$. We get then

$$U^{-1}\partial_\mu U = \frac{\mathrm{i}}{F}\sqrt{\frac{2}{N}}\partial_\mu\phi^0 + \widehat{U}^+\partial_\mu\widehat{U} \tag{4.26}$$

and as a consequence,

$$\mathcal{L}^{(2)} = \frac{1}{2}\partial\phi^0\cdot\partial\phi^0 + \frac{F^2}{4}\langle\partial_\mu\widehat{U}\partial^\mu\widehat{U}^{-1}\rangle. \tag{4.27}$$

Therefore ϕ^0 completely decouples. This means that for the on-shell amplitudes in this model

$$\mathcal{M}^{a_1a_2\ldots a_n}(p_1, p_2, \ldots, p_n) = 0 \tag{4.28}$$

whenever at least one $a_j = 0$. Note that this statement does not depend on the parametrization. We can therefore reproduce the on-shell amplitudes of the $SU(N)$ chiral nonlinear sigma model from that of the $U(N)$ one simply by assigning to the indices a_i the values corresponding the $SU(N)$ Goldstone bosons. Keeping this in mind, in what follows we will freely switch between the $U(N)$ and $SU(N)$ case and use the general parameterizations (4.24) also in the context of the $SU(N)$ chiral nonlinear sigma model.

The fact that the $U(1)$ Goldstone boson decouples gives also a nice physical explanation why the "disconnected" $1/N$ term can be omitted in the relation (4.17) when summing over virtual states in the tree-level Feynman graphs for the $SU(N)$ nonlinear sigma model. This term can be interpreted as the subtraction of the extra $U(1)$ virtual state contained in the first "connected" part. However, because this state decouples, no such correction is in fact needed.

The decoupling of the $U(1)$ Goldstone boson is an effect analogous to the decoupling of the $U(1)$ component of the gauge field in the case of the $U(N)$ Yang-Mills theory. For the tree-level amplitudes (and the corresponding stripped amplitudes) we get as a consequence a set of identities constraining their form. For instance taking only one $a_j = 0$ (say a_1) in (4.28), we get the "dual Ward identity" (or the $U(1)$ decoupling identity)

$$\mathcal{M}(p_1, p_2, p_3, \ldots, p_n) + \mathcal{M}(p_2, p_1, p_3, \ldots, p_n) + \ldots + \mathcal{M}(p_2, p_3, \ldots, p_1, p_n) = 0 \tag{4.29}$$

exactly as in the Yang-Mills case (see e.g. [105] and references therein).

4.2.4 Explicit examples of $SU(N)$ on-shell amplitudes

Using (4.11) we can reconstruct the complete amplitude $\mathcal{M}^{a_1\dots a_n}(p_1,\dots,p_n)$ just from a single stripped amplitude $\mathcal{M}(p_1,\dots p_n)$ which is given by the sum of Feynman diagrams with ordered external legs $\{1,2,\dots n\}$. Though the aim of this chapter is not to calculate scattering amplitudes using the Feynman diagram approach, in this section we provide explicit examples for diagrammatic calculation of the stripped 4pt and 6pt amplitudes of the chiral nonlinear $SU(N)$ sigma model (the 8pt and 10pt amplitudes we postpone to the Appendix 4.7.2) as the reference result for the recursive formula given in section 4.

We can easily see that the only poles in the stripped amplitude are of the form $1/s_{i,j}$ where

$$s_{i,j} = p_{i,j}^2 \qquad \text{with} \qquad p_{i,j} = \sum_{k=i}^{j} p_k \tag{4.30}$$

(Obviously $s_{i,j} = s_{j+1,i-1}$ due to momentum conservation). The variables $s_{i,j}$ are therefore well suited for presentation of the amplitudes.

As we have discussed above, the $SU(N)$ stripped amplitudes are essentially the same as those for the $U(N)$ case and, as we have discussed above, they are independent on the parametrization of the unitary matrix U in (4.3). The most convenient one for diagrammatic calculation of on-shell scattering amplitudes is the *minimal* parametrization [104]

$$U = \sqrt{2}\frac{\mathrm{i}}{F}\phi + \sqrt{1 - 2\frac{\phi^2}{F^2}} = 1 + \sqrt{2}\frac{\mathrm{i}}{F}\phi - 2\sum_{k=1}^{\infty}\left(\frac{1}{2F^2}\right)^k C_{n-1}\phi^{2k} \tag{4.31}$$

where C_n are the Catalan numbers (4.164). The stripped Feynman rules for vertices can be written in terms of $s_{i,j}$ as follows (see Appendix 4.7.1 for details)

$$V_{2n+2}(s_{i,j}) = \left(\frac{1}{2F^2}\right)^n \frac{1}{2}\sum_{k=0}^{n-1} C_k C_{n-k-1} \sum_{i=1}^{2n+2} s_{i,i+2k+1} \tag{4.32}$$

Note that within this parametrization the stripped vertices do not depend on the off-shellness of the momenta entering the vertex and when expressed in terms of the variables $s_{i,j}$ they are identical taken both on-shell or off-shell. This rapidly speeds up the calculation, because there are no partial cancelations between the numerators and propagator denominators within the individual Feynman graphs and it allows us to find the final expressions for the amplitudes in very compact form.

The four-point amplitude is directly given by the Feynman rule in the simple parametrization,

$$2F^2\mathcal{M}(1,2,3,4) = s_{1,2} + s_{2,3}. \tag{4.33}$$

Note that for n-point amplitude $\sum_{k=1}^{n} p_k = 0$ and this can be used to systematically eliminate p_n or equivalently $s_{\cdot,n}$.

The six-point amplitude is given by diagrams in Fig. 4.1. The explicit formula reads

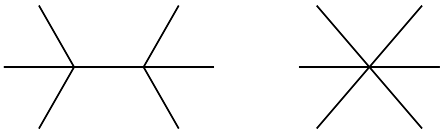

Figure 4.1: Graphical representation of the 6-point amplitude (4.34) with cycling tacitly assumed.

$$
\begin{aligned}
&4F^4\mathcal{M}(1,2,3,4,5,6) = \\
&= -\frac{(s_{1,2}+s_{2,3})(s_{1,4}+s_{4,5})}{s_{1,3}} - \frac{(s_{1,4}+s_{2,5})(s_{2,3}+s_{3,4})}{s_{2,4}} - \frac{(s_{1,2}+s_{2,5})(s_{3,4}+s_{4,5})}{s_{3,5}} \\
&\quad + (s_{1,2}+s_{1,4}+s_{2,3}+s_{2,5}+s_{3,4}+s_{4,5})
\end{aligned} \tag{4.34}
$$

This can be rewritten as

$$
4F^4\mathcal{M}(1,2,3,4,5,6) = -\frac{1}{2}\frac{(s_{1,2}+s_{2,3})(s_{1,4}+s_{4,5})}{s_{1,3}} + s_{1,2} + \text{cycl}\,,
$$

with 'cycl' defined for n-point amplitude as

$$
A[s_{i,j},\ldots,s_{m,n}] + \text{cycl} \equiv \sum_{k=0}^{n-1} A[s_{i+k,j+k},\ldots,s_{m+k,n+k}]\,, \tag{4.35}
$$

which will quite considerably shorten the 8- and 10-point formulae. These are postponed to Appendix 4.7.2.

4.3 Recursive methods for scattering amplitudes

Feynman diagrams are completely universal way how to calculate scattering amplitudes in any theory (that has Lagrangian description). However, it is well-known that in many cases they are also very ineffective. Despite the expansion contains many diagrams each of them being a complicated function of external data, most terms vanish in the sum and the result is spectacularly simple. The most transparent example is Parke-Taylor formula [130] for all tree-level Maximal-Helicity-Violating amplitudes [4]. The simple structure of the result is totally invisible in the standard Feynman diagrams expansion.

Several alternative approaches and methods have been discovered in last decades, let us mention e.g. the Berends-Giele recursive relations for the currents [131] and the more recent BCFW (Britto, Cachazo, Feng and Witten) recursion relations for on-shell tree-level amplitudes that reconstruct the result from its poles using simple Cauchy theorem [111], [112].

4.3.1 BCFW recursion relations

For concreteness let us consider tree-level stripped on-shell amplitudes of n massless particles in $SU(N)$ Yang-Mills theory ("gluodynamics").[5] The partial am-

[4]Scattering amplitudes of gluons where two of them have negative helicity and the other ones have positive helicity.

[5]The recursion relations can be also formulated for more general cases and also for massive particles. See [132] for more details.

plitude $\mathcal{M}_n$ is a gauge-invariant rational function of external momenta and additional quantum numbers h (helicities in case of gluons)

$$\mathcal{M}_n \equiv \mathcal{M}_n(p_1, p_2, \dots p_n; h_1, h_2, \dots h_n). \tag{4.36}$$

The external momenta are generically complex but if we are interested in physical amplitudes we can set them to be real in the end. Let us pick two arbitrary indices i, j and perform following shift.

$$p_i \to p_i(z) = p_i + zq, \qquad p_j \to p_j(z) = p_j - zq \tag{4.37}$$

such that the momentum q is orthogonal to both p_i and p_j, ie. $q^2 = (q \cdot p_i) = (q \cdot p_j) = 0$ and the shifted momenta remain on-shell. Let us note that such q can be found only for the case of spacetime dimensions $d \geq 4$. The amplitude becomes a meromorphic function $\mathcal{M}_n(z)$ of complex parameter z with only simple poles. The original expression corresponds to $z = 0$. If $\mathcal{M}_n(z)$ vanishes for $z \to \infty$ we can use the Cauchy theorem to reconstruct $\mathcal{M}_n = \mathcal{M}_n(0)$,

$$0 = \frac{1}{2\pi \mathrm{i}} \int_{C(\infty)} \frac{dz}{z} \mathcal{M}_n(z) = \mathcal{M}_n(0) + \sum_k \frac{\mathrm{Res}\,(\mathcal{M}_n, z_k)}{z_k} \tag{4.38}$$

where $C(\infty)$ is closed contour at infinity. $\mathcal{M}_n$ can be then expressed as

$$\mathcal{M}_n = -\sum_k \frac{\mathrm{Res}\,(\mathcal{M}_n, z_k)}{z_k} \tag{4.39}$$

where k is sum of all residues of $\mathcal{M}_n(z)$ in the complex z-plane. Residues of $\mathcal{M}_n(z)$ can be straightforwardly calculated for the following reason: the only poles of $\mathcal{M}_n$ are $p_{a,b}^2 = 0$ where $p_{a,b} = (p_a + p_{a+1} + \dots p_b)$. The poles of $\mathcal{M}_n(z)$ have still the same locations just shifted, namely $p_{a,b}^2(z) = 0$ where $i \in (a, a{+}1, \dots b)$ or $j \in (a, a{+}1, \dots b)$. If none of the indices i, j or both of them are in this range, the dependence on z in $p_{a,b}(z)$ cancels and it is not pole in z anymore. It is easy to identify all locations of the corresponding poles z_{ab}. Suppose that particle $i \in (a, a{+}1, \dots b)$,

$$p_{a,b}^2(z) = (p_a + \dots p_{i-1} + (p_i + zq) + p_{i+1} + \dots p_b)^2 = 0 \quad \Rightarrow \quad z_{a,b} = -\frac{p_{a,b}^2}{2(q \cdot p_{a,b})} \tag{4.40}$$

In the original amplitude $\mathcal{M}_n$ the residue on the pole $p_{a,b}^2 = 0$ is given by unitarity: on the factorization channel with given helicity the amplitude factorizes into two sub-amplitudes, and therefore

$$\mathrm{Res}\,(\mathcal{M}_n, z_{a,b}) = \sum_{h_{ab}} \mathcal{M}_L(z_{a,b})^{-h_{ab}} \frac{\mathrm{i}}{2(q \cdot p_{a,,b})} \mathcal{M}_R^{h_{ab}}(z_{a,b}) \tag{4.41}$$

where the summation over the helicities h_{ab} of the one-particle intermediate state is taken. The "left" and "right" sub-amplitudes $\mathcal{M}_{L,R}^{\pm h_{ab}}(z_{a,b})$ are

$$\mathcal{M}_L^{-s_{ab}}(z_{a,b}) = \mathcal{M}_{b-a+2}(p_a, \dots, p_i(z_{a,b}), \dots p_b, -p_{a,b}(z_{a,b}); h_a, \dots, -h_{ab}) \tag{4.42}$$

$$\mathcal{M}_R^{s_{ab}}(z_{a,b}) = \mathcal{M}_{n-(b-a)}(p_{a,b}(z_{a,b}), p_{b+1}, \dots, p_j(z_{a,b}), \dots, p_{a-1}; h_{ab}, \dots, h_a) \tag{4.43}$$

The amplitude $\mathcal{M}_n$ can be then written as

$$\mathcal{M}_n = \sum_{ab,h_{ab}} \mathcal{M}_L^{-h_{ab}}(z_{a,b}) \frac{\mathrm{i}}{p_{a,b}^2} \mathcal{M}_R^{h_{ab}}(z_{a,b}) \tag{4.44}$$

It is convenient to choose i and j to be adjacent because it eliminates the number of factorization channels we have to consider.

4.3.2 Reconstruction formula with subtractions

The BCFW recursion relations discussed above are very generic and applicable for a large class of theories. The main restriction is the requirement of large z behavior: $\mathcal{M}_n(z) \to 0$ for $z \to \infty$. However, this behavior is not guaranteed in general and there exist examples when it is broken no matter which pair of momenta p_i and p_j is chosen to be shifted. In such a case, an additional term (dubbed *boundary term*) is present on the right hand side of eq. (4.44). The boundary term, which is hard to obtain in general case, has been studied by various methods in the series of papers [133], [134] and [135], however no general solution is still available. Sometimes this problem can be cured by means of considering more general approach when all the external momenta p_k are deformed (such an *all-line shift* has been introduced in [136], see also [137])

$$p_k \to p_k(z) = p_k + z q_k. \tag{4.45}$$

where z is a complex parameter and q_k are appropriate vectors compatible with the requirements of the momentum conservation and on-shell constraint for $p_k(z)$, ie. $p_k \cdot q_k = q_k^2 = 0$. The on-shell amplitude

$$\mathcal{M}_n(z) \equiv \mathcal{M}_n(p_1(z), p_2(z), \ldots, p_n(z)) \tag{4.46}$$

become again meromorphic function of the variable z the only singularities of which are simple poles and the residue at these poles have the simple structure (4.41) dictated by unitarity. In some cases the desired behavior $\mathcal{M}_n(z) \to 0$ for $z \to \infty$ can be achieved in this way. However, in general case the behavior of $\mathcal{M}_n(z)$ for $z \to \infty$ is power-like with non-negative power of z. This fact requires some modification of the reconstruction procedure.

This can be done as follows. Let us suppose that we have made any (linear) deformation of the external momenta $p_k \to p_k(z)$ in such a way that the deformed amplitude $\mathcal{M}_n(z)$ is a meromorphic function the only singularities of which are simple poles and let us assume the following asymptotic behavior

$$\mathcal{M}_n(z) \approx z^k \tag{4.47}$$

when $z \to \infty$. Let us denote the poles of $\mathcal{M}_n(z)$ as z_i, $i = 1, 2, \ldots n$. Assume a_j, $j = 1, 2, \ldots, k+1$ to be complex numbers satisfying $|a_j| < R$ different form the poles z_i. Then we can write for $z \neq a_j$ inside the disc $D(R)$ (i.e. inside the domain $|z| < R$ the boundary of which is a circle $C(R)$ of the radius R) the following "$k+1$ times subtracted Cauchy formula" (see Fig.4.2)

$$\begin{aligned} &\frac{1}{2\pi\mathrm{i}} \int_{C(R)} \mathrm{d}w \frac{\mathcal{M}_n(w)}{w - z} \prod_{j=1}^{k+1} \frac{1}{w - a_j} \qquad (4.48) \\ = \; &\mathcal{M}_n(z) \prod_{j=1}^{k+1} \frac{1}{z - a_j} + \sum_{j=1}^{k+1} \frac{\mathcal{M}_n(a_j)}{a_j - z} \prod_{l=1, l\neq j}^{k+1} \frac{1}{a_j - a_l} + \sum_{i=1}^{n_{C(R)}} \frac{\mathrm{Res}\,(\mathcal{M}_n; z_i)}{z_i - z} \prod_{j=1}^{k+1} \frac{1}{z_i - a_j}. \end{aligned}$$

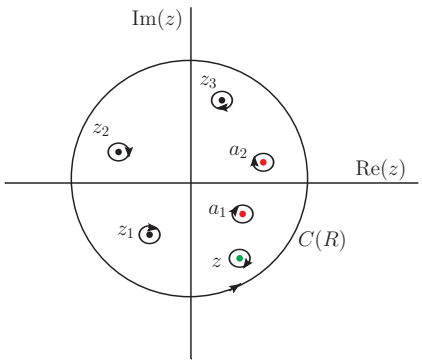

Figure 4.2: Illustration of the contour used for the derivation of the subtracted Cauchy formula (4.48) with $k = 1$ and $n_{C(R)} = 3$.

Here $z_1, z_2, \ldots, z_{n_{C(R)}}$ are the poles inside $D(R)$ and $\mathrm{Res}\,(\mathcal{M}_n; z_i)$ are corresponding residues. In the limit $R \to \infty$ the integral vanishes due to (4.47) and $D(\infty)$ will contain all n poles. As a result we get a reconstruction formula with $k+1$ subtractions

$$\mathcal{M}_n(z) = \sum_{i=1}^{n} \frac{\mathrm{Res}\,(\mathcal{M}_n; z_i)}{z - z_i} \prod_{j=1}^{k+1} \frac{z - a_j}{z_i - a_j} + \sum_{j=1}^{k+1} \mathcal{M}_n(a_j) \prod_{l=1, l\neq j}^{k+1} \frac{z - a_l}{a_j - a_l}. \tag{4.49}$$

This is the desired generalization of the usual prescription. In order to reconstruct the amplitude with the asymptotic behavior (4.47) from its pole structure, we need therefore along with the residues at the poles z_i (which are fixed by unitarity) also supplementary information, namely the $k+1$ values $\mathcal{M}_n(a_j)$ of the amplitude at the points a_j. Such a additional information is the weakest point of the relations (4.49): there exists no universal recipe how to get the values $\mathcal{M}_n(a_j)$ for a general theory. This corresponds to the well known analogous situation of $k+1$ subtracted dispersion relations, which allow to reconstruct a general amplitude from its discontinuities uniquely up to the $k+1$ generally unknown subtraction constants. Note that, provided we choose a_j in such a way that $\mathcal{M}_n(a_j) = 0$ (i.e. a_j are the roots of the deformed amplitude $\mathcal{M}_n(z)$), we can reproduce the formula

$$\mathcal{M}_n(z) = \sum_{i=1}^{n} \frac{\mathrm{Res}\,(\mathcal{M}_n; z_i)}{z - z_i} \prod_{j=1}^{k+1} \frac{z - a_j}{z_i - a_j} \tag{4.50}$$

first written in this context by Benincasa a Conde [138] and further discussed by Bo Feng, Yin Jia, Hui Luo a Mingxing Luo in [139].

4.4 BCFW-like relations for semi-on-shell amplitudes

The straightforward application of the BCFW reconstruction procedure is not possible for the $SU(N)$ nonlinear sigma model because the amplitudes $\mathcal{M}_n(z)$ do

not have appropriate asymptotic behavior for $z \to \infty$. The reason is that due to the derivative coupling of the Goldstone bosons the interaction vertices are quadratic in the momenta. Therefore after the BCFW shift the vertices along the "hard" $z-$dependent line of the Feynman graph are in general linear in z and the linear large z behavior of the propagators cannot compensate for it. For instance, under the shift[6](4.37) with $i = 1$, $j = 2$ we get for the 6pt amplitude (4.34) for $z \to \infty$

$$\begin{aligned} \mathcal{M}_6(z) &= -2z \left(\frac{(q \cdot p_{2,3})\,(s_{1,4} + s_{4,5} - s_{1,3})}{s_{1,3}} + \frac{(q \cdot p_{2,5})\,(q \cdot p_{2,3})}{(q \cdot p_{2,4})} \right. \\ &\quad \left. + \frac{(q \cdot p_{2,5})\,(s_{3,4} + s_{4,5} - s_{3,5})}{s_{3,5}} \right) + O(z^0). \end{aligned} \tag{4.51}$$

and analogously $\mathcal{M}_n(z) = O(z)$ for general[7] n. As discussed in the previous section, in order to reconstruct such an amplitude from its pole structure, it would be sufficient to know the values of $\mathcal{M}_n(z)$ for two fixed values of z. However, such an information is difficult to gain solely from the Feynman graph analysis restricted only to the amplitudes $\mathcal{M}_n$. It is therefore useful to take into account also more flexible objects, namely the semi-on-shell amplitudes, which unlike the on-shell amplitudes depend on the parametrization of the matrix U and from which the on-shell amplitudes can be straightforwardly derived. As we would like to show in this section, appropriate choice of parametrization together with suitable way of BCFW-like deformation of the semi-on-shell amplitudes allows to substitute for the missing information on the amplitudes $\mathcal{M}_n$ and to construct generalized BCFW-like relations for them.

4.4.1 Semi-on-shell amplitudes and Berends-Giele relations

The semi-on-shell amplitudes $J_n^{a_1 a_2 \dots a_n}(p_1, p_2, \dots, p_n)$ (or *currents* in the terminology of the original paper [131], where they were introduced for QCD and more generally for the $SU(N)$ Yang-Mills theory) can be defined in our case as the matrix elements of the Goldstone boson field $\phi^a(0)$ between vacuum and the n Goldstone boson states $|\pi^{a_1}(p_1) \dots \pi^{a_n}(p_n)\rangle$

$$J_n^{a, a_1 a_2 \dots a_n}(p_1, p_2, \dots, p_n) = \langle 0 | \phi^a(0) | \pi^{a_1}(p_1) \dots \pi^{a_n}(p_n) \rangle. \tag{4.52}$$

Here the momentum p_{n+1} attached to $\phi^a(0)$

$$p_{n+1} = -\sum_{j=1}^{n} p_j. \tag{4.53}$$

[6]Under the all-line (anti)holomorphic BCFW shift the large z behavior is the same. Here we can use the general formulae derived in [137] which relate the number n of external particles, the sum H of their helicities and the overall dimension c of the couplings to the asymptotics of the amplitude under the all-line holomorphic ($O(z^a)$) and anti-holomorphic ($O(z^s)$) shift. These formulae reads $2s = 4 - n - c + H$ and $2a = 4 - n - c - H$. In our case $H = 0$ and the only coupling constant is F^{-1}, therefore $c = 2 - n$, therefore in general case $a = s = 1$ independently on n.

[7]The general statement can be derived by induction from Brends-Giele recursive relations discussed in the next subsection.

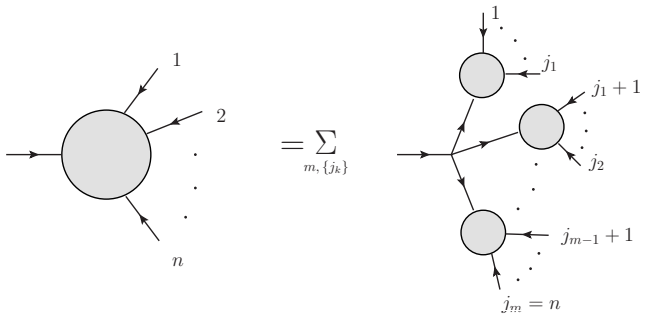

Figure 4.3: Graphical representation of the Berends-Giele recursive relations

is off-shell. Note that $J_n^{a,a_1a_2\ldots a_n}(p_1,p_2,\ldots,p_n)$ has a pole for $p_{n+1}^2=0$.

In complete analogy with the on-shell amplitudes, at the tree level the right hand side of (4.52) can be expressed in terms of the flavor-stripped semi-on-shell amplitudes $J_n(p_1,p_2,\ldots,p_n)$ in the form

$$\langle 0|\phi^a(0)|\pi^{a_1}(p_1)\ldots\pi^{a_n}(p_n)\rangle|_{\rm tree}=\sum_{\sigma\in S_n}{\rm Tr}(t^at^{a_{\sigma(1)}}\ldots t^{a_{\sigma(n)}})J_n(p_{\sigma(1)},p_{\sigma(2)},\ldots,p_{\sigma(n)}). \tag{4.54}$$

Let us note that, at higher orders in the loop expansion the group structure contains also multiple trace terms. We normalize the one particle states according to

$$J_1(p)=1. \tag{4.55}$$

In this section the above semi-on-shell flavor-stripped amplitudes $J_n(p_1,p_2,\ldots,p_n)$ will be the main subject of our interest. The on-shell stripped amplitudes $\mathcal{M}(p_1,p_2,\ldots,p_{n+1})$ can be extracted from them by means of the Lehmann-Symanzik-Zimmermann (LSZ) formulas

$$\mathcal{M}(p_1,p_2,\ldots,p_{n+1})=-\lim_{p_{n+1}^2\to 0}p_{n+1}^2J_n(p_1,p_2,\ldots,p_n). \tag{4.56}$$

The main advantage of the semi-on-shell amplitudes $J_n(p_1,p_2,\ldots,p_n)$ (in what follows we also use short-hand notation $J(1,2,\ldots,n)$) is that they allow to abandon the Feynman diagram approach using appropriate recursive relation. The latter has been first formulated by Berends and Giele in the context of QCD [131] and proved to be very efficient for the calculation of the tree-level multi-gluon amplitudes. For the $U(N)$ nonlinear sigma model the generalized recurrent relations of Berends-Giele type can be written in the form (see Fig.4.3)

$$J(1,2,\ldots,n)=\frac{\rm i}{p_{1,n}^2}\sum_{m=2}^{n}\sum_{\{j_k\}}{\rm i}V_{m+1}(p_{1,j_1},p_{j_1+1,j_2},\ldots p_{j_{m-1}+1,n},-p_{1,n})\prod_{k=1}^{m}J(j_{k-1}{+}1,\ldots,j_k) \tag{4.57}$$

where the sum is over all splittings of the ordered set $\{1,2,\ldots,n\}$ into m non-empty ordered subsets $\{j_{k-1}+1,j_{k-1}+2,\ldots,j_k\}$, (here $j_0=0$ and $j_m=n$)[8],

[8]Explicitly

$$\sum_{\{j_k\}}\equiv\sum_{j_1=1}^{n-m+1}\sum_{j_2=j_1+1}^{n-m+2}\cdots\sum_{j_{m-1}=j_{m-2}+1}^{n-m+(m-1)}.$$

n	2	3	4	5	6	7	8	9	10
$t(2n+1)$	4	12	33	88	232	609	1 596	4 180	10 945
$b(2n+1)$	5	17	50	138	370	979	2 575	6 755	17 700
$f(2n+1)$	4	21	126	818	5 594	39 693	289 510	2 157 150	16 348 960
$t_4(2n+1)$	3	6	10	15	21	28	36	45	55
$b_4(2n+1)$	4	10	20	35	56	84	120	165	220
$f_4(2n+1)$	3	12	55	273	1 428	7 752	43 263	246 675	1 430 715

Table 4.1: A comparison of the number t of the terms on the right hand side of the Berends-Giele recursive relation with the total number b of terms needed for the Berends-Giele recursive calculation of the amplitude $J(1,2,\ldots,2n+1)$ and with the total number f of flavor ordered Feynman graphs contributing to the same amplitude. In the last three row we compare these numbers with the analogous ones for the case of "ϕ^4 theory".

V_{m+1} is the flavor-stripped Feynman rule for vertices with $m+1$ external legs and $p_{i,k} = \sum_{j=i}^{k} p_j$ as above.

Let us note that, because the Lagrangian of the nonlinear sigma model includes infinite number of vertices with increasing number of fields, the above Berends-Giele relation for J_n have to contain vertices up to $n+1$ legs, i.e. much more terms than in the case of power-counting renormalizable theories like QCD where the number of vertices is finite[9]. This fact rather reduces the efficiency of these relation for the calculations of the amplitudes. We illustrate this in the Tab. 1, where the number of terms on the right hand side of the Berends-Giele relation (4.57) written for J_{2n+1} (denoted as $t(2n+1)$) and the total number of terms necessary for the calculation of the same semi-on-shell amplitude using the Berends-Giele recursion (denoted as $b(2n+1)$) is compared with the total number $f(2n+1)$ of the flavor ordered Feynman graphs contributing to J_{2n+1} and with the same numbers valid for the theory with only quadrilinear vertices ("ϕ^4 theory ") denoted with subscript "4" . See Appendix 4.7.3 for more details and for derivation of the explicit formulae for these and other related cases.

On the other hand, as we will see in what follows, the Berends-Giele relations can be used as a very suitable tool for the investigation of the general properties of the semi-on-shell amplitudes. Let us mention e.g. the following simple relations valid for $J(1,2,\ldots,n)$

$$J(1,2,\ldots,2n) = 0 \tag{4.58}$$

$$J(1,2,\ldots,n) = J(n,n-1,\ldots,2,1). \tag{4.59}$$

These relation are valid independently on the field redefinition. However, as we shall see in what follows, some properties of the semi-on-shell amplitudes are not valid universally and are tightly related to a given parametrization.

4.4.2 Cayley parametrization

Unlike the on-shell amplitudes $\mathcal{M}^{a_1\cdots a_n}(p_1,p_2,\ldots,p_n)$, which are physical observables and do not depend on the choice of the field variables provided the different

[9]The number of terms on the right hand side of (4.57) grows exponentially with increasing n in contrast to the polynomial growths typical for the renormalizable theories. See Appendix 4.7.3 for details.

choices are related by means of admissible (generally nonlinear) transformations, the concrete form of $J_n^{a,a_1\ldots a_n}(p_1,p_2,\ldots,p_n)$ as well as the flavor-stripped amplitudes $J_n(p_1,p_2,\ldots,p_n)$ depends on the parametrization of the $U(N)$ nonlinear sigma model. In what follows we will almost exclusively use the so called Cayley parameterizations

$$U=\frac{1+\frac{\mathrm{i}}{\sqrt{2}F}\phi}{1-\frac{\mathrm{i}}{\sqrt{2}F}\phi}=1+2\sum_{n=1}^{\infty}\left(\frac{\mathrm{i}}{\sqrt{2}F}\phi\right)^n, \tag{4.60}$$

where the Goldstone boson fields are arranged into the hermitian matrix $\phi=\phi^a t^a$ with t^a being the $U(N)$ generators. As described in Appendix 4.7.1, representation (4.60) is a special member of a wide class of parameterizations suited for the construction of the flavor-stripped Feynman rules. The interrelation between the field ϕ and analogous field $\widetilde{\phi}$ of the more usual exponential parametrization $U=\exp\left(\frac{\mathrm{i}}{F}\widetilde{\phi}\right)$ is through the following admissible nonlinear field redefinition

$$\phi=2F\tan\left(\frac{\mathrm{i}}{2F}\widetilde{\phi}\right)=\widetilde{\phi}+O\left(\widetilde{\phi}^3\right). \tag{4.61}$$

As is shown in Appendix 4.7.1, the flavor-stripped Feynman rules for vertices read in the Cayley parametrization

$$\begin{aligned}&V_{2n+1}=0\\&V_{2n+2}=-\frac{(-1)^n}{2^{n+1}}\left(\frac{1}{F}\right)^{2n}\sum_{j=0}^{n}\sum_{i=1}^{2n+2}(p_i\cdot p_{i+2j+1})=\frac{(-1)^n}{2^n}\left(\frac{1}{F}\right)^{2n}\left(\sum_{i=0}^{n}p_{2i+1}\right)^2,\end{aligned} \tag{4.62}$$

where we have used the momentum conservation in the last row. For the first non-trivial vertex V_4 we get

$$V_4=-\frac{1}{2F^2}(p_1+p_3)^2=-\frac{1}{2F^2}(p_2+p_4)^2 \tag{4.63}$$

and the first two non-trivial semi-on-shell amplitudes read in the Cayley parametrization

$$J(1,2,3) = \frac{1}{2F^2p_4^2}(p_1+p_3)^2 \tag{4.64}$$

$$\begin{aligned}J(1,2,3,4,5) = \frac{1}{4F^4p_6^2}\Bigg[&\frac{(p_1+p_2+p_3+p_5)(p_1+p_3)^2}{(p_1+p_2+p_3)^2}+\frac{(p_1+p_3+p_4+p_5)^2(p_3+p_5)^2}{(p_3+p_4+p_5)^2}\\&+\frac{(p_1+p_5)^2(p_2+p_4)^2}{(p_2+p_3+p_4)^2}-(p_1+p_3+p_5)^2\Bigg]\end{aligned} \tag{4.65}$$

Let us illustrate explicitly the dependence of the semi-on-shell amplitudes on the parametrization. Using the exponential one we obtain different amplitude $J(1,2,3)$, namely

$$J(1,2,3)_{\exp}=-\frac{1}{6F^2}\frac{(p_1+p_2)^2+(p_2+p_3)^2-2(p_1+p_3)^2}{p_4^2}. \tag{4.66}$$

However, both $J(1,2,3)$ and $J(1,2,3)_{\exp}$ give the same on-shell amplitude (4.33).

In the next subsection we will prove additional useful properties of the semi-on-shell amplitudes.

4.4.3 Scaling properties of semi-on-shell amplitudes

The Cayley parametrization is specific in the sense that the semi-on-shell amplitudes $J_n(p_1,\dots,p_n)$ in this parametrization obey simple scaling properties when some subset of the momenta p_i are scaled $p_i \to tp_i$ and the scaling parameter t is then send to zero. Here we will study two important scaling limits, corresponding to the case when *all odd* or *all even* on-shell momenta are scaled. As we shall see in the following section, these two scaling limits are the key ingredients for the construction of the BCFW-like relations for semi-on-shell amplitudes in the Cayley parametrization.

We will prove that for $n > 1$ and $t \to 0$

$$J_{2n+1}(tp_1, p_2, tp_3, p_4, \dots, p_{2r}, tp_{2r+1}, p_{2r+2}, \dots, p_{2n}, tp_{2n+1}) = O(t^2) \tag{4.67}$$

and

$$\lim_{t\to 0} J_{2n+1}(p_1, tp_2, p_3, tp_4, \dots, tp_{2r}, p_{2r+1}, tp_{2r+2}, \dots, tp_{2n}, p_{2n+1}) = \frac{1}{(2F^2)^n}. \tag{4.68}$$

The general proof of (4.67) and (4.68) is by induction. Let us first verify the base cases. While the second statement holds already for $n = 1$

$$J_3(p_1, tp_2, p_3) = \frac{1}{F^2}\frac{(p_1\cdot p_3)}{(p_1 + tp_2 + p_3)^2} \to \frac{1}{2F^2}, \tag{4.69}$$

the first one is not valid unless $n = 2$. Indeed

$$J_3(tp_1, p_2, tp_3) = \frac{1}{2F^2}\frac{t(p_1\cdot p_3)}{(p_1\cdot p_2) + (p_2\cdot p_3) + t(p_1\cdot p_3)} = O(t). \tag{4.70}$$

On the other hand, using the explicit form of J_5 (cf. (4.65)) we get

$$J_5(tp_1, p_2, tp_3, p_4, tp_5) = O(t^2); \tag{4.71}$$

we can therefore proceed by induction starting at $n = 2$.

Let us first prove the scaling property (4.67). Suppose, that (4.67, 4.68) holds for all $\bar{n}$, where $1 < \bar{n} < n$ and write for the left hand side of (4.67) the Berends-Giele relation (4.57) expressing J_{2n+1} in terms of $J_{2\bar{n}+1}$ with $\bar{n} < n$. After the scaling $p_{2k+1} \to tp_{2k+1}$, the $t \to 0$ behavior of p^2_{2n+2} and V_{m+1} is $O(t^0)$ and $O(t^r)$ where $r \geq 0$ respectively. The scaling of the remaining semi-on-shell amplitudes on the right hand side of (4.57) can be deduced from the induction hypothesis. Note that it depends on the number of the external on-shell legs of $J(j_{i-1}+1,\dots,j_i)$ as well as on the parity of $j_{i-1}+1$, because the semi-on-shell amplitude with scaled even or odd momenta scales differently. Namely, according to the induction hypothesis, the scaling of these building blocks of the right hand side of (4.57) is as follows (see Fig. 4.4)

$$\begin{aligned} &J(j) = 1 = O(t^0), \quad J(2j-1, 2j, 2j+1) = O(t), \quad J(2j,\dots,2k) = O(t^0), \\ &J(2j+1,\dots,2k+1) = O(t^2) \ \text{ for } \ k - j > 1. \end{aligned} \tag{4.72}$$

This implies, that those terms of Berends-Giele relations which are depicted in Fig. 4.5, i.e. those which contain at least one block $J(2j+1,\dots,2k+1) = O(t^2)$

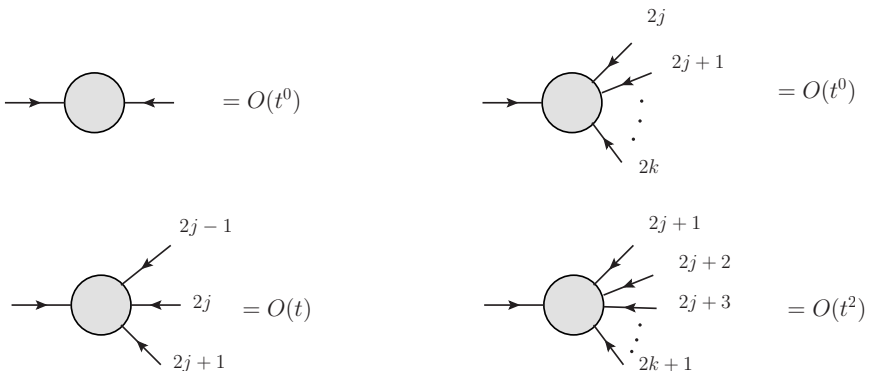

Figure 4.4: Scaling of the building blocks on the right hand hand of the Berends-Giele recursion relation according to the induction hypothesis when the odd momenta are scaled.

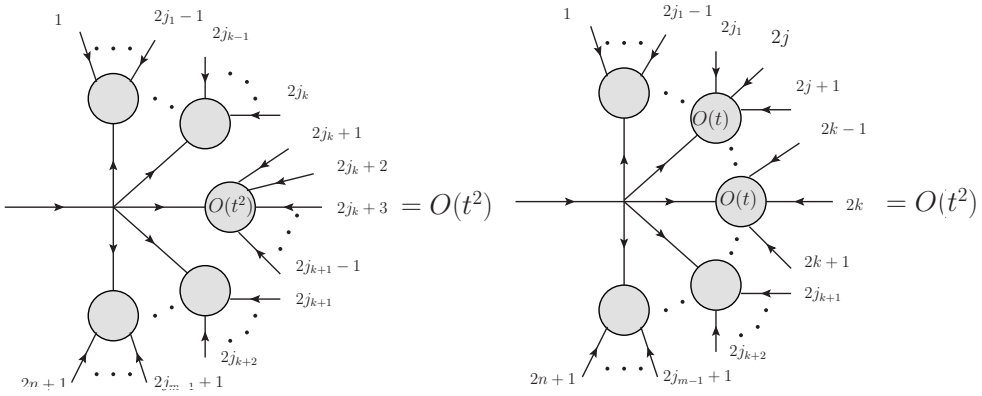

Figure 4.5: The terms on the right hand hand of the Berends-Giele recursion relation which are automatically $O(t^2)$ using the induction hypothesis when the odd momenta are scaled.

with $k-j>1$ or at least two building blocs $J(2j-1,2j,2j+1)$ are automatically $O(t^2)$. Therefore, the only dangerous terms on the right hand side of (4.57) are those without the buildings block of the type $J(2j+1,\ldots,2k+1)=O(t^2)$ with $k-j>1$ and at the same time without (case I) or with just one (case II) building block $J(2j-1,2j,2j+1)=O(t)$ (see Fig. 4.6). To this terms the induction hypothesis cannot be applied directly.

In the case I, the odd lines of the corresponding vertex V_{2m+2} are attached to $J(2j_k+1)=1$ and such a vertex is then proportional to the squared sum of the odd momenta tp_{2j_k+1}, (cf. (4.62))

$$V_{2m+2}(tp_1,p_{2,2j_1},tp_{2j_1+1},\ldots,tp_{2n+1})\sim(tp_1+tp_{2j_1+1}+\cdots+tp_{2n+1})^2 \qquad (4.73)$$

which means that it scales as $O(t^2)$. This is in fact the scaling of the complete contribution of the terms in the case I, because all the remaining building blocs are of the order $O(t^0)$ for $t\to 0$.

In the case II with exactly one building block $J_3(tp_{2j-1},p_{2j},tp_{2j+1})=O(t)$ (note that, it has to be attached to the odd line of the vertex V_{2m+2}), all the

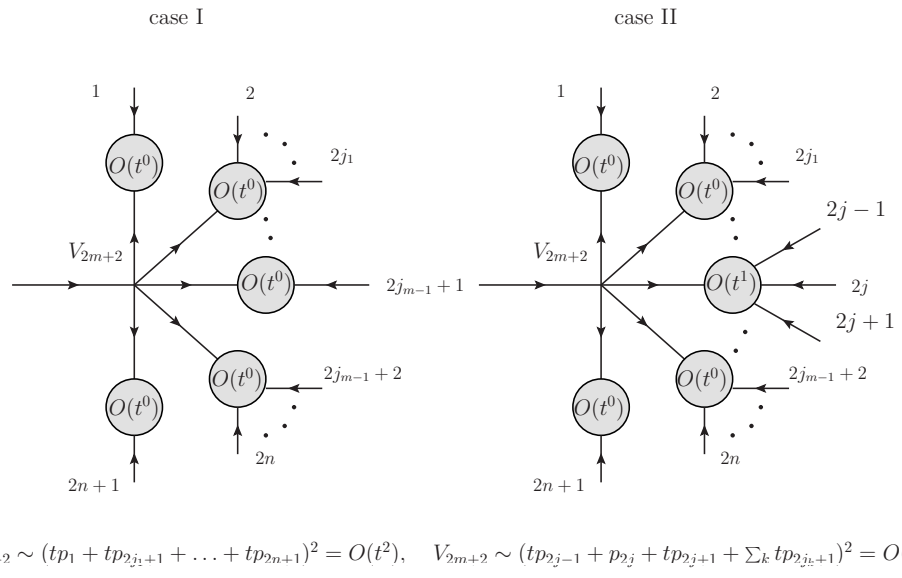

Figure 4.6: Typical terms on the right hand hand of the Berends-Giele recursion relation to which the induction hypothesis (4.67) cannot be applied directly. In both cases, to all (case I) or to all but one (case II) odd lines of the vertex the blocks J_1 are attached. In the case II, one building block J_3 is attached to remaining odd line.

other odd lines of V_{2m+2} are attached to $J(2j_k+1) = 1$ and such a vertex is then proportional to the squared sum of the momenta tp_{2j_k+1} and the momentum of the line which is attached to $J_3(tp_{2j-1}, p_{2j}, tp_{2j+1})$, namely

$$V_{2m+2} \sim \left(tp_{2j-1} + p_{2j} + tp_{2j+1} + \sum_k tp_{2j_k+1} \right)^2 = O(t). \tag{4.74}$$

Therefore the complete contribution of the dangerous terms in the case II is in fact $O(t^2)$ for $t \to 0$ because both V_{2m+2} and $J_3(tp_{2j-1}, p_{2j}, tp_{2j+1})$ scale as $O(t)$ and again all the remaining building blocks are of the order $O(t^0)$ for $t \to 0$. All the other "non-dangerous" terms on the right hand side of the Berends-Giele relations scale at least as $O(t^2)$, which finishes the proof of (4.67).

Let us now prove (4.68), i.e. the case when all even momenta are scaled. Suppose validity of this relation for $\bar{n} < n$ and again write the Berends-Giele relation for the left hand side of (4.68). Thanks to the just proven statement (4.67), the terms on the right hand side of (4.57) with at least one building block $J(j_k+1, \ldots, j_{k+1})$ with odd j_k and $j_{k+1} - j_k > 1$ do not contribute in the limit $t \to 0$. Such a block can be attached only to the even line of the vertex V_{m+1}. Therefore, the only terms which can contribute in the limit $t \to 0$ have the form depicted in Fig. 4.7, i.e. those with the building blocks J_1 attached to all even lines of the vertex.

According to the induction hypothesis and using the explicit form of V_{2k+2} this gives for $t \to 0$

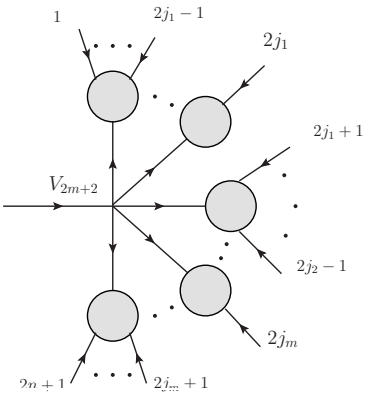

Figure 4.7: Typical terms on the right hand hand of the Berends-Giele recursion relation which contribute to (4.68). Here to all even lines of the vertex the blocks J_1 are attached.

$$-\frac{(-1)^k}{2^k F^{2k}} \prod_{l=1}^{k+1} \frac{1}{(2F^2)^{j_l - j_{l-1}-1}} = -\frac{(-1)^k}{2^n F^{2n}} \tag{4.75}$$

where we denote $j_0 = 0$ and $j_{k+1} = n+1$. Sum of all such contributions is

$$\sum_{k=1}^{n} \sum_{1 \le j_1 < j_2 < \dots, j_k \le n} \frac{(-1)^{k-1}}{2^n F^{2n}} = \frac{1}{2^n F^{2n}} \sum_{k=1}^{n} \left(\begin{array}{c} n \\ k \end{array} \right) (-1)^{k-1} = \frac{1}{2^n F^{2n}}, \tag{4.76}$$

which finishes the proof.

Another independent scaling properties of the semi-on-shell amplitudes J_{2n+1} can be proven using the same strategy. For instance, when all odd momenta and one additional even momentum (say p_{2r}) are scaled, we get

$$\lim_{t \to 0} J_{2n+1}(tp_1, p_2, tp_3, p_4, \dots, tp_{2r-1}, tp_{2r}, tp_{2r+1}, \dots, p_{2N}, tp_{2n+1}) = 0 \tag{4.77}$$

for $n > 1$. We postpone the proof to the Appendix 4.7.4.

Let us note that due to the homogeneity of $J(1, 2, \dots, 2n+1)$ we can rewrite the relations (4.67) and (4.68) as a statement on the asymptotic behavior of the scaled amplitudes for $t \to \infty$, namely

$$\lim_{t \to \infty} J_{2n+1}(tp_1, p_2, \dots, p_{2n}, tp_{2n+1}) = \lim_{t \to \infty} J_{2n+1}(p_1, t^{-1}p_2, \dots, t^{-1}p_{2n}, p_{2n+1}) = \frac{1}{(2F^2)^n} \tag{4.78}$$

and

$$J_{2n+1}(p_1, tp_2, \dots, tp_{2n}, p_{2n+1}) = J_{2n+1}(t^{-1}p_1, p_2, \dots, p_{2n}, t^{-1}p_{2n+1}) = O(t^{-2}). \tag{4.79}$$

4.4.4 BCFW reconstruction

As we have mentioned in the previous subsection, the standard BCFW-like deformation of the external momenta p_i yields deformed amplitudes which behave

as a non-negative power of z for $z \to \infty$. As a result, for the reconstruction of the amplitude from its pole structure we need to use the general reconstruction formula (4.49) for which additional information on the on-shell amplitude (its values at several points) is necessary. However, such an information is not at our disposal. We solve this problems by the following trick: we relax some demands placed on the usual BCFW-like deformation and allow more general ones for which either the reconstruction formula without subtractions can be applied or additional information on the deformed amplitudes is accessible. The momentum conservation cannot be evidently avoided, what remains is the on-shell condition of all the external momenta. It seems therefore to be natural to relax this constraint and instead of the on-shell amplitudes $\mathcal{M}_{2n+2}$ to use the semi-on-shell amplitudes J_{2n+1}, or the cut semi-on-shell amplitudes M_{2n+1} defined as

$$M_{2n+1}\left(p_1, \ldots, p_{2n+1}\right) = p_{1,2n+1}^2 J_{2n+1}\left(p_1, \ldots, p_{2n+1}\right). \tag{4.80}$$

Motivated by the results of the previous section let us assume the following deformation of the semi-on-shell amplitude M_{2n+1} in the Cayley parametrization

$$M_{2n+1}(z) \equiv M_{2n+1}(p_1, zp_2, p_3, zp_4, \ldots, zp_{2r}, p_{2r+1}, zp_{2r+2}, \ldots, zp_{2n}, p_{2n+1}) \tag{4.81}$$

i.e. all even momenta are scaled by the complex parameter z and the odd momenta are not deformed

$$p_{2k}(z) = zp_{2k}, \quad p_{2k+1}(z) = p_{2k+1} \tag{4.82}$$

Note that in contrast to the standard BCFW shift this deformation is possible for general number of space-time dimensions d. The physical amplitude corresponds to $z = 1$. For $n = 1$ we get explicitly

$$M_3(z) = \frac{1}{F^2}(p_1 \cdot p_3) \tag{4.83}$$

For general n let us denote the sums of all odd (even) momenta as

$$p_{\text{-}} = \sum_{k=0}^{n} p_{2k+1}, \quad p_{+} = \sum_{k=1}^{n} p_{2k}\ . \tag{4.84}$$

Then in general case the function $M_{2n+1}(z)$ has the following important properties:

1. With generic fixed p_i it is a meromorphic function of z with simple poles.

2. The asymptotics of $M_{2n+1}(z)$ can be deduced form the known properties of J_{2n+1}, namely for $n > 1$ we get as a consequence of (4.79)

$$M_{2n+1}(z) = (p_+ z + p_-)^2 J_{2n+1}(p_1, zp_2, \ldots, zp_{2n}, p_{2n+1}) = O(z^0). \tag{4.85}$$

3. For $n \geq 1$ we have according to known scaling property (4.68) of J_{2n+1}

$$\lim_{z\to 0} M_{2n+1}(z) = \frac{1}{(2F^2)^n} p_-^2 \tag{4.86}$$

The first two properties allows us to write for $M_{2n+1}(z)$ the reconstruction formula with one subtraction, i.e. the relation (4.49) with $k = 0$. The third property is the key one for the complete reconstruction and determines both the "subtraction point" $a_1 = 0$ and the "subtraction constant" $M_{2n+1}(a_1) = p_-^2/(2F^2)^n$. The resulting formula reads[10]

$$M_{2n+1}(z) = \frac{1}{(2F^2)^n} p_-^2 + \sum_P \frac{\mathrm{Res}\,(M_{2n+1}, z_P)}{z - z_P} \frac{z}{z_P} \tag{4.87}$$

where the sum is over the poles z_P of $M_{2n+1}(z)$. The position of the poles is known and the corresponding residues can be determined recursively as in usual BCFW relations, however, there are some subtleties.

The poles z_P of $M_{2n+1}(z)$ correspond to the vanishing denominators of the deformed propagators $p_P^2(z) = 0$, where

$$p_P^2(z) \equiv p_{i,j}(z)^2 = 0, \quad \text{for} \;\; 2 \leq j - i < 2n \tag{4.88}$$

and where $j - i$ is even; in this formula $p_{i,j}(z) = z p_{i,j}^+ + p_{i,j}^-$ with

$$p_{i,j}^+ = \sum_{i \leq 2k \leq j} p_{2k}, \quad p_{i,j}^- = \sum_{i \leq 2k+1 \leq j} p_{2k+1}, \tag{4.89}$$

i.e. $p_{i,j}^\pm$ is a sum of all even (odd) momenta from the ordered set $p_i, p_{i+1}, \ldots, p_{j-1}, p_j$. Explicitly for $j - i > 2$

$$z_{i,j}^\pm = \frac{-(p_{i,j}^+ \cdot \; p_{i,j}^-) \pm \left(-G(p_{i,j}^+, \; p_{i,j}^-)\right)^{1/2}}{p_{i,j}^{+2}} \tag{4.90}$$

where $G(a,b) = a^2 b^2 - (a \cdot b)^2$ is the Gram determinant, which is nonzero for generic momenta $p_i, \ldots, p_j$. Therefore in the generic case for $j - i > 2$ we deal with doublets of single poles.

The case of three-particle poles corresponding to $j - i = 2$ has to be treated separately. In this case either $p_{i,j}^{+2} = 0$ or $p_{i,j}^{-2} = 0$ (this sets in for $p_{i,j}^+ = p_{i+1}$ or for $p_{i,j}^- = p_{i+1}$ respectively; let us remind that p_k are on-shell). In the first case we have only one pole

$$z_{2j-1,2j+1} = -\frac{(p_{2j-1} \cdot p_{2j+1})}{p_{2j} \cdot (p_{2j-1} + p_{2j+1})} \tag{4.91}$$

while in the second case we have apparently two poles

$$z_{2j,2j+2}^+ \;\; = \;\; 0 \tag{4.92}$$

$$z_{2j,2j+2}^- \;\; \equiv \;\; z_{2j,2j+2} = -\frac{p_{2j+1} \cdot (p_{2j} + p_{2j+2})}{(p_{2j} \cdot p_{2j+2})} \tag{4.93}$$

[10] Let us note, that we could write analogous reconstruction formula directly for the currents J_{2n+1} as we did in [142]. In such a case we do not need any subtraction. The price to pay is that we get two more poles, the residues of which cannot be determined recursively from unitarity. Fortunately, the relation (4.79) and the residue theorem can be used in order to obtain the unknown residues in terms of the remaining ones. The resulting formula is fully equivalent to (4.87), however it is a little bit less elegant.

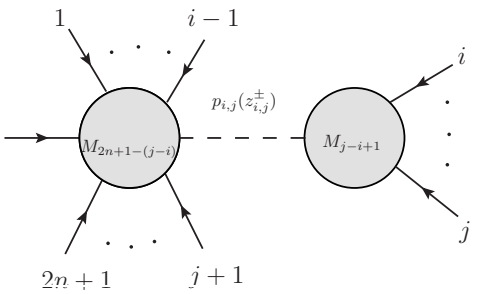

Figure 4.8: Graphical representation of the right hand side of the relation (4.95).

However $z^+_{2j,2j+2} = 0$ cannot be a pole according to (4.86) and the corresponding residue has to be zero.

The residues of the function $M_{2n+1}(z)$ are dictated by unitarity and at the poles they factorize (see Fig. 4.8). Writing for $j - i > 2$

$$(zp^+_{i,j} + p^-_{i,j})^2 = p^{+2}_{i,j}(z - z^+_{i,j})(z - z^-_{i,j}) \tag{4.94}$$

we get for $j - i > 2$

$$\mathrm{Res}\left(M_{2n+1}, z^\pm_{i,j}\right) = \pm \frac{M_L^{(i,j)}(z^\pm_{i,j}) M_R^{(i,j)}(z^\pm_{i,j})}{p^{+2}_{i,j}(z^+_{i,j} - z^-_{i,j})} \tag{4.95}$$

where we denoted

$$M_L^{(i,j)}(z^\pm_{i,j}) = M_{2n+1-(j-i)}(p_1(z^\pm_{i,j}), \ldots, p_{i-1}(z^\pm_{i,j}), p_{i,j}(z^\pm_{i,j}), p_{j+1}(z^\pm_{i,j}), \ldots, p_{2n+1}(z^\pm_{i,j})) \tag{4.96}$$

$$M_R^{(i,j)}(z^\pm_{i,j}) = M_{j-i+1}(p_i(z^\pm_{i,j}), p_{i+1}(z^\pm_{i,j}), \ldots, p_j(z^\pm_{i,j})). \tag{4.97}$$

Note that, while the amplitude $M_L^{(i,j)}$ remains semi-on-shell, the amplitude $M_R^{(i,j)}$ is fully on-shell, because the deformed momentum $p_{i,j}(z)$ is on-shell for $z = z^\pm_{i,j}$.

The formula (4.95) is valid also for the three-particle pole $z_{2j,2j+2}$ given by (4.93). However the pole $z_{2j-1,2j+1}$ deserves a special remark because the corresponding residue is determined by the formula different from (4.95), namely

$$\mathrm{Res}\left(M_{2n+1}, z_{2j-1,2j+1}\right) = \frac{M_L^{(2j-1,2j+1)}(z_{2j-1,2j+1}) M_R^{(2j-1,2j+1)}(z_{2j-1,2j+1})}{2p^+_{2j-1,2j+1} \cdot p^-_{2j-1,2j+1}} \tag{4.98}$$

where $M_{L,R}^{(2j-1,2j+1)}(z_{2j-1,2j+1})$ are given by (4.96) and (4.97) with $z^\pm_{i,j}$ replaced by $z_{2j-1,2j+1}$.

To summarize, we have found a closed system of recursive BCFW-like relations for the tree cut semi-on-shell amplitudes M_{2n+1}, which consists of the reconstruction formula (4.87), the pole positions (4.90), (4.91) and (4.93) and the residue formulae (4.95) and (4.98). Note that the initial condition for the recursion (4.83) can be understood as the special case of (4.87) for $n = 1$ because then there is no pole $z_{i,j}$ with $2 \leq j - i < 2$ and the sum of the residue contributions is empty. The physical amplitude $M_{2n+1}(p_1, \ldots, p_{2n+1})$ corresponds to $z = 1$

$$M_{2n+1}(p_1, \ldots, p_{2n+1}) = \frac{1}{(2F^2)^n} p^2_- + \sum_P \frac{\mathrm{Res}\left(M_{2n+1}, z_P\right)}{z_P} \frac{1}{1 - z_P}. \tag{4.99}$$

As a final result we get then using (4.95), (4.98), (4.91), (4.93) and (4.94)

$$M_{2n+1}(p_1,\dots,p_{2n+1}) = \frac{1}{(2F^2)^n}p_-^2 + \sum_P M_L^{(P)}(z_P)\frac{R_P}{p_P^2}M_R^{(P)}(z_P). \tag{4.100}$$

Note that there is an extra function R_P in contrast to the standard BCFW formula (4.44), namely

$$R_P = \begin{cases} z_P^{-2} & \text{for} \quad z_P = z_{2j,2j+2} \\ z_P^{-1} & \text{for} \quad z_P = z_{2j-1,2j+1} \\ \frac{1}{z_{i,j}^{\pm}-z_{i,j}^{\mp}}\frac{1-z_{i,j}^{\mp}}{z_{i,j}^{\pm}} & \text{for} \quad z_P = z_{i,j}^{\pm} \end{cases} \tag{4.101}$$

For further convenience, we rewrite (4.100) with help of (4.83) in the following more explicit form

$$\begin{aligned} &M_{2n+1}\left(p_1,\dots,p_{2n+1}\right) = \frac{1}{(2F^2)^n}p_-^2 + \\ &+\sum_{j=1}^{n-1} M_L^{(2j,2j+2)}(z_{2j,2j+2})\frac{1}{p_{2j,2j+2}^2}\frac{p_{2j}\cdot p_{2j+2}}{F^2} \\ &-\sum_{j=1}^{n} M_L^{(2j-1,2j+1)}(z_{2j-1,2j+1})\frac{1}{p_{2j-1,2j+1}^2}\frac{p_{2j-1,2j+1}^+\cdot p_{2j-1,2j+1}^-}{F^2} \\ &+\sum_{2<j-i<2n}\frac{1}{z_{i,j}^+ - z_{i,j}^-}\times \\ &\left(M_L^{(i,j)}(z_{i,j}^+)\frac{1}{p_{i,j}^2}M_R^{(i,j)}(z_{i,j}^+)\frac{1-z_{i,j}^-}{z_{i,j}^+} - M_L^{(i,j)}(z_{i,j}^-)\frac{1}{p_{i,j}^2}M_R^{(i,j)}(z_{i,j}^-)\frac{1-z_{i,j}^+}{z_{i,j}^-}\right). \end{aligned} \tag{4.102}$$

The on-shell amplitude is then

$$\mathcal{M}_{2n}(1,2,\dots,2n-1;2n) = -\lim_{p_{1,2n-1}^2\to 0} M_{2n-1}(1). \tag{4.103}$$

4.4.5 Explicit example of application of BCFW relations: 6pt amplitude

As an illustration let us apply the BCFW-like recursive relations (4.87) to the amplitude $M_5(z) \equiv M_5(p_1, zp_2, p_3, zp_4, p_5)$. In this case we have three poles, all of them being three-particle, namely

$$z_{1,3} = 1 - \frac{s_{1,3}}{s_{1,2}+s_{2,3}}, \quad z_{2,4} = \left(1 - \frac{s_{2,4}}{s_{2,3}+s_{3,4}}\right)^{-1}, \quad z_{3,5} = 1 - \frac{s_{3,5}}{s_{3,4}+s_{4,5}} \tag{4.104}$$

where the variables $s_{i,j}$ are given by (4.30).The residues are given by the relations (4.95) for $z_{2,4}$ and (4.98) for $z_{1,3}$ and $z_{3,5}$. After simple algebra using the explicit

form of the poles (4.104) we get

$$\begin{aligned}
\frac{\mathrm{Res}\,(M_5, z_{1,3})}{z_{1,3}} &= \frac{1}{4F^4}(1-z_{1,3})(s_{2,5}-s_{2,4}+s_{3,4}-s_{3,5}) - \frac{1}{4F^4}\,(s_{1,5}-s_{1,4}-s_{4,5}) \\
\frac{\mathrm{Res}\,(M_5, z_{3,5})}{z_{3,5}} &= \frac{1}{4F^4}(1-z_{3,5})(s_{1,4}-s_{1,3}+s_{2,3}-s_{2,4}) - \frac{1}{4F^4}(s_{1,5}-s_{1,2}-s_{2,5}) \\
\frac{\mathrm{Res}\,(M_5, z_{2,4})}{z_{2,4}} &= \frac{1}{4F^4}\,(s_{1,5}-s_{1,4}+s_{2,4}-s_{2,5})\,. \qquad (4.105)
\end{aligned}$$

Note that the potential unphysical poles $z_{i,j}(p_k) = 0$ have canceled completely. We have also

$$(1-z_{1,3})^{-1} = \frac{s_{1,2}+s_{2,3}}{s_{1,3}},\;\; (1-z_{3,5})^{-1} = \frac{s_{3,4}+s_{4,5}}{s_{3,5}},\quad (1-z_{2,4})^{-1} = 1-\frac{s_{2,3}+s_{3,4}}{s_{2,4}} \qquad (4.106)$$

These factors are responsible for setting of the physical poles in the resulting amplitude. After inserting this to the formula (4.99) we get for the individual contributions to the semi-on-shell amplitude in the Cayley parametrization

$$\begin{aligned}
\frac{\mathrm{Res}\,(M_5, z_{1,3})}{z_{1,3}(1-z_{1,3})} &= \frac{1}{4F^2}\left[\frac{(s_{1,4}+s_{4,5}-s_{1,5})\,(s_{1,2}+s_{2,3})}{s_{1,3}} + s_{2,5}-s_{2,4}+s_{3,4}-s_{3,5}\right] \\
\frac{\mathrm{Res}\,(M_5, z_{3,5})}{z_{3,5}(1-z_{3,5})} &= \frac{1}{4F^2}\left[\frac{(s_{1,2}+s_{2,5}-s_{1,5})(s_{3,4}+s_{4,5})}{s_{3,5}} + s_{1,4}-s_{1,3}+s_{2,3}-s_{2,4}\right] \\
\frac{\mathrm{Res}\,(M_5, z_{2,4})}{z_{2,4}(1-z_{2,4})} &= \frac{1}{4F^2}\left[\frac{(s_{1,4}+s_{2,5}-s_{1,5})\,(s_{2,3}+s_{3,4})}{s_{2,4}} + s_{1,5}-s_{1,4}+s_{2,4}\right. \qquad (4.107) \\
&\qquad\qquad \left. -s_{2,5}-s_{2,3}-s_{3,4}\right] \\
\frac{p_-^2}{4F^2} &= \frac{1}{4F^2}\left[s_{1,3}-s_{1,2}-s_{2,3}+s_{1,5}-s_{1,4}+s_{2,4}-s_{2,5}+s_{3,5}-s_{3,4}-s_{4,5}\right]. \qquad (4.108)
\end{aligned}$$

Finally we get

$$\begin{aligned}
&4F^2 M_5(1) = \\
= \;& \frac{(s_{1,4}+s_{4,5}-s_{1,5})\,(s_{1,2}+s_{2,3})}{s_{1,3}} + \frac{(s_{1,2}+s_{2,5}-s_{1,5})(s_{3,4}+s_{4,5})}{s_{3,5}} \qquad (4.109) \\
&+\frac{(s_{1,4}+s_{2,5}-s_{1,5})\,(s_{2,3}+s_{3,4})}{s_{2,4}} + 2s_{1,5}-s_{1,2}-s_{1,4}-s_{2,3}-s_{2,5}-s_{3,4}-s_{4,5}.
\end{aligned}$$

Taking this amplitude on-shell according to (4.103), i.e. setting $s_{1,5} \to 0$ and changing the overall sign, we reproduce the parametrization independent physical amplitude (4.34).

4.5 More properties of stripped semi-on-shell amplitudes

The BCFW recursive relations provides us with a Lagrangian-free formulation of the tree-level nonlinear $SU(N)$ sigma model in the Cayley parametrization.

We can use them similarly as the Berends-Giele relations as a tool for the investigation of further interesting features of the stripped semi-on-shell amplitudes M_{2n+1} and J_{2n+1}. As we have already mentioned, these features are not universal because of the parametrization dependence of M_{2n+1} and J_{2n+1}, however, their implications for the fully on shell amplitudes hold universally[11]. In this section we will concentrate on the problem of single soft limits (Adler zeroes) and double soft limit of the semi-on-shell amplitudes.

The presence of Adler zeroes for the *on-shell* Goldstone boson amplitudes $\mathcal{M}^{a_1\dots a_{2n}}(p_1,\dots,p_{2n})$, i.e. validity of the limit

$$\lim_{p_j\to 0}\mathcal{M}^{a_1a_2\dots a_{2n}}(p_1,p_2,\dots,p_{2n})=0, \tag{4.110}$$

is a well known consequence of the nonlinearly realized chiral symmetry. More generally it is an universal (non-perturbative) feature in the theories with spontaneous breakdown of a global symmetry. In such theories the amplitudes with one extra Goldstone boson π^a in the *out* (or *in*) state vanishes when the Goldstone boson become soft, e.g.

$$\lim_{p\to 0}\langle f+\pi^a(p),\mathrm{out}|i,\mathrm{in}\rangle=0, \tag{4.111}$$

provided the π^a cannot be emitted from the external lines corresponding to the states $|i,\mathrm{in}\rangle$ or $|f,\mathrm{out}\rangle$. In the $SU(N)$ nonlinear sigma model the Adler zero is present also for the stripped on-shell amplitudes $\mathcal{M}_{2n}(p_1,p_2,\dots,p_{2n})$ due to the leading N orthogonality relations (4.20) and corresponding uniqueness of the decomposition (4.11). However, this property is not guaranteed automatically for the semi-on-shell amplitudes M_{2n+1} and the soft Goldstone boson behavior can depend on the parametrization. For instance using the Cayley parametrization, we find for the amplitude $M_3=(p_1\cdot p_3)/F^2$ the Adler zero for soft p_1 and p_3, however there is no zero for soft p_2 in general when keeping p_4 off-shell. For the same amplitude in the exponential parametrization (cf. (4.66)) we have no Adler zero at all. As we shall show in this section, for the semi-on-shell amplitudes M_{2n+1} in the Cayley parametrization we can prove, using the BCFW-like relation, the Adler zero for half of the momenta (namely for those p_j with *odd* index j).

The double soft limit of the Goldstone boson on-shell amplitudes $\mathcal{M}^{a_1a_2\dots a_{2n+2}}(p_1,p_2,\dots,p_{2n+2})$ is more complicated and has been studied relatively recently in connection with the regularized action of the broken generators on the n Goldstone boson states [143]. Motivated by direct inspection of the six Goldstone boson amplitude in the nonlinear chiral $SU(2)$ sigma model it was conjectured that provided the two soft momenta are sent to zero with the same rate, the following limit holds

$$\begin{aligned}&\lim_{t\to 0}\mathcal{M}^{aba_1a_2\dots a_{2n}}(tp,tq,p_1,p_2,\dots,p_{2n})\\ &=\ -\frac{1}{2F^2}\sum_{i=1}^{n}f^{abc}f^{ca_id}\frac{p_i\cdot(p-q)}{p_i\cdot(p+q)}\mathcal{M}^{a_1\dots a_{i-1}da_{i+1}\dots a_{2n}}(p_1,p_2,\dots,p_{2n})\end{aligned} \tag{4.112}$$

where f^{abc} are the structure constants. Analogous statement has been then rigorously proven for the tree-level amplitudes in the $\mathcal{N}=8$ supergravity using

[11] Let us remind that the on-shell amplitudes are parametrization independent.

BCFW relations. In fact, for the on-shell amplitudes, the formula (4.112) can be proven non-perturbatively under some assumptions for the general enough case of the theory with global symmetry breaking (including the case of chiral non-linear sigma model with general chiral group G) using the symmetry arguments only (cf. the PCAC soft-pions theorems [141]) . We postpone the details to the Appendix 4.7.5 .

In terms of the stripped *on-shell* amplitudes the relation (4.112) can be rewritten as

$$\lim_{t\to 0}\mathcal{M}_{2n+2}(p_1,\dots,p_{i-1},tp_i,\dots,tp_j,p_{j+1},\dots p_{2n+2})$$
$$=\frac{1}{4F^2}\delta_{j,i+1}\left(\frac{p_{i+2}\cdot(p_i-p_{i+1})}{p_{i+2}\cdot(p_i-p_{i+1}}-\frac{p_{i-1}\cdot(p_i-p_{i+1})}{p_{i-1}\cdot(p_i-p_{i+1}}\right)\mathcal{M}_{2n}(p_1,\dots,p_{i-1},p_{i+2},\dots p_{2n+2}). \tag{4.113}$$

In this section we will prove this relation also for the tree-level semi-on-shell amplitudes J_{2n+1} (and consequently for M_{2n+1}) of the $SU(N)$ nonlinear sigma model in the Cayley parametrization using suitable form of the generalized BCFW representation.

4.5.1 Adler zeroes

In this subsection we will use the BCFW-like relations (4.102) derived in the previous section and prove the presence an Adler zero at M_{2n+1} when one of the *odd* momenta, say p_{2l-1}, is soft, i.e. we will prove that for $l=1,2,\dots,n+1$

$$\lim_{t\to 0}M_{2n+1}(p_1,p_2,\dots,p_{2l-2},tp_{2l-1},p_{2l+1},\dots,p_{2n+1})=0. \tag{4.114}$$

For the fundamental amplitude $M_3(p_1,p_2,p_3)$ we have explicitly[12]

$$M_3(tp_1,p_2,p_3)=M_3(p_1,p_2,tp_3)=\frac{1}{F^2}t(p_1\cdot p_3)\to 0. \tag{4.115}$$

In the general case the proof of (4.114) is by induction. Let us assume validity of (4.114) for $m<n$. This assumption also means that, taking the cut semi-on-shell amplitude M_{2m+1} on shell, i.e. for $p^2_{1,2n+1}\to 0$, the Adler zero is in fact present at $M_{2m+1}|_{\text{on shell}}=-\mathcal{M}_{2m+2}$ for all momenta, i.e.

$$\lim_{t\to 0}M_{2m+1}(p_1,p_2,\dots,tp_j,\dots p_{2m+1})|_{\text{on shell}}=0 \tag{4.116}$$

for all $j=1,\dots,2m+1$ due to the cyclicity of $\mathcal{M}_{2m+2}$.

Let us now substitute $p_{2l-1}\to tp_{2l-1}$ to the right hand side of (4.102). Note that, under such substitution, the position of the poles $z_{2j,2j+2}$, $z_{2j-1,2j+1}$ and $z^{\pm}_{i,j}$ become $t-$dependent. The $t-$ dependence of the right hand side of (4.102) is therefore both explicit (due to the explicit dependence on p_{2l-1}) and implicit (due to the implicit $t-$dependence of the poles z_P).

[12]Note however that for $t\to 0$ according to (4.68).

$$M_3(p_1,tp_2,p_3)\to\frac{1}{2F^2}(p_1+p_3)^2$$

and therefore the statement analogous to (4.114) for even momenta does not hold.

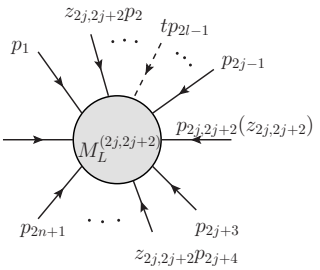

$\times \frac{1}{F^2}\frac{p_{2j}\cdot p_{2j+2}}{p^2_{2j,2j+2}} \to 0$

A) $j \neq l-1$

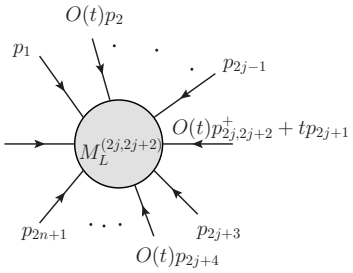

$\times \frac{1}{F^2}\frac{p_{2j}\cdot p_{2j+2}}{(p^+_{2j,2j+2}+tp_{2j_1})^2} \to \frac{1}{(2F^2)^n}p^2_-|_{p_{2l-1}\to 0}$

B) $j = l-1$

Figure 4.9: Graphical representation of the $t \to 0$ limit of the second term on the right hand side of (4.102). The soft momentum is denoted by dashed line in the case A. In the case B, $O(t)$ indicates the order of the $t-$dependent $z_{2j,2j+2}$.

We will now inspect the behavior of the individual terms under the limit $t \to 0$. The first term gives finite limit

$$\frac{1}{(2F^2)^n}p^2_- \to \frac{1}{(2F^2)^n}p^2_-|_{p_{2l-1}\to 0}. \tag{4.117}$$

As far as the second term is concerned, the individual terms of the sum over j vanish in this limit unless $j = l-1$. The reason is as follows. For $j \neq l-1$ (the case A in the Figure 4.9), the kinematical factor $p_{2j}\cdot p_{2j+2}/p^2_{2j,2j+2}$ as well as the position of the pole $z_{2j,2j+2}$ are $t-$independent and because tp_{2l-1} is placed on the *odd* position in $M_L^{(2j,2j+2)}(z_{2j,2j+2})$, we can safely[13] use the induction hypothesis to conclude that

$$\lim_{t\to 0} M_L^{(2j,2j+2)}(z_{2j,2j+2})|_{p_{2l-1}\to 0} = 0.$$

For $j = l-1$ (the case B in the Figure 4.9), the kinematical factor $p_{2j}\cdot p_{2j+2}/p^2_{2j,2j+2}$ becomes explicitly $t-$dependent and tends to $1/2$ for $t \to 0$, while $M_L^{(2j,2j+2)}(z_{2j,2j+2})$ has both explicit (through $p_{2j,2j+2} = z_{2j,2j+2}(p_{2j}+p_{2j+2}) + tp_{2j+1}$) and implicit $t-$dependence. In this case $z_{2j,2j+2} = O(t)$, as can be seen from (4.93). Therefore, all *even* momenta in $M_L^{(2j,2j+2)}(z_{2j,2j+2})$ are scaled by $O(t)$ factor, in the same way as in (4.68). We can therefore conclude with help of (4.68) that

$$\lim_{t\to 0} M_L^{(2j,2j+2)}(z_{2j,2j+2})\frac{1}{p^2_{2j,2j+2}}\frac{p_{2j}\cdot p_{2j+2}}{F^2} = \delta_{j,l-1}\frac{1}{(2F^2)^n}p^2_-|_{p_{2l-1}\to 0}. \tag{4.118}$$

The third term on the right hand side of (4.102) can be treated exactly in the

[13]Indeed, in general the momenta $p_k(z_{2j,2j+2})$ and $p_{2j,2j+2}(z_{2j,2j+2})$ are $t-$independent and

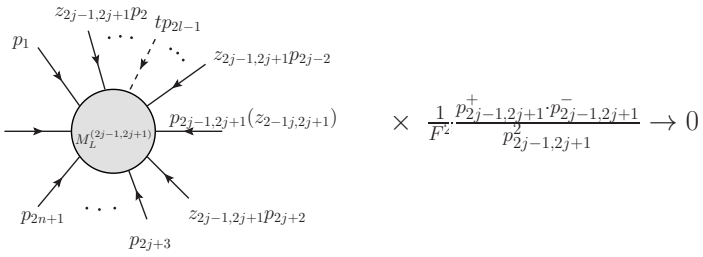

A) $j \neq l, l-1$

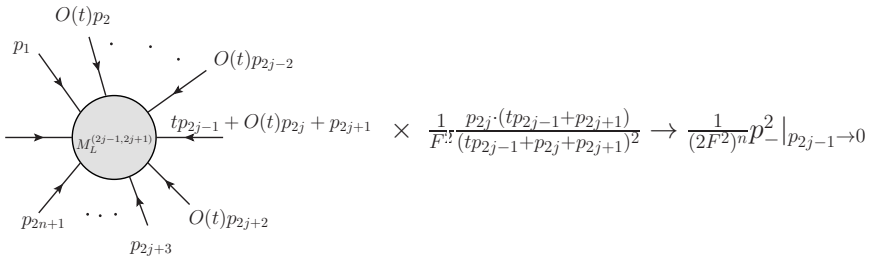

B) $j = l$

Figure 4.10: Graphical representation of the $t \to 0$ limit of the third term on the right hand side of (4.102). The soft momentum is denoted by dashed line in the picture A. In the picture B, we show only the $j = l$ case, the $j = l-1$ case is treated analogously. $O(t)$ indicates the order of the $t-$dependent $z_{2j,2j+2}$.

same way as the second (see Fig. 4.10). Also here the individual terms of the sum over j do not contribute with the only exception of $j = l$ and $j = l-1$ by induction hypothesis applied to $M_L^{(2j-1,2j+1)}(z_{2j-1,2j+1})$ which has for $j \neq l, l-1$ only explicit $t-$dependence. In the remaining two cases $j = l$ and $j = l-1$, the explicitly $t-$dependent kinematical factors $p^+_{2j-1,2j+1} \cdot p^-_{2j-1,2j+1}/p^2_{2j-1,2j+1}$ tend again to $1/2$ and within $M_L^{(2j-1,2j+1)}(z_{2j-1,2j+1})$ the even momenta are scaled by $z_{2j-1,2j+1} = O(t)$ (see (4.91)) and thus (4.68) can be used[14] to conclude that

$$\lim_{t\to 0} M_L^{(2j-1,2j+1)}(z_{2j-1,2j+1})\frac{1}{p^2_{2j-1,2j+1}}\frac{p^+_{2j-1,2j+1}\cdot p^-_{2j-1,2j+1}}{F^2} = (\delta_{j,l}+\delta_{j,l-1})\,\frac{1}{(2F^2)^n}p^2_-|_{p_{2l-1}\to 0}. \tag{4.119}$$

The fourth term on the right hand side of (4.102) vanish completely in the limit $t \to 0$. This is easy to see for those terms of the sum over (i,j) for which[15] $\lim_{t\to 0} z^\pm_{i,j} \neq 0$. In this case either $M_L^{(i,j)}(z^\pm_{i,j})$ or $M_R^{(i,j)}(z^\pm_{i,j})$ have explicit $t-$dependence through tp_{2l-1} (which is for $M_L^{(i,j)}(z^+_{i,j})$ on odd position) and thus the induction hypothesis in the form (4.114) or (4.116) can be used[16]. By direct inspection of (4.90) we find that the only case for which the above argumentation does not apply is the case $j - i = 4$ with i even and $i \leq 2l-1 \leq j$. Here

nonzero.

[14]Note that, the odd momenta are $t-$idependent with the only exception of $p_{2j-1,2j+1}(z_{2j-1,2j+1})|_{p_{2j\mp 1}\to tp_{2j\mp 1}}$ the limit of which is $p_{2j\pm 1}$.

[15]It is easy to realize that $\lim_{t\to 0} z^+_{i,j} \neq \lim_{t\to 0} z^-_{i,j}$ for generic p_k.

[16]Let us remind that $M_R^{(i,j)}(z^+_{i,j})$ is fully on-shell.

$\lim_{t\to 0} z^-_{i,j} \neq 0$ and so for the "minus" part of this (i,j) term we can use the induction hypothesis as above. However, the "plus" part might be problematic because

$$z^+_{i,j} = -\frac{(p_{2l-1}\cdot p_{2l-1\pm 2})}{(p_{2l-1\pm 2}\cdot p^+_{i,j})}t + O(t^2). \tag{4.120}$$

Using this formula and (4.65) we find after some algebra

$$M_R^{(i,j)}(z^+_{i,j}) = M_5(p_i(z^{t+}_{i,j}), \dots tp_{2l-1}, \dots, p_j(z^{t+}_{i,j})) = O(t^2). \tag{4.121}$$

which shows that also the "plus" part has vanishing $t\to 0$ limit.

Putting therefore the only nonzero contributions (4.117), (4.118) and (4.119) together we get finally

$$\begin{aligned}&\lim_{t\to 0} M_{2n+1}(p_1, p_2, \dots, p_{2l-2}, tp_{2l-1}, p_{2l+1}, \dots, p_{2n+1})\\ =\ & \frac{1}{(2F^2)^n} p_-^2|_{p_{2l-1}\to 0}\left(1 + \sum_{j=1}^{n-1}\delta_{j,l-1} - \sum_{j=1}^{n}(\delta_{j,l}+\delta_{j,l-1})\right) = 0,\end{aligned}$$

which finishes the proof.

4.5.2 Double-soft limit

Let us now study the behavior of the semi-on-shell amplitude J_{2n+1} in the Cayley parametrization under the double soft limit, i.e. the case when two external momenta, say p_i and p_j, are scaled according to $p_{i,j}\to tp_{i,j}$ and t is sent to zero. In this section we will prove, that for $1<i<j<2n+1$

$$\begin{aligned}&\lim_{t\to 0} J_{2n+1}(p_1,\dots,p_{2n+1})|_{p_i\to tp_i, p_j\to tp_j}\\ &= \delta_{j,i+1}\frac{1}{2F^2}\left(\frac{(p_i\cdot p_{i+2})}{p_{i+2}\cdot(p_{i+1}+p_i)} - \frac{(p_i\cdot p_{i-1})}{p_{i-1}\cdot(p_{i+1}+p_i)}\right) J_{2n-1}(p_1,\dots,p_{i-1},p_{i+2}\dots,p_{2n+1}),\end{aligned} \tag{4.122}$$

which has an identical form as (4.113)[17]. The key ingredient of the proof is the generalized form of the BCFW representation mentioned in Section 4.3.2 written for a suitable two-parameter complex deformation of the amplitude J_{2n+1}. Such a representation allows us to calculate the double soft limit with help of the known behavior of the poles and corresponding residues in this limit. Useful information on this behavior can be inferred from the statement (4.114) concerning the Adler zeroes proved in the previous subsection.

The above mentioned deformation of J_{2n+1} can be defined as the following function of two complex variables z and t

$$S^n_{i,j}(z,t) = J(p_1,\dots,p_{2n+1})|_{p_i\to tp_i, p_j\to zp_j}, \tag{4.123}$$

[17]Indeed,

$$\frac{(p_i\cdot p_{i+2})}{p_{i+2}\cdot(p_{i+1}+p_i)} - \frac{(p_i\cdot p_{i-1})}{p_{i-1}\cdot(p_{i+1}+p_i)} = \frac{1}{2}\left(\frac{p_{i+2}\cdot(p_i-p_{i+1})}{p_{i+2}\cdot(p_i-p_{i+1})} - \frac{p_{i-1}\cdot(p_i-p_{i+1})}{p_{i-1}\cdot(p_i-p_{i+1})}\right).$$

therefore

$$S^n_{i,j}(1,1) = J_{2n+1}(p_1,\dots,p_{2n+1}) \tag{4.124}$$

Various types of the double soft limit correspond then to various ways of taking the limit $(z,t) \to (0,0)$ in the double complex plane (z,t); the limit (4.122) corresponds to $\lim_{t\to 0} S^n_{i,j}(t,t) \equiv S^{n,0}_{i,j}$.

For $z \to \infty$ and $t > 0$ fixed the following asymptotic behavior holds

$$S^n_{i,j}(z,t) = O(z^0), \tag{4.125}$$

as can be easily proved e.g. by induction with help of the Berends-Giele recursive relations (4.57). We can therefore write the generalized BCFW relation with one subtraction in the form (4.49)

$$S^n_{i,j}(z,t) = S^n_{i,j}(a,t) + \sum_{k,l} \frac{\mathrm{Res}\left(S^n_{i,j}; z_{k,l}(t)\right)}{z - z_{k,l}(t)} \frac{z-a}{z_{k,l}(t)-a}. \tag{4.126}$$

where $a \neq z_{k,l}(t)$ is a priory arbitrary, however, as we shall see in what follows, appropriate choice of a can simplify the calculation.

The poles $z_{k,l}(t)$ for $k \leq j \leq l$ correspond to the conditions $p^2_{k,l}|_{p_i\to tp_i, p_j\to zp_j} = 0$, or explicitly

$$z_{k,l}(t) = -\frac{p^2_{k,l}|_{p_i\to tp_i, p_j\to 0}}{2(p_j\cdot p_{k,l})|_{p_i\to tp_i}}. \tag{4.127}$$

The residues at the poles $z_{k,l}(t)$ factorize

$$\begin{aligned}\mathrm{Res}\left(S^n_{i,j}; z_{k,l}(t)\right) \;=\; & \frac{1}{2(p_j\cdot p_{k,l})|_{p_i\to tp_i}} [J_{2n+1-(l-k)}(p_1,\dots,p_{k-1},p_{k,l},p_{l+1},\dots,p_{2N+1}) \\ & \times M_{l-k+1}(p_k,\dots,p_l)|_{p_i\to tp_i, p_j\to zp_j}]|_{z\to z_{k,l}(t)},\end{aligned} \tag{4.128}$$

where M_{l-k+1} is the cut amplitude (4.80). Namely the latter two formulae along with (4.114) contain sufficient amount of information for the calculation of the double soft limit.

Let us first assume $i < j$ where i is odd and j arbitrary. This choice is a technical one, and as we shall see, the general case can be easily obtained using the symmetry properties of the amplitude. In what follows we set $a = 1$ in (4.126), the double soft limit then simplifies to

$$S^{n,0}_{i,j} \equiv \lim_{t\to 0} S^n_{i,j}(t,t) = \lim_{t\to 0} \sum_{k,l} \frac{\mathrm{Res}\left(S^n_{i,j}; z_{k,l}(t)\right)}{t - z_{k,l}(t)} \frac{t-1}{z_{k,l}(t)-1}, \tag{4.129}$$

where we have used the existence of the Adler zero for
$S^n_{i,j}(1,t) = J_{2n+1}(p_1,\dots,tp_i,\dots,p_{2n+1})$ and i odd (cf. (4.114)).

For generic p_r there exist a finite limit

$$z_{k,l}(0) = \lim_{t\to 0} z_{k,l}(t) \neq 1 \tag{4.130}$$

In fact the only nonzero contributions to the right hand side of (4.129) stem from the cases for which $z_{k,l}(0) = 0$. Indeed, for $z_{k,l}(0) \neq 0$ we get for the corresponding contribution

$$\frac{1}{z_{k,l}(0)(z_{k,l}(0)-1)} \lim_{t\to 0} \mathrm{Res}\left(S^n_{i,j}; z_{k,l}(t)\right), \tag{4.131}$$

and, according to (4.114), on the right hand side of (4.128) we get either

$$\lim_{t\to 0}[M_{l-k+1}(p_k,\ldots,p_l)|_{p_i\to tp_i,p_j\to zp_j}]|_{z\to z_{k,l}(t)}=0 \tag{4.132}$$

for $k\le i<j\le l$ or

$$\lim_{t\to 0} J_{2n+1-(l-k)}(p_1,\ldots,tp_i,\ldots,p(k,l)(t),p_{k+1},\ldots,p_{2n+1})=0 \tag{4.133}$$

for $i<k<j\le l$. In both cases the complementary factor has finite limit and therefore

$$\lim_{t\to 0}\mathrm{Res}\left(S^n_{i,j};z_{k,l}(t)\right)=0. \tag{4.134}$$

Let us therefore discuss the contributions form the poles for which $z_{k,l}(0)=0$. Note that, for generic p_r such a pole does not exist provided $j>i+2$. We can therefore immediately conclude

$$S^{n,0}_{i,j}=0\quad\text{for}\quad j>i+2. \tag{4.135}$$

What remains are the following two alternatives for which the three-particle poles $z_{k,l}(t)$ with $l=k+2$ can vanish in the limit $t\to 0$ (see Fig. 4.11)

1. $j=i+1$ and either $k=i$ or $k=i-1$. In this case either

$$p^2_{i-1,i+1}|_{p_i\to tp_i,p_j\to 0}\to p^2_{i-1}=0 \tag{4.136}$$

or

$$p^2_{i,i+2}|_{p_i\to tp_i,p_j\to 0}\to p^2_{i+2}=0 \tag{4.137}$$

2. $j=i+2$ and $k=i$, in this case

$$p^2_{i,i+2}|_{p_i\to tp_i,p_j\to 0}=p^2_{i+1}=0. \tag{4.138}$$

In what follows we will discuss separately the cases $j=i+1$ and $j=i+2$. Let us first study the double soft limit of two adjacent momenta, i.e. $j=i+1$ where i is odd. We will investigate the contributions of individual poles $z_{k,l}(t)$ on the right hand side of (4.129) separately. In this case we get for $i>1$ only two potentially nonzero contributions (i.e. (4.137) and (4.136)) to the right hand side of (4.129), namely

$$S^{n,0}_{i,i+1}=\lim_{t\to 0}\frac{\mathrm{Res}\left(S^n_{i,i+1};z_{i-1,i+1}(t)\right)}{t-z_{i-1,i+1}(t)}\frac{t-1}{z_{i-1,i+1}(t)-1}+\lim_{t\to 0}\frac{\mathrm{Res}\left(S^n_{i,i+1};z_{i,i+2}(t)\right)}{t-z_{i,i+2}(t)}\frac{t-1}{z_{i,i+2}(t)-1}. \tag{4.139}$$

We get for the poles $z_{i-1,i+1}(t)$ and $z_{i,i+2}(t)$

$$z_{k,k+2}(t)=-\frac{p^2_{k,k+2}|_{p_i\to tp_i,p_j\to 0}}{2(p_j\cdot p_{k,k+2})|_{p_i\to tp_i}}=-t\frac{(p_i\cdot p_r)}{(p_j\cdot p_r)}+O(t^2), \tag{4.140}$$

where either $r=i+2$ (for $k=i$) or $r=i-1$ (for $k=i-1$), and as a consequence,

$$\frac{1}{t-z_{k,k+2}(t)}\frac{t-1}{z_{k,k+2}(t)-1}=\frac{1}{t}\frac{(p_j\cdot p_r)}{p_r\cdot(p_j+p_i)}(1+O(t)). \tag{4.141}$$

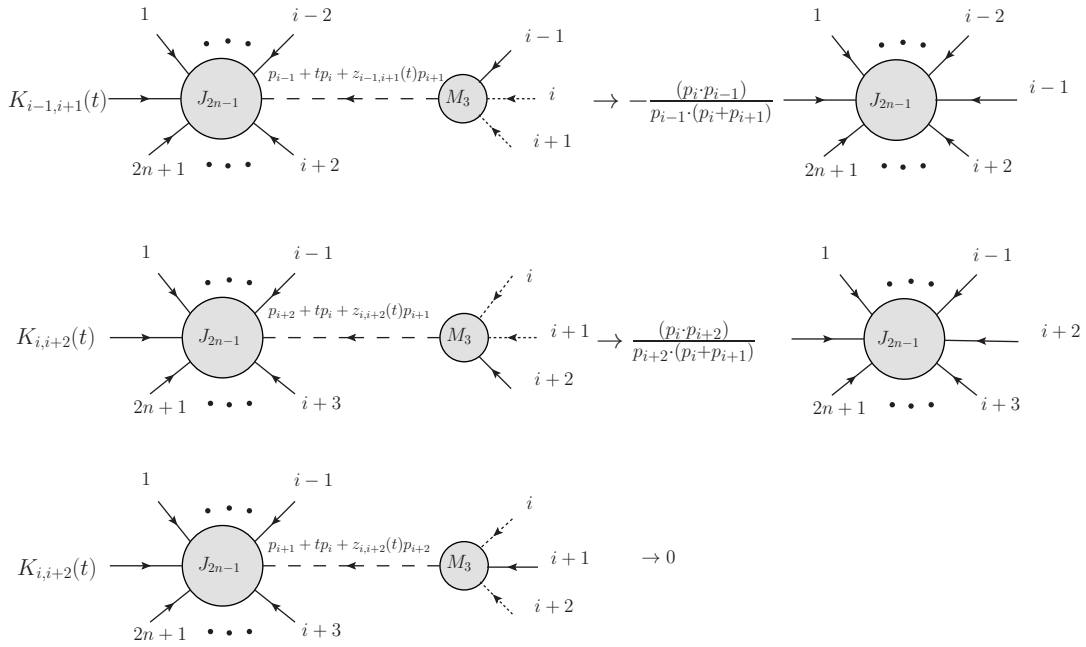

Figure 4.11: Graphical representation of the $t \to 0$ limit of the three cases (4.136), (4.137) and (4.138) for which $z_{k,l}(t) \to 0$. The soft momenta are denoted by dotted lines. The multiplicative factors $K_{k,l}(t)$ stays for $(t-1)/(t-z_{k,l}(t))(z_{k,l}(t)-1)$.

We have further

$$p_{k,k+2}(t) = tp_i + z_{k,k+2}(t)p_j + p_r \to p_r \neq 0 \tag{4.142}$$

and therefore in both cases

$$\lim_{t\to 0} J_{2n-1}(p_1, \ldots, p_{k-1}, p_{k,k+2}(t), p_{k+3}, \ldots, p_{2n+1}) = J_{2n-1}(p_1, \ldots, p_{i-2}, p_{i-1}, p_{i+2}, \ldots, p_{2n+1}). \tag{4.143}$$

For the remaining ingredients of the formula (4.128) we get

$$M_3(tp_i, z_{i,i+2}(t)p_{i+1}, p_{i+2}) = \frac{1}{F^2} t(p_i \cdot p_{i+2}) \tag{4.144}$$

$$M_3(p_{i-1}, tp_i, z_{i-1,i+1}(t)p_{i+1}) = \frac{1}{F^2} z_{i-1,i+1}(t)(p_{i-1} \cdot p_{i+1}) = -t\frac{1}{F^2}(p_i \cdot p_{i-1})(1 + O(t)). \tag{4.145}$$

Inserting this into the formulae (4.128) and (4.139) get finally for $i > 1$

$$S^{n,0}_{i,i+1} = \frac{1}{2F^2}\left(\frac{(p_i \cdot p_{i+2})}{p_{i+2} \cdot (p_{i+1} + p_i)} - \frac{(p_i \cdot p_{i-1})}{p_{i-1} \cdot (p_{i+1} + p_i)}\right) J_{2n-1}(p_1, \ldots, p_{i-2}, p_{i-1}, p_{i+2}, \ldots, p_{2n+1}). \tag{4.146}$$

In the same way, for $i = 1$ only the first term on the right hand side of (4.146) contributes.

Let us proceed to the case 2. when $j = i+2$ and $z_{i,i+2}(t) \to 0$ for $t \to 0$ is the only pole which can give nonzero contribution to (4.129). In this case we have

$$S^{n,0}_{i,i+2} = \lim_{t\to 0} \frac{\mathrm{Res}\left(S^n_{i,i+2}; z_{i,i+2}(t)\right)}{t - z_{i,i+2}(t)} \frac{t-1}{z_{i,i+2}(t)-1}. \tag{4.147}$$

The formulae (4.140, 4.141, 4.142, 4.143) are still valid with $r = i+1$, but now we have

$$M_3(tp_i, p_{i+1}, z_{i,i+2}(t)p_{i+2}) = \frac{1}{F^2} t z_{i,i+2}(t)(p_i \cdot p_{i+2}) = O(t^2). \tag{4.148}$$

which implies $S^{n,0}_{i,i+2} = 0$.

To summarize, we have for $k > 0$

$$\begin{aligned} &\lim_{t\to 0} J_{2n+1}(p_1, \ldots, p_{2k}, tp_{2k+1}, \ldots, tp_j, \ldots, p_{2n+1}) = \\ = \;& \delta_{j,2k+2} \frac{1}{2F^2} J_{2n-1}(p_1, \ldots, p_{2k}, p_{2k+3}, \ldots, p_{2n+1}) \\ & \times \left(\frac{(p_{2k+1} \cdot p_{2k+3})}{p_{2k+3} \cdot (p_{2k+2} + p_{2k+1})} - \frac{(p_{2k+1} \cdot p_{2k})}{p_{2k} \cdot (p_{2k+2} + p_{2k+1})} \right) \end{aligned} \tag{4.149}$$

and for $k = 0$

$$\lim_{t\to 0} J_{2n+1}(tp_1, \ldots, tp_j, \ldots, p_{2n+1}) = \delta_{j,2} \frac{1}{2F^2} \frac{(p_1 \cdot p_3)}{(p_2 \cdot p_3) + (p_1 \cdot p_3)} J_{2n-1}(p_3, \ldots, p_{2n+1}).$$

As it is clear from the above discussion, the "asymmetry" of the latter result stems from the fact that p_{2n+2} is off-shell and therefore the three-particle pole corresponding to $(p_3 + p_4 + \ldots + p_{2n+1})^2 = (p_{2n+2} - p_1 - p_2)^2 \to p^2_{2n+2} \neq 0$ does not contribute.

Because

$$J(1, 2, \ldots, 2n+1) = J(2n+1, 2n, \ldots, 2, 1), \tag{4.150}$$

we get for $j < 2k+1$

$$J_{2n+1}(p_1, \ldots, tp_j \ldots, p_{2k}, tp_{2k+1}, \ldots, , p_{2n+1}) = J_{2n+1}(p_{2n+1,} \ldots, tp_{2k+1}, p_{2k}, \ldots, tp_j, \ldots, p_1). \tag{4.151}$$

On the right hand side of this identity the momentum p_{2k+1} stays on the odd position and thus

$$\begin{aligned} &\lim_{t\to 0} J_{2n+1}(p_1, \ldots, tp_j \ldots, p_{2k}, tp_{2k+1}, \ldots, p_{2n+1}) \\ = \;& \delta_{j,2k} \frac{1}{2F^2} J_{2n-1}(p_1 \ldots, p_{2k-1}, p_{2k+2}, \ldots, p_{2n+1}) \\ & \times \left(-\frac{(p_{2k} \cdot p_{2k-1})}{p_{2k-1} \cdot (p_{2k} + p_{2k+1})} + \frac{(p_{2k} \cdot p_{2k+2})}{p_{2k+2} \cdot (p_{2k} + p_{2k+1})} \right) \end{aligned} \tag{4.152}$$

Putting (4.149) and (4.152) together the final result (4.122) follows.

4.6 Summary and conclusion

We have studied various aspects of the $SU(N)$ chiral nonlinear sigma model which describes the low-energy dynamics of the Goldstone bosons corresponding to the spontaneous chiral symmetry breaking $SU(N) \times SU(N) \to SU(N)$. As we have shown, the tree-level scattering amplitudes of the Goldstone bosons can be constructed from the stripped amplitudes, which are identical as those of the $U(N)$ chiral nonlinear sigma model. It is therefore possible to use this correspondence and to investigate both the $SU(N)$ and $U(N)$ cases on the same footing. Especially we are allowed to choose any parametrization (field redefinition) of the chiral unitary matrix $U(x)$ entering the Lagrangian from the wide class of parametrizations admissible for the extended $U(N)$ case, because the fully on-shell stripped amplitudes do not depend on the parametrization. For the direct calculation of the flavor ordered Feynman graphs, the most convenient choice proved to be the minimal parametrization (4.31), which we have chosen in order to calculate the on-shell amplitudes up to 10 Goldstone bosons.

The proliferation of the Feynman graphs with increasing number of the Goldstone bosons call for alternative methods of calculation. The more efficient method is based on the Berends-Giele recursive relations for the semi-on-shell amplitudes, but due to the infinite number of the interaction vertices in the Lagrangian of the nonlinear sigma model, the number of terms necessary to evaluate the $n-$point amplitude grows much faster (exponentially) with n than for the case of the power-counting renormalizable theories (where the growth is polynomial).

The BCFW recursive relations could make the calculation of the on-shell stripped amplitude as effective as for the renormalizable theories at least as far as the number of terms (which is in both cases related to the number of factorization channels) is concerned. However, the standard way of the BCFW reconstruction is not directly applicable for the nonlinear sigma model because of the bad behavior of the BCFW deformed amplitudes at infinity. We have therefore proposed an alternative deformation of the semi-on-shell amplitudes based on the scaling of all odd or all even momenta, for which we were able to prove exact results concerning the behavior of the semi-on-shell amplitudes when the scaling parameter tended to zero. Using the Berends-Giele recursive relations we were able to prove this scaling properties for general $n-$point amplitude. An essential ingredient of the proof was the fact that the semi-on-shell amplitudes (unlike the on-shell ones) are parametrization dependent and we could therefore make an appropriate choice of the parametrization (the Cayley one). We have then used these exact scaling properties for a generalized BCFW reconstruction formula (with one subtraction) which determines fully all the semi-on-shell amplitudes in the Cayley parametrization including the basic four-point one. Putting then the semi-on-shell amplitudes on-shell we reconstruct simply the parametrization independent on-shell amplitudes. In contrast to the standard BCFW relations our procedure is not restricted to $d \geq 4$ space-time dimensions.

The BCFW recursive relation are also a suitable tool for investigation of the properties of the amplitudes. We have illustrated this in two cases, namely we have proved the presence of the Adler zero and established the general form of the double soft limit for the semi-on-shell amplitudes in the Cayley parametrization.

The existence of BCFW recursion relations for power-counting non-renormalizable

effective theory as the $SU(N)$ chiral nonlinear sigma model gives an evidence that the on-shell methods can be used for much larger classes of theories than has been considered so far. It also indicates that the $SU(N)$ chiral nonlinear sigma model is rather special and deeper understanding of all its properties is desirable. For future directions, it would be interesting to see whether the construction can be re-formulated purely in terms of on-shell scattering amplitudes not using the semi-on-shell ones. Next possibility is to focus on loop amplitudes. As was shown in [113] the loop integrand can be also in certain cases constructed using BCFW recursion relations, it would be spectacular if the similar construction can be applied for effective field theories.

4.7 Appendix

4.7.1 General parametrization

In this Appendix we will discuss a very general class of parameterizations of the $U(N)$ sigma model originally studied in [97], which is suited for a derivation of the stripped Feynman rules. Within this class the field $U(x) \in U(N)$ is expressed in the form

$$U = \sum_{k=0}^{\infty} a_k \left(\sqrt{2}\frac{\mathrm{i}}{F}\phi\right)^k \tag{4.153}$$

where $\phi = t^a\phi^a$, ϕ^a are the Goldstone boson fields, t^a are the $U(N)$ generators normalized according to $\langle t^a t^b\rangle = \delta^{ab}$ and a_k are real coefficients. These coefficients are not completely arbitrary, because the unitarity condition $U^+U = 1$ implies the following constraint

$$\sum_{k=0}^{n} a_k a_{n-k}(-1)^k = \delta_{n,0}. \tag{4.154}$$

For $n = 0$ we get $a_0^2 = 1$ and without lose of generality we can set $a_0 = 1$. In order to preserve the correct normalization of the kinetic term and to keep the interpretation of F as the decay constant for the fields ϕ^a we have to fix also $a_1 = 1$.

For n odd the relations (4.154) are satisfied automatically while for $n = 2k$ we can solve them for a_{2k} and get a recurrent formula for the even coefficients expressed in terms of the odd ones

$$a_{2k} = -\frac{(-1)^k}{2}a_k^2 - \sum_{j=1}^{k-1}(-1)^j a_j a_{2k-j}. \tag{4.155}$$

This gives up to $k = 3$

$$\begin{aligned} a_2 &= \frac{1}{2}a_1^2 = \frac{1}{2} \\ a_4 &= -\frac{1}{2}a_2^2 + a_1 a_3 = -\frac{1}{8} + a_3 \\ a_6 &= \frac{1}{2}a_3^2 + a_1 a_5 - a_2 a_4 = \frac{1}{16} - \frac{1}{2}a_3 + \frac{1}{2}a_3^2 + a_5 \end{aligned} \tag{4.156}$$

The explicit solution of the recurrent relations (4.155) to all orders can be easily found by means of the following trick. Let us introduce the generating function $f(x)$ of the above coefficients a_k

$$f(x) = \sum_{k=0}^{\infty} a_k x^k. \tag{4.157}$$

The relations of unitarity with the initial conditions $a_0 = a_1 = 1$ are then equivalent to

$$f(-x)f(x) = 1,\ f(0) = 1,\ f^{'}(0) = 1 \tag{4.158}$$

which represents a functional equations for the generating functions $f(x)$. Let us define $f_{\pm}(x)$ to be the even and odd part of $f(x)$, i.e. $f_{\pm}(x) = \left(f(x) \pm f(-x)\right)/2$. From (4.158) we get then

$$f_+(x)^2 - f_-(x)^2 = 1 \tag{4.159}$$

or finally

$$f_+(x) = \sqrt{1 + f_-(x)^2}. \tag{4.160}$$

The formal series expansion of both sides of the last equation at $x = 0$ gives the solution of the recurrent relations (4.155), i.e. the explicit expressions for a_{2k} in terms of an infinite number of free parameters a_{2k+1}. The general solution of the functional equation (4.158) is then

$$f(x) = f_-(x) + \sqrt{1 + f_-(x)^2} \tag{4.161}$$

where $f_-(x)$ is arbitrary odd real function analytic for $x = 0$ satisfying $f'(0) = 1$. The minimal parameter-free solution corresponds to the choice $a_{2k+1} = 0$ for $k > 0$, i.e. $f_-^{\min}(x) = x$ and

$$f_{\min}(x) = x + \sqrt{1 + x^2} \tag{4.162}$$

i.e. for $k \geq 1$

$$a_{2k}^{\min} = \frac{(-1)^{k+1}}{2^{2k-1}} C_{k-1}, \tag{4.163}$$

where

$$C_n = \frac{1}{n+1} \left(\begin{array}{c} 2n \\ n \end{array} \right) \tag{4.164}$$

are the Catalan numbers.

Another frequently used choices are the exponential and Cayley parameterizations corresponding to $f_{\exp}(x)$ and $f_{\text{Cayley}}(x)$ respectively, where

$$f_{\exp}(x) = \mathrm{e}^x \tag{4.165}$$

$$f_{\text{Cayley}}(x) = \frac{1 + (x/2)}{1 - (x/2)}, \tag{4.166}$$

or in terms of the coefficients a_k

$$a_k^{\exp} = \frac{1}{k!} \tag{4.167}$$

$$a_k^{\text{Cayley}} = \frac{1}{1 + \delta_{k,0}} \frac{1}{2^{k-1}}. \tag{4.168}$$

These two parameterizations can be understood as minimal parameter-free variants with respect to other two possible forms of the general solutions of the functional equation (4.158), namely

$$f(x) = \exp g(x) \tag{4.169}$$

and

$$f(x) = \frac{h(x)}{h(-x)} \tag{4.170}$$

where $g(x)$ and $h(x)$ are arbitrary real functions analytic for $x = 0$ for which

$$g(x) = -g(-x), \tag{4.171}$$
$$g(0) = 0, \quad g'(0) = 1 \tag{4.172}$$

and

$$h'(0) = \frac{1}{2}h(0) \neq 0. \tag{4.173}$$

As was proved in [97], for $N > 2$ the only parametrization from the class (4.153) admissible also for $SU(N)$ sigma model is the exponential one. The reason is that, under the general axial $SU(N)$ transformation

$$U(x)' = \sum_{k=0}^{\infty} a_k \left(\sqrt{2}\frac{\mathrm{i}}{F}\phi'\right)^k = U_A \sum_{k=0}^{\infty} a_k \left(\sqrt{2}\frac{\mathrm{i}}{F}\phi\right)^k U_A \tag{4.174}$$

which defines corresponding nonlinear transformation of the matrix of the Goldstone boson fields $\phi = \sum_{a=1}^{N^2-1} \phi^a t^a$ the $SU(N)$ condition for the trace $\langle \phi' \rangle = 0$ is not preserved unless $a_k = 1/k!$. Of course, in the case $N > 2$ we can use different admissible parameterizations of $SU(N)$ which, however, do not belong to the class (4.153) (see e.g. [140]).

Let us now find the stripped Feynman rules. Using the general parametrization (4.153) we can write the Lagrangian of the nonlinear $U(N)$ sigma model in the expanded form

$$\mathcal{L}^{(2)} = \frac{F^2}{4}\langle \partial U \cdot \partial U^+ \rangle = \sum_{n,m=0}^{\infty} v_{n,m} \langle \partial\phi\phi^n \cdot \partial\phi\phi^m \rangle. \tag{4.175}$$

where we get for $v_{n,m}$ after some algebra (and using the unitarity condition (4.154))

$$v_{n,m} = (1 + (-1)^{n+m}) \frac{(-\mathrm{i})^{n+m}}{4F^{n+m}} \sum_{k=0}^{m} a_k a_{m+n+2-k} (-1)^{k+1} (k - 1 - m) \tag{4.176}$$

Therefore only the terms with even number of fields survive, explicitly

$$\mathcal{L}^{(2)} = \sum_{n=0}^{\infty} \mathcal{L}^{(2)}_{2n+2} \tag{4.177}$$

where

$$\mathcal{L}^{(2)}_{2n+2} = \sum_{k=0}^{2n} v_{k,2n-k} \langle \partial\phi\phi^k \cdot \partial\phi\phi^{2n-k} \rangle \tag{4.178}$$

The usual Feynman rules for the vertices can be easily obtained as a sum over permutations

$$V_{2n+2}^{a_1,\ldots,a_{2n+2}}(p_1,p_2,\ldots,p_{2n+1};p_{2n+2}) = -2^{n+1}\sum_{\sigma\in S_{2n+2}}\langle t^{a_{\sigma(1)}}\ldots t^{a_{\sigma(2n+2)}}\rangle \times\sum_{k=0}^{2n} v_{k,2n-k}(p_{\sigma(1)}\cdot p_{\sigma(1)+k+1}) \quad (4.179)$$

The stripped Feynman rule then follows in the form

$$V_{2n+2}(p_1,p_2,\ldots,p_{2n+1};p_{2n+2}) = -2^{n+1}\sum_{k=0}^{2n}\sum_{i=1}^{2n+2} v_{k,2n-k}(p_i\cdot p_{i+k+1}) \quad (4.180)$$

Inserting (4.167) into (4.176) we get after some algebra for the exponential parametrization

$$v_{k,2n-k}^{\exp} = \frac{(-1)^n}{2F^{2n}}\frac{(-1)^k}{(2n+2)!}\left(\begin{array}{c}2n\\k\end{array}\right). \quad (4.181)$$

while for the Cayley parametrization we have $v^{\rm Cayley}_{2k+1,2n-2k-1}=0$ and

$$v_{2k,2n-2k}^{\rm Cayley} = \frac{(-1)^n}{2F^{2n}}\frac{1}{2^{2n+1}}. \quad (4.182)$$

Similar calculations can be made also for the minimal parametrization, but the result is much more lengthy and we will not need it explicitly. Instead we will rewrite the Feynman rules for the vertex V_{2n+2} with $2n+2$ external legs in terms of the variables

$$s_{i,j} = p_{i,j}^2 \quad (4.183)$$

where $1\le i<j\le 2n+1$ and

$$p_{i,j} = \sum_{k=i}^{j} p_k \quad (4.184)$$

Here we identify

$$s_{2n+2,2n+2+k} = s_{k+1,2n+1} \quad (4.185)$$

$$s_{i,2n+2+k} = s_{k+1,i-1}. \quad (4.186)$$

The scalar products $(p_i\cdot p_j)$ can be then expressed as

$$(p_i\cdot p_i) = s_{i.i} \quad (4.187)$$

$$(p_i\cdot p_{i+1}) = \frac{1}{2}(s_{i,i+1}-s_{i,i}-s_{i+1,i+1}) \quad (4.188)$$

and for $k\ge 2$

$$(p_i\cdot p_{i+k}) = \frac{1}{2}(s_{i,i+k}-s_{i,i+k-1}+s_{i+1,i+k-1}-s_{i+1,i+k}). \quad (4.189)$$

On-shell we get $s_{i,i}=0$ and $s_{1,2n+1}=0$. The stripped Feynman rule in these variables can be written in the form valid for $n\ge 1$

$$V_{2n+2}(s_{i,j}) = (-1)^n\left(\frac{2}{F^2}\right)^n\sum_{k=0}^{n} w_{k,n}\sum_{i=1}^{2n+2} s_{i,i+k} \quad (4.190)$$

where

$$w_{0,n} = (-1)^n 2F^{2n} \left(2v_{0,2n} - v_{1,2n-1}\right) \tag{4.191}$$

$$w_{k,n} = (-1)^n 2F^{2n} \left(2v_{k,2n-k} - v_{k-1,2n+1-k} - v_{k+1,2n-1-k}\right) \quad \text{for} \quad k < n \tag{4.192}$$

$$w_{n,n} = (-1)^n 2F^{2n} (v_{n,n} - v_{n-1,n+1}). \tag{4.193}$$

Within the general parametrization we get from (4.176) and (4.154) after some algebra

$$w_{k,n} = \frac{(-1)^k}{1+\delta_{kn}} a_{k+1} a_{2n+1-k}. \tag{4.194}$$

For the above special cases this reads for $N \geq 1$

$$w_{k,n}^{\exp} = \frac{(-1)^k}{1+\delta_{kn}} \frac{1}{(2n+2)!} \begin{pmatrix} 2n+2 \\ k+1 \end{pmatrix} \tag{4.195}$$

$$w_{k,n}^{\text{Cayley}} = \frac{(-1)^k}{1+\delta_{kn}} \frac{1}{2^{2n}} \tag{4.196}$$

$$w_{0,n}^{\min} = w_{2k,n}^{\min} = 0 \tag{4.197}$$

$$w_{2k+1,n}^{\min} = \frac{1}{1+\delta_{2k+1,n}} \frac{(-1)^n}{2^{2n}} C_k C_{n-k-1}. \tag{4.198}$$

Note that, for the minimal parametrization the coefficients $w_{0,n}^{\min}$ at $s_{i,i} = p_i^2$ vanish, therefore the stripped Feynman rules for vertices do not depend on the off-shellness of the momenta in this case. This fact has been observed already in [104] without calculating the explicit Feynman rules.

4.7.2 More examples of amplitudes

The eight-point amplitude is

$$\begin{aligned} &8F^6 \mathcal{M}(1,2,3,4,5,6,7,8) = \\ &= \frac{1}{2} \frac{(s_{1,2}+s_{2,3})(s_{1,4}+s_{4,7})(s_{5,6}+s_{6,7})}{s_{1,3}s_{5,7}} + \frac{(s_{1,2}+s_{2,3})(s_{1,4}+s_{4,5})(s_{6,7}+s_{7,8})}{s_{1,3}s_{6,8}} \\ &\quad - \frac{(s_{1,2}+s_{2,3})(s_{4,5}+s_{4,7}+s_{5,6}+s_{5,8}+s_{6,7}+s_{7,8})}{s_{1,3}} + 2s_{1,2} + \frac{1}{2}s_{1,4} + \text{cycl} \end{aligned} \tag{4.199}$$

and graphically in Fig. 4.12. Finally the ten-point amplitude is given by

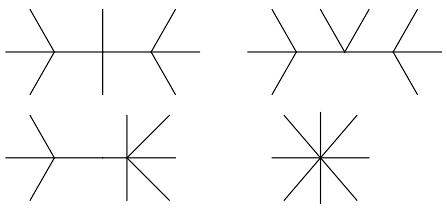

Figure 4.12: Graphical representation of the 8-point amplitude (4.199) with cycling tacitly assumed.

$$
\begin{aligned}
16F^8\mathcal{M}(1,2,3,4,5,6,7,8,9,10) = -\frac{s_{1,2}+s_{2,3}}{s_{1,3}}\Big\{ & \\
& \frac{1}{2}\frac{(s_{1,4}+s_{4,9})(s_{5,8}+s_{6,9})(s_{6,7}+s_{7,8})}{s_{5,9}s_{6,8}} + \frac{1}{2}\frac{(s_{1,4}+s_{4,5})(s_{1,8}+s_{6,9})(s_{6,7}+s_{7,8})}{s_{1,5}s_{6,8}} \\
& + \frac{1}{2}\frac{(s_{1,8}+s_{4,9})(s_{4,5}+s_{5,8})(s_{6,7}+s_{7,8})}{s_{4,8}s_{6,8}} + \frac{(s_{1,4}+s_{4,5})(s_{1,6}+s_{6,7})(s_{1,8}+s_{8,9})}{s_{1,5}s_{1,7}} \\
& + \frac{(s_{1,4}+s_{4,5})(s_{1,6}+s_{6,9})(s_{7,8}+s_{8,9})}{s_{1,5}s_{7,9}} + \frac{(s_{1,8}+s_{4,9})(s_{4,7}+s_{5,8})(s_{5,6}+s_{6,7})}{s_{4,8}s_{5,7}} \\
& + \frac{(s_{1,6}+s_{4,9})(s_{4,5}+s_{5,6})(s_{7,8}+s_{8,9})}{s_{4,6}s_{7,9}} \\
& - \frac{1}{2}\frac{(s_{1,4}+s_{1,8}+s_{4,5}+s_{4,9}+s_{5,8}+s_{6,9})(s_{6,7}+s_{7,8})}{s_{6,8}} \\
& - \frac{(s_{1,8}+s_{4,9})(s_{4,5}+s_{4,7}+s_{5,6}+s_{5,8}+s_{6,7}+s_{7,8})}{s_{4,8}} \\
& - \frac{(s_{1,4}+s_{1,6}+s_{4,5}+s_{4,7}+s_{5,6}+s_{6,7})(s_{1,8}+s_{8,9})}{s_{1,7}} \\
& - \frac{(s_{1,4}+s_{1,6}+s_{4,5}+s_{4,9}+s_{5,6}+s_{6,9})(s_{7,8}+s_{8,9})}{s_{7,9}} \\
& - \frac{(s_{1,4}+s_{4,5})(s_{1,6}+s_{1,8}+s_{6,7}+s_{6,9}+s_{7,8}+s_{8,9})}{s_{1,5}} \\
& - \frac{(s_{1,4}+s_{4,9})(s_{5,6}+s_{5,8}+s_{6,7}+s_{6,9}+s_{7,8}+s_{8,9})}{s_{5,9}} \\
& + 2s_{1,4}+s_{1,6}+2s_{1,8}+2s_{4,5}+s_{4,7}+2s_{4,9}+2s_{5,6}+s_{5,8}+2s_{6,7}+s_{6,9}+2s_{7,8}+2s_{8,9}\Big\} \\
& - \frac{1}{2}\frac{(s_{1,2}+s_{1,4}+s_{2,3}+s_{2,5}+s_{3,4}+s_{4,5})(s_{1,6}+s_{1,8}+s_{6,7}+s_{6,9}+s_{7,8}+s_{8,9})}{s_{1,5}} \\
& + 5s_{1,2}+2s_{1,4}+\text{cycl}
\end{aligned}
\tag{4.200}
$$

with one-to-one correspondence with Fig. 4.13

4.7.3 Relative efficiency of Feynman diagrams and Berends-Giele relations

In this appendix we review the solution of several types of recursive relations which count the number of ordered Feynman graphs needed for the semi-on-shell amplitude $J(1,2,\ldots,n)$ in the nonlinear sigma model and related toy models.

Number of the Feynman graphs

Let us start with the case of nonlinear sigma model, i.e. with the case with infinite number of vertices in the interaction Lagrangian. The above recursive relations, which determine the number $f(2n+1)$ of the (flavor ordered) Feynman graphs which contribute to $J(1,2,\ldots,2n+1)$, are tightly related to the Berends-Giele relations (4.57). Indeed, after making the following substitution to (4.57)

$$
J(1,2,\ldots,2n+1) \to f(2n+1), \quad \frac{\mathrm{i}}{p_{2n+2}^2} \to 1, \quad \mathrm{i}V_{2k+1} \to 0, \quad \mathrm{i}V_{2k+2} = 1, \tag{4.201}
$$

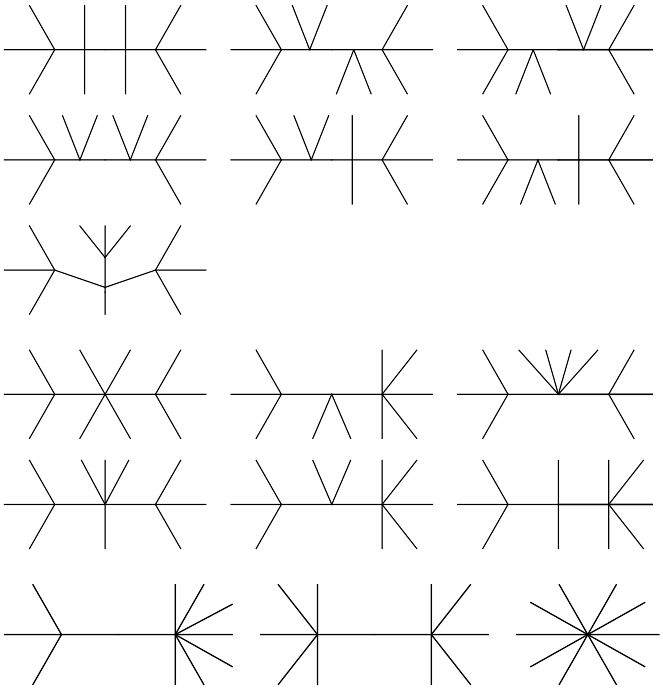

Figure 4.13: Graphical representation of the 10-point amplitude (4.200) with cycling tacitly assumed.

the individual terms on the right hand side just count the number of Feynman graphs generated from these terms by the iterations of the recursive procedure. As a result we get for $f(2n+1)$ the following recursive relation

$$f(2n+1) = \sum_{k=1}^{n} \sum_{\{n_i\}} \prod_{i=1}^{2k+1} f(2n_i+1), \tag{4.202}$$

with the initial condition $f(1) = 1$. In the above formula the sum over $\{n_i\}$ is constrained by the requirement

$$\sum_{i=1}^{2k+1} (2n_i+1) = 2n+1 \Leftrightarrow \sum_{i=1}^{2k+1} n_i = n-k \tag{4.203}$$

i.e. it corresponds to the sum over all possible decompositions of ordered set of $2n+1$ momenta to non-empty clusters with odd number of momenta in each cluster (cf. (4.58) and Fig. 4.3), i.e. more explicitly

$$f(2n+1) = \sum_{k=1}^{n} \sum_{\sum_i n_i = n-k} \prod_{i=1}^{2k+1} f(2n_i+1), \quad f(1) = 1. \tag{4.204}$$

Standard method for solution of this type of recursive relation is based on the generating function defined as

$$A(x) = \sum_{n=0}^{\infty} f(2n+1) x^n. \tag{4.205}$$

The recursive formula (4.204) implies the following equation for $A(x)$

$$A = 1 + \sum_{k=1}^{\infty} x^k A^{2k+1} = 1 + \frac{xA^3}{1 - xA^2} \tag{4.206}$$

or

$$x = \frac{B}{(B+1)^2 (2B+1)} \equiv \frac{B}{g(B)} \tag{4.207}$$

where $B = A-1$ and $g(z) = (z+1)^2(2z+1)$. In this form, the problem is prepared for the application of the Lagrange–Bürmann inversion formula

$$B(x) = \sum_{n=0}^{\infty} \frac{x^n}{n!} \frac{\mathrm{d}^{n-1}}{\mathrm{d}z^{n-1}} g(z)^n|_{z=0} = \sum_{n=1}^{\infty} \frac{x^n}{n!} \frac{\mathrm{d}^{n-1}}{\mathrm{d}z^{n-1}} (z+1)^{2n}(2z+1)^n|_{z=0}. \tag{4.208}$$

After straightforward algebra with help of Leibnitz rule we get for $n \geq 1$

$$f(2n+1) = \frac{2^{n-1}}{n} \sum_{k=0}^{n-1} \left(\begin{array}{c} n \\ k+1 \end{array} \right) \left(\begin{array}{c} 2n \\ k \end{array} \right) 2^{-k} = 2^{n-1}\ {}_2F_1\left(1-n, -2n, 2; \frac{1}{2}\right), \tag{4.209}$$

where ${}_2F_1(\alpha.\beta, \gamma; z)$ is the hypergeometric function. In the same way one can solve the recurrence relations for the number of ordered Feynman graphs for the semi-on-shell amplitudes $J(1, 2, \ldots, n)$ in the cases when only quadrilinear vertices ("ϕ^4 theory"), only trilinear vertices ("ϕ^3 theory") or both trilinear and quadrilinear vertices ("$\phi^3 + \phi^4$ theory") are present in the Lagrangian. In the first case, similarly to the nonlinear sigma model, only $J(1, 2, \ldots, n)$ with n odd can be nonzero, while in the remaining two cases $J(1, 2, \ldots, n)$ both parities of n are generally allowed. Let us denote the number of the Feynman graphs for $J(1, 2, \ldots, n)$ as $f_4(n)$, $f_2(n)$ and $f_{3+4}(n)$ respectively. We get the following recurrence relations

$$f_4(2n+1) = \sum_{n_1+n_2+n_3=n-1,\ n_i \geq 0} f_4(2n_1+1) f_4(2n_2+1) f_4(2n_3+1) \tag{4.210}$$

$$f_3(n) = \sum_{n_1+n_2=n,\ n_i \geq 1} f_3(n_1) f_3(n_2) \tag{4.211}$$

$$f_{3+4}(n) = \sum_{n_1+n_2=n,\ n_i \geq 1} f_{3+4}(n_1) f_{3+4}(n_2) \tag{4.212}$$

$$+ \sum_{n_1+n_2+n_3=n,\ n_i \geq 1} f_{3+4}(n_1) f_{3+4}(n_2) f_{3+4}(n_3) \tag{4.213}$$

with initial conditions $f_j(1) = 1$, $j = 3, 4, 3+4$. The corresponding generating functions

$$A_4(x) = \sum_{n=0}^{\infty} f_4(2n+1) x^n, \quad A_{3,3+4}(x) = \sum_{n=1}^{\infty} f_{3,3+4}(n) x^n \tag{4.214}$$

then satisfy

$$A_4 = 1 + xA_4^3, \quad A_3 = x + A_3^2, \quad A_{3+4} = x + A_{3+4}^2 + A_{3+4}^3. \tag{4.215}$$

n	2	3	4	5	6	7	8	9	10
$f_3(n)$	1	2	5	14	42	132	429	1 430	4 862
$f_{3+4}(n)$	1	3	10	38	154	654	2 871	12 925	59 345
$f_4(2n+1)$	3	12	55	273	1 428	7 752	43 263	246 675	1 430 715
$f(2n+1)$	4	21	126	818	5 594	39 693	289 510	2 157 150	16 348 960

Table 4.2: Number of flavor ordered Feynman graphs for $J(1,\ldots,n)$ and $J(1,\ldots,2n+1)$ in the models of the type ϕ^3, $\phi^3+\phi^4$, ϕ^4 and nonlinear sigma model.

In the second case we get

$$A_3(x) = \frac{1-\sqrt{1-4x}}{2} = \frac{1}{2}\left(1 - \sum_{n=0}^{\infty} \left(\begin{array}{c} 1/2 \\ k \end{array} \right) (-4x)^k \right) \tag{4.216}$$

and therefore

$$f_3(n) = \frac{1}{n} \left(\begin{array}{c} 2(n-1) \\ n-1 \end{array} \right) = C_{n-1} \tag{4.217}$$

where C_n are the Catalan numbers. In the first case, writing

$$x = \frac{A_4 - 1}{A_4^3} = \frac{B_4}{(B_4+1)^3} \tag{4.218}$$

and using the Lagrange–Bürmann inversion formula we get for $n > 0$

$$f_4(2n+1) = \frac{1}{n!} \frac{\mathrm{d}^{n-1}}{\mathrm{d}z^{n-1}} (z+1)^{3n}|_{z=0} = \frac{1}{2n+1} \left(\begin{array}{c} 3n \\ n \end{array} \right). \tag{4.219}$$

In the third case, we get from

$$x = A_{3+4}\left(1 - A_{3+4} - A_3^2\right) \tag{4.220}$$

and using the Lagrange–Bürmann inversion formula

$$f_{3+4}(n) = \frac{1}{n!} \frac{\mathrm{d}^{n-1}}{\mathrm{d}z^{n-1}} \left(\frac{1}{1-z-z^2} \right)^n |_{z=0} = \frac{(-1)^n}{n!} \frac{\mathrm{d}^{n-1}}{\mathrm{d}z^{n-1}} \left(\frac{1}{z_1 - z} \right)^n \left(\frac{1}{z_2 - z} \right)^n |_{z=0} \tag{4.221}$$

(where $z_1 = -\phi$, $z_2 = \phi - 1$ and $\phi = (1+\sqrt{5})/2$ is the Golden ratio) the result

$$\begin{aligned} f_{3+4}(n) &= (-1)^{n+1} \frac{\phi^{1-n}}{n} \sum_{k=0}^{n-1} \left(\begin{array}{c} n-1+k \\ k \end{array} \right) \left(\begin{array}{c} 2(n-1)-k \\ n-1 \end{array} \right) \left(\frac{\phi}{1-\phi} \right)^k \\ &= \left(-\frac{4}{\phi} \right)^{n-1} \Gamma\left(n - \frac{1}{2} \right) \, {}_2F_1\left(1-n, n, 2-2n; \frac{\phi}{1-\phi} \right). \end{aligned} \tag{4.222}$$

The first twelve members of the above sequences are illustrated in the Table 4.2.

Efficiency of the Berends-Giele relations

We can compare this with the number of terms generated by Berends-Giele recursion. For the nonlinear sigma model, the number of terms on the right hand side of (4.57) is just

$$t(2n+1) = \sum_{k=1}^{n} \sum_{\{n_i\}} 1 = \sum_{k=1}^{n} \left(\begin{array}{c} n+k \\ n-k \end{array} \right) = F_{2n+1} - 1 \tag{4.223}$$

where

$$F_n = \frac{1}{\sqrt{5}}\left(\phi^n - (\phi-1)^n\right) \tag{4.224}$$

are the Fibonacci numbers and $\phi = (1+\sqrt{5})/2$ is the Golden ratio. Therefore, using the known results for $J(1,2,\ldots,2m+1)$ with $m<n$ at each step, we need to evaluate altogether

$$b(2n+1) = \sum_{m=1}^{n} t(2m+1) = \frac{1}{\sqrt{5}}\left(\phi^3\frac{\phi^{2n}-1}{\phi^2-1} - (\phi-1)^3\frac{(\phi-1)^{2n}-1}{(\phi-1)^2-1}\right) - n \tag{4.225}$$

terms in order to calculate $J(1,2,\ldots,2n+1)$ using the Berends-Giele recursion. We show the sequences $t(2n+1)$ and $b(2n+1)$ in the first and second row of Tab.1 respectively.

In the same way we can calculate analogous numbers $t_j(n)$ and $b_j(n)$ for $j = 3, 4, 3+4$, i.e. for "ϕ^3 theory" , "ϕ^3 theory" or "$\phi^3+\phi^4$ theory". For instance, for $t_4(2n+1)$ we have (see Tab. 1 for numerical values)

$$t_4(2n+1) = \begin{pmatrix} n+1 \\ 2 \end{pmatrix}, \quad b_4(2n+1) = \sum_{m=1}^{n} t_4(2m+1) = \frac{1}{6}n(n+1)(n+2) \tag{4.226}$$

Note the exponential growth of $t(2n+1)$ and $b(2n+1)$ with increasing n in contrast to the only polynomial growth of $t_4(2n+1)$ and $b_4(2n+1)$.

4.7.4 Other example of scaling properties of the semi-on-shell amplitudes

In this appendix we prove the following scaling limit

$$\lim_{t\to 0} J_{2n+1}(tp_1, p_2, tp_3, p_4, \ldots, tp_{2r-1}, tp_{2r}, tp_{2r+1}, \ldots, p_{2N}, tp_{2n+1}) = 0 \tag{4.227}$$

which is valid for for $n>1$. Let us note, however, that

$$J_3(tp_1, tp_2, tp_3) = J_3(p_1,p_2,p_3) \neq 0. \tag{4.228}$$

On the other hand, for $N=2$ we get by direct calculation

$$\lim_{t\to 0} J_5(tp_1, tp_2, tp_3, p_4, tp_5) = \lim_{t\to 0} J_5(tp_1, p_2, tp_3, tp_4, tp_5) = 0 \tag{4.229}$$

and we can therefore proceed by induction based on Berends-Giele relations almost exactly as in the case of the proof of (4.67). The only modification here is that, along with the "dangerous" contributions without blocks $J(j_k+1,\ldots,j_{k+1})$ where j_k is even and $j_{k+1}-j_k > 1$ attached to the odd line of the vertex V_{m+1}(provided at least one such a block is present, the contribution vanish either by the induction hypothesis or by (4.67)) we have to discuss separately new type of "dangerous" terms with building block $J(p_{2r-1}, p_{2r}, p_{2r+1})$ (this block does not vanish due to (4.228)). The "old" dangerous terms do not in fact contribute as was already discussed within the proof of (4.67). The "new" dangerous terms

have the following general form

$$\frac{\mathrm{i}}{p_{2N+2}^2}\mathrm{i}V_{2k+2}(p_1, p_{2,2j_1}, p_{2j_1+1}, \ldots, p_{2j_l+2,2r-2}, p_{2r-1,2r+1}, p_{2r+2,2j_{l+1}} \cdots$$
$$\ldots, p_{2j_{k-1},2n}, p_{2n+1}, -p_{1,2n+1})$$
$$\times J(p_1)J(2,\ldots,2j_1)J(p_{2j_1+1})\ldots J(2j_l+2,\ldots,2r-2)$$
$$\times J(p_{2r-1},p_{2r},p_{2r+1})J(2r+2,\ldots,2j_{l+1})\cdots J(2j_{k-1},\ldots,2n)J(p_{2n+1}). \quad (4.230)$$

Note that, $p_{2r-1,2r+1}$ is attached to the odd line of the vertex V_{2k+2} and scales as

$$p_{2r-1,2r+1} \to tp_{2r-1,2r+1} \quad (4.231)$$

i.e. in the same way as the remaining momenta attached to the odd lines of the vertex. The vertex being proportional the squared sum of the odd line momenta scales therefore as $O(t^2)$, and the contribution of the "new" dangerous terms vanish. This finishes the proof.

4.7.5 Double soft limit of Goldstone boson amplitudes

In this appendix we will discuss the properties of the on-shell scattering amplitudes of the Goldstone bosons, which are dictated by the symmetry, namely the limits of the amplitudes for soft external momenta. Some of these properties have been obtained in the special case of pions by PCAC methods in the late sixties (see e.g. [141]). Here we enlarge and reformulate them in a more general form appropriate for our purposes with stress on the proof of the double soft limit discussed recently for pions and $\mathcal{N}=8$ supergravity in [143].

Let us assume a general theory with spontaneous symmetry breaking according to the pattern $G \to H$ where the homogeneous space G/H is a symmetric space, i.e. the vacuum little group H is the maximal subgroup invariant with respect to some involutive automorphism of G ("parity"). This implies the following structure of the Lie algebra of G

$$\begin{aligned}[T^a, T^b] &= \mathrm{i}f_T^{abc}T^c \\ [T^a, X^b] &= \mathrm{i}f_X^{abc}X^c \\ [X^a, X^b] &= \mathrm{i}F^{abc}T^c. \end{aligned} \quad (4.232)$$

Here T^a and X^a are the unbroken and broken generators respectively and f_T^{abc}, f_X^{abc} and F^{abc} are the structure constants. The chiral nonlinear sigma model is a special case for which $f_T^{abc} = f_X^{abc} = F^{abc} = f^{abc}$.

The invariance of the theory with respect to the group G can be expressed in terms of the Ward identities for the correlators in the general form

$$\mathrm{i}p^\mu\langle\widetilde{V}_\mu^a(p)\widetilde{O}_1(p_1)\ldots\widetilde{O}_n(p_n)\rangle = -\sum_{i=1}^n \mathrm{i}\langle\widetilde{O}_1(p_1)\ldots\delta_T^a\widetilde{O}_i(p_i+p)\ldots\widetilde{O}_n(p_n)\rangle \quad (4.233)$$

$$\mathrm{i}p^\mu\langle\widetilde{A}_\mu^a(p)\widetilde{O}_1(p_1)\ldots\widetilde{O}_n(p_n)\rangle = -\sum_{i=1}^n \mathrm{i}\langle\widetilde{O}_1(p_1)\ldots\delta_X^a\widetilde{O}_i(p_i+p)\ldots\widetilde{O}_n(p_n)\rangle. \quad (4.234)$$

Here $V^a_\mu(x)$ and $A^a_\mu(x)$ are the Noether currents corresponding to the generators T^a and X^a respectively (in analogy with the chiral theories we will call them *vector* and *axial* currents in what follows and to the Ward identities (4.233) and (4.234) we will refer to the *vector* and *axial* WI) , $O_i(x)$ are (generally composite) local operators, $\delta^a_T O_i(x)$ and $\delta^a_X O_i(x)$ are their infinitesimal transforms with respect to the generators T^a and X^a . The tilde means the Fourier transform

$$\widetilde{O}_i(p) = \int \mathrm{d}^4x e^{\mathrm{i}p\cdot x} O_i(x). \tag{4.235}$$

According to the Goldstone theorem the spectrum of the theory contains as many Goldstone bosons π^a as the broken generators X^a for which the currents $A^a_\mu(x)$ play the role of the interpolating fields, i.e.

$$\langle 0|A^a_\mu(0)|\pi^b(p)\rangle = \mathrm{i}p_\mu F\delta^{ab}. \tag{4.236}$$

where F is the Goldstone boson decay constant. Let as denote $M^{a_1\dots a_n}(p_1,\dots,p_n)$ the on-shell scattering amplitude of the Goldstone bosons $\pi^{a_1}(p_1),\dots,\pi^{a_n}(p_n)$. In what follows we will concentrate on the properties of $M^{a_1\dots a_n}(p_1,\dots,p_n)$ dictated by the symmetry, i.e. those which are encoded in the WI (4.233) and (4.234).

Vector WI and symmetry with respect to H

The invariance with respect to the unbroken subgroup H implies

$$\sum_{i=1}^n f^{aa_ib}_X M^{a_1\dots a_{i-1}ba_{i+1}\dots a_n}(p_1,\dots,p_n) = 0. \tag{4.237}$$

This can be understood as the consequence of the vector WI of the form

$$-\mathrm{i}p^\mu\langle\widetilde{V}^a_\mu(p)\widetilde{A}^{a_1}_{\mu_1}(p_1)\dots\widetilde{A}^{a_n}_{\mu_n}(p_n)\rangle = -\sum_{i=1}^n \mathrm{i}\langle\widetilde{A}^{a_1}_{\mu_1}(p_1)\dots\delta^a_T\widetilde{A}^{a_i}_{\mu_i}(p+p_i)\dots\widetilde{A}^{a_n}_{\mu_n}(p_n)\rangle \tag{4.238}$$

Note that the infinitesimal transformations $\delta^a V^b_\nu$ and $\delta^a A^b_\nu$ of these currents with respect to the generator T^a of the unbroken subgroup H are as follows

$$\delta^a_T A^b_\nu = -f^{abc}_X A^c_\nu \tag{4.239}$$

$$\delta^a_T V^b_\nu = -f^{abc}_T V^c_\nu. \tag{4.240}$$

Because there is no pole for $p\to 0$ in the correlator on the left hand side of (4.238), we get in this limit

$$\sum_{i=1}^n f^{aa_ib}\langle\widetilde{A}^{a_1}_{\mu_1}(p_1)\dots\widetilde{A}^{b}_{\mu_i}(p_i)\dots\widetilde{A}^{a_n}_{\mu_n}(p_n)\rangle = 0. \tag{4.241}$$

Using the LSZ formula we get according to (4.236)

$$\langle\widetilde{A}^{a_1}_{\mu_1}(p_1)\dots\widetilde{A}^{a_n}_{\mu_n}(p_n)\rangle = \left(\prod_{i=1}^n \frac{\mathrm{i}}{p_i^2}Z_{\mu_i}\right) M^{a_1\dots a_n}(p_1,\dots,p_n) + R^{a_1\dots}_{\mu_1\dots} \tag{4.242}$$

where $Z_{\mu_i} = \mathrm{i}Fp_{i\mu_i}$ and the remnant $R^{a_1\dots}_{\mu_1\dots}$ is regular on shell in the sense that

$$\lim_{p_i^2\to 0}\left(\prod_{i=1}^n p_i^2\right) R^{a_1\dots}_{\mu_1\dots} = 0. \tag{4.243}$$

which implies (4.237) for the on-shell amplitude $M^{a_1\dots a_n}(p_1,\dots,p_n)$.

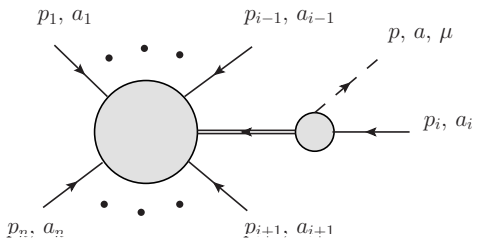

Figure 4.14: Graphical representation of the singular contributions to the matrix element (4.244).

Soft vector current singularity

Let us assume now the following matrix element

$$\langle \widetilde{V}^a_\mu(p)|\pi^{a_1}(p_1)\dots\pi^{a_i}(p_i)\dots\pi^{a_n}(p_n)\rangle. \tag{4.244}$$

In what follows we will discuss the behavior of this object in the limit $p \to 0$. On the level of the Feynman graphs, the only singularities in the soft limit $p \to 0$ are those which stem from the one-Goldstone-boson-reducible graphs for which the vector current $\widetilde{V}^a_\mu(p)$ is attached to the external Goldstone boson line. The potential singularities are therefore of the form (see Fig. 4.14)

$$\langle \widetilde{V}^a_\mu(p)\phi^{a_j}(0)|\pi^{a_i}(p_1)\rangle_{1PI}\mathrm{i}\Delta^{a_j a_k}((p-p_i)^2)\langle\phi^{a_k}(0)|\pi^{a_1}(p_1)\dots\widehat{\pi^{a_i}(p_i)}\dots\pi^{a_n}(p_n)\rangle_{1PI} \tag{4.245}$$

where the subscript $1PI$ means one-Goldstone-boson-irreducible block, the hat means omitting of the corresponding particle, $\phi^a(x)$ is the Goldstone boson interpolating field normalized as

$$\langle 0|\phi^a(0)|\pi^b(p)\rangle = \delta^{ab} \tag{4.246}$$

and $\Delta^{a_j a_k}(q^2)$ is a Goldstone boson propagator. For $q^2 \to 0$ we have

$$\Delta^{a_j a_k}(q^2) = \frac{\delta^{a_j a_k}}{q^2}\left(1 + O(q^2)\right). \tag{4.247}$$

As a consequence of the Lorentz invariance, invariance with respect to H and LSZ formulae we have

$$\langle \widetilde{V}^a_\mu(p)\phi^{a_j}(0)|\pi^{a_i}(p_i)\rangle_{1PI} = \mathrm{i}f_X^{aa_ia_j}F_V(p^2)(2p_i-p)_\mu + O((p-p_i)^2) \tag{4.248}$$

where $F_V(p^2)$ is the on-shell vector form-factor defined as[18]

$$\langle \pi^{a_j}(p-p_i)|\widetilde{V}^a_\mu(p)|\pi^{a_i}(p_i)\rangle = \mathrm{i}f_X^{aa_ia_j}F_V(p^2)(2p_i-p)_\mu. \tag{4.249}$$

We can fix the normalization of the vector currents V^a_μ in such a way that

$$F_V(p^2) = 1 + O(p^2). \tag{4.250}$$

[18]The form of the right hand side is dictated by H-invariance, Bose and crossing symmetry.

Analogously we have

$$\langle\phi^{a_k}(0)|\pi^{a_1}(p_1)\dots\widehat{\pi^{a_i}(p_i)}\dots\pi^{a_n}(p_n)\rangle_{1PI} = M^{a_1\dots a_{i-1}a_k a_{i+1}\dots a_n}(p_1,\dots,p_n)+O((p-p_i)^2). \tag{4.251}$$

Using $(p-p_i)^2 = -2(p\cdot p_i)+p^2$ and putting all the ingredients together we get for $p\to 0$

$$\begin{aligned}&\langle\widetilde{V}^a_\mu(p)|\pi^{a_1}(p_1)\dots\pi^{a_i}(p_i)\dots\pi^{a_n}(p_n)\rangle\\ &\quad=\sum_{i=1}^n f^{aa_id}_X\frac{(2p_i-p)_\mu}{2(p\cdot p_i)}M^{a_1\dots a_{i-1}da_{i+1}\dots a_n}(p_1,\dots,p_n)+O(1)\end{aligned} \tag{4.252}$$

Axial WI and Adler zero

To illustrate the method which we will use in the next subsection, let us briefly recapitulate the textbook example of the derivation of the Adler zero for the amplitude $M^{a_1\dots a_n}(p_1,\dots,p_n)$ (see e.g. [144]). Let us start with the axial WI in the form

$$-\mathrm{i}p^\mu\langle\widetilde{A}^a_\mu(p)\widetilde{A}^{a_1}_{\mu_1}(p_1)\dots\widetilde{A}^{a_n}_{\mu_n}(p_n)\rangle = -\sum_{i=1}^n\mathrm{i}\langle\widetilde{A}^{a_1}_{\mu_1}(p_1)\dots\delta^a_X\widetilde{A}^{a_i}_{\mu_i}(p+p_i)\dots\widetilde{A}^{a_n}_{\mu_n}(p_n)\rangle \tag{4.253}$$

where now

$$\begin{aligned}\delta^a_X A^b_\nu &= -F^{abc}V^c_\nu\\ \delta^a_X V^b_\nu &= -f^{abc}_X A^c_\nu.\end{aligned} \tag{4.254}$$

Applying on both sides of (4.253) the LSZ reduction to all but one axial currents, we get the conservation of the axial current in terms of the transversality of the matrix element of A^a_μ between the initial and final states $|i\rangle$ and $\langle f|$

$$-\mathrm{i}p^\mu\langle f|\widetilde{A}^a_\mu(p)|i\rangle = 0. \tag{4.255}$$

On the other hand from (4.242) we get the Goldstone boson pole dominance for $p^2\to 0$

$$-\mathrm{i}p^\mu\langle f|\widetilde{A}^a_\mu(p)|i\rangle = \frac{1}{p^2}p^\mu Z_\mu\langle f+\pi^a(p)|i\rangle - \mathrm{i}p^\mu R^a_{\mu,fi} \tag{4.256}$$

where $Z_\mu = \mathrm{i}Fp_\mu$ and the remnant $R^a_{\mu,fi}$ is regular in this limit

$$\lim_{p^2\to 0}p^2R^a_{\mu,fi} = 0. \tag{4.257}$$

Putting (4.255) and (4.256) together we get for the amplitude with emition of the Goldstone boson $\pi^a(p)$ in the final state

$$\langle f+\pi^a(p)|i\rangle = \frac{1}{F}p^\mu R^a_{\mu,fi}. \tag{4.258}$$

Provided the following stronger regularity condition holds

$$\lim_{p\to 0}p^\mu R^a_{\mu,fi} = 0, \tag{4.259}$$

we get

$$\langle f + \pi^a(0)|i\rangle = 0, \tag{4.260}$$

i.e. the Adler zero for $p \to 0$.

An useful off-shell generalization of the formula (4.256) reads

$$-\mathrm{i}p^\mu\langle\widetilde{A}^a_\mu(p)\widetilde{A}^{a_1}_{\mu_1}(p_1)\dots\widetilde{A}^{a_n}_{\mu_n}(p_n)\rangle = \mathrm{i}F\langle\pi^a(p)|\widetilde{A}^{a_1}_{\mu_1}(p_1)\dots\widetilde{A}^{a_n}_{\mu_n}(p_n)\rangle - \mathrm{i}p^\mu R^{a,a_1\dots}_{\mu,\mu_1\dots} \tag{4.261}$$

where

$$\lim_{p^2\to 0} p^2 R^{a,a_1\dots}_{\mu,\mu_1\dots} = 0. \tag{4.262}$$

and using the Ward identity (4.253) and (4.254) we get

$$\begin{aligned} & F\langle\pi^a(p)|\widetilde{A}^{a_1}_{\mu_1}(p_1)\dots\widetilde{A}^{a_n}_{\mu_n}(p_n)\rangle \\ = \;& p^\mu R^{a,a_1\dots}_{\mu,\mu_1\dots} + \sum_{i=1}^n F^{aa_ic}\langle\widetilde{A}^{a_1}_{\mu_1}(p_1)\dots\widetilde{V}^c_{\mu_i}(p+p_i)\dots\widetilde{A}^{a_n}_{\mu_n}(p_n)\rangle. \end{aligned} \tag{4.263}$$

Double soft limit

Our starting point is the axial WI (4.253) rewritten in the form

$$\begin{aligned} -\mathrm{i}p^\mu\langle\widetilde{A}^a_\mu(p)\widetilde{A}^b_\nu(q)\widetilde{A}^{a_1}_{\mu_1}(p_1)\dots\widetilde{A}^{a_n}_{\mu_n}(p_n)\rangle \;=\; & -\mathrm{i}\langle\delta^a_X\widetilde{A}^b_\nu(p+q)\widetilde{A}^{a_1}_{\mu_1}(p_1)\dots\widetilde{A}^{a_n}_{\mu_n}(p_n)\rangle \\ & -\sum_{i=1}^n \mathrm{i}\langle\widetilde{A}^b_\nu(q)\widetilde{A}^{a_1}_{\mu_1}(p_1)\dots\delta^a_X\widetilde{A}^{a_i}_{\mu_i}(p+p_i)\dots\widetilde{A}^{a_n}_{\mu_n}(p_n)\rangle \end{aligned} \tag{4.264}$$

Multiplying then both sides by $-\mathrm{i}q^\nu$ and using the axial WI (4.253) once again we get

$$\begin{aligned} & -p^\mu q^\nu\langle\widetilde{A}^a_\mu(p)\widetilde{A}^b_\nu(q)\widetilde{A}^{a_1}_{\mu_1}(p_1)\dots\widetilde{A}^{a_n}_{\mu_n}(p_n)\rangle \\ = \;& q^\nu F^{abc}\langle\widetilde{V}^c_\nu(p+q)\widetilde{A}^{a_1}_{\mu_1}(p_1)\dots\widetilde{A}^{a_n}_{\mu_n}(p_n)\rangle \\ + \;& \sum_{i\neq j;i,j=1}^n F^{aa_jc}F^{ba_id}\langle\widetilde{A}^{a_1}_{\mu_1}(p_1)\dots\widetilde{V}^d_{\mu_i}(p_i+q)\dots\widetilde{V}^c_{\mu_j}(p+p_j)\dots\widetilde{A}^{a_n}_{\mu_n}(p_n)\rangle \\ & + \sum_{i=1}^n F^{aa_ic}f^{bcd}_X\langle\widetilde{A}^{a_1}_{\mu_1}(p_1)\dots\widetilde{A}^d_{\mu_i}(p+q+p_i)\dots\widetilde{A}^{a_n}_{\mu_n}(p_n)\rangle. \end{aligned} \tag{4.265}$$

The left hand side of (4.265) is symmetric with respect to the interchange of $(p,a) \leftrightarrow (q,b)$; its right hand side can be therefore rewritten in the manifestly symmetric form

$$\begin{aligned} & -p^\mu q^\nu\langle\widetilde{A}^a_\mu(p)\widetilde{A}^b_\nu(q)\widetilde{A}^{a_1}_{\mu_1}(p_1)\dots\widetilde{A}^{a_n}_{\mu_n}(p_n)\rangle \\ = \;& -\frac{1}{2}(p-q)^\nu F^{abc}\langle\widetilde{V}^c_\nu(p+q)\widetilde{A}^{a_1}_{\mu_1}(p_1)\dots\widetilde{A}^{a_n}_{\mu_n}(p_n)\rangle \\ + \;& \sum_{i\neq j;i,j=1}^n F^{aa_jc}F^{ba_id}\langle\widetilde{A}^{a_1}_{\mu_1}(p_1)\dots\widetilde{V}^d_{\mu_i}(p_i+q)\dots\widetilde{V}^c_{\mu_j}(p+p_j)\dots\widetilde{A}^{a_n}_{\mu_n}(p_n)\rangle \\ & + \frac{1}{2}\sum_{i=1}^n \left(F^{aa_ic}f^{bcd}_X + F^{ba_ic}f^{acd}_X\right)\langle\widetilde{A}^{a_1}_{\mu_1}(p_1)\dots\widetilde{A}^d_{\mu_i}(p+q+p_i)\dots\widetilde{A}^{a_n}_{\mu_n}(p_n)\rangle. \end{aligned} \tag{4.266}$$

On the other hand, the LSZ formula gives for $p^2, q^2 \to 0$

$$\langle \widetilde{A}^a_\mu(p)\widetilde{A}^b_\nu(q)\widetilde{A}^{a_1}_{\mu_1}(p_1)\dots\widetilde{A}^{a_n}_{\mu_n}(p_n)\rangle = \sum_{c,d}\frac{\mathrm{i}}{p^2}\langle 0|A^a_\mu|\pi^c(p)\rangle\frac{\mathrm{i}}{q^2}\langle 0|A^b_\nu|\pi^d(q)\rangle \times \langle \pi^c(p)\pi^d(q)|\widetilde{A}^{a_1}_{\mu_1}(p_1)\dots\widetilde{A}^{a_n}_{\mu_n}(p_n)\rangle + R^{ab,\dots}_{\mu\nu} \tag{4.267}$$

where the regular remnant satisfies

$$\lim_{p^2,q^2\to 0} p^2q^2R^{ab,\dots}_{\mu\nu} = 0. \tag{4.268}$$

Therefore, using (4.236) we get

$$\begin{aligned} & -p^\mu q^\nu\langle \widetilde{A}^a_\mu(p)\widetilde{A}^b_\nu(q)\widetilde{A}^{a_1}_{\mu_1}(p_1)\dots\widetilde{A}^{a_n}_{\mu_n}(p_n)\rangle \\ = \;& F^2\langle \pi^a(p)\pi^b(q)|\widetilde{A}^{a_1}_{\mu_1}(p_1)\dots\widetilde{A}^{a_n}_{\mu_n}(p_n)\rangle - p^\mu q^\nu R^{ab,\dots}_{\mu\nu} \end{aligned} \tag{4.269}$$

On the other hand applying the LSZ reduction to (4.265, 4.266) (let us note that only the first terms on the right hand side has the appropriate poles at $p^2, q^2 \to 0$) we get

$$\begin{aligned} & p^\mu q^\nu\langle \widetilde{A}^a_\mu(p)\widetilde{A}^b_\nu(q)|\pi^{a_1}(p_1)\dots\pi^d(p_i)\dots\pi^{a_n}(p_n)\rangle \\ = \;& q^\nu F^{abc}\langle \widetilde{V}^c_\nu(p+q)|\pi^{a_1}(p_1)\dots\pi^d(p_i)\dots\pi^{a_n}(p_n)\rangle \\ = \;& p^\mu F^{bac}\langle \widetilde{V}^c_\mu(p+q)|\pi^{a_1}(p_1)\dots\pi^d(p_i)\dots\pi^{a_n}(p_n)\rangle \\ = \;& -\frac{1}{2}F^{abc}(p-q)^\mu\langle \widetilde{V}^c_\mu(p+q)|\pi^{a_1}(p_1)\dots\pi^d(p_i)\dots\pi^{a_n}(p_n)\rangle \end{aligned} \tag{4.270}$$

and as a consequence of LSZ reduction of (4.269)

$$\begin{aligned} & F^2\langle \pi^a(p)\pi^b(q)|\pi^{a_1}(p_1)\dots\pi^{a_i}(p_i)\dots\pi^{a_n}(p_n)\rangle \\ & = -\frac{1}{2}F^{abc}(p-q)^\mu\langle \widetilde{V}^c_\mu(p+q)|\pi^{a_1}(p_1)\dots\pi^d(p_i)\dots\pi^{a_n}(p_n)\rangle + p^\mu q^\nu R^{ab,\dots}_{\mu\nu}|_{LSZ}. \end{aligned} \tag{4.271}$$

According to (4.252) we have for $p, q \to 0$

$$\begin{aligned} & -\frac{1}{2}F^{abc}(p-q)^\mu\langle \widetilde{V}^c_\mu(p+q)|\pi^{a_1}(p_1)\dots\pi^d(p_i)\dots\pi^{a_n}(p_n)\rangle \\ = \;& -\frac{1}{2}\sum_{i=1}^n F^{abc}f^{ca_id}_X\frac{(2p_i-p-q)\cdot(p-q)}{2((p+q)\cdot p_i)}\langle \pi^{a_1}(p_1)\dots\pi^d(p_i)\dots\pi^{a_n}(p_n)\rangle + O(p-q) \\ = \;& -\frac{1}{2}\sum_{i=1}^n F^{abc}f^{ca_id}_X\frac{p_i\cdot(p-q)}{p_i\cdot(p+q)}\langle \pi^{a_1}(p_1)\dots\pi^d(p_i)\dots\pi^{a_n}(p_n)\rangle \\ & +O\left(p-q, \frac{p^2-q^2}{p_i\cdot(p+q)}\right) \end{aligned} \tag{4.272}$$

For $p^2 = q^2 = 0$ we finally get

$$\begin{aligned} & F_0^2\langle \pi^a(p)\pi^b(q)|\pi^{a_1}(p_1)\dots\pi^{a_i}(p_i)\dots\pi^{a_n}(p_n)\rangle \\ = \;& -\frac{1}{2}\sum_{i=1}^n F^{abc}f^{ca_id}_X\frac{p_i\cdot(p-q)}{p_i\cdot(p+q)}\langle \pi^{a_1}(p_1)\dots\pi^d(p_i)\dots\pi^{a_n}(p_n)\rangle \\ & +p^\mu q^\nu R^{ab,\dots}_{\mu\nu}|_{LSZ} + O\left(p-q\right). \end{aligned} \tag{4.273}$$

Provided condition stronger than (4.268) holds, namely $\lim_{p,q\to 0} p^\mu q^\nu R_{\mu\nu}^{ab,\cdots}|_{LSZ} = 0$ (cf. (4.259)), we get as a result

$$\begin{aligned} & \lim_{t\to 0} F_0^2 \langle \pi^a(tp)\pi^b(tq)|\pi^{a_1}(p_1)\dots\pi^{a_i}(p_i)\dots\pi^{a_n}(p_n)\rangle \\ = \; & -\frac{1}{2}\sum_{i=1}^{n} F^{abc} f_X^{ca_id} \frac{p_i\cdot(p-q)}{p_i\cdot(p+q)} \langle \pi^{a_1}(p_1)\dots\pi^d(p_i)\dots\pi^{a_n}(p_n)\rangle. \end{aligned} \quad (4.274)$$

For the chiral nonlinear sigma model corresponding to the symmetry breaking $G\times G\to G$, we have $F^{abc} = f_X^{abc} = f_T^{abc}$ and we get the formula (4.112) as a special case.

Conclusion

Quantum Chromodynamics is a theory that accurately describes the sector of strong interactions of the Standard model. However, it is a strongly coupled theory and the fundamental degrees of freedom – quarks and gluons are not physical degrees of freedom at low energies. We are forced to use the effective field theory approach to be able to do any calculations.

In this thesis we studied different aspects of effective field theories for QCD. In first two chapters we worked in the context of the effective field theory for resonances. In the first chapter we calculated the SS-PP correlator at one-loop and matched the result with low energy expansion in Chiral perturbation theory and high energy OPE and obtained both the resonance saturation of low energy constants as well as non-trivial constraints between resonance couplings. In the second chapter we focused on more conceptual problem of one loop renormalization and dynamical generation of new degrees of freedom that do not propagate at tree-level. We showed that this indeed can happen even inside the resonance region. In the last chapter we studied the tree-level amplitudes in the non-linear sigma model which serves as a leading order low energy effective field theory for QCD. Inspired by BCFW recursion relations in Yang-Mills theory we constructed the recursion relations for all tree-level amplitudes using the non-trivial behavior of amplitudes under certain shifts. This provides further insight on the well known theory.

Bibliography

[1] S. Weinberg, Physica A **96** (1979) 327.

[2] J. Gasser and H. Leutwyler, Annals Phys. **158** (1984) 142.

[3] J. Gasser and H. Leutwyler, Nucl. Phys. B **250** (1985) 465.

[4] J. Bijnens, G. Colangelo and G. Ecker, Annals Phys. **280** (2000) 100-139 [arXiv:hep-ph/9907333]; JHEP **9902** (1999) 020 [arXiv:hep-ph/9902437].

[5] G. Amorós, J. Bijnens and P. Talavera, Nucl. Phys. B **568** (2000) 319-363 [arXiv:hep-ph/9907264].

[6] G. Amorós, J. Bijnens and P. Talavera, Nucl. Phys. B **602** (2001) 87 [arXiv:hep-ph/0101127].

[7] J. Bijnens and I. Jemos, [arXiv:0909.4477 [hep-ph]].

[8] G. Ecker, J. Gasser, A. Pich and E. de Rafael, Nucl. Phys. B **321** (1989) 311.

[9] G. Ecker, J. Gasser, H. Leutwyler, A. Pich and E. de Rafael, Phys. Lett. B **223** (1989) 425.

[10] G. 't Hooft, Nucl. Phys. B **72** (1974) 461; **75** (1974) 461; E. Witten, Nucl. Phys. B **160** (1979) 57.

[11] K. Kampf, J. Novotny and J. Trnka, Eur. Phys. J. C **50** (2007) 385 [arXiv:hep-ph/0608051].

[12] K. Kampf, J. Novotný and J. Trnka, Acta Phys. Polon. B **38** (2007) 2961-2966 [arXiv:hep-ph/0701041].

[13] J. Bijnens and E. Pallante, Mod. Phys. Lett. A **11** (1996) 1069-1080 [arXiv:hep-ph/9510338].

[14] P. D. Ruiz-Femenia, A. Pich and J. Portoles, JHEP **0307** (2003) 003 [arXiv:hep-ph/0306157].

[15] V. Cirigliano, G. Ecker, M. Eidemuller, R. Kaiser, A. Pich and J. Portolés, Nucl. Phys. B **753** (2006) 139-177 [arXiv:hep-ph/0603205].

[16] V. Cirigliano, G. Ecker, M. Eidemüller, R. Kaiser, A. Pich and J. Portolés, JHEP **0504** (2005) 006 [arXiv:hep-ph/0503108].

[17] V. Cirigliano, G. Ecker, M. Eidemuller, J. Portoles and A. Pich, Phys. Lett. B **596** (2004) 96 [arXiv:hep-ph/0404004].

[18] B. Moussallam, Phys. Rev. D **51** (1995) 4939-4949 [arXiv:hep-ph/9407402]; Nucl. Phys. B **504** (1997) 381 [arXiv:hep-ph/9701400]; JHEP bf 0008 (2000) 005 [arXiv:hep-ph/0005245]; B. Ananthanarayan and B. Moussallam, JHEP **0406** (2004) 047 [arXiv:hep-ph/0405206].

[19] J. Bijnens, E. Gamiz, E. Lipartia and J. Prades, JHEP **0304** (2003) 055 [arXiv:hep-ph/0304222].

[20] M. Knecht and A. Nyffeler, Eur. Phys. J. C **21** (2001) 659-678 [arXiv:hep-ph/0106034].

[21] K. Kampf and B. Moussallam, Eur. Phys. J. C **47** (2006) 723-736 [arXiv:hep-ph/0604125].

[22] P. Roig, [arXiv:0709.3734 [hep-ph]]; D. Gómez-Dumm, P. Roig, A. Pich and J. Portolés, [arXiv:0911.2640 [hep-ph]].

[23] S. Ivashyn and A.Yu. Korchin, Eur. Phys. J. C **54** (2008) 89-106 [arXiv:0707.2700 [hep-ph]].

[24] S. Ivashyn and A.Yu. Korchin, [arXiv:0904.4823 [hep-ph]].

[25] Z. H. Guo, J. J. Sanz-Cillero and H. Q. Zheng, Phys. Lett. B **661** (2008) 342-347 [arXiv:0710.2163 [hep-ph]].

[26] M. Jamin, J.A. Oller and A. Pich, Nucl. Phys. B bf 587 (2000) 331-362 [arXiv:hep-ph/0006045].

[27] Pere Masjuan, [arXiv:0910.0140 [hep-ph]].

[28] Z.-H. Guo and J.J. Sanz-Cillero, Phys. Rev. D **79** (2009) 096006 [arXiv:0903.0782 [hep-ph]].

[29] O. Cata and S. Peris, Phys. Rev. D **65** (2002) 056014 [arXiv:hep-ph/0107062].

[30] I. Rosell, J. J. Sanz-Cillero and A. Pich, JHEP **0408** (2004) 042 [arXiv:hep-ph/0407240].

[31] I. Rosell, J. J. Sanz-Cillero and A. Pich, JHEP **0701** (2007) 039 [arXiv:hep-ph/0610290].

[32] A. Pich, I. Rosell and J. J. Sanz-Cillero, JHEP **0807** (2008) 042 [arXiv:0803.1567 [hep-ph]].

[33] I. Rosell, P. Ruiz-Femenía and J. Portolés, JHEP **0512** (2005) 020 [arXiv:hep-ph/0510041].

[34] J.J. Sanz-Cillero, Phys. Lett. B **649** (2007) 180-185 [arXiv:hep-ph/0702217].

[35] L.Y. Xiao and J.J. Sanz-Cillero, Phys. Lett. B **659** (2008) 452-456 [arXiv:0705.3899 [hep-ph]]; J. J. Sanz-Cillero [arXiv:0709.3363].

[36] K. Kampf, J. Novotny and J. Trnka, Fizika B **17** (2008) 2, 349 - 354 [arXiv:0803.1731 [hep-ph]].

[37] K. Kampf, J. Novotny and J. Trnka, Nucl. Phys. Proc. Suppl. **186** (2009) 153-156 [arXiv:0810.3842 [hep-ph]].

[38] J.J. Sanz-Cillero, Phys. Lett. B **681** (2009) 100-104 [arXiv:0905.3676 [hep-ph]].

[39] A. Pich, [arXiv:0812.2631 [hep-ph]], and references therein.

[40] M. Golterman and S. Peris, Phys. Rev. D **74** (2006) 096002 [arXiv:hep-ph/0607152].

[41] M.A. Shifman, A.I. Vainshtein and V.I. Zakharov, Nucl. Phys. B **147** (1979) 385-447; **147** (1979) 448-518.

[42] S. Weinberg, Phys. Rev. Lett. **18** (1967) 507.

[43] P. Masjuan and S. Peris, JHEP **0705** (2007) 040 [arXiv:0704.1247 [hep-ph]].

[44] M. Knecht and E. de Rafael, Phys. Lett. B **424** (1998) 335-342 [arXiv:hep-ph/9712457]; S. Peris, M. Perrottet and E. de Rafael, JHEP **9805** (1998) 011 [arXiv:hep-ph/9805442].

[45] K. Kampf, J. Novotny and J. Trnka, Fizika B **17** (2008) 349; Nucl. Phys. Proc. Suppl. **186** (2009) 153; arXiv:0905.1348 [hep-ph]; in preparation.

[46] I. Rosell, Ph.D.Thesis (U. Valencia, 2007) [arXiv:hep-ph/0701248];

[47] I. Rosell, P. Ruiz-Femenía and J.J. Sanz-Cillero, Phys. Rev. D **79** (2009) 076009 [arXiv:0903.2440 [hep-ph]]; J. Portolés, I. Rosell and Pedro Ruiz-Femenia, Phys. Rev. D **75** (2007) 114011 [arXiv:hep-ph/0611375].

[48] J.J. Sanz-Cillero, Ph.D. Thesis (U. Valencia, 2004).

[49] M. F. L. Golterman and S. Peris, Phys. Rev. D **61** (2000) 034018 [arXiv:hep-ph/9908252].

[50] H. Leutwyler, Nucl. Phys. Proc. Suppl. **64** (1998) 223-231 [arXiv:hep-ph/9709408]; R. Kaiser and H. Leutwyler, Eur. Phys. J. C **17** (2000) 623-649 [arXiv:hep-ph/0007101]; [arXiv:hep-ph/9806336].

[51] C. Amsler et al. (Particle Data Group), Phys. Lett. B 667 (2008) 1 (2008) and 2009 partial update for the 2010 edition, http://pdglive.lbl.gov .

[52] S.-Z. Jiang, Y. Zhang, C. Li and Q. Wang, [arXiv:0907.5229 [hep-ph]].

[53] A. Bazavov *et al.* (MILC Collaboration), [arXiv:0910.3618 [hep-lat]].

[54] J. Bijnens, Prog. Part. Nucl. Phys. **58** (2007) 521 [arXiv:hep-ph/0604043].

[55] S. R. Coleman, J. Wess and B. Zumino, Phys. Rev. **177** (1969) 2239.

[56] C. G. . Callan, S. R. Coleman, J. Wess and B. Zumino, Phys. Rev. **177**, 2247 (1969).

[57] V. Cirigliano, G. Ecker, M. Eidemuller, R. Kaiser, A. Pich and J. Portoles, Nucl. Phys. B **753** (2006) 139 [arXiv:hep-ph/0603205].

[58] K. Kampf and B. Moussallam, Eur. Phys. J. C **47** (2006) 723 [arXiv:hep-ph/0604125].

[59] P. C. Bruns and U. G. Meißner, Eur. Phys. J. C **40** (2005) 97 [arXiv:hep-ph/0411223].

[60] K. Kampf, J. Novotny and J. Trnka, Eur. Phys. J. C **50**, 385 (2007)

[61] J. Gasser, M. E. Sainio and A. Svarc, Nucl. Phys. B **307** (1988) 779.

[62] I. Rosell, J. J. Sanz-Cillero and A. Pich, JHEP **0408**, 042 (2004).

[63] I. Rosell, J. J. Sanz-Cillero and A. Pich, JHEP **0701** (2007) 039

[64] J. J. Sanz-Cillero and J. Trnka, [arXiv:0912.0495 [hep-ph]]

[65] A. Pich, I. Rosell and J. J. Sanz-Cillero, JHEP **0807** (2008) 014

[66] J. J. Sanz-Cillero, Phys. Lett. B **681** (2009) 100 [arXiv:0905.3676 [hep-ph]].

[67] I. Rosell, P. Ruiz-Femenia and J. J. Sanz-Cillero, Phys. Rev. D **79** (2009) 076009 [arXiv:0903.2440 [hep-ph]].

[68] J. J. Sanz-Cillero, Phys. Lett. B **649** (2007) 180 [arXiv:hep-ph/0702217].

[69] J. J. Sanz-Cillero and J. Trnka, arXiv:0912.0495 [hep-ph].

[70] I. Rosell, P. Ruiz-Femenia and J. Portoles, JHEP **0512** (2005) 020 [arXiv:hep-ph/0510041].

[71] K. Kampf, J. Novotny and J. Trnka, FIZIKA B **17** (2008) 2, 349 - 354 [arXiv:0803.1731 [hep-ph]].

[72] K. Kampf, J. Novotny and J. Trnka, Nucl. Phys. Proc. Suppl. **186** (2009) 153 [arXiv:0810.3842 [hep-ph]].

[73] V. Pascalutsa, M. Vanderhaeghen and S. N. Yang, Phys. Rept. **437** (2007) 125 [arXiv:hep-ph/0609004].

[74] K. Johnson and E. C. G. Sudarshan, Annals Phys. **13** (1961) 126.

[75] G. Velo and D. Zwanziger, Phys. Rev. **186** (1969) 1337.

[76] H. Krebs, E. Epelbaum and U. G. Meißner, Phys. Rev. C **80** (2009) 028201 [arXiv:0812.0132 [hep-th]].

[77] M. Boglione and M. R. Pennington, Phys. Rev. D **65** (2002) 114010 [arXiv:hep-ph/0203149].

[78] N. A. Tornqvist, Z. Phys. C **68** (1995) 647 [arXiv:hep-ph/9504372].

[79] N. A. Tornqvist and M. Roos, Phys. Rev. Lett. **76** (1996) 1575 [arXiv:hep-ph/9511210].

[80] M. F. M. Lutz and S. Leupold, Nucl. Phys. A **813** (2008) 96 [arXiv:0801.3821 [nucl-th]].

[81] M. Harada and K. Yamawaki, Phys. Rept. **381** (2003) 1 [arXiv:hep-ph/0302103].

[82] B. Moussallam, Phys. Rev. D **51** (1995) 4939 [arXiv:hep-ph/9407402].

[83] R. Kaiser and H. Leutwyler, arXiv:hep-ph/9806336.

[84] R. Kaiser and H. Leutwyler, Eur. Phys. J. C **17** (2000) 623 [arXiv:hep-ph/0007101].

[85] J. Prades, Z. Phys. C **63** (1994) 491 [Erratum-ibid. C **11** (1999) 571] [arXiv:hep-ph/9302246].

[86] M. Knecht and A. Nyffeler, Eur. Phys. J. C **21** (2001) 659 [arXiv:hep-ph/0106034].

[87] P. D. Ruiz-Femenia, A. Pich and J. Portoles, JHEP **0307** (2003) 003.

[88] M. J. Ablowitz and A. S. Fokas, *Complex Variables: Introduction and Applications*, Cambridge University Press, 1997.

[89] L. Castillejo, R. H. Dalitz and F. J. Dyson, Phys. Rev. **101** (1956) 453.

[90] N. N. Achasov and A. V. Kiselev, Phys. Rev. D **70** (2004) 111901 [arXiv:hep-ph/0405128].

[91] F. Giacosa and G. Pagliara, Phys. Rev. C **76** (2007) 065204 [arXiv:0707.3594 [hep-ph]].

[92] P. J. Redmond, Phys. Rev. **112** (1958) 1404.

[93] N. N. Bogolyubov, A. A. Logunov and D. V. Shirkov, Sov. Phys. JETP **37** (1960) 574.

[94] F. Lambert, Nucl. Phys. **B62** (1973) 301.

[95] J. Caro, E. Ruiz Arriola and L. L. Salcedo, Phys. Rev. C **55** (1997) 1767 [arXiv:nucl-th/9609031].

[96] K. Symanzik, J. Math. Phys., 1 (1960)249.

[97] J. A. Cronin, "Phenomenological model of strong and weak interactions in chiral U(3) x U(3)," Phys. Rev. **161** (1967) 1483.

[98] S. Weinberg, "Dynamical approach to current algebra," Phys. Rev. Lett. **18** (1967) 188.

[99] S. Weinberg, "Nonlinear realizations of chiral symmetry," Phys. Rev. **166** (1968) 1568.

[100] L. S. Brown, "Field Theory Of Chiral Symmetry," Phys. Rev. **163** (1967) 1802.

[101] P. Chang and F. Gursey, "Unified Formulation of Effective Nonlinear Pion-Nucleon Lagrangians," Phys. Rev. **164** (1967) 1752.

[102] L. Susskind and G. Frye, "Algebraic aspects of pionic duality diagrams," Phys. Rev. D **1** (1970) 1682.

[103] H. Osborn, "Implications of adler zeros for multipion processes," Lett. Nuovo Cim. **2S1** (1969) 717 [Lett. Nuovo Cim. **2** (1969) 717].

[104] J. R. Ellis and B. Renner, "On the relationship between chiral and dual models," Nucl. Phys. B **21** (1970) 205.

[105] M. L. Mangano and S. J. Parke, "Multiparton amplitudes in gauge theories," Phys. Rept. **200** (1991) 301 [hep-th/0509223].

[106] L. J. Dixon, "Calculating scattering amplitudes efficiently," In *Boulder 1995, QCD and beyond* 539-582 [hep-ph/9601359].

[107] B. Feng and M. Luo, "An Introduction to On-shell Recursion Relations," arXiv:1111.5759 [hep-th].

[108] J. M. Drummond, "Hidden Simplicity of Gauge Theory Amplitudes," Class. Quant. Grav. **27** (2010) 214001 [arXiv:1010.2418 [hep-th]].

[109] Z. Bern, L. J. Dixon, D. C. Dunbar and D. A. Kosower, "One loop n point gauge theory amplitudes, unitarity and collinear limits," Nucl. Phys. B **425**, 217 (1994) [hep-ph/9403226].

[110] Z. Bern, L. J. Dixon, D. C. Dunbar and D. A. Kosower, "Fusing gauge theory tree amplitudes into loop amplitudes," Nucl. Phys. B **435**, 59 (1995) [hep-ph/9409265].

[111] R. Britto, F. Cachazo and B. Feng, "New recursion relations for tree amplitudes of gluons," Nucl. Phys. B **715** (2005) 499 [hep-th/0412308].

[112] R. Britto, F. Cachazo, B. Feng and E. Witten, "Direct proof of tree-level recursion relation in Yang-Mills theory," Phys. Rev. Lett. **94** (2005) 181602 [hep-th/0501052].

[113] N. Arkani-Hamed, J. L. Bourjaily, F. Cachazo, S. Caron-Huot and J. Trnka, "The All-Loop Integrand For Scattering Amplitudes in Planar N=4 SYM," JHEP **1101** (2011) 041 [arXiv:1008.2958 [hep-th]].

[114] C. F. Berger, Z. Bern, L. J. Dixon, F. Febres Cordero, D. Forde, T. Gleisberg, H. Ita and D. A. Kosower *et al.*, "Precise Predictions for W + 4 Jet Production at the Large Hadron Collider," Phys. Rev. Lett. **106** (2011) 092001 [arXiv:1009.2338 [hep-ph]].

[115] E. Witten, "Perturbative gauge theory as a string theory in twistor space," Commun. Math. Phys. **252**, 189 (2004) [hep-th/0312171].

[116] Z. Bern, L. J. Dixon and V. A. Smirnov, "Iteration of planar amplitudes in maximally supersymmetric Yang-Mills theory at three loops and beyond," Phys. Rev. D **72**, 085001 (2005) [hep-th/0505205].

[117] L. F. Alday and J. M. Maldacena, "Gluon scattering amplitudes at strong coupling," JHEP **0706**, 064 (2007) [arXiv:0705.0303 [hep-th]].

[118] L. F. Alday, J. Maldacena, A. Sever and P. Vieira, "Y-system for Scattering Amplitudes," J. Phys. A **43**, 485401 (2010) [arXiv:1002.2459 [hep-th]].

[119] J. M. Drummond, J. Henn, G. P. Korchemsky and E. Sokatchev, "Dual superconformal symmetry of scattering amplitudes in N=4 super-Yang-Mills theory," Nucl. Phys. B **828**, 317 (2010) [arXiv:0807.1095 [hep-th]].

[120] J. M. Drummond, J. Henn, G. P. Korchemsky and E. Sokatchev, "On planar gluon amplitudes/Wilson loops duality," Nucl. Phys. B **795**, 52 (2008) [arXiv:0709.2368 [hep-th]].

[121] J. M. Drummond, J. M. Henn and J. Plefka, "Yangian symmetry of scattering amplitudes in N=4 super Yang-Mills theory," JHEP **0905**, 046 (2009) [arXiv:0902.2987 [hep-th]].

[122] Z. Bern, J. J. M. Carrasco and H. Johansson, "New Relations for Gauge-Theory Amplitudes," Phys. Rev. D **78**, 085011 (2008) [arXiv:0805.3993 [hep-ph]].

[123] N. Arkani-Hamed, J. L. Bourjaily, F. Cachazo, A. B. Goncharov, A. Postnikov and J. Trnka, "Scattering Amplitudes and the Positive Grassmannian," arXiv:1212.5605 [hep-th].

[124] N. Arkani-Hamed, F. Cachazo, C. Cheung and J. Kaplan, "A Duality For The S Matrix," JHEP **1003**, 020 (2010) [arXiv:0907.5418 [hep-th]].

[125] L. J. Mason and D. Skinner, "Dual Superconformal Invariance, Momentum Twistors and Grassmannians," JHEP **0911**, 045 (2009) [arXiv:0909.0250 [hep-th]].

[126] L. J. Mason and D. Skinner, "The Complete Planar S-matrix of N=4 SYM as a Wilson Loop in Twistor Space," JHEP **1012**, 018 (2010) [arXiv:1009.2225 [hep-th]].

[127] J. Bedford, A. Brandhuber, B. J. Spence and G. Travaglini, "A Recursion relation for gravity amplitudes," Nucl. Phys. B **721** (2005) 98 [hep-th/0502146].

[128] F. Cachazo and P. Svrcek, "Tree level recursion relations in general relativity," hep-th/0502160.

[129] C. Cheung, "On-Shell Recursion Relations for Generic Theories," JHEP **1003** (2010) 098 [arXiv:0808.0504 [hep-th]].

[130] S. J. Parke and T. R. Taylor, "An Amplitude for n Gluon Scattering," Phys. Rev. Lett. **56** (1986) 2459.

[131] F. A. Berends and W. T. Giele, "Recursive Calculations for Processes with n Gluons," Nucl. Phys. B **306** (1988) 759.

[132] S. D. Badger, E. W. N. Glover, V. V. Khoze and P. Svrcek, "Recursion relations for gauge theory amplitudes with massive particles," JHEP **0507** (2005) 025 [hep-th/0504159].

[133] B. Feng, J. Wang, Y. Wang and Z. Zhang, "BCFW Recursion Relation with Nonzero Boundary Contribution," JHEP **1001** (2010) 019 [arXiv:0911.0301 [hep-th]].

[134] B. Feng and C. -Y. Liu, "A Note on the boundary contribution with bad deformation in gauge theory," JHEP **1007** (2010) 093 [arXiv:1004.1282 [hep-th]].

[135] B. Feng and Z. Zhang, "Boundary Contributions Using Fermion Pair Deformation," JHEP **1112** (2011) 057 [arXiv:1109.1887 [hep-th]].

[136] K. Risager, "A Direct proof of the CSW rules," JHEP **0512** (2005) 003 [hep-th/0508206].

[137] T. Cohen, H. Elvang and M. Kiermaier, "On-shell constructibility of tree amplitudes in general field theories," JHEP **1104** (2011) 053 [arXiv:1010.0257 [hep-th]].

[138] P. Benincasa and E. Conde, "On the Tree-Level Structure of Scattering Amplitudes of Massless Particles," JHEP **1111** (2011) 074 [arXiv:1106.0166 [hep-th]].

[139] B. Feng, Y. Jia, H. Luo and M. Luo, "Roots of Amplitudes," arXiv:1111.1547 [hep-th].

[140] J. Bijnens, K. Kampf and S. Lanz, "Leading logarithms in N-flavour mesonic Chiral Perturbation Theory," arXiv:1303.3125 [hep-ph].

[141] R. F. Dashen and M. Weinstein, "Soft pions, chiral symmetry, and phenomenological lagrangians," Phys. Rev. **183** (1969) 1261.

[142] K. Kampf, J. Novotny and J. Trnka, "Recursion Relations for Tree-level Amplitudes in the SU(N) Nonlinear Sigma Model," arXiv:1212.5224 [hep-th].

[143] N. Arkani-Hamed, F. Cachazo and J. Kaplan, "What is the Simplest Quantum Field Theory?," JHEP **1009** (2010) 016 [arXiv:0808.1446 [hep-th]].

[144] S. Weinberg, "The quantum theory of fields. Vol. 2: Modern applications," Cambridge, UK: Univ. Pr. (1996) 489 p